DOE/RL/87-09
PNL-6200
UC-11

DISCLAIMER

THE REMEDIAL ACTION PRIORITY SYSTEM (RAPS): MATHEMATICAL FORMULATIONS

G. Whelan
D. L. Strenge
J. G. Droppo, Jr.
B. L. Steelman
J. W. Buck

DOE/RL--87-09

DE88 001699

August 1987

Prepared by:
Pacific Northwest Laboratory
Richland, Washington 99352
under Contract DE-AC06-76RLO 1830

Prepared for:
Assistant Secretary,
Environment, Safety, and Health
Office of Environmental
Guidance and Compliance
U.S. Department of Energy
Washington, D.C. 20545

PREFACE

In 1985 and 1986, the Pacific Northwest Laboratory (PNL) developed the Remedial Action Priority System (RAPS). The RAPS methodology represents an approach that prioritizes hazardous and radioactive mixed-waste disposal sites in a scientific and objective manner based on limited site information. The RAPS methodology provides the U.S. Department of Energy's Office of Environment, Safety, and Health (DOE-ESH) with a management tool for assistance in prioritizing funding and human resource allocations for further investigations and possible remediation at its inactive waste sites that may produce long-term releases of contaminants to the environment.

Under the guidance of DOE-ESH, PNL has developed a program to review, analyze, test, and enhance major aspects of the RAPS methodology. The completion date of this program is October 1988. This report represents one of the first steps of this program. Other steps represented in the program are outlined as follows:

- Independent Peer Review -- The methodology and its mathematical formulations have been independently peer reviewed by leading outside authorities in the private and public sectors.
- Demonstration of the Methodology -- The various components of the RAPS methodology have been implemented at actual sites where contaminant levels have been monitored in the environment. The monitored contaminant levels were then compared to simulated contaminant levels associated with the application of RAPS to these sites. The purpose of the comparison was to demonstrate the applicability of the RAPS methodology to a variety of hazardous waste sites or releases of contaminants into the environment.
- Sensitivity Analysis -- An extensive sensitivity analysis is planned to determine the effects of 1) specific input parameters, 2) initial and boundary conditions, 3) distributions of input parameters, and 4) interrelationships that exist among input parameters on model response over short and long time frames.

- Test Applications of the Methodology -- The methodology is being implemented at a suite of hazardous waste sites, which have been independently chosen, to rank these sites according to their potential hazard to the surrounding human population. These results will then be compared with those from other methodologies that have ranked these same sites. These results will be reviewed by a panel of exposure assessment experts to determine the strengths and weaknesses of each methodology. The purpose of the applications is to illustrate the flexibility, strengths, and weaknesses of the methodologies and to identify discrepancies between the different ranking techniques.

- Enhanced Features to the Methodology -- Several features not outlined in this report will be included in the methodology before the October 1988 completion date. The major enhancements include the following:

  - complex-terrain model for the atmospheric component of the methodology
  - sedimentation submodels to address aggradation/degradation issues associated with the surface water component of the methodology
  - lake or large impoundment (e.g., reservoirs) model for the surface water component of the methodology
  - retrofitting or back-calculating techniques to help calibrate components of the methodology at those sites where measured environmental data (including contaminant levels) are available
  - algorithms to address short-term, batched, or infrequent releases of contaminants to the environment.

As with the components outlined in the following chapters of this report, each enhanced feature will be independently peer reviewed and

tested. This new, enhanced version of the RAPS methodology will be called the Multimedia Environmental Pollutant Assessment System (MEPAS).

- Documentation of the Methodology -- Documentation represents a key feature of the RAPS program. Key documentation will include the following:
  - complete description of the mathematical formulations forming the basis of the RAPS methodology (represented by this manual)
  - documentation of the extensive sensitivity analysis
  - a complete listing of data bases used by the methodology
  - instruction manual identifying sources of pertinent data outside the data bases
  - guidelines for implementing the methodology
  - a user's manual.

  Any future modifications to the methodology will be documented in addenda and appropriately distributed.

When completed, the RAPS methodology will be available for implementation by those personnel specifically trained in its application. When appropriately applied, RAPS will represent a powerful tool for prioritizing environmental issues associated with sites that potentially release contaminants into the environment.

EXECUTIVE SUMMARY

The Remedial Action Priority System (RAPS) represents a methodology that prioritizes inactive hazardous and radioactive mixed-waste disposal sites in a scientific and objective manner based on limited site information. This methodology is intended to bridge the technology gap between the initial site evaluation using the Hazard Ranking System (HRS) and the time-consuming process of actual field site characterization, assessment, and remediation efforts.

The RAPS methodology provides the U.S. Department of Energy (DOE) with a management tool for assistance in prioritizing funding and human resource allocations for further investigations and possible remediations at its inactive waste sites. Use of RAPS will help DOE ensure that those sites posing the highest potential risk are addressed first.

The RAPS methodology uses empirically, analytically, and semianalytically based mathematical algorithms to predict the potential for contaminant migration from a site to receptors of concern using pathways analyses. Four major pathways of contaminant migration are considered in the RAPS methodology: groundwater, overland, surface water, and atmospheric. Using the predictions of contaminant transport, simplified exposure assessments are performed for important receptors. The risks associated with the site can then be calculated relative to the risks of other sites for each pathway and for all pathways together.

The RAPS methodology considers 1) specific site information and constituent characteristics associated with the transport pathways; 2) both chemical and radioactive wastes; 3) the potential direction of contaminant movement; 4) contaminant mobility and persistence, where applicable; 5) population distributions; 6) various routes of exposure (e.g., inhalations, ingestion, and external exposure); 7) contaminant toxicities; 8) duration of exposure of the surrounding population; and 9) contaminant arrival time to sensitive receptors. Because RAPS is based on specific site information and constituent characteristics, the scoring system of the RAPS methodology reduces the subjectivity that is associated with other ranking methods.

Upon completion of the RAPS methodology and upon completion of its implementation at DOE sites, the staff at DOE will then consolidate the rankings provided by the RAPS methodology with other environmental concerns such as compliance, enforcement, and state and local concerns. Following a consolidation of this other information, any modifications to the risk-based ranking will be on a case-by-case basis. These modifications will be developed and justified by DOE staff based on the knowledge of the site. Each modification will be documented and shall include the basis for the consideration (e.g., violation of an air permit). The modifications to the risk-based rankings are expected to come under close scrutiny by DOE management and outside concerns; therefore, the extent of the documentation shall be sufficient to ensure an adequate understanding of the circumstances by reviewers of the decision.

The purpose of this report is to present the preliminary mathematical algorithms forming the basis of the RAPS methodology. The preliminary mathematical formulations associated with the environmental transport pathways, the exposure assessment component of RAPS, and the environmental health effects components are represented. An overview of the RAPS methodology and the rationale associated with its development is included. Four hypothetical case studies are presented that illustrate the application of RAPS.

ACKNOWLEDGMENTS

Developing a multimedia contaminant environmental exposure and risk assessment methodology incorporates a wide spectrum of engineering and scientific technologies and involves the specialized expertise of several researchers. One researcher cannot adequately address the complexities associated with an assessment methodology that covers contaminant migration through four major transport environments (i.e., overland, groundwater, surface water, and air), human dose through four routes of exposure (i.e., ingestion, inhalation, dermal contact, and external dose), and health effects associated with exposure to carcinogenic and noncarcinogenic constituents. The principal contributors to this report, listed after the chapter to which they contributed, are

- Chapter 1.0 -- G. Whelan and B. L. Steelman
- Chapter 2.0 -- G. Whelan and B. L. Steelman
- Chapter 3.0 -- G. Whelan
- Chapter 4.0 -- G. Whelan
- Chapter 5.0 -- G. Whelan
- Chapter 6.0 -- G. Whelan
- Chapter 7.0 -- J. G. Droppo, Jr. and J. W. Buck
- Chapter 8.0 -- D. L. Strenge
- Chapter 9.0 -- D. L. Strenge
- Chapter 10.0 -- G. Whelan, D. L. Strenge, and B. L. Steelman.

This report has been peer reviewed by independent, outside [i.e., not related to the U.S. Department of Energy (DOE) or Pacific Northwest Laboratory (PNL)] peer reviewers. The following reviewers provided valuable comments for this report: L. Mulkey of the U.S. Environmental Protection Agency (EPA) in Athens, Georgia; C. DeRosa of EPA in Cincinnati, Ohio; R. Codell of the U.S. Nuclear Regulatory Commission (NRC) in Washington, D.C.; J. Reyes of the Agency for Toxic Substances and Disease Registry in Atlanta, Georgia; D. Pollock of the U.S. Geological Survey in Washington, D.C.; M. Amdurer of EBASCO; D. Buss of GeoTrans; S. Hanna of Sigma Research; and T. Gallagher of HydroQual. Their valuable comments are greatly appreciated and have been incorporated into this document, where appropriate. In addition to the outside peer reviews,

technical comments and guidance were provided by the following DOE personnel and their associated Operations Offices: P. Krupin of DOE Richland, Washington; C. Travis, D. Kocher, L. Barnthouse, G. Suter, and L. D. Eyman of Oak Ridge National Laboratory; R. W. Taft of Nevada; and W. Holman and J. T. Davis of San Francisco. The authors greatly appreciate the comments by each DOE reviewer.

The authors would like to thank K. A. Hawley of PNL for 1) providing material associated with the Hazard Ranking System (HRS) and modified Hazard Ranking System (mHRS) and 2) calculating the HRS and mHRS ranking scores associated with the example case studies. The authors would also like to thank G. W. Gee, R. L. Skaggs, Y. Onishi, E. A. Jacobson, J. K. Soldat, B. A. Napier, R. W. Wallace, and P. J. Mellinger of PNL for reviewing portions of the document and for providing valuable comments in the development of the Remedial Action Priority System (RAPS) methodology. Many of the concepts associated with the compositely coupled assessment methodology were developed in concert with Y. Onishi. Appreciation is extended to D. R. Simpson, J. L. Baer, J. L. Downs, S. A. Kreml, and P. C. Hays of PNL for editing the document and to PNL Word Processing for typing the document.

Special thanks go to K. Semac and R. Aiken of DOE's Office of Environment, Safety, and Health (ESH), and to P. vanHaagen and V. J. DeCarlo, formerly of DOE-ESH, for their comments, guidance, and support in the development of the RAPS methodology. This work is supported by DOE-ESH under contract DE-AC06-76RLO 1830.

CONTENTS

FIGURES

TABLES

1.0 INTRODUCTION

Over the years, federal, state, and local agencies have become concerned about the release of contaminants into the environment from a variety of sources. The potential danger these releases present to humans and the environment is of utmost concern. Federal legislation mandates the analysis and evaluation of contaminant effluent effects on the environment. Establishing effective regulatory programs, however, requires that water quality and effluent standards be based on a comparative relationship between risks, costs, and benefits associated with emission criteria. Taking this into consideration, the federal government enacted the following legislation, among others, to establish effluent standards controlling toxic pollutants and to help restore and/or maintain the chemical, physical, and biological integrity of the nation's natural resources (Whelan et al. 1987):

- Water Quality Act of 1965
- Federal Water Pollution Control Action (FWPCA) Amendments of 1972
- Safe Drinking Water Act of 1974
- Resource Conservation and Recovery Act (RCRA) of 1976
- Clean Water Act of 1977
- Comprehensive Environmental Response, Compensation, and Liability Act (CERCLA or Superfund) of 1980
- Hazardous and Solid Waste Amendments of 1984
- Superfund Amendments and Reauthorization Act (SARA) of 1986.

With the passage of RCRA, CERCLA, and SARA, Congress has mandated a much closer scrutiny of the management of hazardous wastes generated currently and in the future and of the restoration of disposal sites contaminated by improper management in the past. Legislative language, regulatory intent, and prudent judgment call for the use of risk assessment techniques to aid in the decision-making process; this applies to facilities operated for the U.S. Department of Energy (DOE) just as it does to private industrial facilities.

The U.S. Department of Energy's inactive hazardous waste disposal sites are currently being evaluated under its CERCLA program to determine whether migration of hazardous substances has occurred and whether remediation will be required (DOE 1985). Consequently, DOE is in the process of locating, identifying, and evaluating potential problems associated with its inactive hazardous and radioactive waste disposal facilities, and of controlling the migration of hazardous substances from such facilities to minimize potential hazards to health, safety, and the environment.

It is the intent of all environmental regulations to minimize, if not eliminate, the risks to man and his environment that arise from the regulated activity. Because lower levels of risk are usually accompanied by higher costs of control, optimal management is achieved by a balancing of risks and costs. Hence, in selecting between alternatives, the decision maker must have access to data and methods for quantifying residual risks for each available option. With respect to the DOE inactive hazardous waste site management program, the development and application of an objective, scientifically based methodology for assessing the potential risk of contaminant migration represents an invaluable risk assessment tool.

1.1 OBJECTIVE

Limited resources are available to conduct detailed site investigations and characterizations of all identified potentially hazardous and radioactive mixed-waste sites. Therefore, an assessment methodology is required to prioritize waste sites according to risk, based on limited available information, so that detailed site characterizations are performed first on those sites that exhibit the highest potential risks.

For an initial identification of sites that may pose significant problems to public health, safety, and/or the environment, DOE is utilizing the Hazard Ranking System (HRS), developed by the U.S. Environmental Protection Agency (EPA), and a modified Hazard Ranking system (mHRS), developed by Pacific Northwest Laboratory (PNL), to assess waste sites containing radionuclides (Hawley and Napier 1984). The HRS and mHRS were not developed to quantify the relative risks of sites (EPA 1982). Consequently, PNL was requested to develop a risk

assessment methodology called the Remedial Action Priority System (RAPS). The RAPS methodology will provide DOE with a management tool to assist them in determining priorities for further site investigation.

1.2 SCOPE OF WORK

Releases of chemical, radioactive, or mixed wastes from an inactive hazardous waste site into the environment can occur through a number of pathways. After contaminants are released into the environment, they may undergo complex processes of transport, degradation/decay, transformation, biological uptake, and intermedia transfer between atmospheric, overland, subsurface (groundwater), and surface water environments. A multimedia contaminant environmental exposure and risk assessment methodology can be obtained by systematically integrating computer-based models that represent the various environmental transport pathways and routes of human exposure to estimate the relative risks associated with the exposure.

The primary focus of the work outlined in this report is the development of the RAPS methodology, which ranks inactive hazardous and radioactive mixed-waste disposal facilities in an objective, scientifically based manner with regard to their hazard potential. In developing the RAPS methodology, a number of characteristics had to be considered to build a framework that could be applied at a wide number of sites. In this case, the framework had to

- address inactive landfills in its analysis
- address holding ponds in its analysis
- consider hazardous and radioactive mixed wastes
- consider the direction of solute migration
- consider size and location of the surrounding populations
- consider lifetime exposure to a surrounding population
- consider the duration of exposure of the population to the contaminant

- consider the time frame associated with the exposure (e.g., is the population initially exposed after 1 year or does the contaminant require 10,000 years of travel time to come into contact with the surrounding population?)
- consider the relative risks to a population from exposure to contaminants
- consider the mobility, persistence, toxicity, and nature of the waste constituents
- consider the potential for contaminating drinking-water supplies
- discriminate the potential hazard according to transport pathway
- include specific site and constituent characteristics in its analysis
- minimize user subjectivity
- provide rapid and inexpensive predictions
- be based on a system that can be applied by users with a limited background in the area of hazardous waste assessment
- be based on data available at most sites
- be based on previously developed techniques
- be transferable between sites
- be based on a compatible computing system that is available to most users
- represent an initial step in quantitatively ranking the potential for hazard at one site relative to other sites and identifying sites that may pose a significant risk to public health.

Because computer codes can effectively integrate a wide variety of complex processes into a single, cogent framework, they form the basis of the assessment methodology. Employing mathematical codes to describe specific site and constituent characteristics removes much of the subjectivity that exists with current methodologies that describe the hazard potential at inactive hazardous waste facilities. However, to address all of the constraints listed, the

assessment methodology must be composed of computer codes that are not overly complex and/or based on unreasonably onerous data requirements.[a] As a result, screening-level codes best fit the level of detail required by the modeling constraints listed.[b]

The RAPS methodology is composed of computer codes that are analytically, semianalytically, and empirically based. The contaminant transport pathways and routes of exposure have a set of codes that describe contaminant migration (i.e., movement of the contaminant in the environment) and fate (i.e., form and location of the contaminant in the environment) through various environmental media and exposure (i.e., dose to the individual) and relative risk (i.e., health effects associated with the exposure) to the surrounding populations.

1.3 APPLICATION LIMITATIONS

Although simplified codes are required for the purposes of RAPS, inherent deficiencies are associated with their application. At first glance, simplified codes appear ideal. They are easy to implement on a computing system; they have small input data requirements; they are inexpensive to operate; they have a small number of algorithms and components (as compared to a complex numerical code); and their documentation is more easily understood. However, a potential drawback associated with simplified codes is that they are also potentially easier to misuse than a more complex code. The code user must remember that the applicability of a code is defined by its assumptions and limitations of its algorithms.

All computer codes, no matter how complex, represent simplifications of real-world conditions. Complex codes are usually developed to address detailed mechanistic phenomena, hence the large number of input parameters. Simplified codes handle less of the detailed phenomenological aspects of real-world

---

(a) Numerically based computer codes using finite difference or finite element algorithms illustrate examples of complex codes.

(b) Computer codes based on analytical, semianalytical, and/or empirical relationships illustrate examples of screening-level codes.

conditions by combining many of these aspects into fewer parameters; it is, therefore, difficult to ensure the absolute accuracy of results at all sites under all conditions.

To help alleviate this problem, the RAPS methodology is being developed to be used in a comparative mode, not in a predictive mode. Although RAPS generates a risk-based ranking and is based on algorithms for which an assigned risk to a human population can be determined, it does not purport to use this risk in an absolute manner. Rather, the risk is convoluted and normalized with standard exposure and risk factors; these factors are used in the ranking process. The output results from one site are then compared, in a relative sense, to the output results of other sites to determine their significance.

The RAPS methodology can quantitatively identify the sites that are potentially most hazardous to their surrounding populations relative to other sites, but because of its relative simplicity and the unknown distributions and variances associated with many of the parameters, RAPS cannot currently associate an uncertainty with that risk. In fact, no methodology that uses simplified codes for a wide variety of applications at different sites can guarantee accurate results for all applications in an absolute sense. See the following references for more information associated with the philosophical aspects of computer modeling: Simmons and Cole (1985), Whelan et al. (1987), Kincaid et al. (1984a,b), Bachmet et al. (1980), Mercer and Faust (1980a-e), and Anderson (1979).

1.4 STRUCTURE OF THE REPORT

This report is divided into 10 chapters. Chapter 2.0 presents an overview of the RAPS methodology and the rationale associated with its development. Chapters 3.0 through 7.0 discuss the mathematical formulations associated with the environmental transport pathways. Chapter 3.0 presents the algorithms used in quantifying the source-term leachate and overland runoff volumes, while Chapters 4.0 through 7.0 review the mathematical formulations for computing contaminant transport in the overland, groundwater, surface water, and atmospheric environments, respectively. Chapters 8.0 and 9.0 present the mathematical algorithms associated with the exposure assessment and health risk

evaluation components, respectively, of RAPS. Finally, Chapter 10.0 illustrates the application of the RAPS methodology to four hypothetical case studies. These case studies demonstrate the utility of RAPS in simulating the migration and fate of hazardous and radioactive mixed wastes through and between various environmental media, their interaction with the media, exposure to surrounding populations, and subsequent risks associated with the exposure.

This report represents the results of the initial phase in the development of the RAPS methodology and presents the preliminary mathematical formulations associated with all major aspects of RAPS. Following several applications of RAPS to actual DOE hazardous and radioactive mixed-waste facilities, the mathematical formulations associated with RAPS will be updated, where applicable, and the various components of the framework will be finalized.

1.5 REFERENCES

Anderson, M. P. 1979. "Ground-Water Modeling - The Emperor has No Clothes." Ground Water 21(2):666-669.

Bachmet, Y., J. Bredehoeft, B. Andrews, D. Holte and S. Sebastian. 1980. Groundwater Management: The Use of Numerical Models. Water Resources Monograph #5. American Geophysical Union, Washington, D.C.

DOE. 1985. Comprehensive Environmental Response Compensation, and Liability Act Program. DOE Order 5480.14, U.S. Department of Energy, Washington, D.C.

EPA. 1982. "Appendix A - Uncontrolled Hazardous Waste Site Ranking System: A User's Manual." U.S. Environmental Protection Agency, 37(137) Fed. Reg. 31219-31243 (July 16, 1982).

Hawley, K. A., and B. A. Napier. 1984. "A Ranking System for Mixed Radioactive and Hazardous Waste Sites." In Proceedings of the Fifth DOE Environmental Protection Information Meeting, CONF-841187, U.S. Department of Energy, Washington, D.C.

Kincaid, C. T., J. R. Morrey and J. E. Rogers. 1984a. Geohydrochemical Models for Solute Migration: The Selection of Computer Codes and Description of Solute Migration Processes. Vol. I. EPRI RP-1619-1, Electric Power Research Institute, Palo Alto, California.

Kincaid, C. T., J. R. Morrey, S. B. Yabusaki, A. R. Felmy and J. E. Rogers. 1984b. Geohydrochemical Models for Solute Migration: Preliminary Evaluation of Selected Computer Codes for Modeling Aqueous Solutions and Solute Migration in Soils and Geologic Media. Vol. II. EA-3417, EPRI RP-2485-02, Electric Power Research Institute, Palo Alto, California.

Mercer, J. W., and C. R. Faust. 1980a. "Ground-Water Modeling: An Overview." Ground Water 18(2):108-115.

Mercer, J. W., and C. R. Faust. 1980b. "Ground-Water Modeling: Mathematical Models." Ground Water 18(3):212-227.

Mercer, J. W., and C. R. Faust. 1980c. "Ground-Water Modeling: Numerical Models." Ground Water 18(4):395-409.

Mercer, J. W., and C. R. Faust. 1980d. "Ground-Water Modeling: Applications." Ground Water 18(6):486-497.

Mercer, J. W., and C. R. Faust. 1980e. "Ground-Water Modeling: Recent Developments." Ground Water 19(6):569-577.

Simmons, C. S., and C. R. Cole. 1985. Guidelines for Selection and Evaluation of Groundwater Transport Models. PNL-4980, Pacific Northwest Laboratory, Richland, Washington.

Whelan, G., S. M. Brown, D. L. Strenge, A. P. Schwab and P. J. Mitchell. 1987. Contaminant Assessment Modeling Under the Resource Conservation and Recovery Act. EA-5342. Electric Power Research Institute, Palo Alto, California.

2.0 OVERVIEW OF THE RAPS METHODOLOGY

For several decades, DOE and its predecessor agencies have been involved in a wide range of activities that generate hazardous substances, both chemical and radioactive. In some cases, these substances have migrated from the disposal sites, and further site investigations and possibly site remediation are needed. These circumstances, coupled with the enactment of environmental regulations such as CERCLA, require that action be taken to identify and reduce or eliminate, in an environmentally responsible manner, the potential hazards related to the past disposal activities.

The DOE policy (DOE 1985) is to identify and evaluate potential problems associated with inactive hazardous waste disposal sites and to provide steps to help control the migration of hazardous substances from such facilities to minimize potential hazards to health, safety, and the environment. A typical approach in accomplishing the goals of this policy is to locate and identify those inactive hazardous waste disposal sites that may pose an unacceptable risk to health, safety, and the environment; to quantify the presence or absence of hazardous substances for sites that may pose an unacceptable risk, by conducting preliminary surveys and comprehensive investigations if necessary; to develop a site remediation plan for sites confirmed to pose an unacceptable risks, by evaluating alternative technologies for controlling the migration of hazardous substances or decontaminating the inactive disposal site; to implement the recommended remedial measures; and to prepare documentation of remedial actions and to establish any site monitoring requirements necessary to verify the effectiveness of the actions.

The work presented in this report is associated with locating and identifying these inactive hazardous waste disposal sites. To accomplish this objective (i.e., identify sites that may pose unacceptable risks), all potentially hazardous inactive waste disposal sites must be identified and sufficient information gathered to allow preliminary evaluation of the potential risks.

To fully comprehend the approach being considered for identifying and evaluating those hazardous waste sites that may pose an unacceptable risk to the surrounding environment, this section presents the rationale behind the

development of the RAPS methodology. Additionally, this section briefly 1) reviews other types of assessment methodologies developed for addressing concerns related to the migration, fate, and exposure of contaminants released into the environment; 2) briefly highlights the appropriate tools for quantitatively prioritizing sites based on their relative risk; and 3) reviews a proposed integrated framework employing a suite of methodologies coupled with RAPS, which can be used for identifying and evaluating potential problems associated with inactive hazardous and radioactive mixed-waste disposal facilities. These discussions are followed by a description of the structure of RAPS, the various components that comprise the system, and the key features and characteristics of the system.

2.1 ASSESSMENT METHODOLOGIES

Assessment methodologies or frameworks have been and are being developed to address concerns related to risks and the migration, fate, and exposure of contaminants released into the environment. These contaminants can undergo complex processes of transport, degradation and decay, transformation, biological uptake, and intermedia transfer among atmospheric, overland, groundwater, and surface water pathways. The interactions of these various media pathways and linkages to man are illustrated in Figure 2.1. The assessment frameworks integrate many of these complex components in an attempt to address a complicated environmental setting in a logical, consistent, cogent, objective manner. Each assessment framework is developed to meet a particular objective and, therefore, cannot arbitrarily be applied to all assessment situations. For example, the RAPS methodology is being developed for DOE to rank, according to potential risk, inactive hazardous and radioactive mixed-waste sites so the most hazardous sites can be further investigated first (Whelan and Steelman 1984). The RAPS methodology addresses contaminant migration, fate, exposure, and risk through four major environmental transport pathways (i.e., groundwater, overland, surface water, and atmospheric). Because of the level of sophistication of the RAPS methodology, it can only be employed to rank sites according to their relative hazard potential; it cannot be used in a predictive

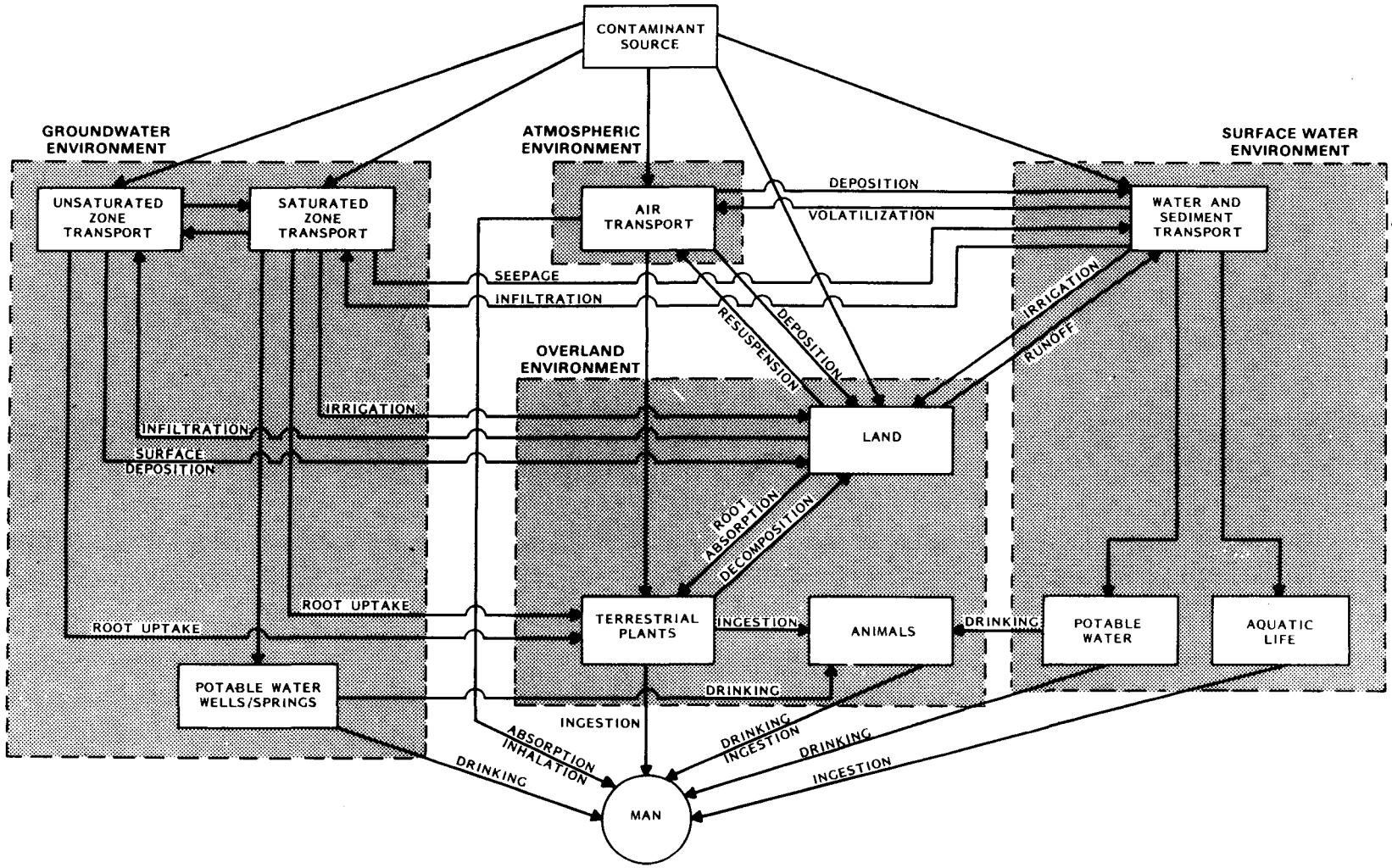

FIGURE 2.1. Schematic Diagram Illustrating the Interactions Between the Various Contaminant Transporting Media and How the Contaminants Affect Man Through His Environment (After Whelan et al. 1983)

mode to simulate the actual risks posed by a particular site resulting from the release of contaminants into the environment (Whelan et al. 1986). The RAPS methodology, therefore, meets the needs of DOE but may not meet the needs of other government agencies or private groups for conducting different types of assessments.

Several computer-based methodologies have been developed to effectively integrate and analyze complex processes involved in the migration and fate of contaminants through various transport pathways. Assessment methodologies can be grouped according to any number of traits. For example, they can be described according to their level of sophistication. At one end, frameworks exist based on simple questionnaires and check lists; at the other end, frameworks exist based on several highly sophisticated computer models. Whelan et al. (1987) took another approach and divided the various assessment methodologies into three categories according to their structure: check list/questionnaire (CL/Q), fully coupled, and compositely coupled. A brief review of these approaches follows.

2.1.1 Check List/Questionnaire Methodology

Check list or questionnaire methodologies are generally based on a questionnaire that divides site and condition characteristics into predetermined categories that are each assigned a point value. The user describes the characteristics of the site, waste, demography, etc. by identifying the categories that most closely correspond to those characteristics. The points associated with each category are usually totaled, and a score for the site is assigned. This method attempts to provide a simplistic, systematic means of assessing the hazards associated with waste disposal. Although the CL/Q frameworks are easily applied, Whelan and Steelman (1984) and JRB (1982)[(a)] note that they include inherent deficiencies:

- Key parameters, particularly important in describing the migration, fate, exposure, and risks of a contaminant, are usually not directly

(a) JRB. 1982. "The Establishment of Guidelines for Modeling Groundwater Contamination from Hazardous Waste Facilities." Discussion Draft Report. JRB Associates, Inc., McLean, Virginia.

considered in the assessment; these usually include, but are not limited to, dispersion coefficients, hydraulic conductivities, degradation rates, modes of exposure (e.g., inhalation, ingestion, dermal contact), and dose-response information.

- The total waste volume is usually assumed to be composed of the most toxic substance present at the site (HWN 1984), almost totally without regard for that constituent's concentration. This assumption even applies to innocuous material, such as soils, that contains relatively low levels of contamination.
- The potential direction of migrating contaminants is not usually addressed (EPA 1984).
- The site and contaminant characteristics that are employed in the methodology represent oversimplifications of real conditions.
- The time of contaminant arrival to sensitive receptors and the duration of exposure of surrounding populations are not usually addressed.
- All contaminant pathways are usually analyzed using similar, if not identical, questions.
- Little or no information on exposure is included in the CL/Q methodologies. The exposure assessment should include an analysis of the type of exposure (i.e., inhalation, ingestion, dermal contact, and external dose), time until exposure (i.e., the arrival time of the contaminant from the waste site to important receptors), and duration of exposure (i.e., the amount of time a population is continually exposed to a contaminant).
- The scoring system is highly subjective; that is, the score assigned is often a matter of personal interpretation of the questionnaire and possible responses to questions.

Typical examples of CL/Q methodologies include the LeGrand model (LeGrand 1983), the Surface Impoundment Assessment (SIA) model (Silka and Swearingen

1978, as reported by JRB 1982[a]), the JRB Rating Methodology model (Kufs et al. 1980), the HRS model (EPA 1982a), the mHRS model (Hawley and Napier 1984, 1985[b]; Hawley et al. 1986; Stenner et al. 1986), and the DRASTIC methodology (Aller et al. 1985).

2.1.2 Fully Coupled Methodology

With a fully coupled approach, each component of the assessment methodology (usually representing a transport pathway or exposure assessment component) is represented by a submodel, with the submodels internally combined into a single code. In effect, each submodel represents a part of the overall multimedia model. In some instances, submodels may interact (i.e., data and information transfer) with other submodels on both a temporal and spacial level. Interfacing and information transfer between submodels are managed by a central executive program, and information transfer readily occurs between pathways.

The pathway submodels are chosen a priori (by the original developer of the program), thereby limiting the type of sites and the number of release scenarios that can be addressed at a particular site. The fully coupled approach is intended to allow consistent and unified descriptions of environmental systems. Such methodologies are expected to eliminate user bias and achieve consistency from site to site. Because of the complex phenomena associated with the various pathways, however, a unified model of this type can become extremely large and cumbersome to implement; consequently, simplified models are usually used to reduce the quantity and complexity of information exchanged between components, achieve reasonable computer core size, and obtain more efficient code execution times. Assessment methodologies that may be considered fully coupled include the RCRA Risk-Cost Analysis (WET) model (ICF 1984),

---

(a) JRB. 1982. "The Establishment of Guidelines for Modeling Groundwater Contamination from Hazardous Waste Facilities." Discussion Draft Report. JRB Associates, Inc., McLean, Virginia.

(b) Hawley, K. A., and B. A. Napier. 1985. A Ranking System for Sites with Mixed-Radioactive and Hazardous Wastes. Prepared for the U.S. Department of Energy, Office of Operational Safety by Pacific Northwest Laboratory, Richland, Washington (Draft).

Air Land Water Analysis System (ALWAS)[a] model (Tucker et al. 1984), Hydrologic Simulation Program in FORTRAN (HSPF)[a] model (Johanson et al. 1980; Donigian et al. 1983a), Water Transport Model (WTM) (Fletcher and Dodson 1971; Fletcher et al. 1973), Simplified Codes for Performance Evaluation (SCOPE) methodology (Petrie et al. 1983), and Unified Transport Model (UTM)[a] (Patterson et al. 1974; Baes et al. 1976; Patterson 1986).

2.1.3 Compositely Coupled Methodology

With a compositely coupled (i.e., integrated systems) approach, each transport pathway is represented by an independent model. The models are externally coupled by the user to address the appropriate level of detail dictated by the environmental system and the type of assessment required. Therefore, the conceptualization of the modeling scenario is the responsibility of the user, whereas the conceptualization of the modeling scenario using the fully coupled approach is determined before its use. Modeling with a compositely coupled approach occurs in a sequential order; codes for individual pathways do not interact directly between themselves. Interfacing and information transfer occurs by assigning the output file from one pathway model to the input file of the next pathway model. Feedback (i.e., reversing the direction of data transfer) between the pathway models is addressed by the user when assessing the site, and the user decides the specific pathway to address. For example, two codes could be compositely coupled to simulate contaminant movement in a saturated groundwater environment. One code would model the movement of the water (i.e., transporting medium); the other code would model the movement of the contaminant. Each code functions independently and, therefore, can be independently updated or replaced.

The compositely coupled approach allows each component or code to be replaced as the scenario being modeled changes or as technological advances are made. This approach allows the user to customize frameworks to address specific modeling needs and to allocate resources to optimize the resource requirements of the analysis in relation to the goals of the assessment.

(a) Although the components used in this methodology are fixed, certain components may be more easily updated or changed than with other fully coupled methodologies.

Overall, the compositely coupled approach is more flexible than the fully coupled approach because only the necessary pathway models are used for a given problem. Examples of sequential pathway modeling, using the compositely coupled approach, include the Land Disposal Restriction (LDR) methodology (EPA 1986), the Chemical Migration and Risk Assessment (CMRA) methodology (Onishi et al. 1979, 1980, 1981; Parkhurst et al. 1981; Whelan and Parkhurst 1983), and the Multimedia Contaminant Environmental Exposure Assessment (MCEA) methodology (Onishi et al. 1982a,b; Whelan et al. 1982, 1983; Whelan and Onishi 1983). Bolten et al. (1983) expanded the MCEA methodology to include cost and risk analysis components.

2.2 INTEGRATED ASSESSMENT METHODOLOGY FOR INACTIVE WASTE SITES

Currently, the EPA uses HRS (a CL/Q methodology) to evaluate hazardous waste sites that fall within the jurisdiction of CERCLA. The HRS is probably the most widely used standardized assessment methodology. The EPA uses the HRS to identify sites for nomination to the NPL; it is designed as an initial screening tool to discriminate between hazardous wastes that do not pose and those that are likely to pose significant problems to human health, safety, and/or the environment.

The HRS examines three primary and two secondary pathways or routes of exposure (i.e., air, surface water, and groundwater, and direct contact and fire/explosion, respectively) in scoring a site being considered for nomination to the NPL. Each route score is normalized to a scale of 0 to 100. To obtain a total site migration score, the three route scores are geometrically averaged. Figure 2.2 reviews the basic logic used in scoring the primary routes of exposure in HRS.

The HRS was not designed to assess waste sites containing radionuclides. Radioactive wastes are at a disadvantage because their detection limits are significantly lower than those of traditional hazardous wastes (DOE 1985). Although the public is well served by lower detection limits for radioactive wastes, the implication is that chemical wastes (when not detected) are not present, and therefore the hazards appear higher for the radioactive wastes; in fact, the opposite may be true. Radioactive sites are likely to receive

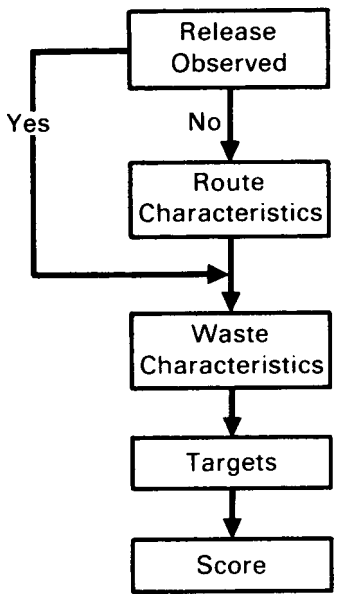

FIGURE 2.2. HRS Logic Diagram (After Whelan et al. 1985)

high scores because of the way the HRS methodology scores the toxicity and persistence of radionuclides in its waste characteristics section. The HRS waste characteristics scores are based on three waste criteria: 1) persistence, 2) toxicity or incompatibility/reactivity, and 3) quantity. By HRS definition, all radionuclides potentially cause severe toxic effects such as cancer (EPA 1984); therefore, radionuclides automatically receive the highest possible toxicity score. In addition, because many radionuclides have relatively long half-lives and/or because many radionuclides are also metals, most receive a maximum persistence score. By treating most radionuclides alike (i.e., having a maximum toxicity/persistence score), the HRS tends to overestimate the potential hazards of radioactive sites relative to chemical sites and fails to discriminate between the potential risks of sites containing different radionuclides.

Hawley and Napier (1984), Hawley et al. (1986), and Stenner et al. (1986) modified the HRS so radiological hazards would be addressed in a manner consistent with that of chemical wastes in the HRS. The resulting mHRS operates within the existing framework of the HRS, without changing the HRS scoring system. The mHRS allows information to be used in the route characteristics and

targets sections common to that of the HRS. The mHRS splits the waste characteristics sections into two subsections -- one for nonradioactive or chemical wastes and one for radioactive wastes (see Figure 2.3). At a mixed-waste site (i.e., one containing both radioactive and nonradioactive wastes), the mHRS develops two waste characteristics scores for each exposure route -- one for chemical and one for radioactive wastes. In calculating the migration scores for each route, the higher of the two waste characteristics scores is used in further analyses. For purely chemical sites, the mHRS yields results identical to those of the HRS (Whelan et al. 1985).

The mHRS calculates waste characteristics scores for radionuclides using dose factors and maximum observable or potential radiocontaminant concentrations in the environment. Dose factors convert data about the types of radionuclides present at the site, their half-lives, and environmental characteristics into values that, when combined with concentrations, reflect the

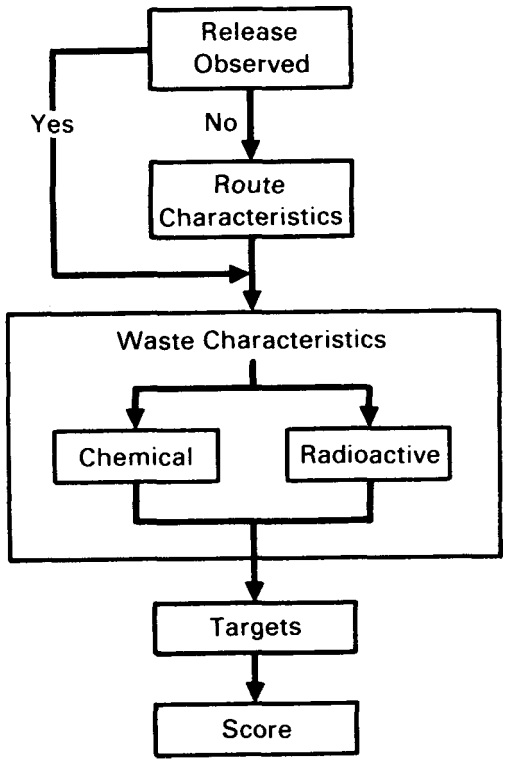

FIGURE 2.3. Modified HRS Logic Diagram (After Whelan et al. 1985)

relative maximum potential dose and, therefore, risk to man that could result from releases of the radionuclides into the environment.

Although these modifications to the HRS alleviate its major limitations in assessing radioactive sites, the mHRS still retains many of the limitations inherent in extremely simple ranking systems. Because of these CL/Q limitations, the HRS/mHRS cannot be used to prioritize sites based on their relative potential hazards. However, as a preliminary screening tool, the HRS/mHRS is useful for identifying those sites that may pose significant risk to human health, safety, and/or the environment.

Currently, DOE field offices are identifying those inactive hazardous waste disposal sites that may pose an unacceptable risk to health, safety, and the environment. Two ranking methodologies are used to identify and prioritize, according to risk, waste sites requiring further investigation. For identifying sites that may pose significant risk to health, safety, and/or the environment, DOE is using both the HRS and mHRS methodologies. The sites are then classified into one of two groups: those that may and those that do not pose a potential risk to the surrounding environment. For those sites that do not pose a potential risk to the surrounding environment, no further evaluation is required. Those sites that may pose a significant potential risk can be further evaluated and prioritized according to their potential risk (in a relative sense) by the RAPS methodology. Figure 2.4 illustrates the utility of integrating the HRS/mHRS methodologies with the RAPS methodology.

2.3 REMEDIAL ACTION PRIORITY SYSTEM

The RAPS methodology uses empirically, analytically, and semianalytically based mathematical algorithms and a pathways analysis to predict the potential for contaminant migration from a waste site to important environmental receptors. Four major transport pathways for contaminant migration are considered in RAPS: subsurface (groundwater), overland, surface water, and atmospheric. Using the predictions of contaminant transport, simplified exposure assessments are performed for important receptors. The risks associated with the sites are then calculated relative to other sites for all pathways of concern.

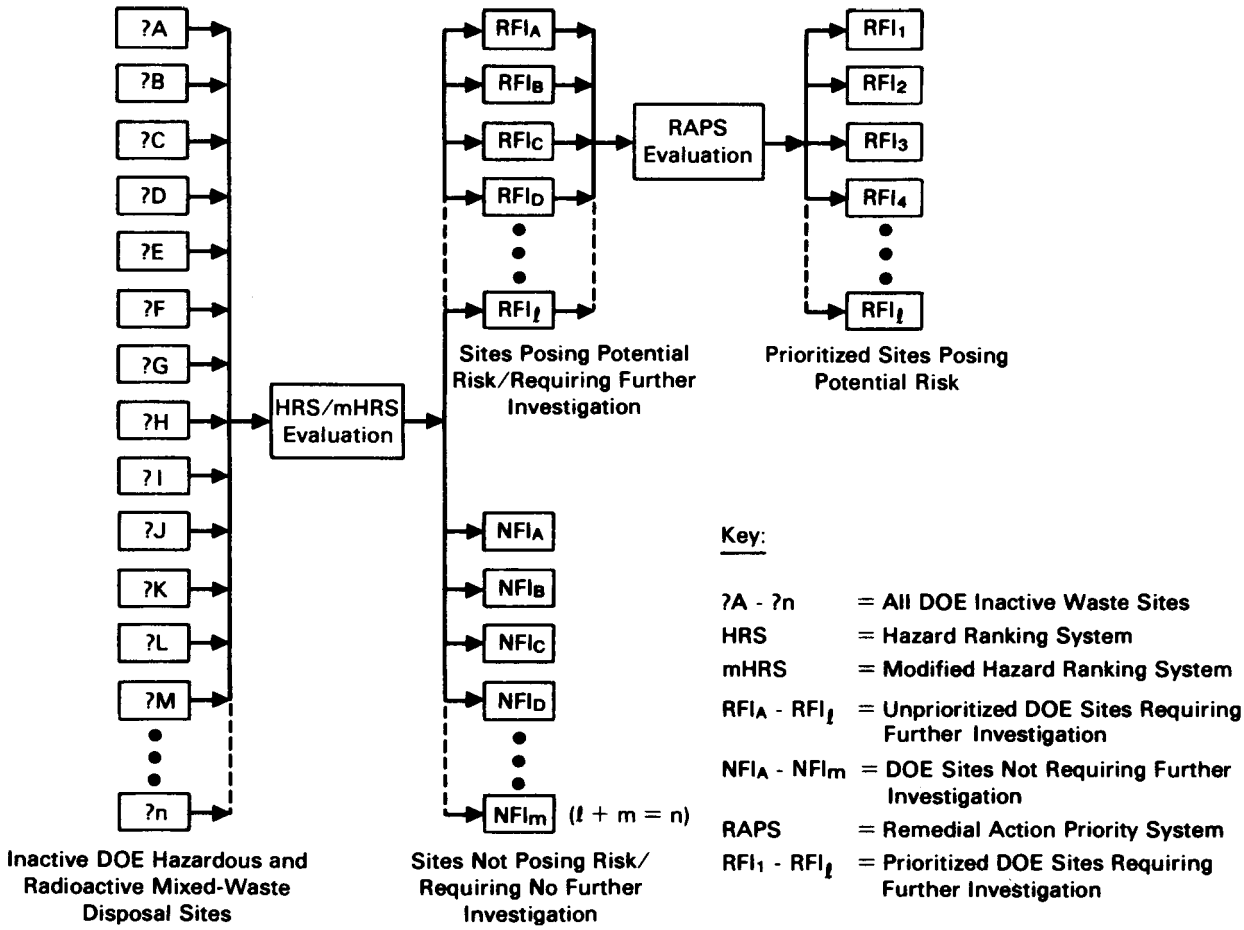

FIGURE 2.4. Utility of the HRS/mHRS and RAPS Methodologies in Locating, Identifying, and Prioritizing Sites Posing a Potential Risk to the Surrounding Environment (After Steelman and DeCarlo 1985)

Based on input data that are readily available at DOE facilities, the RAPS methodology considers 1) specific site information and constituent characteristics associated with the pathways; 2) chemical (certain organic and inorganic) and radioactive wastes; 3) the potential direction of contaminant movement; 4) contaminant mobility, dispersion, and decay/degradation, where applicable; 5) contaminant toxicities; 6) population distributions; 7) various routes or types of exposure (e.g., inhalation, ingestion, dermal contact, and external dose); 8) time until a population is exposed or exposure begins (i.e., time of contaminant arrival); and 9) duration of exposure (i.e., the length of time a population is continually exposed to a contaminant). Time of contaminant arrival and duration of exposure are critical considerations in a site

prioritization; the sooner a population is exposed, the greater the urgency for site characterization and possible remediation. Likewise, the longer a population is exposed to a contaminant the greater the potential severity of that exposure. Consideration of both of these factors is absent from more simplified ranking methodologies.

2.3.1 Structure of RAPS

Structurally, the RAPS methodology is based on the pseudocompositely coupled multimedia modeling approach. Although modular components of the methodology have been chosen a priori by the code developers (e.g., fully coupled approach), RAPS does not allow its components to spacially and temporally interact (i.e., two-way data transfer), as it is designed along lines similar to the compositely coupled approach (i.e., use of independent modules, unidirectional transfer of information, and ease of updating and replacing components as the state of the art advances). Each transport pathway addressed by RAPS has a set of codes that describe the migration and fate of contaminants. These transport pathway codes are systematically integrated with an exposure assessment component that considers the type, time, and duration of exposure and the location and size of the population exposed. Figure 2.5 presents a simplified diagram outlining the various pathways and their interactions, as considered by the RAPS methodology.

To implement the methodology at a site, the user designates the appropriate transport pathways by identifying the path [i.e., route(s)] the contaminants may take from the waste site through the various media. The user is then prompted to supply site and constituent (i.e., contaminant) information. Based on these data, the migration and fate of the contaminants are simulated from the source through the designated transport pathways to important environmental receptors. The exposure route to the population is integrated into the analysis, and the subsequent risk [i.e., the Hazard Potential Index (HPI)] to the population is computed for the site. The site HPI is compared to HPIs at other sites that have been previously analyzed. The sites are then objectively ranked in order of increasing risk, according to the HPI for each site.

The HPI is a parameter that reflects the results of the multimedia transport calculations, the exposure assessment, and the effects of an exposure to a

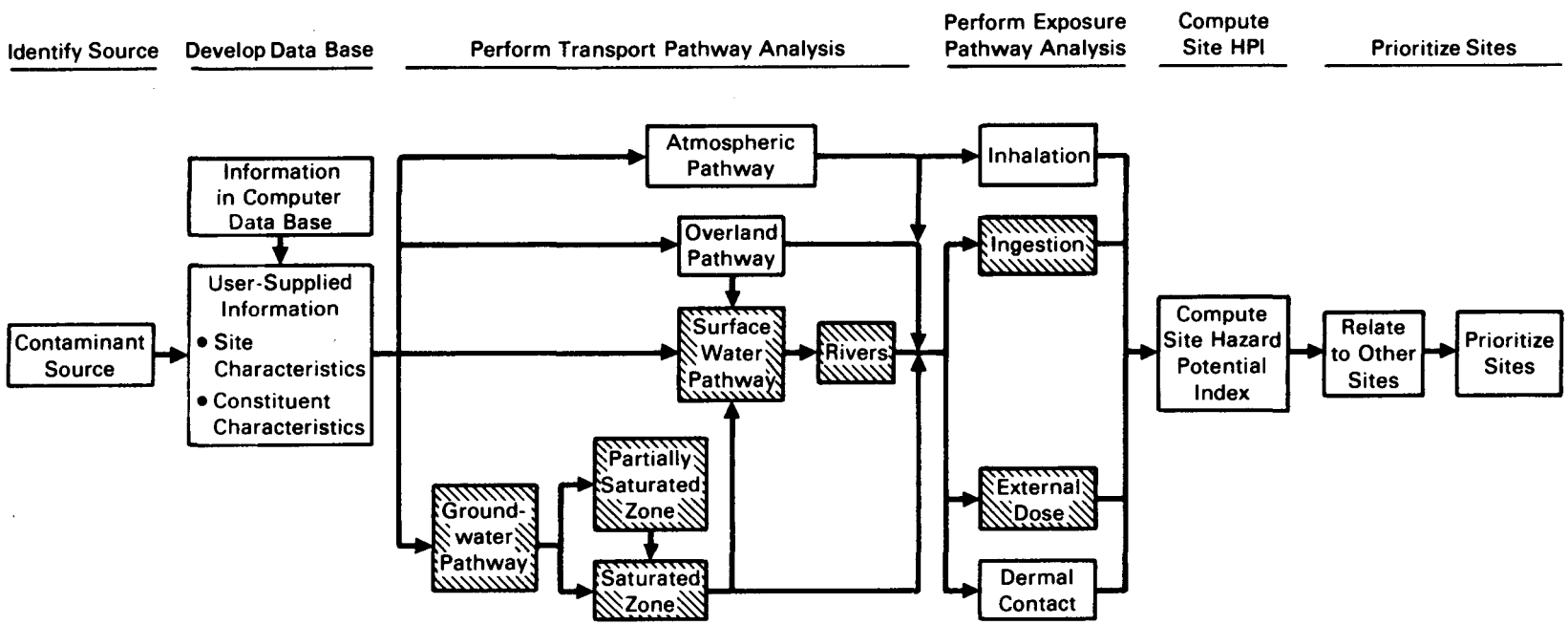

FIGURE 2.5. Simplified Diagram Outlining the Interactions Between the Transport Pathways and Exposure Assessment Components of the RAPS Methodology (Shaded boxes indicate a potential contaminant transport and exposure route using the RAPS methodology) (After Whelan et al. 1986)

population of concern. It directly considers contaminant levels that reflect persistence and mobility at important receptors, population distributions, contaminant toxicity, routes and levels of exposure, duration of exposure, and the time until a population is exposed. It is also based on scientifically accepted dose-health effects relationships. The HPI is used as a relative marker for quantitatively comparing the potential for the migration, fate, and effects of hazardous substances. By itself, an HPI does not indicate the absolute risk at a site but does indicate whether one site potentially presents a higher risk to surrounding receptors of concern than another site. The HPI is discussed in greater detail in Chapter 9.0.

The shaded boxes in Figure 2.5 illustrate an example application of the RAPS methodology. According to this example, leachate leaves the waste site and enters the groundwater pathway, travels through the partially saturated zone, enters and travels through the saturated zone, leaves the groundwater pathway and enters the surface water pathway, and migrates through a nearby river. At designated usage locations, the population is externally exposed to contaminants of concern and, in addition, ingests a portion of the contaminated river water. An HPI is computed based on the exposure to the population and is compared to HPIs for other sites to prioritize the site, relative to others, based on relative risk.

2.3.2 RAPS Solute Transport Pathways and Exposure Assessment Component

As illustrated in Figure 2.5, four transport pathways and an exposure component are addressed by the RAPS framework. For each pathway, contaminant retardation is described, where applicable, by an equilibrium (i.e., partition or distribution) coefficient. First-order degradation/decay is assumed for all contaminants that do not result in toxic decay products (e.g., radionuclides).

For contaminants that decay, the parent contaminants are initially treated as conservative substances (i.e., no decay products or degradation). Upon reaching the environmental receptor, radiological decay is corrected in a separate calculation, and the code subsequently computes the temporal distribution of each decay product. The Bateman equation is then used to calculate the concentrations of all important decay products in the chain (Bateman 1910, as

reported by Codell et al. 1982). The approach for analyzing each of the pathways considered in RAPS is briefly discussed below.

2.3.2.1 Groundwater Pathway

The quantity of leachate likely to be generated during the operational lifetime of an inactive hazardous waste facility is a major factor controlling the degree to which a site will require analysis. The site leachate quantity is controlled by local meteorologic, geologic, and hydrologic conditions and the design and operation of the facility. Given the limited availability of literature data on leachate quantities generated by sites with contaminated soils (e.g., inactive landfills), available estimation techniques are used to quantify the leachate.

A modified method of that proposed by Thornthwaite and Mather (1955, 1957), Fenn et al. (1975), and Dass et al. (1977) is currently under consideration for computing leachate quantities from contaminated soils. The methodology is based on a water-budget analysis; it estimates the quantity of leachate produced at a given site with contaminated soils and involves a water-balance calculation, using monthly estimates of precipitation, potential evapotranspiration, temperature, and runoff. The principal source of moisture is precipitation (rainfall and snowfall) over the site. Of the precipitation that falls on a site, a portion runs off, some is lost to evapotranspiration, and the remainder percolates through the soil or waste. Water that percolates through the fill eventually exits as leachate. Simpler methods have been proposed (e.g., Knight et al. 1980); however, these methods are not nearly as precise. More complex methods also have been proposed and developed (e.g., ICF 1984; Schroeder et al. 1984), but their complexity precludes their use in a preliminary ranking system scheme. A review of the mathematical algorithms that describe the technique for computing leachate quantities from landfills is given in Chapter 3.0.

The RAPS methodology is being developed to address long-term average environmental conditions resulting from the release of contaminants from an inactive hazardous waste site. Because the analyses are performed assuming no changes to current land use, groundwater, or surface water practices (such as remedial actions to the waste or population changes), the potential health

exposure associated with the migration and fate of contaminants from a waste site may continue for hundreds to thousands of years, particularly for the groundwater transport pathway. At this time, the exposure analysis component of RAPS is, therefore, based on 70-year increments (i.e., approximately one human life span), with average concentrations defined for each increment.

Contaminants exiting the bottom of the contaminated soils, landfill, or pond migrate through a partially saturated or saturated groundwater zone. In the partially saturated zone, flow is usually assumed to be in a vertical direction. Because this flow is generally unidirectional, one-dimensional modeling is performed. The RAPS methodology uses a one-dimensional, unsteady, semianalytical code to simulate contaminant leaching and movement through the partially saturated zone. The solution algorithm to the advective-dispersive equation is based on homogeneous and isotropic soil parameters (see Van Genuchten and Alves 1982; Donigian et al. 1983b). The partially saturated soil beneath the waste site is assumed at a unit potential hydraulic gradient. The moisture content is assumed to fluctuate between field capacity and saturation. If the percolation rate (leach rate) from the waste site is less than the soil transmission rate, as described by the general equation for liquid flow in the partially saturated zone (see Hanks and Ashcroft 1980; Hillel 1980), the leachate moves through the soil at the percolation rate. For an percolation rate equal to or greater than the transmission rate, the leaching water is assumed to move at the transmission rate, as is the case for ponded wastes.

The predominant movement of the leachate in the saturated zone is assumed to be in the direction of the groundwater flow. A three-dimensional advective-dispersive equation describes the migrating plume as it disperses and attenuates through the saturated aquifer. Advection represents the transport of solute caused by the mass motion of water, while dispersion represents solute transport by unaccounted variations in the fluid velocity and molecular motion. Dispersion is considered in the longitudinal, lateral, and vertical directions. Soil properties are assumed to be homogeneous, and the flow is assumed steady and only in the longitudinal direction.

Solutions for the advective-dispersive equations for the partially saturated and saturated zones have been formulated in terms of an instantaneous contaminant release (i.e., a pulse release over zero time). The RAPS methodology generalizes these solutions for arbitrary time-varying releases by convoluting response functions (i.e., temporally varying contaminant leach or flow rates) with instantaneous contaminant release solutions.

The RAPS groundwater component computes contaminant levels at wells and at the edge of streams and calculates solute fluxes from the groundwater environment to the surface water environment. The solution algorithms are based on Green's functions and have been reported by several researchers (e.g., Codell et al. 1982; Yeh 1981; Van Genuchten and Alves 1982). Figure 2.5 illustrates the potential interactions between the groundwater pathway and the other environmental transport pathways addressed by the RAPS methodology. A preliminary review of the mathematical algorithms describing the groundwater pathway is presented in Chapter 5.0.

2.3.2.2 Surface Water Pathway

Of the many possible surface water components (e.g., nontidal rivers, estuaries, lakes, open coasts, reservoirs, impoundments, etc.), RAPS is currently capable of addressing nontidal rivers. Nontidal rivers refer to freshwater bodies with unidirectional flow in definable channels. Because the RAPS methodology is compositely coupled, other surface water pathways can be added when deemed necessary.

At many sites, the temporal distribution associated with the release of contaminants to the surface water environment is longer than the near-field residence time of the contaminant in the surface water. In addition, the current application of the exposure component of RAPS bases its health effects calculations on lifetime dose. Because of these reasons, the current version of the surface water component of the RAPS methodology was not designed to take into account releases over relatively "short" time periods. Because transient solutions for contaminant migration and fate calculations are most applicable for batch and infrequent releases over relatively short periods of time (Codell et al. 1982), steady-state solutions to the advective-dispersive equation are

most applicable for the long-term assessments addressed by RAPS. The three-dimensional, steady-state, vertically integrated mass balance equation for contaminant transport in a riverine environment (where longitudinal advection dominates longitudinal dispersion) forms the basis for all surface water solution algorithms (Codell et al. 1982). Contaminants released into a surface water body are transported through the system by the processes of advection and dispersion. Dispersion is considered in the longitudinal and lateral directions. A description of contaminant movement is based on steady, unidirectional flow in a straight, rectangular channel. Figure 2.5 illustrates the potential interactions between the surface water pathway and the other environmental transport pathways addressed in RAPS. A review of the mathematical algorithms describing the surface water pathway is presented in Chapter 6.0.

2.3.2.3 Overland Pathway

Overland flow is that portion of precipitation that ultimately appears as flowing water on the ground surface; it occurs primarily because of rainfall or snowmelt in excess of abstraction demands (i.e., interception, evapotranspiration, infiltration, etc.) and/or the emergence of soil water into drainage pathways. The overland component of the RAPS methodology has two functions.

First, results from the overland assessment are used in computing leachate quantities percolating from a nonponded waste site (e.g., see Section 2.3.2.1). This component estimates long-term, average monthly runoff volumes for use in the water-balance calculations for estimating leach quantities. These calculations are based on monthly average precipitation events.

Second, the overland component estimates the migration and fate of contaminated water and sediment that moves from contaminated surface soils (e.g., exposed wastes at unprotected landfills and soils contaminated through atmospheric wet and dry deposition). Because the majority of soil loss at a site is traditionally transported by overland runoff from precipitation events larger than the monthly average, these calculations are based on events with higher return periods (e.g., higher intensity and larger volume).

The algorithms used in computing the volume of overland flow are based on data that are easily attainable. Estimation techniques are based on the curve

number technique of the U.S. Department of Agriculture's Soil Conservation Service (SCS), as presented by SCS (1972, 1982), Kent (1973), USBR (1977), and Haun and Barfield (1978). The SCS curve number technique incorporates into its computations soil classifications, soil cover, land use treatment or practice, hydrologic condition for infiltration, locale (i.e., location within the United States), initial moisture abstraction, antecedent moisture conditions, and potential maximum moisture retention. The algorithms are empirically based and represent a method of estimating direct runoff volumes from storms.

The driving mechanism transporting contaminants through the overland pathway is overland flow. Many of the characteristics describing the watershed and hazardous waste sites are used in computing overland water and sediment movement and subsequent contaminant transport. If an unlimited supply of contamination were available for transport, then the overland flow rate would control the mass flux of contaminant moving downgradient. As the flow rate increases, the potential for increasing the contaminant mass flux would also rise.

The movement of contaminated sediments from the waste site is described by the Universal Soil Loss Equation (USLE). The USLE is an empirically derived formula that is based on 10,000 plot-years of erosion field research data. The USLE considers 1) the erosive force and intensity of precipitation and runoff in a normal year, 2) the susceptibility of soil particles to detachment and transport by precipitation and runoff, 3) the combined effects of slope length and gradient, and 4) the soil loss from lands under varying vegetative conditions (Goldman et al. 1986). It provides average-annual sediment loss from field-sized plots. This standard method and subsequent modified versions have been recommended and used over the last 30 years by numerous researchers (e.g., Goldman et al. 1986; Mills et al. 1985; Riggins and Bandy 1981; Novotny and Chesters 1981; Whelan 1980; Mitchell and Bubenzer 1980; Wischmeier and Smith 1958, 1978; Onstad et al. 1977; Foster 1976; Williams and Bernt 1976; Kuh et al. 1976; Onstad and Foster 1975; Stewart et al. 1975; Meyer 1974; Foster and Wischmeier 1973).

For locations with known contaminated sediment producing runoff events, a modified version of the USLE can be used. This USLE version, when combined

with overland flow computations using the method of characteristics and kinematic wave approximation, will be able to estimate sediment loss from a field-sized plot for each precipitation event (see Onstad and Foster 1975; Foster et al. 1977). The method of characteristics defines the path of wave propagation along which partial differential equations become ordinary differential equations with analytic solutions. Use of the method of characteristics has been illustrated by Eagleson (1970), Hjelmfelt (1976), Witinok (1979), Whelan (1980), and Witinok and Whelan (1980).

As Figure 2.5 indicates, the overland transport pathway can interact with the surface water pathway or directly supply the exposure assessment component with contaminant levels for computing the site HPI. A review of the mathematical algorithms describing the overland pathway is presented in Chapter 4.0.

2.3.2.4 Atmospheric Pathway

Complex phenomena are associated with the migration and fate of contaminants released to the atmosphere (Cupitt 1980). The atmospheric component of the RAPS methodology considers release mechanisms and characteristics, dilution and transport, washout by cloud droplets and precipitation, and deposition on the underlying surface cover. The atmospheric pathway model provides a realistic computation of these processes within the constraints of using limited, readily available site information.

The prediction of contaminant movement through the atmospheric pathway involves the use of codes that address atmospheric suspension/emission, transport, diffusion, and deposition. Input to the codes includes site-specific climatologic information such as wind direction, wind speed, and precipitation. Output from the models consists of average air and surface contaminant levels that are then used as input to the exposure assessment component. Currently, contaminant transport is assumed to occur sufficiently fast that chemical transformations can be neglected. The validity of this assumption needs to be confirmed for the various contaminants that exist at DOE inactive hazardous waste sites.

The atmospheric pathway is modeled in a manner to maximize the validity of comparisons between sites. The suspension/emission rates are based mainly on

empirical relationships using site characteristics. The atmospheric transport and dispersion are computed in terms of sector-averaged values using Gaussian dispersion principles similar to those proposed by Busse and Zimmerman (1973) and examined by Culkowski (1984). Deposition is computed as the sum of outputs from empirical wet and dry deposition algorithms described in Van Voris et al. (1984).

The relative importance of the atmospheric pathway between different sites is controlled by a combination of geographic and climatic influences. Distances, directions, winds, and atmospheric stability are controlling parameters. The dispersion relationships used in the atmospheric component depend on local site characteristics (Pasquill and Smith 1983). Because the dispersion is a strong function of downwind distance from the source, the physical distances between the contaminant sites and population centers are of prime importance. The relative proximities of sites and population centers are important in terms of the local frequencies of wind directions, particularly in areas with topographic channeling of winds. The relative rates of atmospheric dilution between the sites are mainly a function of local wind speeds and atmospheric stability parameters.

In the operational mode, the atmospheric pathway component computes contaminant levels as a function of the direction and distance that coincides with population centers surrounding the site. Inhalation represents the major route of exposure to contaminants via the atmospheric pathway. RAPS also considers the ingestion route of exposure through the food chain and from wet and dry deposition on vegetation and subsequent ingestion of contaminated food materials derived from the soils. In addition, external dose can be addressed, although its effects are usually insignificant as compared to the inhalation exposure route. The interaction and coupling between the atmospheric pathway and exposure assessment components of the RAPS methodology are illustrated in Figure 2.5. A preliminary review of the mathematical algorithms describing the atmospheric pathway is presented in Chapter 7.0.

2.3.2.5 Exposure Assessment Component

Results from each of the four transport pathways are used in the exposure assessment component to calculate the HPI for each important waste-site contaminant. The exposure assessment component considers potential exposure of the surrounding population through the following exposure routes: 1) external dermal contact to chemicals; 2) external dose from radiation; 3) inhalation of airborne contaminants; and 4) ingestion of contaminated drinking water, soil, crops, animal products, and aquatic foods. In evaluating the HPI values, the important exposure routes and populations at risk are first defined. Then, based on the air, water, and soil contaminant levels provided by the transport pathway analyses, an estimate is made of the average daily human exposure to each contaminant. Estimation of the daily exposure is based on simple multiplicative models describing the transfer of pollutants from air, water, or soil to humans. The daily exposure rate is next converted to an average individual risk factor using mathematical codes for radionuclides, carcinogenic chemicals, and noncarcinogenic chemicals. The risk factor is intended to indicate the level of potential health impact to an average member of the exposed population. For radionuclides, the risk factor is based on cancer risk estimates of the National Academy of Sciences Committee on the Biological Effects of Ionizing Radiation (NAS 1980). The risks from chemical carcinogens are currently based on cancer potency factors defined by the EPA (1982b). Risk estimates for noncarcinogenic chemicals are based on reference dose levels (RfD), as defined by the EPA.

One of the key features of the exposure assessment component is the estimation of the average exposure. The exposure modes included in RAPS are as follows:

- drinking-water ingestion -- For groundwater, overland, and surface water transport pathways. Factors may be applied to the water concentration to account for purification of the water in a treatment plant.
- aquatic food ingestion (fish and invertebrates) -- For overland, surface water, and groundwater transport pathways. Average daily intake is estimated using bioconcentration factors and average daily ingestion rates for aquatic foods.

- crops -- For all transport pathways. Crops may be contaminated from irrigation with contaminated water or by direct deposition onto plants and soil. Two crop types are considered: leafy vegetables with the edible portion subject to direct deposition and other crops such as root and pod vegetables and fruit. Crop concentrations are estimated using soil-to-plant transfer factors and air-to-edible-plant transfer factors. Average daily intake is estimated using average daily ingestion rates for vegetables and leafy vegetables.

- animal product -- For all transport pathways. Contaminated animal products result from animal ingestion of contaminated water and contaminated feed. Feed contamination may occur from direct deposition onto feed crops or pasture from air or through use of contaminated irrigation water. Use of contaminated animal drinking water is only considered for the three water transport pathways (i.e., overland, groundwater, and surface water). The concentration of contaminant in animal meat and milk is estimated using animal ingestion to animal product transfer factors. Average daily intake of exposed individuals is estimated using average daily ingestion rates for meat and milk.

- water immersion (domestic bathing and swimming) -- For groundwater and surface water transport pathways. Dermal contact (for chemicals) and radiation exposure are included for domestic bathing for both water transport pathways. Inhalation of volatile organics during showering with groundwater is also included. Exposure from swimming in contaminated water is considered for the surface water pathway. For chemicals, an equivalent daily intake amount is estimated based on dermal contact time and absorption characteristics of the chemical pollutant. For radiation exposures, the dose from immersion in water is estimated using dose conversion factors. A contribution to radiation dose may also be included for recreational boating and shoreline fishing.

- soil ingestion -- For the atmospheric transport pathway. Contaminated soil is assumed to be ingested each day with the ingestion rate based on a lifetime average.

- inhalation -- Atmospheric transport pathway. The daily average intake is estimated using an average inhalation rate for the exposed population.

The interaction and coupling between the exposure assessment component and the transport pathways of the RAPS methodology are illustrated in Figure 2.5. Reviews of the mathematical algorithms describing the exposure and health effects assessments are presented in Chapters 8.0 and 9.0, respectively.

2.4 SUMMARY

When fully developed, RAPS will prioritize inactive hazardous waste sites in a scientific and objective manner based on limited site information. The RAPS methodology is more sophisticated than more simplistic CL/Q methods and bases its approach on site and constituent (i.e., chemical and radionuclide) characteristics. The RAPS methodology requires minimum user knowledge of risk assessment and the least possible amount of required input data. It takes into consideration four major transport pathways for contaminant migration: groundwater, overland, surface water, and atmospheric. Each pathway is described by empirically, analytically, and/or semianalytically based mathematical algorithms with the results being expressed as the dimensionless parameter (modified according to constituent toxicity and human exposure) called the Hazard Potential Index (HPI). The risks of a site, based on HPIs, are calculated relative to the risks of other sites for each pathway and for all pathways together; sites are then ranked and identified for additional site investigation and possible remediation.

2.5 REFERENCES

Aller, L., T. Bennett, J. H. Lehr and R. J. Petty. 1985. DRASTIC: A Standardized System for Evaluating Ground Water Pollution Potential Using Hydrogeologic Settings. EPA/600/2-85/018. Prepared by the National Water Well Association for the Robert S. Kerr Environmental Research Laboratory, U.S. Environmental Protection Agency, Ada, Oklahoma.

Baes, C. F., C. L. Begovich, W. M. Culkowski, K. R. Dixon, D. E. Fields, J. T. Holdeman, D. D. Huff, D. R. Jackson, N. M. Larson, R. J. Luxmoore, J. K. Munro, M. R. Patterson, R. J. Raridon, M. Reeves, O. C. Stein, J. L. Stolzy and T. C. Tucker. 1976. "The Unified Transport Model." In Ecology and Analysis of Trace Contaminants Progress Report October 1974 - December 1975, eds. R. I. Van Hook and W. D. Shults. ORNL/NSF/EATC-22, pp. 13-62.

Bateman, H. 1910. "The Solution of a System of Differential Equations Occurring in the Theory of Radioactive Transformations." Proc. Cambridge Philos. Soc. 16:423-427.

Bolten, J. G., P. F. Morrison and K. A. Soloman. 1983. Risk-Cost Assessment Methodology for Toxic Pollutants from Coal-Fired Power Plants. WD-1589 EPRI RP1826-5, Electric Power Research Institute, Palo Alto, California.

Busse, A. D., and J. R. Zimmerman. 1973. User's Guide for the Climatological Dispersion Model. EPA-RA-73-024, U.S. Environmental Protection Agency, Research Triangle Park, North Carolina.

Codell, R. B., K. T. Key and G. Whelan. 1982. A Collection of Mathematical Models for Dispersion in Surface Water and Groundwater. NUREG-0868, Office of Nuclear Reactor Regulation, U.S. Nuclear Regulatory Commission, Washington, D.C.

Culkowski, W. M. 1984. An Initial Review of Several Meteorological Models Suitable for Low-Level Waste Disposal Facilities. NUREG/CR-3838, U.S. Nuclear Regulatory Commission, Washington, D.C.

Cupitt, L. T. 1980. Fate of Toxic and Hazardous Materials in the Air Environment. EPA-600/3-80-084, U.S. Environmental Protection Agency, Research Triangle Park, North Carolina.

Dass, P., G. R. Tamke and C. M. Stoffel. 1977. "Leachate Production at Sanitary Landfills." J. Environ. Eng. Div. Proc. ASCE 103(EE6).

DOE. 1985. Comprehensive Environmental Response Compensation, and Liability Act Program. DOE Order 5480.14, U.S. Department of Energy, Washington, D.C.

Donigian, A. S., Jr., J. C. Imhoff, B. R. Bicknell, J. L. Baker, D. A. Haith and M. F. Walter. 1983a. Application of Hydrologic Simulation Program - FORTRAN (HSPF) in Iowa Agricultural Watersheds. EPA-600/S3-83-069, U.S. Environmental Protection Agency, Athens, Georgia.

Donigian, A. S. Jr., T. Y. R. Lo and E. W. Shanahan. 1983b. Rapid Assessment of Potential Groundwater Contamination Under Emergency Response Conditions. U.S. Environmental Protection Agency, Athens, Georgia.

Eagleson, P. S. 1970. Dynamic Hydrology. McGraw-Hill, New York.

EPA. 1982a. "Appendix A - Uncontrolled Hazardous Waste Site Ranking System: A User's Manual." U.S. Environmental Protection Agency, 37(137) Fed. Reg. 31219-31243 (July 16, 1982).

EPA. 1982b. Health Effects Assessment Summary for 300 Hazardous Organic Constituents. Environmental Criteria and Assessment Office, U.S. Environmental Protection Agency, Cincinnati, Ohio.

EPA. 1984. Uncontrolled Hazardous Waste Site Ranking System, a User's Manual (HW-10). U.S. Environmental Protection Agency, Washington, D.C.

EPA. 1986. "Hazardous Waste Management System Land Disposal Restrictions; Proposed Rule." Part III. U.S. Environmental Protection Agency, 40 CFR (260) Fed. Reg. 1601-1766 (January 14, 1986).

Fenn, D. G., K. J. Hanley and T. V. DeGeare. 1975. Use of the Water Balance Method for Predicting Leachate Generation from Solid Waste Disposal Sites. SW-168, U.S. Environmental Protection Agency, Washington, D.C.

Fletcher, J. F., and W. L. Dodson. 1971. Hermes-A Digital Computer Code for Estimating Regional Radiological Effects from the Nuclear Power Industry. USAEC Rep. HEDL-TME-71-1968.

Fletcher, J. F., W. L. Dodson, D. E. Peterson and R. P. Betson. 1973. "Modeling the Regional Transport of Radionuclide in a Major United States River Basin." In Environmental Behavior of Radionuclide Released in the Nuclear Industry. IAEA, Vienna.

Foster, G. R. 1976. "Sediments, General: Reporter's Comments." In Proceedings of the National Symposium on Urban Hydrology, Hydraulics, and Sediment Control, pp. 129-138, University of Kentucky, Lexington, Kentucky, July 26-29, 1976.

Foster, G. R., and W. H. Wischmeier. 1973. Evaluating Irregular Slopes for Soil Loss Prediction. Trans. ASAE (Am. Soc. Agric. Eng.) 17.

Foster, G. R., L. D. Meyer and C. A. Onstad. 1977. "An Erosion Equation Derived from Basic Erosion Principles." Trans. ASAE (Am. Soc. Agric. Eng.) 20:678-682.

Goldman, S. J., K. Jackson and T. A. Bursztynsky. 1986. Erosion and Sediment Control Handbook. McGraw-Hill, New York.

Hanks, R. J., and G. L. Ashcroft. 1980. Applied Soil Physics. Springer-Verlag, New York.

Haun, C. F., and B. J. Barfield. 1978. "Hydrology and Sedimentology of Surface-Mined Lands." University of Kentucky, Lexington, Kentucky.

Hawley, K. A., and B. A. Napier. 1984. "A Ranking System for Mixed Radioactive and Hazardous Waste Sites." In Proceedings of the Fifth DOE Environmental Protection Information Meeting, CONF-841187, U.S. Department of Energy, Washington, D.C.

Hawley, K. A., R. A. Peloquin and R. D. Stenner. 1986. Modified Hazard Ranking System for Sites with Mixed Radioactive and Hazardous Wastes -- User Manual. PNL-5841, Pacific Northwest Laboratory, Richland, Washington.

Hillel, D. 1980. Fundamentals of Soil Physics. Academic Press, New York.

Hjelmfelt, A. T. Jr. 1976. Modeling of Soil Movement Across a Watershed. Completion Report for Project A-076-MO, Missouri Water Resources Center, University of Missouri, Columbia, Missouri.

HWN. September 17, 1984. 6(37)290. Hazardous Waste News. Business Publishers, Silver Spring, Maryland.

ICF. 1984. The Risk-Cost Analysis Model: Phase III Report. Prepared by ICF, Inc., for the Office of Solid Waste, Economic Analysis Branch, U.S. Environmental Protection Agency, Washington, D.C.

Johanson, R. C., J. C. Imhoff and H. H. Davis, Jr. 1980. User's Manual for Hydrologic Simulation Program - FORTRAN (HSPF). EPA-600/9-80-015, U.S. Environmental Protection Agency, Athens, Georgia.

Kent, K. M. 1973. A Method for Estimating Volume and Rate of Runoff in Small Watersheds. SCS-TP-149, U.S. Department of Agriculture, Soil Conservation Service, Washington, D.C.

Knight, R. G., E. H. Rothfuss and K. D. Yard. 1980. FGD Sludge Disposal Manual. 2nd ed. EPRI CS-1515, Electric Power Research Institute, Palo Alto, California.

Kuh, H., D. L. Raddell and E. A. Hiler. 1976. Two-Dimensional Model of Erosion from a Watershed. Paper 76-2539. American Society of Agricultural Engineers, St. Joseph, Michigan.

Kufs, C., D. Twedell, S. Paige, R. Wetzel, P. Spooner, R. Colonna and M. Kilpatrick. 1980. "Rating the Hazard Potential of Waste Disposal Facilities." In Proceedings on the Management of Uncontrolled Hazardous Waste Sites, U.S. Environmental Protection Agency National Conference. Hazardous Materials Control Research Institute, Washington, D.C.

LeGrand, H. E. 1983. A Standardized System for Evaluating Waste-Disposal Sites. 2nd ed. National Water Well Association, Worthington, Ohio.

Meyer, L. D. 1974. "Overview of the Urban Erosion and Sedimentation Processes." In Proceedings of the National Symposium on Urban Rainfall and Runoff and Sediment Control, University of Kentucky, Lexington, Kentucky, July 29-31, 1974.

Mills, W. B., D. B. Porcella, M. J. Ungs, S. A. Gherini, K. V. Summers, L. Mok, G. L. Rupp and G. L. Bowie. 1985. WATER QUALITY ASSESSMENT: A Screening Procedure for Toxic and Conventional Pollutants in Surface and Groundwater. Vols. I and II. EPA/600/6-85/002. NTIS PB86-12249 6, U.S. Environmental Protection Agency, Athens, Georgia.

Mitchell, J. K., and G. D. Bubenzer. 1980. "Oil Loss Estimation." In Soil Erosion, p. 312, eds. M. J. Kirby and R. P. C. Morgan. Wiley, New York.

NAS. 1980. "The Effects on Populations of Exposure to Low Levels of Ionizing Radiation." National Academy of Sciences Committee on the Biological Effects of Ionizing Radiations, National Research Council, Washington, D.C.

Novotny, V., and G. Chesters. 1981. Handbook of Nonpoint Pollution. Van Nostrand Reinhold, New York.

Onishi, Y., S. M. Brown, A. R. Olsen and M. A. Parkhurst. 1981. "Chemical Migration and Assessment Methodology." In Proceedings of the Conference on Environmental Engineering, American Society of Civil Engineers, Atlanta, Georgia.

Onishi, Y., S. M. Brown, A. R. Olsen, M. R. Parkhurst and S. E. Wise. 1979. Assessment Methodology for Overland and Instream Migration and Risk Assessment of Pesticides. Battelle, Pacific Northwest Laboratories, Richland, Washington.

Onishi, Y., G. Whelan, M. A. Parkhurst, A. R. Olsen and P. J. Gutknecht. 1980. Preliminary Assessment of Toxophene Migration and Risk in the Yazoo River Basin, Mississippi. Battelle, Pacific Northwest Laboratories, Richland, Washington.

Onishi, Y., G. Whelan and R. L. Skaggs. 1982a. Development of a Multimedia Radionuclide Exposure Model for Low-Level Management. PNL-3370, Pacific Northwest Laboratory, Richland, Washington.

Onishi, Y., S. B. Yabusaki, C. R. Cole, W. E. Davis and G. Whelan. 1982b. Multimedia Contaminant Environmental Exposure Assessment (MCEA) Methodology for Coal-Fired Power Plants. Vols. I and II. Battelle, Pacific Northwest Laboratories, Richland, Washington.

Onstad, C. A., and G. R. Foster. 1975. "Erosion Modeling over Watershed." Trans. ASAE (Am. Soc. Agric. Eng.) 18(2):288-292.

Onstad, C. A., C. K. Mutchler and A. J. Bowie. 1977. "Predicting Sediment Yields." In National Symposium on Soil Erosion and Sedimentation by Water. American Agricultural Engineers Proceedings, St. Joseph, Michigan, December 1977.

Parkhurst, M. A., G. Whelan, Y. Onishi and A. R. Olsen. 1981. Simulation of the Migration, Fate, and Effects of Diazinon in Two Monticello Stream Channels. Battelle, Pacific Northwest Laboratories, Richland, Washington.

Pasquill, F., and F. B. Smith. 1983. Atmospheric Diffusion. 3rd ed. Wiley, New York.

Patterson, M. R. 1986. "Unified Transport Model for Organics." In Proceedings of the First Workshop on Pollutant Transport and Accumulation in a Multimedia Environment, January 22-24, 1986, Los Angeles, California.

Patterson, M. R., J. K. Munro, D. E. Fields, R. D. Ellison, A. A. Brooks and D. D. Huff. 1974. A User's Manual for the Fortran IV Version of the Wisconsin Hydrologic Transport Model. ORNL-NSF-EATC-7, Oak Ridge National Laboratory, Oak Ridge, Tennessee.

Petrie, G. M., S. C. Sneider, B. A. Napier and J. C. Barnard. 1983. Simplified Codes for Performance Evaluation (SCOPE) of Radionuclide Transport: Version 1.0. PNL-4737, Pacific Northwest Laboratory, Richland, Washington.

Riggins, R. E. and J. T. Bandy. 1981. "R-Factor for Soil Loss Impact Prediction". J. Environ. Eng. Div., Proc. ASCE 107(EE4):851-857.

Schroeder, P. R., A. C. Gibson and M. D. Smolen. 1984. The Hydrologic Evaluation of Landfill Performance (HELP) Model. U.S. Environmental Protection Agency, Cincinnati, Ohio.

SCS. 1972. "Hydrology Guide for Use in Watershed Planning." SCS National Engineering Handbook, Section 4, Hydrology, Supplement A. U.S. Department of Agriculture, Soil Conservation Service, Washington, D.C.

SCS. 1982. SCS National Engineering Handbook, Section 4, Hydrology, 1982 Update. U.S. Department of Agriculture, Soil Conservation Service, Washington, D.C.

Silka, L. R., and T. L. Swearingen. 1978. A Manual for Evaluating Contamination Potential of Surface Impoundments. EPA 570/9-78-003, Groundwater Protection Branch, U.S. Environmental Protection Agency, Washington, D.C.

Steelman, B. L., and V. J. DeCarlo. 1985. "Management and Ranking of Department of Energy Radioactive Mixed-Waste Sites." In Transactions of the American Nuclear Society 1985 Winter Meeting, American Nuclear Society, La Grange Park, Illinois, November 10-14, 1985.

Stenner, R. D., R. A. Peloquin and K. A. Hawley. 1986. Modified Hazard Ranking System/Hazard Ranking System for Sites with Mixed Radioactive and Hazardous Wastes -- Software Documentation. PNL-6066. Prepared for the U.S. Department of Energy, Office of Environment, Safety, and Health, Washington, D.C.

Stewart, B. A., D. A. Woolhiser, W. H. Wischmeier, J. H. Caro and M. H. Frere. 1975. Control of Water Pollution from Croplands. Vols. I and II. EPA-600/2-75-026, U.S. Environmental Protection Agency, Washington, D.C.

Thornthwaite, C. W., and J. R. Mather. 1955. "The Water Balance." Publications in Climatology, Vol. VIII, No. 1. Drexel Institute of Technology, Laboratory of Climatology, Centerton, New Jersey.

Thornthwaite, C. W., and J. R. Mather. 1957. "Instructions and Tables for Computing Potential Evapotranspiration and the Water Balance." Publications in Climatology, Vol. X, No. 3. Drexel Institute of Technology, Laboratory of Climatology, Centerton, New Jersey.

Tucker, W. A., A. Q. Eschenroeder and G. C. Magill. 1984. Air Land Water Analysis System (ALWAS): A Multi-Media Model for Toxic Substances. EPA-600/S3-84-052, NTIS PB 84-171 743, U.S. Environmental Protection Agency, Athens, Georgia.

USBR. 1977. Design of Small Dams. U.S. Department of the Interior, Bureau of Reclamation, U.S. Government Printing Office, Washington, D.C.

Van Genuchten, M. T., and W. J. Alves. 1982. Analytical Solutions of the One-Dimensional Convective-Dispersive Solute Transport Equation. Technical Bulletin No. 1661, U.S. Department of Agriculture.

Van Voris, P., T. L. Page, W. H. Rickard, J. G. Droppo and B. E. Vaughan. 1984. Environmental Implications of Trace Element Releases from Canadian Coal-Fired Generating Stations, Phase II Final Report, Volume II, Appendix B and Appendix C. Contract No. 001G194, Battelle, Pacific Northwest Laboratories, Richland, Washington.

Whelan, G. 1980. Distributed Model for Sediment Yield. Master's Thesis, Iowa Institute of Hydraulic Research, University of Iowa, Iowa City, Iowa.

Whelan, G., and Y. Onishi. 1983. "In-Stream Contaminant Interaction and Transport." In Proceedings of the Tenth International Symposium on Urban Hydrology, Hydraulics, and Sediment Control, July 25-28, 1983, University of Kentucky, Lexington, Kentucky.

Whelan, G., and M. A. Parkhurst. 1983. "Simulation of the Migration, Fate and Effects of Diazinon In-Stream." In Proceedings of the D. B. Simons Symposium on Erosion and Sedimentation, July 27-29, 1983, Colorado State University, Fort Collins, Colorado.

Whelan, G., and B. L. Steelman. 1984. "Development of Improved Risk Assessment Tools for Prioritizing Hazardous and Radioactive Mixed-Waste Disposal Sites." In Proceedings of the Fifth DOE Environmental Protection Information Meeting, CONF-841187, U.S. Department of Energy, Washington, D.C.

Whelan, G., F. L. Thompson and S. B. Yabusaki. 1983. Multimedia Contaminant Environment Exposure Assessment Methodology as Applied to Los Alamos, New Mexico. PNL-4546, Pacific Northwest Laboratory, Richland, Washington.

Whelan G., B. L. Steelman, D. L. Strenge and J. G. Droppo. 1986. "Overview of the Remedial Action Priority System (RAPS)." In Pollutants in a Multimedia Environment, ed. Y. Cohen, pp. 191-227. Plenum Press, New York.

Whelan, G., B. L. Steelman, D. L. Strenge and K. A. Hawley. 1985. "Development of the Remedial Action Priority System: An Improved Risk Assessment Tool for Prioritizing Hazardous and Radioactive Mixed-Waste Disposal Sites." In Proceedings of Management of Uncontrolled Hazardous Waste Sites, November 4-6, 1985. Hazardous Materials Control Research Institute, Silver Spring, Maryland.

Whelan, G., S. M. Brown, D. L. Strenge, A. P. Schwab and P. J. Mitchell. 1987. Contaminant Assessment Modeling Under the Resource Conservation and Recovery Act. EA-5342. Electric Power Research Institute, Palo Alto, California.

Whelan, G., Y. Onishi, C. A. Simmons, T. W. Horst, S. K. Gupta, M. M. Orgill and C. A. Newbill. 1982. Multimedia Radionuclide Exposure Assessment Modeling. PNL-4545, Pacific Northwest Laboratory, Richland, Washington.

Williams, J. R., and H. D. Berndt. 1976. Sediment Yield Prediction Based on Watershed Hydrology. Paper No. 76-2535. American Society of Agricultural Engineers, St. Joseph, Michigan.

Wischmeier, W. H., and D. D. Smith. 1978. "Rainfall Energy and Its Relationship to Soil Loss." Trans. Am. Geophys. Union. 39(2):258-291.

Wischmeier, W. H., and D. D. Smith. 1978. Predicting Rainfall Erosion Losses: A Guide to Conservation Planning. Agricultural Handbook No. 537. U.S. Department of Agriculture, Washington, D.C.

Witinok, P. M. 1979. Distributed Watershed and Sedimentation Model. Master's Thesis, University of Iowa, Iowa City, Iowa.

Witinok, P. M., and G. Whelan. 1980. "Distributed Parameter Sedimentation Model." Proc. Iowa Acad. Sci. 87(3)103-111.

Yeh, G. T. 1981. AT123D: Analytical Transient One-, Two-, and Three-Dimensional Simulation of Waste Transport in the Aquifer System. Publications No. 1439, ORNL-5602, Oak Ridge National Laboratory, Oak Ridge, Tennessee.

3.0 PRECIPITATION-GENERATED LEACHATE AND OVERLAND RUNOFF VOLUME QUANTIFICATION

3.1 INTRODUCTION

Water from a precipitation event moves downward through the soil under the influence of gravity as long as there is a sufficient quantity to overcome the restraining forces of capillary hydraulic potential (i.e., matrix potential). Water is extracted from the partially saturated zone as surface evaporation and as transpiration by growing plant roots; together, these processes are called evapotranspiration. The rates of both extraction processes depend directly on available solar energy (i.e., heat radiation) and surface winds (Simmons and Gee 1981).

The process of water movement through a soil matrix is mechanistically complex (Simmons and Gee 1981). This passage of water is very dynamic and depends on detailed variations in the hydraulic properties of the water in the soil. Water storage by a soil profile is characterized by a water content distribution, which ultimately depends on the detailed spacial variability of hydraulic properties. Infiltrating water that exceeds the soil water-holding capacity will contribute to percolation (i.e., "deep" drainage); therefore, a single set of measured hydraulic properties cannot accurately represent an areal region (Simmons and Gee 1981).

This chapter presents a relatively simple methodology for estimating the fraction of precipitation (i.e., rainfall and snowmelt) that percolates (i.e., the portion of water that enters the soil minus evapotranspiration) into an inactive hazardous waste site and the fraction that is lost to overland runoff. A schematic diagram illustrating the movement of water in and around an inactive disposal site is presented in Figure 3.1. The percolation techniques are based on those described by Viessman et al. (1977) and used by Thornthwaite and Mather (1955, 1957), Fenn et al. (1975), and Dass et al. (1977). The overland runoff volume is estimated using techniques described by SCS (1972, 1982), Kent (1973), and USBR (1977). Computations describing the runoff volume in more detail are found in Chapter 4.0.

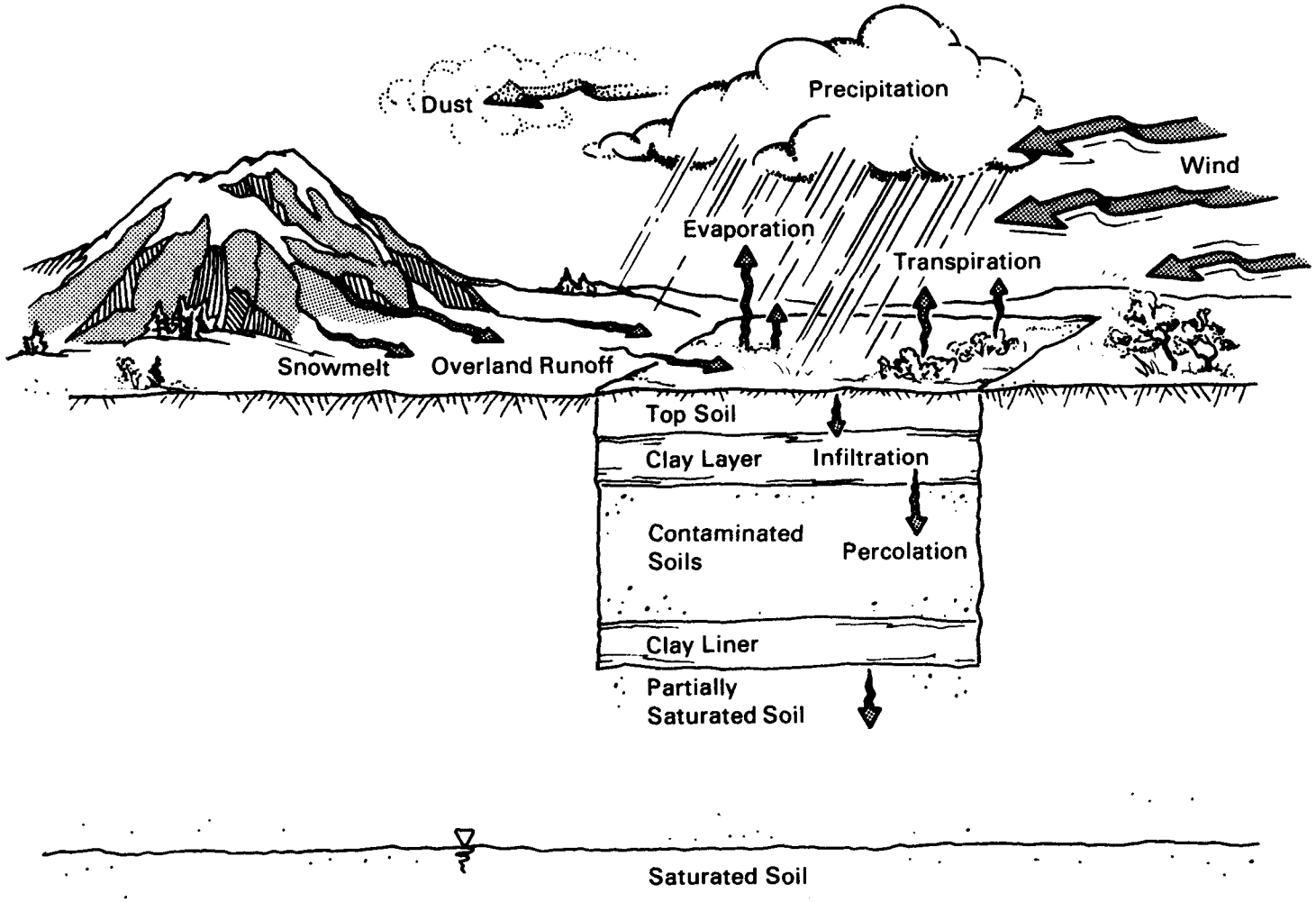

FIGURE 3.1. Schematic Diagram Illustrating the Movement of Water in and Around an Inactive Waste Site

Quantifying the leachate volume is an important component of the RAPS methodology because the volume of water that percolates into an inactive hazardous waste site (i.e., nonponded sites) is assumed in RAPS to eventually percolate from the site, thereby distributing contaminants in the groundwater environment. Because a relatively simple methodology is being proposed to quantify the percolation volume, these techniques must be tested against actual site data and/or computer models (e.g., see Thompson and Tyler 1984) that include a more complete description of the phenomena governing the movement of water through the upper horizons of a partially saturated soil.

It is assumed that water only percolates during periods of precipitation and snowmelt. Of the precipitation that falls on a site with contaminated soils, a portion runs off, some is lost to evapotranspiration, and the remainder percolates through the contaminated soils (e.g., landfill or soils contaminated by atmospheric wet and dry deposition). Water that percolates through the fill can eventually leave as leachate when the moisture content of the fill is between field capacity and saturated conditions. Thornthwaite and Mather (1955, 1957), Fenn et al. (1975), and Dass et al. (1977) have attempted to quantify leachate quantities using physically based principles. Knight et al. (1980) note that, although simpler methods have been proposed, they are not as precise in estimating leachate quantities. More complex methods also have been proposed and developed (e.g., Schroeder et al. 1983; ICF 1984), but their complexity and data requirements preclude their use in a preliminary ranking system scheme. A preliminary ranking system methodology is too simple to be completely accurate in describing the complex processes governing flow and/or solute movement through a partially saturated site with contaminated soils.

Leachate quantities from contaminated soils can be estimated based on the method proposed by Thornthwaite and Mather (1955, 1957), Fenn et al. (1975), and Dass et al. (1977), and used by Whelan et al. (1987). The method involves a monthly water-balance calculation using a variety of meteorologic and site information including monthly estimates of precipitation, potential evapotranspiration, snowmelt, temperature, and runoff. Although the method is not able to simulate the dominant mechanisms governing the movement of soil moisture

through the soil waste matrix in a completely accurate way, it can indicate how a site might respond to different meteorologic and hydrologic conditions.

Long-term meteorological data can be obtained from the Local Climatic Data: Annual Summary with Comparative Data for 1984, published by the Environmental Data Service, National Oceanic and Atmospheric Administration (NOAA), National Climatic Data Center, U.S. Department of Commerce (USDC).[a] Required site information includes data similar to that used by the overland pathway (see Chapter 4.0), because the Soil Conservation Service (SCS) Curve Number (CN) technique forms the basis for estimating overland runoff from the site.

The volume of leachate generated from contaminated soils and the net volume of precipitation that results in overland runoff are computed in monthly time steps. Monthly time steps were chosen because

- Collated, easily attainable data on the United States are available on a monthly basis (see the example LCD summary presented in Figure 3.2).
- Lifetime average exposure is being used as the basis for determining health effects. Using smaller time increments would not increase the computational accuracy for determining contaminant dose response. Throughout this chapter, the index 'i' in the equations refers to the month of the year (i.e., i = 1 for January, 2 for February,..., and 12 for December). Information for areas of the United States pertaining to each month is contained in LCDs (see Figure 3.2). The monthly tabulated data for 30 years of record are under "Normals, Means, and Extremes" in the LCDs.

Source-term quantification calculations are divided into the following 14 steps for computing the potential leachate and net overland runoff volume:

- unadjusted average monthly temperature -- The unadjusted average monthly temperature represents the average monthly temperature at the

(a) The Local Climatic Data Annual Summaries are designated by LCD.

Meteorological Data For The Current Year

Station: CONCORDIA, KANSAS 8 13984 — BLOSSER MUNICIPAL AIRPORT — Standard time used: CENTRAL — Latitude: 39° 33' N — Longitude: 97° 39' W — Elevation (ground): 1470 feet — Year: 1983

Month	Temperature °F: Averages: Daily maximum	Daily minimum	Monthly	Extremes: Highest	Date	Lowest	Date	Degree days Base 65 °F: Heating	Cooling	Precipitation in inches: Water equivalent: Total	Greatest in 24 hrs.	Date	Snow, ice pellets: Total	Greatest in 24 hrs.	Date	Relative humidity, pct.: Hour 00 (Local time)	Hour 06 (Local time)	Hour 12 (Local time)	Hour 18 (Local time)	Wind: Resultant: Direction	Speed m.p.h.	Average speed m.p.h.	Fastest mile: Speed m.p.h.	Direction	Date	Percent of possible sunshine	Average sky cover, tenths, sunrise to sunset	Number of days: Sunrise to sunset: Clear	Partly cloudy	Cloudy	Precipitation .01 inch or more	Snow, ice pellets 1.0 inch or more	Thunderstorms	Heavy fog, visibility ¼ mile or less	Temperature °F: Maximum (b): 90° and above	32° and below	Minimum: 32° and below	0° and below	Average station pressure mb: Elev. 1484 feet m.s.l.
JAN	35.2	22.0	28.6	59	13	6	27	1121	0	1.69	0.71	28-29	12.2	7.5	30-31	80	83	75	74	26	1.4	12.7	35	35	19	43	7.7	5	6	20	9	*	0	4	0	14	30	0	985.1
FEB	39.9	25.9	32.9	62	19	5	*	889	0	1.09	0.52	1-2	8.7	6.4	1	82	83	75	73	20	2.0	13.3	37	17	19	49	7.1	6	5	17	7	3	1	6	0	10	20	0	983.7
MAR	48.9	32.5	40.7	74	2	17	10	748	0	3.42	1.05	4-5	5.3	3.6	26-27	76	79	66	63	06	3.1	14.6	35	19	30	40	8.1	4	3	24	11	2	1	0	0	1	17	0	957.3
APR	53.7	36.1	44.9	76	26	24	15	596	0	1.92	0.98	31-1	6.1	2.6	4-5	77	80	61	61	03	4.5	14.9	38	02	1	43	7.1	7	4	19	10	2	4	2	0	0	15	0	958.7
MAY	68.8	46.9	57.9	85	27	35	15	236	23	2.98	1.48	13-14	0.0	0.0		74	84	59	56	05	0.8	12.8	36	27	6	63	5.7	7	15	9	7	0	5	1	0	0	0	0	959.7
JUN	79.5	59.3	69.4	96	30	43	6	38	177	3.59	2.25	10-11	0.0	0.0		82	91	67	61	18	5.7	11.3	28	18	12	67	5.7	11	4	15	10	0	0	3	0	0	0	0	959.4
JUL	95.1	69.1	82.1	108	27	60	26	0	536	0.16	0.09	28	0.0	0.0		69	79	42	38	19	7.9	13.7	26	23	3	86	2.6	22	5	4	2	0	1	0	23	0	0	0	962.1
AUG	97.2	71.8	84.5	108	16	59	12	0	610	2.58	1.13	20	0.0	0.0		59	76	47	40	18	5.8	11.2	28	34	23	79	4.1	14	12	5	6	0	5	0	28	0	0	0	963.1
SEP	83.2	57.2	70.2	99	8	33	23	77	240	1.72	0.76	19-20	0.0	0.0		63	77	46	41	18	5.7	13.6	37	35	12	75	3.8	15	9	6	6	0	6	0	10	0	0	0	962.8
OCT	65.0	46.2	55.6	89	2	33	13	317	32	3.60	1.64	18-19	0.0	0.0		79	85	66	65	13	1.7	11.7	32	19	14	83	6.5	8	6	17	8	0	3	1	0	0	0	0	964.8
NOV	48.0	32.5	40.3	70	1	7	30	736	0	1.84	1.03	26-27	7.3	7.3	26-27	84	88	78	78	31	2.0	12.5	32	36	9	30	7.3	5	5	20	6	1	5	0	5	19	0	0	958.3
DEC	19.3	4.9	12.1	40	8	-16	27	1634	0	0.85	0.35	27-28	16.7	8.9	20-21	65	65	62	63	33	4.2	13.0	29	01	8	33	6.9	8	3	20	5	*	0	2	0	26	31	10	968.5
					AUG		DEC					JUN			DEC										APR													
YEAR	61.2	42.0	51.6	108	16	-16	22	6390	1616	25.59	2.25	10-11	56.5	8.9	20-21	74	81	62	59	18	1.4	12.9	38	07	1	56	6.1	112	77	176	87	16	35	23	68	56	132	10	961.8

Normals, Means, And Extremes

Month	Temperatures °F: Normal: Daily maximum	Daily minimum	Monthly	Extremes: Record highest	Year	Record lowest	Year	Normal Degree days Base 65 °F: Heating	Cooling	Precipitation in inches: Water equivalent: Normal	Maximum monthly	Year	Minimum monthly	Year	Maximum in 24 hrs.	Year	Snow, ice pellets: Maximum monthly	Year	Maximum in 24 hrs.	Year	Relative humidity pct.: Hour 00 (Local time)	Hour 06 (Local time)	Hour 12 (Local time)	Hour 18 (Local time)	Wind: Mean speed m.p.h.	Prevailing direction thru 1963	Fastest mile: Speed m.p.h.	Direction	Year	Pct. of possible sunshine	Mean sky cover, tenths, sunrise to sunset	Mean number of days: Sunrise to sunset: Clear	Partly cloudy	Cloudy	Precipitation .01 inch or more	Snow, ice pellets 1.0 inch or more	Thunderstorms	Heavy fog, visibility ¼ mile or less	Temperatures °F: Max. (b): 90° and above	32° and below	Min.: 32° and below	0° and below	Average station pressure mb: Elev. 1484 feet m.s.l.
(a)				22		22					22		22		22		22		22		21	21	21	21	21	1	19	19		21	21	21	21	21	21	21	21	21	21	21	21	11
J	35.0	14.7	24.9	71	1981	-17	1979	1243	0	0.61	1.89	1983	0.07	1964	0.73	1971	13.7	1979	8.5	1971	76	80	66	69	12.1	N	50	NW	1965	62	5.9	10	7	14	6	2	*	3	0	13	29	5	966.0
F	41.7	20.1	30.9	76	1972	-15	1979	955	0	0.84	2.50	1971	0.01	1976	1.26	1966	20.6	1971	13.2	1965	75	79	63	62	12.5	NNW	56	NE	1976	64	5.8	9	7	12	5	2	*	2	0	9	25	2	964.8
M	51.3	28.4	39.9	87	1972	-7	1978	778	0	1.86	7.37	1973	0.02	1968	2.04	1979	9.2	1971	7.5	1975	72	79	57	56	13.9	S	68	NW	1971	64	6.1	9	7	15	8	1	2	2	0	2	20	*	960.2
A	64.8	40.9	52.9	92	1965	14	1975	367	0	2.26	4.41	1976	0.84	1966	1.71	1964	6.1	1983	3.8	1970	72	81	54	51	14.2	SSE	51	SE	1963	66	6.0	9	8	13	10	*	6	1	*	*	5	0	960.6
M	74.8	51.7	63.3	99	1967	26	1967	137	84	3.99	9.74	1970	0.26	1966	5.15	1970	T	1967	T	1967	76	84	57	54	12.3	SSE	54	E	1971	69	5.9	9	9	13	11	0	8	1	1	0	*	0	959.6
J	85.2	61.7	73.5	109	1983	41	1964	16	271	4.25	14.14	1967	1.27	1980	5.46	1967	0.0		0.0		76	85	55	51	12.0	SSE	67	NE	1967	77	5.2	10	11	9	9	0	10	*	9	0	0	0	960.2
J	90.9	67.0	79.0	109	1983	48	1972	0	436	3.37	10.17	1971	0.16	1983	3.94	1971	0.0		0.0		71	81	51	47	11.6	SSE	61	NW	1968	79	4.5	14	10	7	9	0	11	*	10	0	0	0	961.9
A	89.2	65.4	77.3	108	1983	45	1964	0	381	3.35	10.72	1977	0.38	1971	4.56	1968	0.0		0.0		72	83	54	49	11.3	ENE	47	NW	1980	77	4.6	13	10	8	9	0	9	1	14	0	0	0	962.4
S	79.8	55.6	67.7	104	1976	33	1983	65	196	3.00	8.49	1973	0.55	1976	3.18	1973	0.0		0.0		75	85	56	54	11.5	SSE	53	NW	1969	71	4.7	13	7	10	8	0	7	1	5	0	0	0	963.4
O	69.1	44.2	56.7	96	1963	17	1972	277	20	1.83	6.82	1979	0.22	1965	4.15	1979	4.6	1970	4.6	1970	70	79	52	54	12.0	S	49	N	1970	71	4.8	14	6	11	6	*	3	1	1	0	3	0	963.9
N	52.0	30.2	41.1	84	1980	-4	1976	717	0	1.05	4.88	1971	0.03	1965	3.20	1971	10.1	1972	7.3	1983	76	82	61	65	11.8	SSE	43	NW	1975	60	5.8	10	6	14	5	1	1	2	0	2	16	*	963.9
D	40.8	20.7	30.8	82	1964	-16	1983	1060	0	0.70	3.06	1973	T	1976	1.67	1973	16.7	1983	12.5	1966	76	79	65	68	12.0	WSW	45	NW	1963	58	6.0	10	6	15	5	1	*	2	0	9	29	2	964.7
					JUL		JAN					JUN		DEC		JUN			FEB										MAR												
YR	64.6	41.7	53.2	109	1980	-17	1979	5615	1340	27.11	14.14	1967	T	1976	5.46	1967	20.6	1971	13.2	1965	74	81	57	56	12.3	SSE	68	NW	1971	69	5.4	130	90	141	89	8	58	17	48	35	129	9	962.6

NOTE: NORMAL COOLING DEGREE DATA PUBLISHED IN THE 1982 ANNUAL WERE FOR THE 1951-1980 PERIOD.

NORMALS, MEANS, AND EXTREMES TABLE NOTE(S):
1. Wind under Fastest Mile heading is through September 1981.

(a) Length of record, years, through the current year unless otherwise noted, based on January data.
(b) 70° and above at Alaskan stations.
* Less than one half.
T Trace.
BLANK entries denote missing or unreported data.

NORMALS - Based on record for the 1951-1980 period.
MEANS - Length of record in (a) is for complete data years.
EXTREMES- Length of record in (a) may be for other than complete or consecutive data years. Date is the most recent in cases of multiple occurrence.
WIND DIRECTION - Numerals indicate tens of degrees clockwise from true north. 00 indicates calm.
FASTEST MILE WIND - Speed is fastest observed 1-minute value when direction is in tens of degrees.

Means and extremes above are from existing and comparable exposures. Annual extremes have been exceeded at other sites in the locality as follows:

Temperature
Highest: 116 in Aug. 1936.
Lowest: -25 in Feb. 18994.

Precipitation
Maximum in 24 hours: 6.46 in May 1950.

Snowfall
Maximum monthly: 25.0 in Mar. 1891.
Maximum in 24 hours: 17.2 in Mar. 1924.

FIGURE 3.2. Example of Local Climatological Data (After NOAA 1984)

LCD station, and it has not been adjusted for the elevation difference that may exist between the site proper and the LCD station. The elevation of the LCD station is provided for in the LCDs and is illustrated in Figure 3.2.

- adjusted average monthly temperature -- This step adjusts the LCD station temperature to the site elevation temperature using adiabatic lapse rates. The user must supply only the site elevation to make the adjustment.

- potential evapotranspiration -- The modified Blaney-Criddle (MBC) method (Doorenbos and Pruitt 1977) and the Penman method with correction factor (PMCF) are used to estimate the potential evapotranspiration (PET) at the site. The MBC and PMCF methods are based on average air temperature, minimum relative humidity, ratio of actual to maximum possible sunshine hours, and average wind speed. The PMCF is also based on the maximum relative humidity and latitude. These parameters can be defined by using the LCDs (see Figure 3.2) and are different than those used by Thornthwaite and Mather (1955, 1957), Fenn et al. (1975), and Dass et al. (1977).

- monthly precipitation as rainfall -- This step identifies the total monthly precipitation when adjusted monthly temperatures are above freezing. This information is obtained from LCDs (see Figure 3.2).

- monthly precipitation as snowfall -- All precipitation occurring during a month when the adjusted monthly temperature is below freezing is assumed to be in the form of snowfall. This information (precipitation) is obtained in the same location on the LCDs as the monthly precipitation as rainfall (see Figure 3.2).

- precipitation adjusted for snowmelt -- Snowfall is assumed to occur before any considerable ground-surface freezing has taken place. This assumption is important because when snowmelt occurs, percolation can also occur. It is also assumed that the snow is stored on the ground during the months when the adjusted average monthly temperature is below freezing. During the spring melt, a portion of the

snowmelt is combined with the precipitation. The adjusted precipitation is used in the overland runoff and percolation computations. Snowmelt computations consider melt from rainfall, vapor condensation, convection, and radiation. Typically required parameters include average temperature, average wind speed, site elevation, mean sky cover (i.e., degree of cloudiness), and monthly precipitation as rainfall. This information is supplied by LCDs (Figure 3.2).

- monthly overland runoff -- The SCS CN technique forms the basis of estimating the net monthly overland runoff. This technique is described in Chapter 4.0 and will not be discussed in detail here. To adjust the computations, the monthly overland runoff is computed based on the number of precipitation events that occur in a given month. The number of precipitation events for each month are provided with the LCDs (Figure 3.2).

- maximum percolation -- The maximum percolation represents the difference between the precipitation adjusted for snowmelt and monthly overland runoff when the adjusted temperature is above freezing.

- potential percolation -- The potential percolation represents the difference between the maximum percolation and the PET when the adjusted temperature is above freezing.

- accumulated potential water loss -- This step represents the potential soil moisture water loss during a year. It is computed using the potential percolation and the soil moisture retention tables provided by Thornthwaite and Mather (1957).

- soil moisture storage -- This step identifies the soil moisture contained in the soil column at the end of each month. Soil moisture storage is computed using the PET and the soil moisture retention tables provided by Thornthwaite and Mather (1957). Because the soil moisture storage calculations are based on the PET, this computational step has a significant influence on the amount of water that percolates into the waste site.

- change in soil moisture storage -- The change in soil moisture storage for a current month is computed by taking the difference of the current and previous month's soil moisture.
- actual evapotranspiration -- The actual evapotranspiration (AET) equals the PET, if the PET is less than or equal to the difference between the maximum percolation and the change in soil moisture storage. If the PET is greater than this difference, the AET equals the maximum percolation minus the change in soil moisture storage.
- leachate generation -- The leachate generated from a soil column is zero if the adjusted monthly temperature is below zero. If the temperature is above zero, the leachate generated equals the maximum percolation minus the AET and change in soil moisture storage.

A complete description of the algorithms on which the source-term quantification is based for each of the steps highlighted above is provided below.[a]

3.2 UNADJUSTED AVERAGE MONTHLY TEMPERATURE

The LCD station nearest and most representative to the actual site provides unadjusted average monthly temperatures. Example values are presented in Figure 3.1 (see "Monthly Temperature" in Figure 3.2).

3.3 ADJUSTED AVERAGE MONTHLY TEMPERATURE

The unadjusted average monthly temperature is adjusted to account for the elevation difference that may exist between the LCD station and the actual site. In general, air temperatures decrease about 0.5° to 0.9°C for every 100 m (3° to 5°F for every 1000 ft) of rise in altitude (Mockus 1971). Using the ideal gas law with the assumption of dry adiabatic conditions, Eagleson (1970) derived an approximate lapse rate (i.e., rate of change of temperature with height in the free atmosphere) as 1°C decrease per 100 m (5.5°F decrease per 1000 ft). This dry adiabatic lapse rate is a maximum rate (excluding superadiabatic conditions). A mean lapse rate as suggested by Linsley et al.

(a) Many of the original equations in this chapter were developed using English units. For consistency, all parameters and equations are expressed in metric units, unless otherwise noted.

(1975) is a decrease of about 0.7°C per 100 m (3.8°F per 1000 ft) of vertical rise. By using the mean lapse rate as suggested by Linsley et al. (1975), an adjusted average monthly temperature can be computed as follows:

$$T_i = Tu_i - 0.007\ (h_1 - h_0) \qquad (3.1)$$

where T_i = adjusted average monthly temperature at the actual site for the i-th month (°C)

Tu_i = unadjusted average monthly temperature at the LCD station for the i-th month (°C)

h_1 = elevation of actual site (m)

h_0 = elevation of LCD station (m)

i = index on month ($1 \leq i \leq 12$ with $i = 1$ for January, $i = 2$ for February,..., and $i = 12$ for December).

3.4 POTENTIAL EVAPOTRANSPIRATION

Potential evapotranspiration represents the most critical parameter in this methodology. If the PET estimate is too high, then the methodology will underpredict the volume of leachate from the waste disposal site. If the PET estimate is too low, then conservative estimates may result; in arid regions, this conservatism may be violated because most of the techniques used for estimating PET were not developed for arid regions.

Rosenberg (1974) notes that the concept of PET has been widely accepted and defines it as follows:

> "Potential evapotranspiration (PET) is the evaporation from an extended surface of short green . . . (vegetation) . . . which fully shades the ground, exerts little or negligible resistance to the flow of water, and is always well supplied with water. Potential evapotranspiration cannot exceed free water evaporation under the same weather conditions."

He continues to note that AET differs from PET under most circumstances. He attributes these differences to 1) the influences of surfaces that are not extended (i.e., great fetch), 2) varying heights in vegetation, 3) partial vegetative cover, 4) internal resistance in vegetation to water flow, 5) periodic water deficits (i.e., periods during which vegetation is not well supplied with water), and 6) vegetation using more water in arid and dry regions than that suggested by pan evaporation (i.e., PET exceeding free water evaporation).

Rosenberg (1974) notes that in humid regions (i.e., where advection of sensible heat is unimportant) free water evaporation from pans gives realistic estimates of the PET. In more arid localities and where advection is considerable, the pan evaporation may give unrealistic values; in fact, he continues to note that the differences between pan evaporation and PET may be "very pronounced." In an effort to present a consistent methodology that can be applied uniformly throughout the country, the PET is estimated by RAPS using well-accepted formulations (e.g., Penman's method), as opposed to being assumed equal to the pan evaporation.

Doorenbos and Pruitt (1977) present four techniques for estimating PET: modified Blaney-Criddle method, Penman method with correction factor, Radiation method, and Pan Evaporation method. Gee and Simmons (1979) applied three of these techniques (i.e., modified Blaney-Criddle method, Penman method with correction factor, and Radiation method) along with the original Penman formulation to the arid Pacific Northwest. Their results indicate that all methods yielded nearly the same cumulative PET over the 2-year simulation period except for the Penman method, which consistently overpredicted PET. Of the four methods mentioned above, the modified Blaney-Criddle method, the Penman method, and the Penman method with correction factor are used to estimate PET. The Blaney-Criddle method was chosen because it was developed for the arid western portions of the United States (Israelsen and Hansen 1962). The Penman method and Penman method with correction factor were chosen because Doorenbos and Pruitt (1977) believe that they offer the best results with the minimum possible error. Each method is applied at each site; the one estimating the lowest PET is used in that site's assessment.

Each method is described below. Because only a correction factor represents the difference between the Penman method and Penman method with correction factor, only the Penman method with correction factor is described in this chapter.

3.4.1 Modified Blaney-Criddle Method

The original Blaney-Criddle equation (Blaney and Criddle 1950) involves calculating evapotranspiration from a consumptive-use factor, mean monthly temperature, and percentage of total annual daylight hours occurring during the period being considered (Doorenbos and Pruitt 1977). An empirically determined consumptive-use crop coefficient is then applied to establish evapotranspiration water requirements. However, Israelsen and Hansen (1962) note that this simplified formula was developed for the arid western portion of the United States and provides good estimates of seasonal water needs under these conditions. Doorenbos and Pruitt (1977) note that the effect of climate is insufficiently defined by temperature and day length and that vegetative requirements will vary between climates having different temperatures and lengths of days.

For a better definition of the effect of climate on vegetative requirements, Doorenbos and Pruitt (1977) present a modified version of the Blaney-Criddle technique to include monthly parameters, such as relative humidity, daytime wind speed, ratio of actual to maximum possible sunshine hours, temperature, latitude, and mean daily percentage of total annual daytime hours.

The governing equations as presented by Doorenbos and Pruitt (1977) are as follows:

$$PET_i = a\ b\ c_i\ p_i\ (0.46\ T_i + 8) \qquad \text{for } T_i > 0^0C \qquad (3.2)$$

$$PET_i = 0 \qquad \text{for } T_i \leq 0^0C \qquad (3.3)$$

where PET_i = potential evapotranspiration rate for month i (mm/day)

a = coefficient that is a function of elevation

b = coefficient that is a function of latitude

c_i = adjustment factor that depends on minimum relative humidity, sunshine hours, and daytime wind speed estimates for month i

p_i = mean daily percentage of total annual daytime hours as a function of latitude and month i

T_i = adjusted average monthly temperature for month i (°C).

The mean daily percentage of total annual daytime hours (p_i) can be obtained from Table 3.1 when the latitude of the site and the corresponding month are known. The latitude of the site can be obtained from the LCD (see Figure 3.2). The adjustment factor has been incorporated into a series of figures that relate [p (0.46 T + 8)] to the PET. The series of figures developed by Doorenbos and Pruitt (1977) is presented in Figure 3.3. This figure requires information on the minimum relative humidity for the month (Rh_{min}), the ratio of actual to maximum possible sunshine hours (n/N), and the daytime wind speed. The Rh_{min} and n/N can be obtained directly from the LCD. The daytime wind speed for the month must be calculated from the average wind speed for the month. The wind speed values presented in the LCD represent the average over a 24-hr period throughout the month. The ratio between the mean daytime and nighttime wind speeds is approximately 2; to obtain daytime wind speeds, the average monthly wind speeds must be adjusted by a factor of 1.33 (Doorenbos and Pruitt 1977). This relationship is given by

$$U_i = 1.33\ \bar{U}_i \tag{3.4}$$

where U_i = average monthly daytime wind speed for month i (m/s)

$\bar{U}_i$ = average wind speed for month i, obtained from LCD (m/s).

TABLE 3.1. Mean Daily Percentage (p) of Annual Daytime Hours for Different Latitudes (After Doorenbos and Pruitt 1977)

North/ South Latitude[a] (degrees)	Jan Jul	Feb Aug	Mar Sep	Apr Oct	May Nov	Jun Dec	Jul Jan	Aug Feb	Sep Mar	Oct Apr	Nov May	Dec Jun
60	0.15	0.20	0.26	0.32	0.38	0.41	0.40	0.34	0.28	0.22	0.17	0.13
58	0.16	0.21	0.26	0.32	0.37	0.40	0.39	0.34	0.28	0.23	0.18	0.15
56	0.17	0.21	0.26	0.32	0.36	0.39	0.38	0.33	0.28	0.23	0.18	0.16
54	0.18	0.22	0.26	0.31	0.36	0.38	0.37	0.33	0.28	0.23	0.19	0.17
52	0.19	0.22	0.27	0.31	0.35	0.37	0.36	0.33	0.28	0.24	0.20	0.17
50	0.19	0.23	0.27	0.31	0.34	0.36	0.35	0.32	0.28	0.24	0.20	0.18
48	0.20	0.23	0.27	0.31	0.34	0.36	0.35	0.32	0.28	0.24	0.21	0.19
46	0.20	0.23	0.27	0.30	0.34	0.35	0.34	0.32	0.28	0.24	0.21	0.20
44	0.21	0.24	0.27	0.30	0.33	0.35	0.34	0.31	0.28	0.25	0.22	0.20
42	0.21	0.24	0.27	0.30	0.33	0.34	0.33	0.31	0.28	0.25	0.22	0.21
40	0.22	0.24	0.27	0.30	0.32	0.34	0.33	0.31	0.28	0.25	0.22	0.21
35	0.23	0.25	0.27	0.29	0.31	0.32	0.32	0.30	0.28	0.25	0.23	0.22
30	0.24	0.25	0.27	0.29	0.31	0.32	0.31	0.30	0.28	0.26	0.24	0.23
25	0.24	0.26	0.27	0.29	0.30	0.31	0.31	0.29	0.28	0.26	0.25	0.24
20	0.25	0.26	0.27	0.28	0.29	0.30	0.30	0.29	0.28	0.26	0.25	0.25
15	0.26	0.26	0.27	0.28	0.29	0.29	0.29	0.28	0.28	0.27	0.26	0.25
10	0.26	0.27	0.27	0.28	0.28	0.29	0.29	0.28	0.28	0.27	0.26	0.26
5	0.27	0.27	0.27	0.28	0.28	0.28	0.28	0.28	0.28	0.27	0.27	0.27
0	0.27	0.27	0.27	0.27	0.27	0.27	0.27	0.27	0.27	0.27	0.27	0.27

(a) Southern latitudes: apply 6-month difference as shown.

Doorenbos and Pruitt (1977) suggest that the evapotranspiration can be adjusted downwards by 10% for each 1000-m (3281-ft) altitude change above sea level. The coefficient a in Equation (3.2) can be modified to address the influence of elevation on evapotranspiration by defining the coefficient as follows:

$$a = \frac{10{,}000 - h_1}{10{,}000} \qquad \text{for } h_1 \leq 10{,}000 \qquad (3.5)$$

where h_1 = elevation of actual site (m).

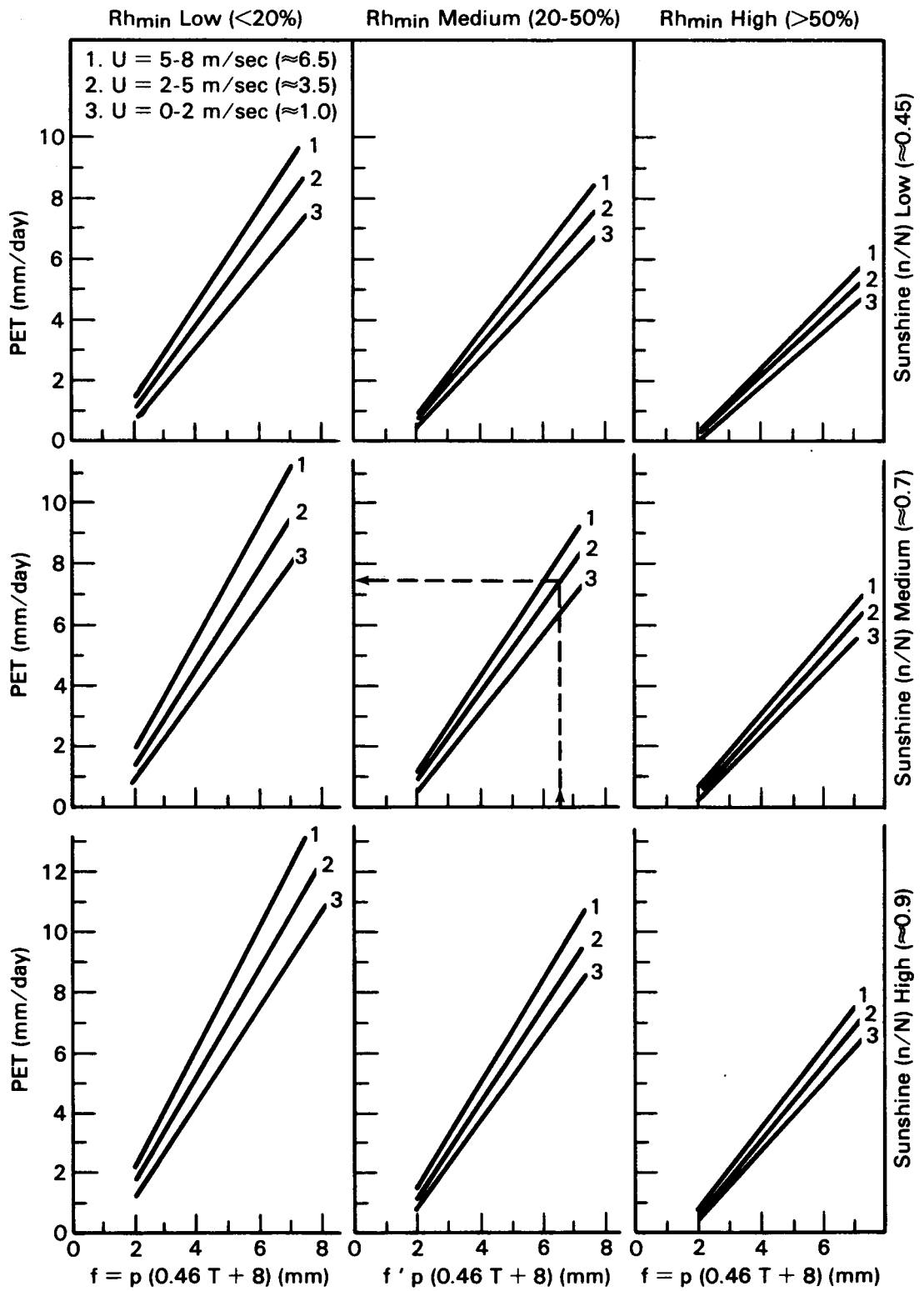

FIGURE 3.3. Prediction of PET from Blaney-Criddle f Factor for Different Conditions of Minimum Relative Humidity, Sunshine Duration, and Daytime Wind (After Doorenbos and Pruitt 1977)

In areas at latitudes of 55° or more, the calculated evapotranspiration should be reduced as much as 15%. To address latitudes greater than 55°, the coefficient b in Equation (3.2) can be described as follows:

$$b = \frac{288.33 - Lat}{233.33} \qquad \text{for } 55^0 \leq Lat \leq 90^0 \qquad (3.6)$$

where Lat = latitude of actual site.
Otherwise, the coefficient b equals unity.

3.4.2 Penman Method with Correction Factor

The original Penman method (Penman 1948) is one of the most theoretically based approaches for estimating evapotranspiration because it is connected to incoming solar energy (i.e., radiation) and aerodynamic characteristics (e.g., wind and humidity). The relative importance of each term varies with climatic conditions. Doorenbos and Pruitt (1977) note that under calm weather conditions the aerodynamic term is usually less important than the energy term, and the results appear to predict evapotranspiration rather closely. They continue to note that under windy conditions and particularly in the more arid regions the aerodynamic term becomes relatively more important; thus, errors may result in predicting evapotranspiration. Israelsen and Hansen (1962) appear to concur with Doorenbos and Pruitt (1977) by noting that the coefficients used in the Penman equation " . . . were determined for a rather humid area not far from the ocean and essentially covered with growing vegetation. Experience indicates that the Penman formula applies better under these conditions than in arid, low-humidity areas where temperature and radiant energy may not be as nearly balanced as . . . (in a humid area near the ocean)."

Doorenbos and Pruitt (1977) developed the modified version of the Penman method, PMCF; it differs from the Penman method by using a revised wind function term in its formulation. The PMCF is based on climatic parameters such as maximum, minimum, and mean relative humidity; ratio of actual to maximum possible sunshine hours; average wind speed; average air temperature; saturation and actual vapor pressures; and net shortwave and longwave solar radiation parameters. The governing PET equations in the PMCF are as follows:

$$PET_i = c_i \left[W_i \, Rn_i + (1 - W_i) \, f(\bar{U})_i \, (es_i - ea_i)\right] \quad \text{for } T_i > 0^0C \qquad (3.7)$$

$$PET_i = 0 \quad \text{for } T_i \leq 0^0C \qquad (3.8)$$

where c_i = adjustment factor to compensate for the effect of day and night weather conditions for month i

W_i = temperature-related weighting factor for the i-th month

Rn_i = net radiation in equivalent evaporation for month i (mm/day)

$f(\bar{U})_i$ = wind-related function for month i

es_i = saturation vapor pressure at mean air temperature for month i (mb)

ea_i = mean actual vapor pressure of the air for month i (mb).

The maximum and minimum relative humidities (Rh_{max} and Rh_{min}, respectively) can be obtained from the LCD tables (see Figure 3.2). The average relative humidity (Rh_{ave}) is computed by averaging Rh_{max} and Rh_{min}. Humidity is expressed here as the saturation vapor pressure deficit (es - ea): the difference between the mean saturation water vapor pressure (es) and the mean actual water vapor pressure (ea) (Doorenbos and Pruitt 1977). The value of 'es' can be estimated from Table 3.2, or from the following equation proposed by Bosen (1960), as reported by Linsley et al. (1975):

$$es_i \simeq 33.8639 \left[(0.00738 \, T_i + 0.8072)^8 - 0.000019 \, ABS \, (1.8 \, T_i + 48) + 0.001316\right] \qquad (3.9)$$

Linsley et al. (1975) note that this "formula yields values of saturation vapor pressure over water that are approximated to within one percent in the range of -50 to +55°C (-58 to +131°F)". The value of 'ea' is defined as the multiple of Rh_{ave} (in fractional form) and 'es'.

TABLE 3.2. Vapor Pressure Versus Temperature (After Linsley et al. 1975; Doorenbos and Pruitt 1977)

Temperature (°C)	Vapor Pressure (mb)
0	6.1
1	6.6
2	7.1
3	7.6
4	8.1
5	8.7
6	9.3
7	10.0
8	10.7
9	11.5
10	12.3
11	13.1
12	14.0
13	15.0
14	16.1
15	17.0
16	18.2
17	19.4
18	20.6
19	22.0
20	23.4
21	24.9
22	26.4
23	28.1
24	29.8
25	31.7
26	33.6
27	35.7
28	37.8
29	40.1
30	42.4
31	44.9
32	47.6
33	50.3
34	53.2
35	56.2
36	59.4
37	62.8
38	66.3
39	69.9
40	73.8
50	123.4
60	199.3
70	311.7
80	473.7
90	701.1
100	1013.3

The wind function ($f(\bar{U})$) is defined in the PMCF as

$$f(\bar{U})_i = 0.27\ (1 + j_i\ \bar{U}_i\ 0.01) \tag{3.10}$$

in which

$$j_i = (2/Hu)^{0.17} \quad \text{for } Hu > 2 \tag{3.11}$$

$$j_i = (2/Hu)^{0.22} \quad \text{for } Hu \leq 2 \tag{3.12}$$

where j_i = correction factor for month i for wind speeds not measured at a 2-m height

Hu = height above the ground at which the wind velocity measurements are made.

In many instances, the height above the ground at which the wind velocity measurements are made is included on a separate page with the LCD tables. If no information is available on Hu, assume Hu = 10 m (based on a typical 10-m meteorological tower).

The temperature-related weighting factor (W) is a function of altitude as well as temperature. The value for W can be obtained from Table 3.3.

The total net radiation (Rn) is equal to the difference between the net shortwave radiation (Rns) and the net longwave radiation (Rnl). When converted to heat, Rn can be related to the energy [i.e., extraterrestrial radiation (Ra)] required to evaporate water from an open surface (Doorenbos and Pruitt 1977). To calculate Rn, the following steps are involved:

- Based on latitude (provided in the LCD tables) and month of year, compute Ra from Table 3.4.

TABLE 3.3. Values of Weighting Factor (W) for the Effect of Radiation on PET at Different Temperatures and Altitudes (After Doorenbos and Pruitt 1977)

Temperature (°C)	2	4	6	8	10	12	14	16	18	20	22	24	26	28	30	32	34	36	38	40
Altitude (m)																				
0	0.43	0.46	0.49	0.52	0.55	0.58	0.61	0.64	0.66	0.69	0.71	0.73	0.75	0.77	0.78	0.80	0.82	0.83	0.84	0.85
500	0.44	0.48	0.51	0.54	0.57	0.60	0.62	0.65	0.67	0.70	0.72	0.74	0.76	0.78	0.79	0.81	0.82	0.84	0.85	0.86
1000	0.46	0.49	0.52	0.55	0.58	0.61	0.64	0.66	0.69	0.71	0.73	0.75	0.77	0.79	0.80	0.82	0.83	0.85	0.86	0.87
2000	0.49	0.52	0.55	0.58	0.61	0.64	0.66	0.69	0.71	0.73	0.75	0.77	0.79	0.81	0.82	0.84	0.85	0.86	0.87	0.88
3000	0.52	0.55	0.58	0.61	0.64	0.66	0.69	0.71	0.73	0.75	0.77	0.79	0.81	0.82	0.84	0.85	0.86	0.87	0.88	0.89
4000	0.54	0.58	0.61	0.64	0.66	0.69	0.71	0.73	0.75	0.77	0.79	0.81	0.82	0.84	0.85	0.86	0.87	0.89	0.90	0.90

TABLE 3.4. Extraterrestrial Radiation (Ra) for the Northern Hemisphere Expressed in Equivalent Evaporation (mm/day) (After Doorenbos and Pruitt 1977)

	Month											
Lat	Jan	Feb	Mar	Apr	May	June	July	Aug	Sep	Oct	Nov	Dec
50°	3.8	6.1	9.4	12.7	15.8	17.1	16.4	14.1	10.9	7.4	4.5	3.2
48	4.3	6.6	9.8	13.0	15.9	17.2	16.5	14.3	11.2	7.8	5.0	3.7
46	4.9	7.1	10.2	13.3	16.0	17.2	16.6	14.5	11.5	8.3	5.5	4.3
44	5.3	7.6	10.6	13.7	16.1	17.2	16.6	14.7	11.9	8.7	6.0	4.7
42	5.9	8.1	11.0	14.0	16.2	17.3	16.7	15.0	12.2	9.1	6.5	5.2
40	6.4	8.6	11.4	14.3	16.4	17.3	16.7	15.2	12.5	9.6	7.0	5.7
38	6.9	9.0	11.8	14.5	16.4	17.2	16.7	15.3	12.8	10.0	7.5	6.1
36	7.4	9.4	12.1	14.7	16.4	17.2	16.7	15.4	13.1	10.6	8.0	6.6
34	7.9	9.8	12.4	14.8	16.5	17.1	16.8	15.5	13.4	10.8	8.5	7.2
32	8.3	10.2	12.8	15.0	16.5	17.0	16.8	15.6	13.6	11.2	9.0	7.8
30	8.8	10.7	13.1	15.2	16.5	17.0	16.8	15.7	13.9	11.6	9.5	8.3
28	9.3	11.1	13.4	15.3	16.5	16.8	16.7	15.7	14.1	12.0	9.9	8.8
26	9.8	11.5	13.7	15.3	16.4	16.7	16.6	15.7	14.3	12.3	10.3	9.3
24	10.2	11.9	13.9	15.4	16.4	16.6	16.5	15.8	14.5	12.6	10.7	9.7
22	10.7	12.3	14.2	15.5	16.3	16.4	16.4	15.8	14.6	13.0	11.1	10.2
20	11.2	12.7	14.4	15.6	16.3	16.4	16.3	15.9	14.8	13.3	11.6	10.7
18	11.6	13.0	14.6	15.6	16.1	16.1	16.1	15.8	14.9	13.6	12.0	11.1
16	12.0	13.3	14.7	15.6	16.0	15.9	15.9	15.7	15.0	13.9	12.4	11.6
14	12.4	13.6	14.9	15.7	15.8	15.7	15.7	15.7	15.1	14.1	12.8	12.0
12	12.8	13.9	15.1	15.7	15.7	15.5	15.5	15.6	15.2	14.4	13.3	12.5
10	13.2	14.2	15.3	15.7	15.5	15.3	15.3	15.5	15.3	14.7	13.6	12.9
8	13.6	14.5	15.3	15.6	15.3	15.0	15.1	15.4	15.3	14.8	13.9	13.3
6	13.9	14.8	15.4	15.4	15.1	14.7	14.9	15.2	15.3	15.0	14.2	13.7
4	14.3	15.0	15.5	15.5	14.9	14.4	14.6	15.1	15.3	15.1	14.5	14.1
2	14.7	15.3	15.6	15.3	14.6	14.2	14.3	14.9	15.3	15.3	14.8	14.4
0	15.0	15.5	15.7	15.3	14.4	13.9	14.1	14.8	15.3	15.4	15.1	14.8

- Compute the solar radiation (Rs) by correcting Ra for the ratio of the actual to the maximum possible sunshine hours [(n/N), Pct. of possible sunshine in the LCD tables].

$$Rs_i = [0.25 + 0.50\ (n/N)_i]\ Ra_i \tag{3.13}$$

- Compute Rns by correcting Rs for the reflectiveness of the land surface with the correction parameter α (equaling 0.25) (Doorenbos and Pruitt 1977).

$$Rns_i = (1 - \alpha_i)\ Rs_i \tag{3.14}$$

- The calculation for estimating Rnl is based on the average temperature, ea, and n/N as follows:

$$Rnl_i = \sigma\ (T_i + 273.15)^4\ [0.34 - 0.044\ (ea_i)^{0.5}]\ [0.1 + 0.9\ (n/N)_i] \tag{3.15}$$

where σ = constant parameter equaling 2.0×10^{-9}
273.15 = units conversion from °C to °K.

- Compute Rn as the algebraic difference between Rns and Rnl:

$$Rn_i = Rns_i - Rnl_i \tag{3.16}$$

The adjustment factor c, which compensates for the effects of day and night weather conditions, can be estimated from Rh_{max}, Rs, and U [Equation (3.4)]. By assuming that the ratio of the daytime- to nighttime-average wind speeds is equal to 2 (see Section 3.4.1), the factor c can be estimated from Table 3.5.

TABLE 3.5. Adjustment Factor (c) in the PMCF Equation (After Doorenbos and Pruitt 1977)

Rs (mm/d)	Rh_{max} = 30%				Rh_{max} = 60%				Rh_{max} = 90%			
U (m/s)	3	6	9	12	3	6	9	12	3	6	9	12
0	0.86	0.90	1.00	1.00	0.96	0.98	1.05	1.05	1.02	1.06	1.10	1.10
3	0.69	0.76	0.85	0.92	0.83	0.91	0.99	1.05	0.89	0.98	1.10	1.14
6	0.53	0.61	0.74	0.84	0.70	0.80	0.94	1.02	0.79	0.92	1.05	1.12
9	0.37	0.48	0.65	0.76	0.59	0.70	0.84	0.95	0.71	0.81	0.96	1.06

3.5 PRECIPITATION AS RAINFALL

The average monthly precipitation is supplied by LCDs, as illustrated in Figure 3.2. The precipitation can fall as rain (i.e., nonfrozen) or snow (i.e., frozen). It is assumed that the monthly precipitation is represented by rainfall if the adjusted average monthly temperature is above freezing. This assumption is not completely accurate, because rainfall and snowfall can frequently occur during the same month, especially during springtime months. If the temperature for the month is above freezing, though, much of the snowfall will melt and represent a source of water for percolation and overland runoff.

3.6 MONTHLY PRECIPITATION AS SNOWFALL

If the adjusted average monthly temperature is below freezing, the monthly precipitation is assumed as snowfall. The snowfall is assumed to accumulate on the land surface and to be stored until the first month arrives with an adjusted average monthly temperature greater than zero. The monthly precipitation values are presented in the LCDs (see Figure 3.2).

3.7 PRECIPITATION ADJUSTED FOR SNOWMELT

In many areas, a dominant source of runoff or percolation may be from snowmelt. The assumption used in this methodology is that snow is stored on the ground when the adjusted average monthly air temperature is less than or equal to 0°C (32°F); when the average monthly air temperature rises above 0°C (32°F), the snow melts and is available for percolation and runoff.

Because crude calculations are employed for estimating the source term, simple empirical relationships are used to estimate snowmelt. The heat necessary to induce snowmelt is derived from radiation, condensation of vapor, convection, air and ground conduction, and rainfall. The four most important sources are vapor condensation, convection, radiation, and rainfall. Of these sources, vapor condensation is considered one of the most important factors, while rainfall ranks fourth as an important heat source (Linsley and Franzini 1972; Linsley et al. 1975; Viessman et al. 1977). Each of these four sources is discussed below.

3.7.1 Vapor Condensation

Viessman et al. (1977) note that heat given off by condensing water vapor in a snowpack is often the most important heat source. A water vapor supply at the snow surface is formed by the turbulent exchange process; consequently, a mass transfer equation similar to those presented for evaporation studies fits the melt process (Viessman et al. 1977). An expression for a 6-hr snowmelt is given as (Light 1941 as reported by Viessman et al. 1977)

$$M'_{vc} = K_1 V (ea - 6.11) \qquad \text{for } T_6 > 0^{0}C \qquad (3.17)$$

$$M'_{vc} = 0 \qquad \text{for } T_6 \leq 0^{0}C \qquad (3.18)$$

where M'_{vc} = 6-hr snowmelt from vapor condensation (cm)
K_1 = a theoretical constant assumed to equal 0.02557 (cm-s)/(mb-m) [0.00450 (hr-in.)/(mb-mi)]
V = average 6-hr wind velocity measured at 15 m (50 ft) (m/s)
ea = vapor pressure of the air (mb; 1 mb = 0.0145 lb/in.^{2})
T_6 = average 6-hr temperature (°C).

The value of K_1 reportedly varies from 0.01818 to 0.03284 (cm-s)/(mb-m) [0.00320 to 0.00578 (hr-in.)/(mb-mi)] (Light 1941 and Wilson 1941, as reported by Viessman et al. 1977); an average value of 0.02557 (cm-s)/(mb-m)

[0.0045 (hr-in.)/(mb-mi)] is chosen for K_1. If the wind velocity measurements were not made at 15 m (50 ft), then they can be calculated using Equation (3.11) as

$$V \approx 1.59\ (Hu)^{-0.17}\ \bar{U} \tag{3.19}$$

Because available data are on a monthly basis, it is assumed that the 6-hr snowmelt computations can be extended over the month by using adjusted averaged monthly temperatures and wind velocities. By assuming that no evaporation of snow occurs, the monthly estimate of snowmelt from vapor condensation can be expressed as follows:

$$Mvc_i = 0.102\ d_i\ V_i\ (ea_i - 6.11) \qquad \text{for } T_i > 0^0C \tag{3.20}$$

$$Mvc_i = 0 \qquad \text{for } T_i \leq 0^0C \tag{3.21}$$

where Mvc_i = average monthly snowmelt from vapor condensation for the ith month (cm)

d_i = number of days in the i-th month.

The vapor pressure of the air is estimated using the PMCF methodology outlined in Section 3.4.2.

3.7.2 Convection

Heat for snowmelt is transferred from the atmosphere to the snowpack by convection (Viessman et al. 1977). The amount of snowmelt by this process is related to temperature and wind velocity. Wilson (1941) and Light (1941), as reported by Viessman et al. (1977), provide an expression for estimating the 6-hr depth of snowmelt by convection in centimeters as

$$M_c' = K_2\ V\ T_6 \qquad \text{for } T_6 > 0^0C \tag{3.22}$$

$$M_c' = 0 \qquad \text{for } T_6 \leq 0^0C \tag{3.23}$$

in which

$$K_2 = 10^{(-1.725 - 5.12\ 10^5\ h_1)} \qquad (3.24)$$

where M_c' = 6-hr snowmelt from convection (cm)

K_2 = heat exchange coefficient as a function of elevation [(cm-s)/(°C-m)].

It is assumed that the 6-hr snowmelt can be extended over the month by using adjusted averaged monthly temperatures and wind velocities. The monthly estimate for snowmelt from convection is given by

$$Mc_i = 4\ d_i\ K_2\ V_i\ T_i \qquad \text{for } T_i > 0^0C \qquad (3.25)$$

$$Mc_i = 0 \qquad \text{for } T_i \leq 0^0C \qquad (3.26)$$

where Mc_i = average monthly snowmelt from convection for the i-th month (cm).

3.7.3 Radiation

The net amount of shortwave and longwave radiation received by a snowpack can be a very important source of heat energy for snowmelt (Viessman et al. 1977). Viessman et al. (1977) note that, under clear skies, the most significant variables in radiation melt are insolation, albedo of snow, and air temperature. USCOE (1956) show that cloud cover and height can significantly affect snowmelt from radiation. An approximate method of estimating 12-hr snowmelt from direct solar radiation is given by Wilson (1941). The relationship is of the following form:

$$M_r' = K\ (1 - 0.75\ m_c) \qquad \text{for } T_{12} > 0^0C \qquad (3.27)$$

$$Mr' = 0 \qquad \text{for } T_{12} \leq 0^{0}C \qquad (3.28)$$

where Mr' = 12-hr snowmelt from radiation (cm)

K = snowmelt occurring in a half-day in clear weather (cm)

m_c = degree of cloudiness (0 for clear weather and 1.0 for completely overcast) (see LCD tables, Figure 3.2)

T_{12} = average 12-hr temperature (°C).

It is assumed that the 12-hr snowmelt can be extended over the month by using monthly averaged degree of cloudiness. The monthly estimate of snowmelt from radiation is given by

$$Mr_i = d_i K_i (1 - 0.75 m_c) \qquad \text{for } T_i > 0^{0}C \qquad (3.29)$$

$$Mr_i = 0 \qquad \text{for } T_i \leq 0^{0}C \qquad (3.30)$$

where Mr_i = average monthly snowmelt from radiation for the i-th month (cm)

K_i = average snowmelt occurring in a half-day in clear weather for the i-th month (cm).

Viessman et al. (1977) provide estimates of the parameter K_i as a function of month (Table 3.6).

3.7.4 Rainfall

Viessman et al. (1977) note that heat derived from rainfall is generally small; when rainfall occurs on a snowpack, the temperature of the rain is probably quite low. At higher temperatures, rainfall may constitute a significant heat source; it affects the aging process of the snow, frequently to a great degree. Based on Viessman et al. (1977) and USCOE (1960), daily snowmelt by rainfall can be estimated by

$$M_p' = 0.032\ P'\ T_{24} \qquad \text{for } T_{24} > 0^0C \qquad (3.31)$$

$$M_p' = 0 \qquad \text{for } T_{24} \leq 0^0C \qquad (3.32)$$

where M_p' = daily snowmelt during a rainfall event (cm)
P' = daily precipitation volume (cm)
T_{24} = is the average daily air temperature (°C).

TABLE 3.6. Half-Day Snowmelt During Clear Weather as a Function of Month (After Viessman et al. 1977)

i	Month	K_i (cm)
3	March	0.89
4	April	1.07
5	May	1.22
6	June	1.33

It is assumed that snowmelt from rainfall occurs only during rainfall events, and the number of events per month is assumed equal to the mean number of days per month when the precipitation volume is 3.9×10^{-3} cm (0.01 in.) or more, as indicated by the LCDs (see Figure 3.2). It is also assumed that the daily snowmelt can be extended over the entire month by using adjusted averaged monthly temperatures. The monthly estimate of snowmelt from rainfall is given by

$$Mp_i = 0.032\ Pm_i\ T_i \qquad \text{for } T_i > 0^0C \qquad (3.33)$$

$$Mp_i' = 0 \qquad \text{for } T_i \leq 0^0C \qquad (3.34)$$

where Mp_i = monthly snowmelt from rainfall for the i-th month (cm)
Pm_i = average monthly precipitation volume for the i-th month (cm).

3.7.5 Monthly Snowmelt

The total inventory of snowmelt on a monthly basis can be estimated by combining Equations (3.20), (3.21), (3.24), (3.25), (3.26), (3.29), (3.30), (3.33), and (3.34):

$$M_i = Mvc_i + Mc_i + Mr_i + Mp_i \qquad \text{for } T_i > 0^0C \qquad (3.35)$$

$$M_i = 0 \qquad \text{for } T_i \leq 0^0C \qquad (3.36)$$

where M_i = total monthly snowmelt for the i-th month (cm).

The volume of snowmelt is limited by the amount of snow stored on the overland surface. When a month has an adjusted monthly temperature greater than freezing and follows a month with a subfreezing temperature, the monthly precipitation volume is adjusted to account for snowmelt as follows:

$$Pms_i = Pm_i + M_i \qquad (3.37)$$

where Pms_i = monthly precipitation adjusted for snowmelt for the i-th month (cm).

The parameter Pms_i represents the precipitation volume used to compute the net overland runoff volume and percolation volume.

3.8 OVERLAND RUNOFF VOLUME

The SCS CN technique (SCS 1972, 1982; Kent 1973; USBR 1977) is used to compute the overland runoff portion of the monthly water balance at the hazardous waste site. Computations for computing percolation using the CN technique are based on the contaminated soil surface characteristics. The soil cover represents the soil type, and the vegetation cover represents the vegetation type. To distribute the monthly volume of precipitation into daily precipitation amounts, we assume the following:

1. The monthly volume of precipitation can be equally distributed among the total number of recorded precipitation events with 3.9×10^{-3} cm (0.01 in.) or more of volume.

2. The number of precipitation events can be defined by the LCD.

3. Precipitation is stored on the land surface in the form of snow when adjusted average monthly temperatures are equal to or below freezing; precipitation is in the form of rainfall when temperatures are above freezing.

Using the curve number technique, the total monthly runoff from the waste site can be estimated as follows:

$$Vm_i = \frac{[Pms_i(CN) - 0.2\ a\ m_i\ [1000 - 10\ (CN)]]^2}{(CN)[Pms_i\ (CN) + 0.8\ a\ m_i\ [1000 - 10\ (CN)]]} \qquad (3.38)$$

$$\text{for} \begin{cases} [Pms_i(CN)] \geq [0.2\ a\ m_i\ [1000 - 10\ (CN)]] \\ T_i > 0^0C \end{cases}$$

$$Vm_i = 0 \qquad (3.39)$$

$$\text{for} \begin{cases} [Pms_i\ (CN)] < [0.2\ a\ m_i\ [1000 - 10\ (CN)]] \\ T_i \leq 0^0C \end{cases}$$

where Vm_i = monthly runoff volume for the i-th month (cm)
a = conversion parameter between centimeters and inches ($a = 2.54$)
m_i = number of precipitation events during the i-th month
CN = curve number.

It is assumed that using the CN technique for the runoff calculations is applicable, although snow may be covering the land surface. This condition rarely occurs, because most snow is usually melted in the first month the average temperature rises above freezing. A complete discussion reviewing the development of Equations (3.38) and (3.39) is presented in Chapter 4.0.

3.9 MAXIMUM PERCOLATION

The maximum amount of moisture available for percolation (i.e., maximum percolation) is represented by the precipitation adjusted for snowmelt, during months in which the adjusted average monthly temperature is greater than freezing minus the average monthly runoff. The maximum percolation is expressed by the following expressions:

$$fmax_i = Pms_i - Vm_i \qquad \text{for } T_i > 0^0C \qquad (3.40)$$

$$fmax_i = 0 \qquad \text{for } T_i \leq 0^0C \qquad (3.41)$$

where $fmax_i$ = maximum amount of moisture available for percolation (cm).

3.10 POTENTIAL PERCOLATION

The potential percolation is defined as the difference between the maximum monthly percolation ($fmax_i$) and the monthly PET. Mathematically, the potential percolation is expressed as follows:

$$fp_i = fmax_i - PET_i \qquad \text{for } T_i > 0^0C \qquad (3.42)$$

$$fp_i = 0 \qquad \text{for } T_i \leq 0^0C \qquad (3.43)$$

where fp_i = potential percolation for the i-th month (cm).

3.11 ACCUMULATED POTENTIAL WATER LOSS

Accumulated potential water loss refers to the potential deficiency of moisture in the soil water storage when the PET is significantly larger than the maximum potential percolation. During these periods, the moisture can be depleted from the soil reservoir creating a moisture deficit below saturated conditions. This condition usually occurs during the summer months in arid areas of the country (e.g., southwestern United States or arid Pacific Northwest).

The methodology outlined by Thornthwaite and Mather (1955, 1957) is used to compute the accumulated potential water loss. The intent of this subsection is to present the mathematical expressions forming the basis for computing the accumulated potential water loss; no examples are presented. For detailed examples, see Thornthwaite and Mather (1955, 1957).

A site has the potential for a yearly averaged moisture deficit in the soil column if the sum of the monthly fp_i values is negative. In humid areas, the sum of the monthly fp_i values will be positive. Because a yearly soil moisture deficit exists in arid regions and 'excess' water exists in humid areas, different computational methods are employed for computing the accumulated potential water loss.

3.11.1 Humid Regions

In humid areas, the value of accumulated potential water loss with which to start accumulating depletion of water moisture from the soil[(a)] is zero. This value of zero is assigned to the last month having a positive value of fp_i. This month is used because the soil moisture at the end of the 'wet' season (i.e., the consecutive months with positive fp_i) is at field capacity. The current month's accumulated potential water loss is computed by summarizing it with the previous months' accumulated potential water loss. Mathematically, we have the following:

$$WL_{\ell-1} = WL_o \tag{3.44}$$

$$WL_{i+1} = \sum_{i=\ell}^{L} (WL_i + fp_{i+1}) \tag{3.45}$$

in which

(a) The value with which to start accumulating negative values of fp_i.

$$WL_0 = 0 \qquad \text{for} \sum_{i=1}^{n} (fp_i) \geq 0 \qquad (3.46)$$

where WL_i = accumulated potential water loss for the i-th month (cm).

WL_0 = accumulated water loss during the last month of the wet season (i.e., 1 month before month ℓ) (cm)

ℓ = index for the first month with a negative fp_i

L = index for the last month with a negative fp_L value (Note that L can be less than ℓ; for example, January with an i = 1 can follow December with an i = 12)

n = number of months in a year (n = 12).

As Equation (3.45) indicates, the summation occurs as long as the fp_i value remains negative (i.e., during the 'dry' season). For the remaining months (i.e., when fp_i is positive), the soil does not lose water but gains it from percolation; therefore, no value is associated with these months.

3.11.2 Arid and Semiarid Regions

In arid or dry areas, soil moisture at the end of the wet season is below field capacity; therefore, it is necessary to find an initial value of the accumulated potential water loss with which to start accumulating the negative values of fp_i. This initial value may be estimated by employing the method of successive approximations, as outlined by Thornthwaite and Mather (1957). The basis for the methodology is that the rate of water loss from the soil is proportional to the soil moisture content; that is, as the soil moisture decreases toward the wilting point, extracting water from the soil becomes increasingly more difficult. The initial value of the accumulated potential water loss for an arid or dry area using the method of successive substitution is computed as follows:

1. Identify the wilting point and field capacity of the soil root zone volume.

2. Compute the available water in the root zone of the soil. The available water equals the difference between the field capacity and wilting point times the root zone depth.

3. Use a suite of soil moisture retention tables provided by Thornthwaite and Mather (1957) to compute the accumulated potential water loss (WL_o) during the last month of the wet season. A portion of one of the tables is presented in Table 3.7. Thornthwaite and Mather (1957) also tabulated a chart to help the user select the most appropriate table that reflects soil type, root zone depth, and available water; their chart is illustrated in Table 3.8.

4. Sum the negative fp_i values (WL_n) for the year.

$$WL_n = \sum_{i=\ell}^{L} [\text{negative } (fp_i)] \qquad (3.47)$$

where WL_n = sum of the negative fp_i values.

This step and the following steps are outlined in the flow diagram illustrated in Figure 3.4. As an initial step, assume WL_o equals WL_n.

5. Use the retention table chosen in Step 3 along with the WL_o value to obtain the first estimate of the soil moisture storage value (ST) (i.e., soil moisture retained). The ST value represents the moisture storage in the soil if the moisture storage at the beginning of the dry period equaled the soil water-holding capacity (i.e., field capacity minus wilting point times the root zone depth). The actual value is less than the soil water-holding capacity because the soil moisture content is at some value less than the water-holding capacity at the beginning of the dry period.

TABLE 3.7. Example Soil Moisture Retention Table for 150-mm Water-Holding Capacity of the Root Zone (After Thornthwaite and Mather 1957)(a)

-WL ↓	Soil Moisture Storage (ST) → 0	1	2	3	4	5	6	7	8	9
10	140	139	138	137	136	135	134	133	132	131
20	131	130	129	128	127	127	126	125	124	123
30	122	122	121	120	119	118	117	116	115	114
40	114	113	113	112	111	111	110	109	108	107
50	107	106	106	105	104	103	103	102	101	100
60	100	99	98	97	97	97	96	95	94	93
70	93	92	92	91	90	90	89	89	88	87
80	87	86	86	85	84	84	84	83	83	82
90	82	81	81	80	79	79	78	77	77	76
100	76	76	75	75	74	74	73	72	72	71
110	71	71	70	70	69	69	68	68	67	67
120	66	66	66	65	65	64	64	63	63	62
130	62	62	61	61	60	60	60	59	59	58
140	58	58	57	57	56	56	55	55	54	54
150	54	53	53	53	52	52	52	52	51	51
160	51	51	50	50	50	49	49	48	48	47
170	47	47	47	46	46	46	45	45	45	44
180	44	44	44	43	43	43	42	42	42	41
190	41	41	41	40	40	40	40	39	39	39
200	39	38	38	38	37	37	37	37	36	36
210	36	36	35	35	35	35	35	34	34	34
220	34	34	33	33	33	33	33	32	32	32
230	32	31	31	31	31	31	30	30	30	30
240	30	29	29	29	29	29	28	28	28	28
250	28	27	27	27	27	27	26	26	26	26
260	26	26	25	25	25	25	25	24	24	24
270	24	24	24	23	23	23	23	23	23	23
280	22	22	22	22	22	22	22	22	21	21
290	21	21	21	20	20	20	20	20	20	20
300	20	19	19	19	19	19	19	19	18	18
310	18	18	18	18	18	18	18	17	17	17
320	17	17	17	17	17	17	17	16	16	16
330	16	16	16	16	16	16	16	15	15	15
340	15	15	15	15	15	15	14	14	14	14
350	14	14	14	14	14	14	14	13	13	13
360	13	13	13	13	13	13	13	12	12	12
370	12	12	12	12	12	12	12	12	11	11
380	11	11	11	11	11	11	11	11	11	11
390	11	11	11	10	10	10	10	10	10	10
400	10	10	10	10	10	10	10	10	9	9
410	9	9	9	9	9	9	9	9	9	9
420	9	9	9	8	8	8	8	8	8	8
430	8	8	8	8	8	8	8	8	8	8
440	8	8	8	7	7	7	7	7	7	7

(a) Soil moisture retained after different amounts of potential evapotranspiration have occurred. Water-holding capacity of the soil root zone is 150 mm.

TABLE 3.8. Relationship Between Soil Moisture Retention Tables and Soil and Vegetation Characteristics (After Thornthwaite and Mather 1957)[a]

Soil Type	Available Water (Field Capacity Minus Wilting Point)		Root Zone Depth		Most Applicable Soil Moisture Retention Table (Available Water x Root Zone Depth)	
	mm/m	in./ft	m	ft	mm	in.
Shallow-rooted crops (spinach, peas, beans, beets, carrots, etc.)						
Fine sand	100	1.2	0.50	1.67	50	2.0
Fine sandy loam	150	1.8	0.50	1.67	75	3.0
Silt loam	200	2.4	0.62	2.08	125	5.0
Clay loam	250	3.0	0.40	1.33	100	4.0
Clay	300	3.6	0.25	0.83	75	3.0
Moderately deep-rooted crops (corn, cotton, tobacco, cereal grains)						
Fine sand	100	1.2	0.75	2.50	75	3.0
Fine sandy loam	150	1.8	1.00	3.33	150	6.0
Silt loam	200	2.4	1.00	3.33	200	8.0
Clay loam	250	3.0	0.80	2.67	200	8.0
Clay	300	3.6	0.50	1.67	150	6.0
Deep-rooted crops (alfalfa, pastures, shrubs)						
Fine sand	100	1.2	1.00	3.33	100	4.0
Fine sandy loam	150	1.8	1.00	3.33	150	6.0
Silt loam	200	2.4	1.25	4.17	250	10.0
Clay loam	250	3.0	1.00	3.33	250	10.0
Clay	300	3.6	0.67	2.22	200	8.0
Orchards						
Fine sand	100	1.2	1.50	5.00	150	6.0
Fine sandy loam	150	1.8	1.67	5.55	250	10.0
Silt loam	200	2.4	1.50	5.00	300	12.0
Clay loam	250	3.0	1.00	3.33	250	10.0
Clay	300	3.6	0.67	2.22	200	8.0
Closed mature forest						
Fine sand	100	1.2	2.50	8.33	250	10.0
Fine sandy loam	150	1.8	2.00	6.66	300	12.0
Silt loam	200	2.4	2.00	6.66	400	16.0
Clay loam	250	3.0	1.60	5.33	400	16.0
Clay	300	3.6	1.17	3.90	350	14.0

(a) These figures are for mature vegetation. Young cultivated crops, seedlings, and other immature vegetation will have shallower root zones and, hence, have less water available for the use of the vegetation. As the plant develops from a seed or a young sprout to the mature form, the root zone will increase progressively from only a few inches to the values listed above. Use of a series of soil moisture retention tables with successively increasing values of available moisture permits the soil moisture to be determined throughout the growing season.

6. Add to the ST value, obtained from the retention table, the sum of the positive values of fp_i; the summation provides a new ST value (see Figure 3.4). The sum of the positive values of fp_i is defined as follows:

$$WL_p = \sum_{i=k}^{K} [\text{positive } (fp_i)] \tag{3.48}$$

where WL_p = sum of the positive fp_i values

k = index for the first month with a positive fp_i

K = index for the last month with a positive fp_i values (note that K can be less than k; for example, January with a k = 1 can follow December with a k = 12).

7. Use the new ST value computed in Step 6 in conjunction with the retention table to obtain a new estimate of the potential water loss WL_o (see Figure 3.4). Note that Step 7 represents the reverse procedure of Step 5.

8. Add WL_n (computed in Step 4) to WL_o (computed in Step 7) to provide a new estimate of WL_o (see Figure 3.4).

9. Use the retention table and WL_o (computed in Step 8) to estimate a new ST value (see Figure 3.4).

10. Repeat Steps 6 through 9 until ST value does not change between iterations. When no change occurs, the potential water loss value WL_o (computed in Step 8) represents the initial value of the accumulated potential water loss. This value is assigned to the last month having a positive value of fp_i. For succeeding months, the accumulated potential water loss is computed using Equations (3.42) and (3.43) but not using Equation (3.46).

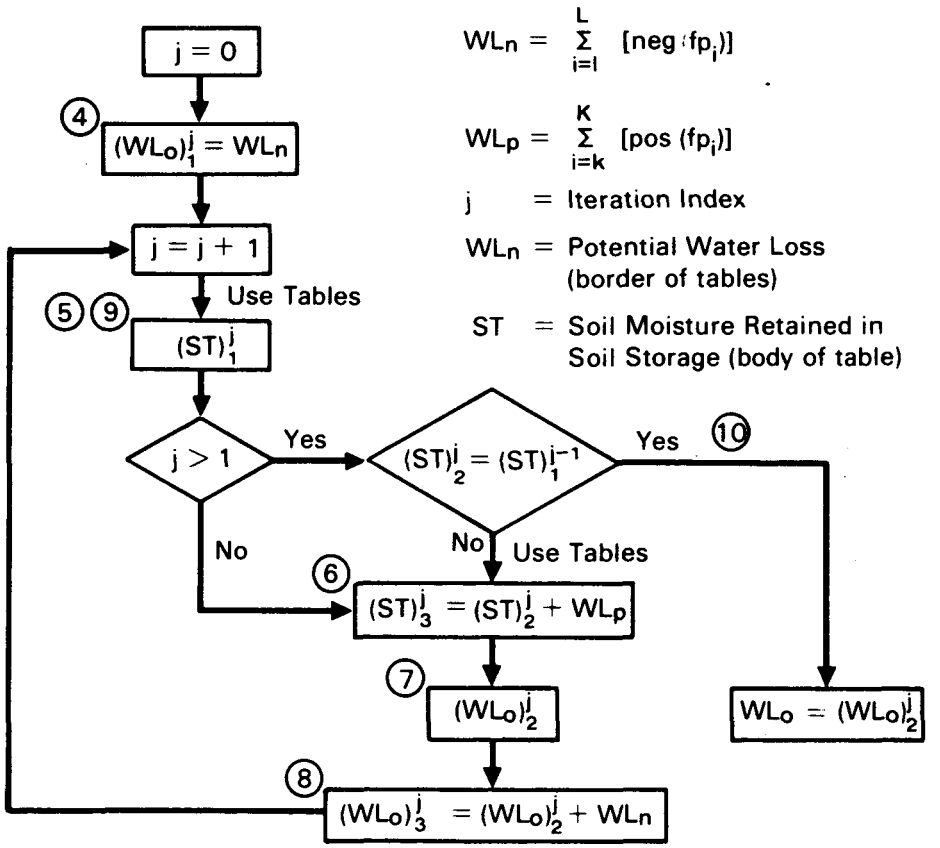

FIGURE 3.4. Flow Diagram Illustrating the Method of Successive Substitution for Computing WL_o for Arid Regions

3.12 SOIL MOISTURE STORAGE

The ST value represents the soil moisture that is retained in the soil after a given amount of accumulated potential water loss or gain has occurred. For humid areas

$$\text{i.e.,} \quad \sum_{i=1}^{n} (fp_i) \geq 0$$

the initial value for soil moisture storage is assigned to the last month having a positive value of fp_i (i.e., the last month of the wet season). This initial value is calculated at field capacity by multiplying the available water per unit depth of soil (i.e., field capacity minus wilting point) by the

root zone depth. This value should coincide with the applicable soil moisture retention table used for computing the accumulated potential water loss (as indicated by Table 3.8). Knisel (1980) notes that the root zone depth is usually estimated to be approximately 1 m (3 ft), although it varies with vegetation type. In an arid setting, depending on soil characteristics and plant cover, the root zone depth can vary from 2 to as much as 6 m (6 to 20 ft). Table 3.8 illustrates root zone depth values as a function of soil type, vegetation cover, and available water; the values range from 0.15 m (0.83 ft) for shallow-rooted crops in clay soils to 2.54 m (8.33 ft) for closed-mature forest in fine sands.

For arid areas

$$\text{i.e.,} \quad \sum_{i=1}^{n} (fp_i) < 0$$

the initial soil moisture storage is known from Step 10 of the accumulated potential water loss calculation (see Subsection 3.11.2). As with humid areas, this initial ST value is also assigned to the last month having a positive value of fp_i.

For both humid and arid areas, the soil moisture storage (ST_i) during the dry season (i.e., when $fp_i < 0$) is estimated using accumulated potential water loss values (WL_i) and the Thornthwaite and Mather (1957) soil moisture retention tables (see Table 3.7). The soil moisture retention tables correlate the relationship between WL_i and ST_i. Using the proper retention table, ST_i can be identified for each WL_i for each dry-season month.

For the first month and succeeding months of the wet season (i.e., first month following the dry season with a positive fp_i), the soil moisture storage is computed as follows:

$$ST_i = \sum_{i=k}^{K} (ST_{i-1} + fp_i) \qquad (3.49)$$

The maximum value for the soil moisture storage (ST_i) is field capacity minus the wilting point times the root zone depth.

3.13 CHANGE IN SOIL MOISTURE STORAGE

The change in the soil moisture storage is defined as the difference between the current and previous month's soil moisture storage. Mathematically, the change in this storage is computed as follows:

$$\Delta ST_i = ST_i - ST_{i-1} \tag{3.50}$$

where ΔST_i = change in soil moisture storage for the i-th month (cm).

3.14 ACTUAL EVAPOTRANSPIRATION

When the PET is less than or equal to the difference between the maximum potential percolation and change in soil moisture storage (note the potential negative sign), the AET is equal to the PET. When the PET is greater, the AET is equal to the difference between the maximum potential percolation and change in soil moisture storage (note the potential negative sign). Mathematically, the AET is computed as follows:

$$AET_i = PET_i \qquad \text{for } PET_i \leq (fmax_i - \Delta ST_i) \tag{3.51}$$

$$AET_i = fmax_i - \Delta ST_i \qquad \text{for } PET_i > (fmax_i - \Delta ST_i) \tag{3.52}$$

where AET_i = AET for the i-th month (cm).

3.15 LEACHATE GENERATION

In addition to the functional relationships discussed in previous sections, the moisture generated as leachate during any month is also a function of the adjusted average monthly temperature. When T_i is below freezing, zero leachate is generated.

$$LG_i = 0 \qquad \text{for } T_i \leq 0^0C \qquad (3.53)$$

where LG_i = leachate generation for the i-th month (cm).

When T_i is greater than freezing, the leachate generated from the site is computed as follows:

$$LG_i = fmax_i - AET_i - \Delta ST_i \qquad \text{for } T > 0^0C \qquad (3.54)$$

Like the cover material over the waste site, the underlying waste exhibits a certain water-holding capacity. Fenn et al. (1975) note that the amount of water that can be added and stored in the waste material depends on the composition of the waste and its initial moisture content (which can vary widely) when delivered to the site.

Theoretically speaking, water movement through a waste layer will act in a similar manner as water movement through a soil layer; the field capacity must be exceeded before leachate movement. Practically speaking, some channeling of water, from the heterogeneities associated with the waste, will occur before the attainment of field capacity.

In an effort to avoid the complex nature associated with various waste forms, the RAPS methodology assumes that the moisture content of the waste equals field capacity. The moisture that percolates through the soil layer covering the waste is assumed to eventually exit at the bottom of the waste.

3.16 SUMMARY

The quantity of leachate likely to be generated during the operational lifetime of an inactive hazardous waste facility is a major factor controlling the degree to which a site will require analysis. This quantity is controlled by local meteorologic, geologic, and hydrologic conditions and the design and operation of the facility. Given the limited availability of literature data on leachate quantities generated by inactive landfills, soils contaminated by atmospheric wet and dry deposition, or spills, available estimation techniques are used to quantify the leachate.

A modified method of those proposed by Thornthwaite and Mather (1955, 1957), Fenn et al. (1975), and Dass et al. (1977) is currently employed for computing precipitation-generated leachate quantities from contaminated soils. The methodology is based on a water-budget analysis; it estimates the quantity of leachate and involves a water-balance calculation using monthly estimates of precipitation, potential evapotranspiration, temperature, and runoff. The principal source of moisture is precipitation (rainfall and snowfall) over the contaminated site. Of the precipitation that falls on the contaminated site, a portion runs off, some is lost to evapotranspiration, and the remainder percolates through. Water that percolates through eventually exits as leachate. At this time, the RAPS methodology assumes that the waste leaches at a constant annual-average rate from the site.

3.17 REFERENCES

Blaney, H. F., and W. D. Criddle. 1950. Determining Water Requirements in Irrigated Areas from Climatological and Irrigation Data. USDA(SCS)TP-96, U.S. Department of Agriculture, Washington, D.C.

Bosen, J. F. 1960. "A Formula for Approximation of the Saturation Vapor Pressure over Water." Mon. Weather Rev. 88:275.

Dass, P., G. R. Tamke and C. M. Stoffel. 1977. "Leachate Production at Sanitary Landfills." J. Environ. Eng. Division., Proc. ASCE 103 (EEG).

Doorenbos, J., and W. O. Pruitt. 1977. Crop Water Requirements. FAO Irrigation and Drainage Paper 24 (Revised), Food and Agriculture Organization of the United States, Rome.

Eagleson, P. S. 1970. Dynamic Hydrology. McGraw-Hill, New York.

Fenn, D. G., K. J. Hanley and T. V. DeGeare. 1975. Use of the Water Balance Method for Predicting Leachate Generation from Solid Waste Disposal Sites. SW-168, U.S. Environmental Protection Agency, Washington D.C.

Gee, G. W., and C. S. Simmons. 1979. Characterization of the Hanford 300 Area Burial Grounds: Task III - Fluid Transport and Modeling. PNL-2921, Pacific Northwest Laboratory, Richland, Washington.

ICF. 1984. The Risk-Cost Analysis Model: Phase III Report. Prepared by ICF, Incorporated for the Office of Solid Waste, Economic Analysis Branch, U.S. Environmental Protection Agency, Washington, D.C.

Israelsen, O. W., and V. E. Hansen. 1962. Irrigation Principles and Practices. Wiley, New York.

Kent, K. M. 1973. A Method for Estimating Volume and Rate of Runoff in Small Watersheds. SCS-TP-149, U.S. Department of Agriculture, Soil Conservation Service, Washington, D.C.

Knight, R. G., E. H. Rothfuss and K. D. Yard. 1980. FGD Sludge Disposal Manual. 2nd ed. EPRI CS-1515, Electric Power Research Institute, Palo Alto, California.

Knisel, W. G., ed. 1980. CREAMS: A Field-Scale Model for Chemical, Runoff, and Erosion from Agricultural Management Systems. Conservation Report No. 26, U.S. Department of Agriculture, Washington, D.C.

Light, P. 1941. "Analysis of High Rates of Snow Melting." Trans. Am. Geophys. Union 22:1.

Linsley, R. K., and J. B. Franzini. 1972. Water-Resources Engineering. McGraw-Hill, New York.

Linsley, R. K., Jr., M. A. Kohler and J. L. H. Paulhus. 1975. Hydrology for Engineers. McGraw-Hill, New York.

Mockus, V. 1971. "Estimation of Direct Runoff from Snowmelt." SCS National Engineering Handbook, Section 4: Hydrology. U.S. Department of Agriculture, Soil Conservation Service, Washington, D.C.

NOAA. 1984. Local Climatological Data: Annual Summaries for 1983. National Oceanic and Atmospheric Administration, National Environmental Satellite, Data, and Information Service, National Climatic Data Center, Ashville, North Carolina.

Penman, H. L. 1948. "Natural Evaporation from Open Water, Bare Soil, and Grass." Proc. R. Soc. Lond. 193:120-145.

Rosenberg, N. J. 1974. MICROCLIMATE: the Biological Environment. McGraw-Hill, New York. 315 pp.

SCS. 1972. "Hydrology Guide for Use in Watershed Planning." SCS National Engineering Handbook, Section 4: Hydrology, Supplement A. U.S. Department of Agriculture, Soil Conservation Service. Washington, D.C.

SCS. 1982. SCS National Engineering Handbook, Section 4: Hydrology. (1982 Update.) U.S. Department of Agriculture, Soil Conservation Service, Washington, D.C.

Schroeder, P. R., A. C. Gibson and M. D. Smolen. 1983. The Hydrologic Evaluation of Landfill Performance (HELP) Model. U.S. Environmental Protection Agency, Cincinnati, Ohio.

Simmons, C. S., and G. W. Gee. 1981. Simulation of Water Flow and Retention in Earthen Cover Materials Overlying Uranium Mill Tailings. UMT/0203, U.S. Department of Energy, Washington, D.C.

Thompson, F. L., and S. W. Tyler. 1984. Comparison of Two Groundwater Flow Models -- UNSAT1D and HELP. EPRI CS-3695, Project 1406-1, Electric Power Research Institute, Palo Alto, California.

Thornthwaite, C. W., and J. R. Mather. 1955. "The Water Balance." Publications in Climatology, Vol. VIII, No. 1. Drexel Institute of Technology, Laboratory of Climatology, Centerton, New Jersey.

Thornthwaite, C. W., and J. R. Mather. 1957. "Instructions and Tables for Computing Potential Evapotranspiration and the Water Balance." Publications in Climatology, Vol. X, No. 3. Drexel Institute of Technology, Laboratory of Climatology, Centerton, New Jersey.

USBR. 1977. Design of Small Dams. U.S. Department of the Interior, Bureau of Reclamation. U.S. Government Printing Office, Washington, D.C.

USCOE. 1956. Snow Hydrology. U.S. Army Corps of Engineers, North Pacific Division, Portland, Oregon.

USCOE. 1960. "Runoff from Snowmelt." Engineering and Design Manuals, EM 1110-2-1406. U.S. Army Corps of Engineers, North Pacific Division, Portland, Oregon.

Viessman, W., Jr., J. W. Knapp, G. L. Lewis and T. E. Harbaugh. 1977. Introduction to Hydrology. Harper and Row, New York.

Whelan, G., S. M. Brown, D. L. Strenge, A. P. Schwab and P. J. Mitchell. 1987. Contaminant Assessment Modeling Under the Resource Conservation and Recovery Act. EA-5342. Electric Power Research Institute, Palo Alto, California.

Wilson, W. T. 1941. "An Outline of the Thermodynamics of Snowmelt." Trans. Am. Geophys. Union 22, Part 1.

4.0 OVERLAND PATHWAY

4.1 INTRODUCTION

Mills et al. (1985) note that receiving water bodies are subject to waste loads from point, nonpoint, and atmospheric deposition. Point sources are identifiable discrete discharges from municipal, institutional, and industrial waste water collection and treatment systems. Nonpoint sources are traditionally associated with land drainage or overland runoff, which enters a water body through often poorly defined pathways. Atmospheric waste sources are represented by constituent and particulate matter that is deposited on land and water surfaces through wet and dry deposition (e.g., see Chapter 7.0).

Surface soils and those soils near the land surface can be contaminated in a number of ways (e.g., accidental spills, intentional dumping, authorized land disposal, and atmospherically deposited contamination through wet and dry deposition). Once surface soils are contaminated, the constituents can migrate to the subsurface (i.e., groundwater) environment by precipitation-generated leaching and to nearby surface water bodies (e.g., holding pond or river) with contaminated runoff water and contaminated surface soil loss. This chapter addresses the migration and fate of 1) contaminated surface water leaching into the subsurface environment and 2) contaminated runoff water and contaminated surface soil loss to nearby receiving water bodies.

The driving mechanism transporting contaminants through the overland pathway and distributing them through the overland environment is overland flow. Overland flow is that portion of precipitation that ultimately appears as flowing water on the ground surface. It occurs primarily because of the incidence of rainfall or snowmelt in excess of abstraction demands (i.e., interception, evapotranspiration, infiltration, etc.) and/or the emergence of soil water into drainage pathways.

The overland pathway is based on the processes controlling the movement of water generated from representative precipitation events. Many of the characteristics describing the waste site and the surrounding watershed are used in computing overland water movement. If an unlimited supply of contamination were available for transport, then the overland flow rate would control the

mass flux of contaminants moving downgradient. As the flow rate increases, the potential for increasing the contaminant mass flux would also rise. The overland flow rate is combined with the initial source-term contaminant concentration and adjusted for contaminant persistence and toxicity. A population center or water body represents the final target for contaminant movement in the overland environment.[a] A schematic diagram illustrating the overland environment is presented in Figure 4.1.

The overland component of the RAPS methodology has two functions. First, results from the overland assessment are used in computing leachate quantities percolating from a nonponded waste site (e.g., see Chapter 3.0). This component estimates long-term, average monthly runoff volumes for use in the water balance calculations described in Chapter 3.0. These calculations are based on monthly average precipitation events. Second, the overland component estimates the migration and fate of contaminated water and sediment that move from contaminated surface soils (e.g., exposed wastes at unprotected landfills and soils contaminated through atmospheric wet and dry deposition). Because the majority of soil loss at a site is traditionally transported by overland runoff from precipitation events larger than the monthly average, these calculations are based on events with higher return periods or recurrence intervals (e.g., higher intensity and larger volume).

The algorithms on which the overland pathway analyses are based are presented in this chapter. The methodology is based on data that are easily attainable and readily available. Estimation techniques are based on

- the U.S. Department of Agriculture Soil Conservation Service's (SCS) curve number methodology, as presented in SCS (1972), Kent (1973), USBR (1977), and Haun and Barfield (1978)
- the Universal Soil Loss Equation (USLE), as presented by Goldman et al. (1986), Mills et al. (1985), Riggins and Bandy (1981), Novotny and Chesters (1981), Whelan (1980), Mitchell and Bubenzer (1980),

---

(a) Root uptake of contaminants is addressed by the exposure assessment component of the RAPS methodology. See Chapter 8 for more information.

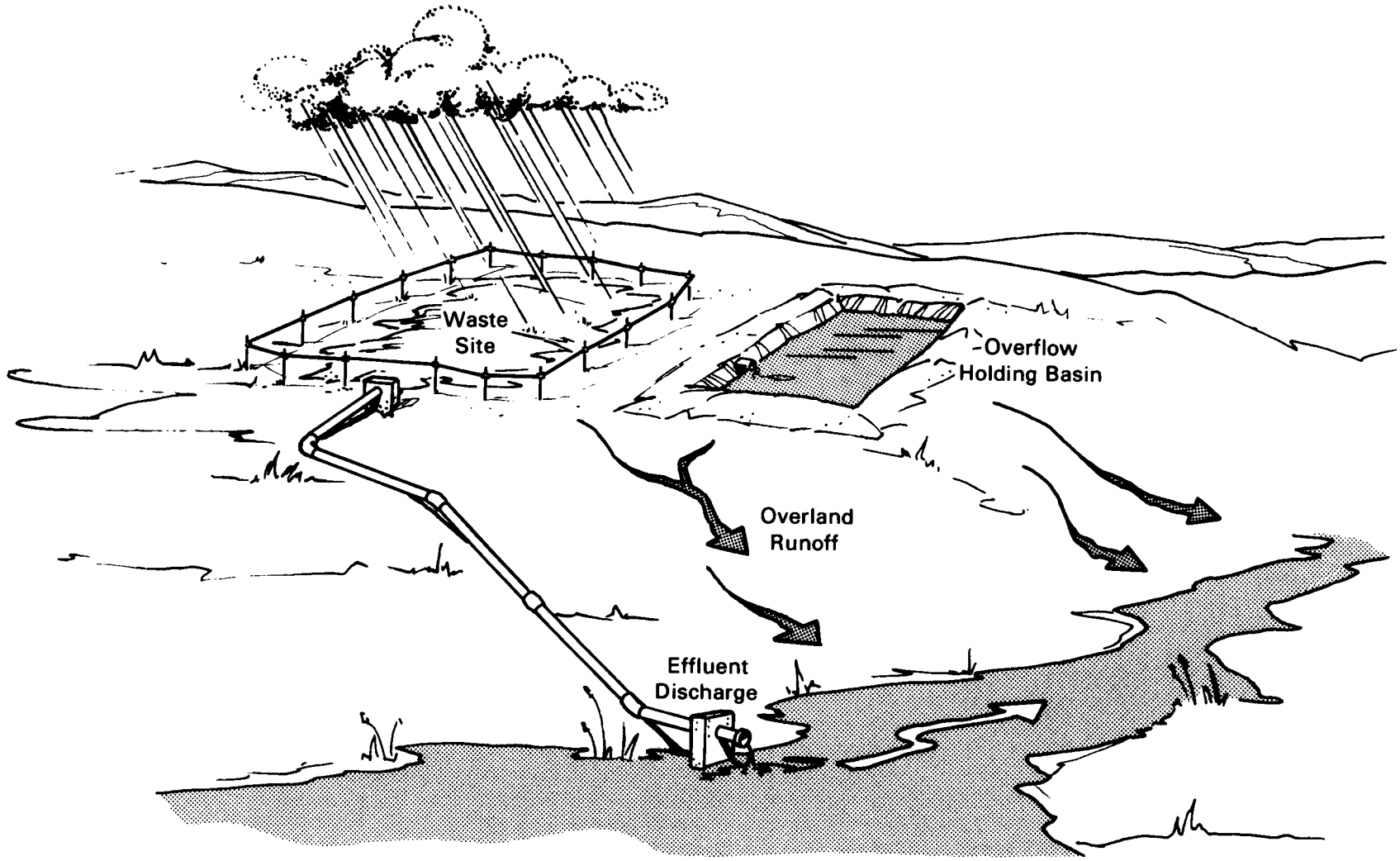

FIGURE 4.1. Schematic Diagram Illustrating the Overland Environment

Wischmeier and Smith (1958, 1978), Onstad et al. (1977), Foster (1976), Williams and Bernt (1976), Kuh et al. (1976), Onstad and Foster (1975), Stewart et al. (1975), Meyer (1974), and Foster and Wischmeier (1973).

The SCS curve number technique incorporates into its computations soil classifications, soil cover, land use treatment or practice, hydrologic condition for infiltration, locale (i.e., location within the United States), initial moisture abstraction, antecedent moisture conditions, and potential maximum moisture retention. The algorithms are empirically based and represent a method of estimating direct runoff volumes from storms.

The movement of contaminated sediments from the waste site is described with the Universal Soil Loss Equation (USLE). The USLE is an empirically derived formula that is based on 10,000 plot-years of erosion field research data. The USLE considers 1) the erosive force and intensity of precipitation and runoff in a normal year, 2) the susceptibility of soil particles to detachment and transport by precipitation and runoff, 3) the combined effects of slope length and gradient, and 4) the soil loss from lands under varying vegetative conditions (Goldman et al. 1986). It provides average-annual sediment loss from field-sized plots.

For locations with known contaminated sediment producing runoff events (e.g., known storm duration and intensity or precipitation-frequency information), a modified version of the USLE can be used. This modified USLE version, when combined with overland flow computations using the method of characteristics and kinematic wave approximation, estimates sediment loss from a field-sized plot for individual precipitation events (see Onstad and Foster 1975; Foster et al. 1977). The method of characteristics defines the path of wave propagation along which partial differential equations become ordinary differential equations to which analytical solutions are available; its use has been illustrated by Eagleson (1970), Hjelmfelt (1976), Croley (1978), Witinok (1979), Whelan (1980), and Witinok and Whelan (1980).

The procedure for implementing the algorithms associated with the overland pathway is diagrammed in Figure 4.2 and outlined on the following page.

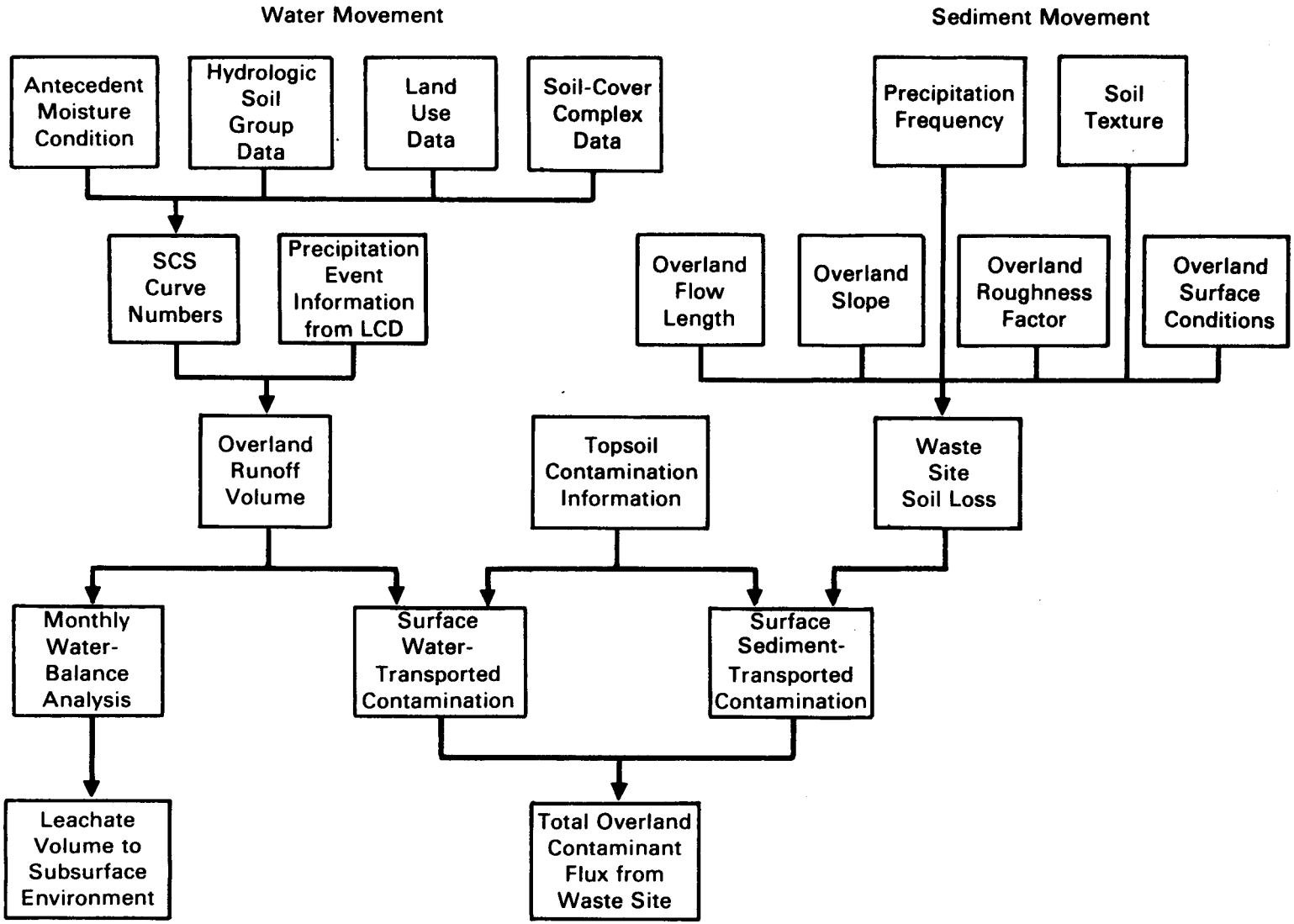

FIGURE 4.2. Flow Diagram of Overland Pathway Procedure (SCS = Soil Conservation Service)

A. Long-Term Average Runoff and Percolation

1. Determine overland runoff volume for historically averaged precipitation events

   a. Identify the average number of precipitation events that historically occur each month of the year and the average volume of precipitation for each month of the year. Assume that the volume of each precipitation event is equivalent to the monthly precipitation volume divided by the number of monthly events (see Section 3.8). The average monthly volume of precipitation can be obtained from Local Climatological Data: Annual Summary with Comparative Data for 1984, published by the Environmental Data Service, National Oceanic and Atmospheric Administration, National Climatic Data Center, U.S. Department of Commerce; this document is designated as LCD in this report. Each precipitation event has an associated runoff volume computed using the SCS curve number technique. The algorithms for combining the individual runoff volumes from each precipitation event are described in Chapter 3.0.

   b. Identify the catchment antecedent moisture conditions (AMC). The AMC refers to the moisture condition of the catchment with regard to the potential runoff of overland flow. The AMC can be crudely defined from low-resolution maps of the United States that cross-correlate surface soil groups, vegetative cover, temperature, moisture, land forms, and mineral and organic deposits (Shirazi et al. 1985[a]).

   c. Identify representative hydrologic soil groups within the catchment (i.e., soils that are classified according to runoff potential). The soil types in the region of concern can be obtained from county soil surveys developed by SCS. Nine thousand soil

(a) Shirazi, M. A., S. A. Peterson and J. W. Hart. 1985. "Computer-Based Mapping for Management of Hazardous Waste." Working Paper. U.S. Environmental Protection Agency, Corvallis, Oregon.

groupings have been developed by SCS. The county surveys can be combined with soil groupings to identify representative hydrologic soil groups.

d. Classify land use and treatment practices (i.e., types of land use and treatment practices that are classified on a runoff-producing basis). Guidance in determining land use and treatment practices is provided by SCS (1972).

e. Determine hydrologic soil-cover complexes (i.e., soil group and land use and treatment classes that are combined into hydrologic soil-cover complexes for determining curve numbers). The soil-cover complexes can be determined using SCS (1972).

f. Determine curve numbers from SCS (1972) or USBR (1977).

g. Compute the overland runoff volume based on curve numbers and precipitation events.

2. Determine the leachate volume to the subsurface environment by incorporating the overland runoff calculations from step 1 with the monthly water-balance analysis outlined in Chapter 3.0 to estimate the leachate volume to the subsurface environment.

3. Determine waste site soil loss

   a. Identify the rainfall volume associated with the 2-year, 6-hr precipitation-frequency event; these events can be defined using National Oceanic and Atmospheric Administration (NOAA) Precipitation-Frequency atlases of the United States.

   b. Determine the five factors that comprise the USLE. These factors incorporate precipitation frequency, soil texture, overland flow length, overland slope, surface roughness, and surface conditions.

   c. Estimate the soil loss from the waste site using the USLE.

B. Single Storm Event Runoff[a]

1. Determine overland flow hydrograph for single precipitation events

   a. Identify the design storm duration and intensity.

   b. Determine the overland runoff volume using the SCS curve number technique (e.g., similar to step A).

   c. Compute a representative overland slope. Data for computing overland slopes can be obtained from U.S. Geological Survey (USGS) 7.5-minute topographic contour maps.

   d. Estimate a representative overland roughness. The roughness value is based on information about land use, vegetative cover, and soil characteristics, among others, and can be obtained from Novotny and Chesters (1981), Foster et al. (1980), Whelan (1980), Morgan (1980), Novotny (1976), Rovey et al. (1977), Woolhiser (1974), Crawford and Linsley (1966), Henderson (1966a), and Chow (1959).

   e. Compute overland flow hydrographs by using the method of characteristics to spacially and temporally distribute the overland runoff volume determined earlier.

2. Determine waste site soil loss

   a. Identify the runoff volume and the rainfall intensity and volume associated with the design storm event's precipitation frequency (e.g., 2-year, 6-hr event); this event can be defined using NOAA Precipitation-Frequency atlases of the United States.

   b. Determine the five factors that comprise a modified version of the USLE. These factors incorporate precipitation frequency, soil texture, overland flow length, overland slope, surface roughness, and surface conditions.

(a) Note that steps A and B are separate, unrelated procedures.

c. Estimate the soil loss from the waste site using the modified USLE.

C. Overland Contaminant Flux from the Site

1. Identify or estimate contaminant levels on surface soils.

2. Determine the flux of contaminants transported by overland runoff (i.e., dissolved-phase flux). This contaminant flux can be computed by combining the overland runoff from step A or B with the contaminant levels identified in step 5a.

3. Determine the flux of contaminants transported with soils by overland runoff (i.e., solid-phase or particulate flux). This flux can be computed by combining the waste site soil loss determined in step A3 or B2 with the contaminant levels identified in step 5a.

4. Determine the total overland contaminant flux leaving the site by combining the solid- and dissolved-phase contaminant fluxes.

A complete description of the mathematical algorithms on which the overland pathway is based is provided in the following subsections. The runoff volume computations are described first; sediment loss calculations are described second; single-event overland flow equations that spacially and temporally distribute the overland runoff volume are described third; and finally, overland contaminant flux calculations are presented.

4.2 RUNOFF VOLUME COMPUTATIONS

This subsection presents the algorithms for estimating the volume of precipitation that eventually represents overland flow. The calculations are based on the SCS curve number technique as presented by SCS (1972, 1982), Kent (1973), and USBR (1977).

The amount of water retained for overland runoff can be expressed as

$$R = V_{max} - V \tag{4.1}$$

where R = actual retention after runoff begins (cm)[a]

V_{max} = maximum potential runoff or actual rainfall after runoff starts, including abstraction (cm)

V = actual runoff (cm).

The maximum potential runoff or actual rainfall after runoff begins, including abstraction, can be expressed as

$$V_{max} = P - I_a \tag{4.2}$$

where P = precipitation (cm)[b]

I_a = initial abstraction (cm).

Rainfall and runoff data from a large number of small experimental watersheds empirically indicated (SCS 1972; Kent 1973) that the initial abstraction is related to the potential maximum retention by

$$I_a = 0.2\ S \tag{4.3}$$

where S = potential maximum retention by any means after runoff begins (cm)

The assumed relationship between precipitation runoff and retention, as indicated by Schroeder et al. (1984), can be expressed as

$$\frac{R}{S} = \frac{V}{V_{max}} \tag{4.4}$$

(a) The SCS curve number technique uses English units (e.g., inches). To be consistent with other chapters of the report, all equations have been converted to account for appropriate metric units.

(b) Precipitation includes rainfall and snowfall. Overland runoff occurs only when the monthly average temperature is above freezing. The equivalent water volume for any snowfall accumulated during subfreezing months is linearly added to the precipitation of the next month in which the average monthly temperature is above freezing. This topic is discussed in more detail in Chapter 3.0.

Rearranging Equation (4.4) and substituting Equations (4.1), (4.2), and (4.3) gives

$$V = \frac{(P - 0.2\ S)^2}{(P + 0.8\ S)} \quad \text{for} \quad P \geq 0.2\ S \tag{4.5}$$

In SCS (1972), the potential retention is related to a curve number parameter that represents the soil type and soil characteristics. The relationship is expressed as

$$CN = \frac{1000}{\frac{S}{2.54} + 10} \tag{4.6}$$

where CN = curve number.
The curve number expresses the relationship between rainfall, runoff, and AMC.

The amount of rainfall in a period of 5 to 30 days before a particular storm is referred to as antecedent rainfall, and the resulting condition of the watershed with regard to potential runoff is the AMC (USBR 1977). Three types of antecedent moisture conditions are identified by SCS (1972) and USBR (1977):

- Type I (AMC-I) refers to watershed soils under dry conditions.
- Type II (AMC-II) refers to watershed soils under normal moisture conditions.
- Type III (AMC-III) refers to watershed soils under wet conditions.

The AMC of a catchment is difficult to define for a particular storm; however, research by Schumm (1977), after Langbein and Schumm (1958) and Langbein et al. (1949), shows that overland runoff can indirectly be a function of mean annual precipitation, vegetative cover, and mean annual temperature. Schumm (1977) illustrates this relationship with a series of figures, one of which is shown in Figure 4.3.

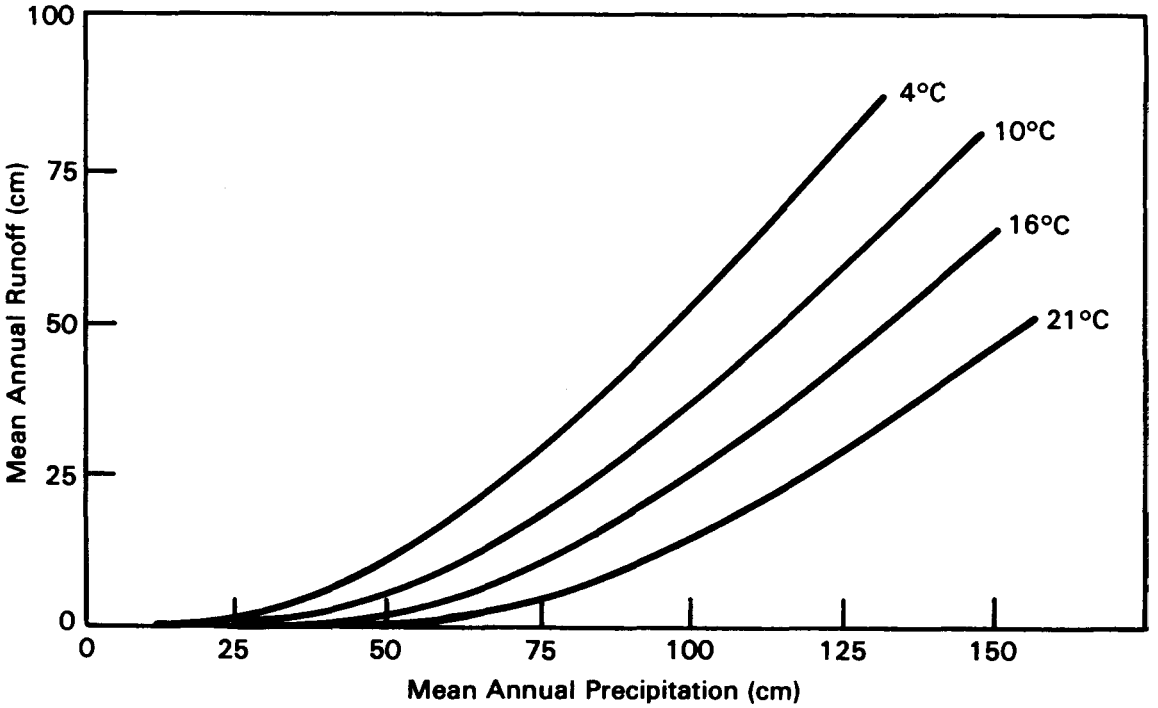

FIGURE 4.3. The Effect of Average Temperature on the Relationship Between Mean Annual Runoff and Mean Annual Precipitation (1 in. = 2.54 cm) (After Langbein et al. 1949 as reported by Schumm 1977)

Shirazi et al. (1985)[a] have developed low-resolution maps of the United States that cross-correlate surface soil groups, vegetative cover, temperature, moisture, land forms, and mineral and organic deposits. Figure 4.4, one of these maps, shows aridity as a function of location. Based on this map, the AMC can be estimated as follows:

- AMC-I conditions are represented by warm and dry soil designations.
- AMC-II conditions are represented by warm and moist and by cool and moist soil designations.
- AMC-III conditions are represented by warm and wet and by cool and wet soil designations.

(a) Shirazi, M. A., S. A. Peterson and J. W. Hart. 1985. "Computer-Based Mapping for Management of Hazardous Waste." Working Paper. U.S. Environmental Protection Agency, Corvallis, Oregon.

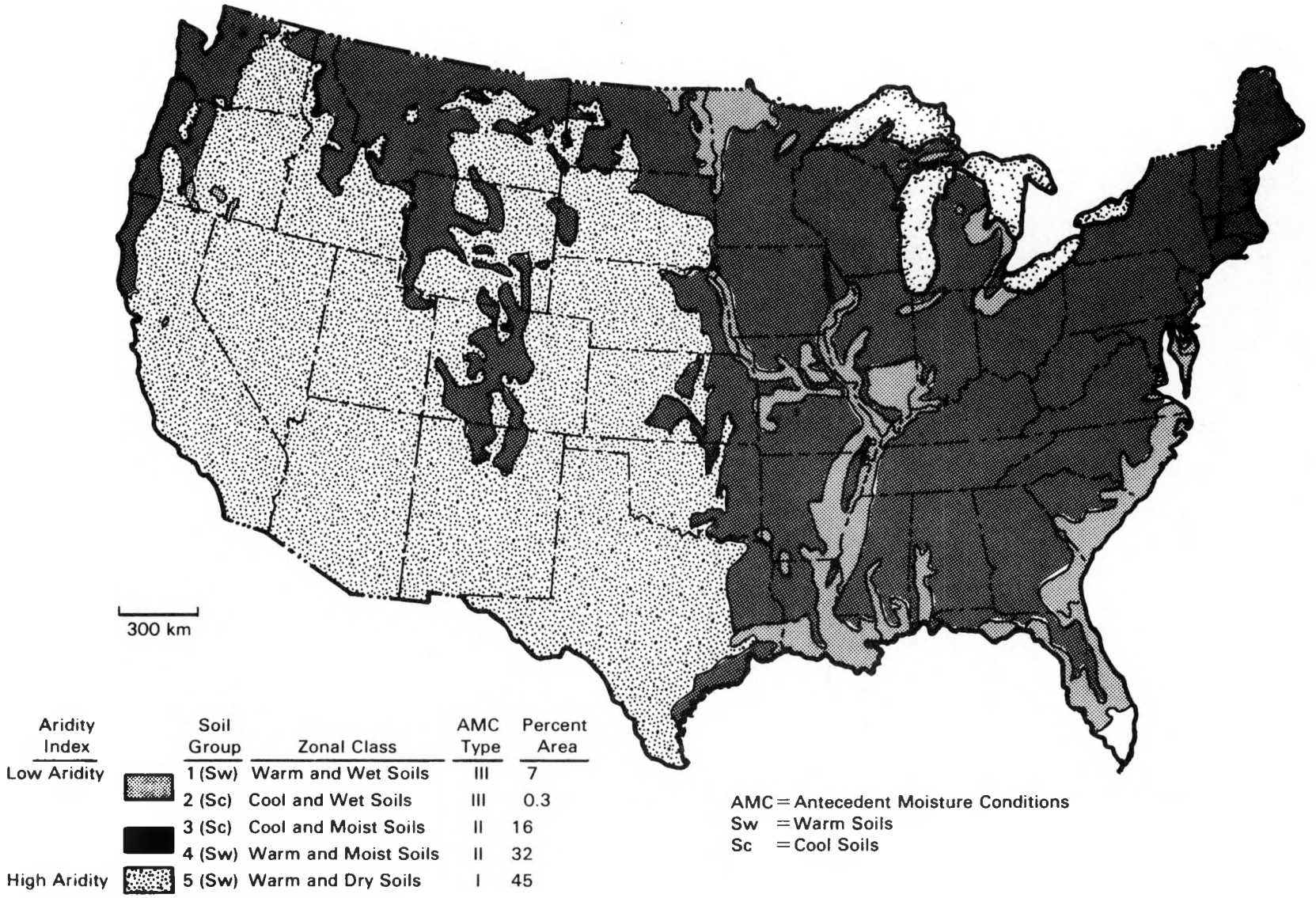

FIGURE 4.4. Zonal Soils of the United States Based on Aridity (Source: M. A. Shirazi, S. A. Peterson and J. W. Hart. 1985. "Computer-Based Mapping for Management of Hazardous Waste." Working Paper. U.S. Environmental Protection Agency, Corvallis, Oregon.)

The relationships between curve numbers and AMC-I, AMC-II, and AMC-III are presented in Table 4.1. The table can also be used to relate AMC-I curve numbers with those of AMC-II and AMC-III.

The low-resolution maps crudely define watershed characteristics on a regional scale. Areas not having meteorological information are placed with areas described by the meteorological data, even though each of the areas may have significantly different characteristics. For example, on the basis of its aridity index, Figure 4.4 indicates the absence of forests in some of the western areas of the United States, although forests exist. For these areas, the user should assume a moist soil condition and use AMC-II data.

To assess the runoff volume from an overland segment that was caused by a particular precipitation event using Equation (4.5), the curve number and, hence, the potential maximum retention (S) for that segment must be determined. Based on research by SCS, USBR (1977) presents a methodology for estimating curve numbers for various hydrologic soil groups, land uses, and hydrologic soil-cover complexes in the eastern and western United States. They have subdivided this analysis into three steps (which are described separately in Section 4.2.1):

1. identification of representative hydrologic soil groups -- Soils are classified according to runoff potential by being identified with one of four soil groups (A, B, C, or D).

2. classification of land use and treatment practices -- Types of land use and treatment practices are classified on a runoff-producing basis.

3. determination of hydrologic soil-cover complexes -- Soil group and land use and treatment classes are combined into hydrologic soil-cover complexes for determining curve numbers.

TABLE 4.1. Relative Curve Numbers for Antecedent Moisture Conditions Types I, II, and III (After USBR 1977)

AMC-I	AMC-II	AMC-III	AMC-I	AMC-II	AMC-III
100	100	100	40	60	78
97	99	100	39	59	77
94	98	99	38	58	76
91	97	99	37	57	75
89	96	99	36	56	75
87	95	98	35	55	74
85	94	98	34	54	73
83	93	98	33	53	72
81	92	97	32	52	71
80	91	97	31	51	70
78	90	96	31	50	70
76	89	96	30	49	69
75	88	95	29	48	68
73	87	95	28	47	67
72	86	94	27	46	66
70	85	94	26	45	65
68	84	93	25	44	64
67	83	93	25	43	63
66	82	92	24	42	62
64	81	92	23	41	61
63	80	91	22	40	60
62	79	91	21	39	59
60	78	90	21	38	58
59	77	89	20	37	57
58	76	89	19	36	56
57	75	88	18	35	55
55	74	88	18	34	54
54	73	87	17	33	53
53	72	86	16	32	52
52	71	86	16	31	51
51	70	85	15	30	50
50	69	84	12	25	43
48	68	84	9	20	37
47	67	83	6	15	30
46	66	82	4	10	22
45	65	82	2	5	13
44	64	81	0	0	0
43	63	80			
42	62	79			
41	61	78			

4.2.1 Hydrologic Soil Groups

Four major soil groups are used in estimating overland runoff (USBR 1977):

- Group A soils have high infiltration rates[a] and low runoff potential even when thoroughly wetted and consist chiefly of deep, well-drained to excessively drained sands or gravels. These soils have a high rate of water transmission[b] (i.e., percolation).
- Group B soils have moderate infiltration rates when thoroughly wetted and consist chiefly of moderately deep to deep, moderately well-drained to well-drained soils with moderately fine to moderately coarse textures. These soils have a moderate rate of water transmission.
- Group C soils have slow infiltration rates when thoroughly wetted and consist chiefly of soils with a layer that impedes downward movement of water or soils with moderately fine to fine texture. These soils have a slow rate of water transmission.
- Group D soils have very slow infiltration rates and high runoff potential when thoroughly wetted and consist chiefly of clay soils with a high swelling potential, soils with a permanently high water table, soils with a claypan or clay layer at or near the surface, and shallow soils over nearly impervious material. These soils have a very slow rate of water transmission.

Each overland segment is classified as being in one of the four major hydrologic groups. A portion of the major U.S. soil types listed by SCS (1982) (those that are of major importance locally or of major extent) is presented in Table 4.2. The capital letter following the soil type in Table 4.2 represents the soil group designation. Soils with unknown soil groups can be compared to the table for assigning a soil group. Soil names for particular areas can be

---

(a) The infiltration rate, the rate at which water enters the soil at the surface, is controlled by surface conditions.
(b) The transmission rate, the rate at which the water moves in the soil, is controlled by the soil horizons.

TABLE 4.2. Example Soil Names and Hydrologic Soil Group Classifications (After SCS 1982)

AABAB	D	ACKLEY	B	ADRIAN	A/D
AABERG	D	ACKMEN	B	ADVOKAY	D
AASTAD	B	ACKMORE	B	AECET	C
AAZDANL	B	ACKWATER	D	AENEAS	B
ABAC	D	ACME	C	AFTADEN	D
ABAJG	C	ACO	B	AFTOM	C/D
ABARCA	B	ACOMA	C	AGAIPAH	D
ABBOTT	D	ACORD	C	AGAN	D
ABBOTTSTOWN	C	ACOVE	C	AGAR	B
ABCAL	D	ACREDALE	D	AGASSIZ	D
ABEGG	B	ACREE	C	AGATE	D
ABELA	B	ACRELANE	C	AGATHA	B
ABELL	B	ACTON	B	AGAMAN	B
ABERDEEN	C	ACUFF	B	AGENCY	C
ABERONE	B	ACUNA	C	AGER	D
ABERT	B	ACY	C	AGET	B
ABES	D	ADA	C	AGNAL	D
ABGESE	B	ADAIR	C	AGNESTON	B
ABILENE	C	ADAMS	A	AGNESTON, COBBLY SUBSTRATUM	C
ABIQUA	C	ADAMSON	B		
ABO	C	ADAMSVILLE	C	AGNEW	C
ABOR	D	ADATON	D	AGNOS	D
ABRA	C	ADAVEN	C	AGUA	B
ABRA, BEDROCK SUBSTRATUM	B	ADDICKS	D	AGUA DULCE	B
		ADDIELOU	B	AGUA FRIA	B
ABRA, DRY	B	ADE	A	AGUADILLA	A
ABRAHAM	B	ADEL	B	AGUALT	B
ABRAZO	D	ADELAIDE	D	AGUEDA	B
ABRAZO, GRAVELLY	C	ADELANTO	B	AGUILARES	B
ABRAZO, COBBLY	D	ADELINO	B	AGUILITA	B
ABREU	B	ADELINO, SALINE-ALKALI	C	AGUIRRE	D
ABSAROKEE	C			AGUSTIN	B
ABSCOTA	A	ADELPHIA	C	AHL	C
ABSHER	D	ADENA	C	AHLSTROM	D
ABSTED	C	ADGER	D	AHMEEK	C
ABSTON	C	ADILIS	B	AHOLT	D
ACACIO	B	ADJUNTAS	C	AHREN	B
ACADEMY	C	ADKINS	B	AHRNKLIN	C
ACADIA	D	ADKINS, ALKALI	B	AHTANUM	D
ACANA	D	ADKINS, WET	C	AHTANUM, DRAINED	C
ACANOD	C	ADKINS, HARDPAN SUBSTRATUM	B	AHWAHNEE	B
ACASCO	D			AIBONITO	C
ACEITUNAS	B	ADKINS, GRAVELLY SUBSTRATUM	B	AIDO	D
ACEL	C			AIKEN	B
ACKER	B	ADLER	C	AIKMAN	D
ACKERMAN	A/D	ADMAN	D	AIKMAN, STONY	C
ACKERVILLE	C	ADOLPH	B/D	AILEY	B
ACKETT	D	ADOS	C	AIMELIIK	B

found on agricultural soil maps (e.g., SCS county soil survey maps) that are available for most of the United States. The maps describe the characteristics of the land surface [to depths up to 18 m (6.0 ft)] and indicate soil classifications according to color, structure, texture, physical constitution, chemical composition, biological characteristics, and morphology; a map of the area surveyed is usually included (USBR 1977).

If an overland segment is composed of several soil groups that are interspersed, soil groupings are determined as a percentage of the total area. An example of these computations by SCS (1982) is presented in Figure 4.5. The SCS (1982) notes that precise measurement of soil group areas, such as by planimetry of soil areas on maps or by weighing map cuttings, is seldom necessary for hydrologic purposes. The detail should not go beyond that illustrated by Figure 4.5. In Figure 4.5a, the individual soils in a hydrologic unit are shown on a sketch map; in Figure 4.5b, the soil types are classified into soil groups; in Figure 4.5c, a grid is placed over the map, and the numbers of grid intersections falling on each group are counted and tabulated; and in Figure 4.5d, a typical computation and tabulation of soil group percentages is shown. Simplified versions of this procedure are generally used in practice.

4.2.2 Land Use and Treatment Classification

After the soil groups of the catchment have been identified, types of land use and treatment are classified. The greater the ability of a given land use or treatment pattern to increase the total retention time of overland runoff, the lower the runoff volume will be.

Various land use and treatment classes are identified by USBR (1977). Each class is briefly discussed below.

- native pasture and range -- Three hydrologic conditions not associated with forage production are used to describe native pastures or ranges.
  - poor pasture or range: The pasture or range is heavily grazed, has no mulch (a mixture of manure and compost, used as a fertilizer), or has plant cover of less than 50%.

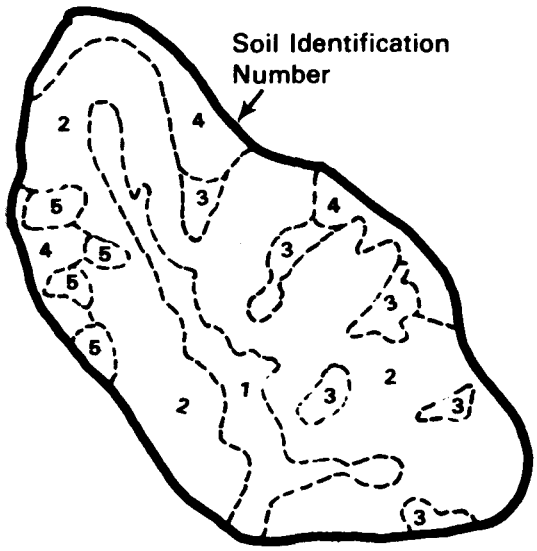

(a) Detailed Soils Map

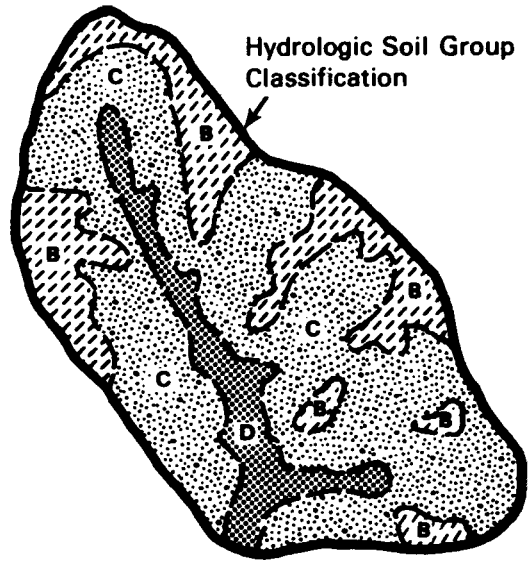

(b) Hydrologic Soil Group Map

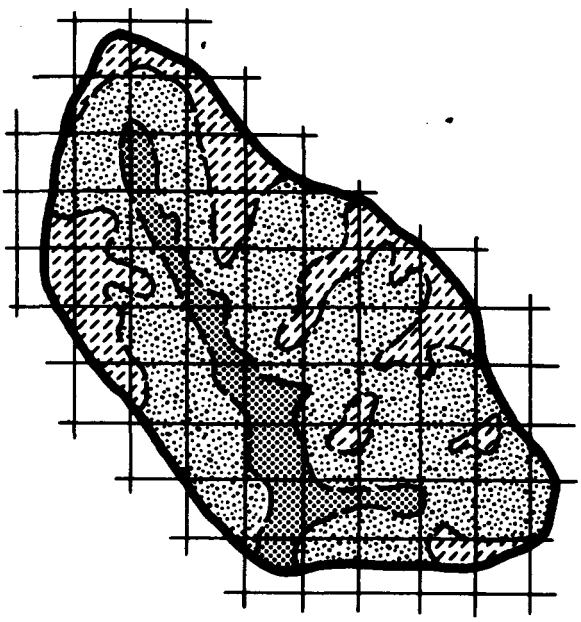

(c) Grid on Soil Group Map

Soil Group	Number Grid Intersections	Percent
B	12	23*
C	63	63
D	7	14
Total	51	100

*Percent for B: (100) 12/51 = 23

(d) Computations

FIGURE 4.5. Steps in Determining Percentages of Soil Groups (After SCS 1982)

- fair pasture or range: The pasture or range has plant cover of 50% to 75% and is not heavily grazed.

- good pasture or range: The pasture or range has plant cover of more than 75% and is slightly grazed.

- farm woodlots -- Three hydrologic factors not based on timber production are used to describe farm woodlots.

  - poor woodlots: Poor woodlots are heavily grazed and regularly burned in a manner that destroys litter, small trees, and brush.

  - fair woodlots: Fair woodlots may be grazed but not burned and may have some litter.

  - good woodlots: Good woodlots are protected from grazing so that litter and shrubs cover the soil.

- forest -- The hydrologic condition classes for forest cover are determined by the depth and quality of litter and humus, and the compactness of humus. They are also divided between the western and eastern portions of the United States.

- crop rotations -- Hydrologic effects of crop rotation range from poor (or weak) to good (or strong), based largely on the amount of dense vegetation in the rotation. The sequence of rotation of crops on a land segment must be evaluated on the basis of its hydrologic effects.

  - poor rotation: Row crop or small grain is planted in the same field year after year. A poor rotation may combine row crops, small grains, or fallow in various ways.

  - good rotation: Alfalfa or other close-seeded legumes or grasses are included in the rotation to improve tilth and increase infiltration.

- straight-row farming -- This class includes up-and-down and cross-slope farming in straight rows. In areas of 1% to 2% slope, cross-slope farming in straight rows is almost the same as contour farming.

- contouring -- Contour farming reduces surface runoff with increasing effectiveness as the overland slope decreases. Contour furrows may be small or large, depending on planting, cultivation, and climatic conditions. Average conditions from experimental watersheds with slopes of 3% to 8% are assumed in curve number calculations.

- terracing -- The effects of graded and open-level terraces are considered in computing curve numbers; the effects of both contouring and grass waterway outlets are considered. Closed-end terraces should be handled like contour furrows.

- miscellaneous -- Farmsteads, roads, and urban areas, where significant, are considered in determining curve numbers. However, these areas are usually very small and may be included with one of the other land use cover types, where applicable. In areas where a significant portion of the overland segment is developed, the curve number would equal 100.

4.2.3 Hydrologic Soil-Cover Complexes

The SCS (1972) and USBR (1977) combine soil groups and land use and treatment practices into hydrologic soil-cover complexes for the actual determination of curve numbers. The determination of curve numbers is presented in Tables 4.3 through 4.5 and Figures 4.6 and 4.7. The relationships for converting from AMC-II to AMC-I or AMC-III are presented in Table 4.1.

Table 4.3 presents runoff curve numbers for hydrologic soil-cover complexes, not including forested lands. Forest cover is included in Tables 4.4 and 4.5 and Figures 4.6 and 4.7. For all of the tables and figures, curve numbers associated with AMC-II are assumed. Because Table 4.3 is self-explanatory, only the figures and tables associated with forested lands will be discussed further.

Forest in the Eastern United States

In the humid forest regions of the eastern United States, three parameters are used to determine the curve number: the humus depth, compactness factor, and hydrologic condition class. Each is discussed below (USBR 1977).

TABLE 4.3. Runoff Curve Numbers Associated with AMC-II for Various Hydrologic Soil-Cover Complexes (After USBR 1977)

Land Use and Treatment or Practice	Hydrologic Condition	Hydrologic Soil Group A	B	C	D
Fallow					
Straight row	--	77	86	91	94
Row crops					
Straight row	Poor	72	81	88	91
Straight row	Good	67	78	85	89
Contoured	Poor	70	79	84	88
Contoured	Good	65	75	82	86
Contoured and terraced	Poor	66	74	80	82
Contoured and terraced	Good	62	71	78	81
Small grain					
Straight row	Poor	65	76	84	88
Straight row	Good	63	75	83	87
Contoured	Poor	63	74	82	85
Contoured	Good	61	73	81	84
Contoured and terraced	Poor	61	72	79	82
Contoured and terraced	Good	59	70	78	81
Close-seeded legumes or rotation meadow					
Straight row	Poor	66	77	85	89
Straight row	Good	58	72	81	85
Contoured	Poor	64	75	83	85
Contoured	Good	55	69	78	83
Contoured and terraced	Poor	63	73	80	83
Contoured and terraced	Good	51	67	76	80
Pasture or range					
No mechanical treatment	Poor	68	79	86	89
No mechanical treatment	Fair	49	69	79	84
No mechanical treatment	Good	39	61	74	80
Contoured	Poor	47	67	81	88
Contoured	Fair	25	59	75	83
Contoured	Good	6	35	70	79
Meadow	Good	30	58	71	78
Woods	Poor	45	66	77	83
	Fair	36	60	73	79
	Good	25	55	70	77
Farmsteads	--	59	74	82	86
Roads[a]					
Dirt	--	72	82	87	89
Hard surface	--	74	84	90	92

Forest lands (eastern and western United States) - See Figures 4.6 and 4.7 and Tables 4.7 and 4.5.

(a) Including rights-of-way.

TABLE 4.4. Runoff Curve Numbers Associated with AMC-II for Various Hydrologic Condition Classes (After USBR 1977)

Hydrologic Condition Class	Hydrologic Soil Group A	B	C	D
I. Poorest	56	75	86	91
II. Poor	46	68	78	84
III. Medium	36	60	70	76
IV. Good	26	52	62	69
V. Best	15	44	54	61

TABLE 4.5. Runoff Curve Numbers Associated with AMC-II for Various Forest Range Areas in the Western United States (After USBR 1977)

Cover	Condition	Soil Groups A	B	C	D
Herbaceous	Poor		78	85	92
	Fair		68	81	88
	Good		59	71	84
Sagebrush	Poor		64	78	
	Fair		46	67	
	Good		35	46	
Oak-Aspen	Poor		63	71	
	Fair		40	54	
	Good		30	40	
Juniper	Poor		73	84	
	Fair		54	70	
	Good		40	59	

- humus depth -- The undecomposed leaves, needles, twigs, bark, and other vegetative debris on the forest floor form the litter from which humus is derived. Humus is therefore the organic layer immediately below the litter layer from which it is derived. Natural litter protects humus from oxidation (i.e., decomposition) and, therefore, indirectly enters into its determination. The humus layer may consist of mor or mull. Mor (also known as mor humus) is practically pure organic matter unrecognizable as to its origin from the material lying on the forest floor; mull is an intimate mixture of organic

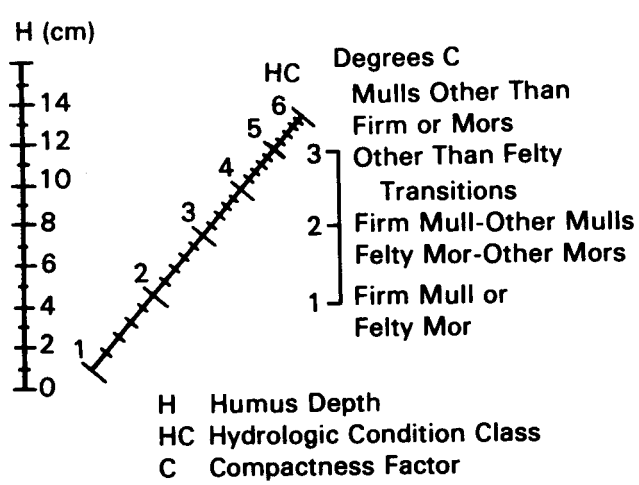

(a) Present Hydrologic Condition of Forest and Woodland

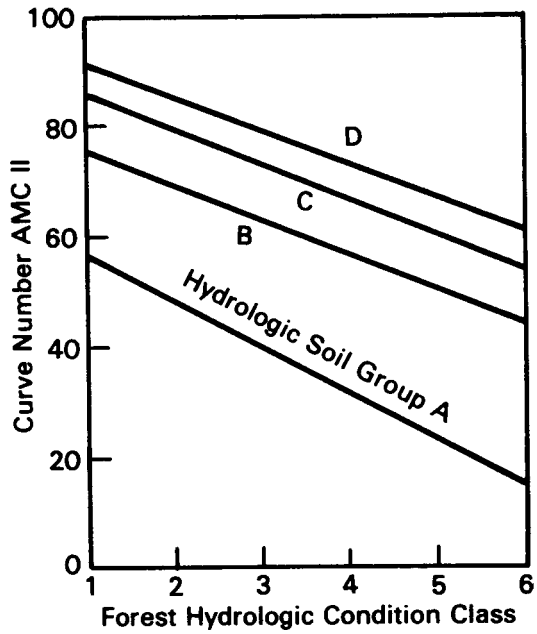

(b) Curve Number by Hydrologic Soil Group and Forest Hydrologic Condition Classes

FIGURE 4.6. Chart for Determining Curve Number for Humid Forest Regions in the Eastern United States (1 in. = 2.54 cm) (After USBR 1977)

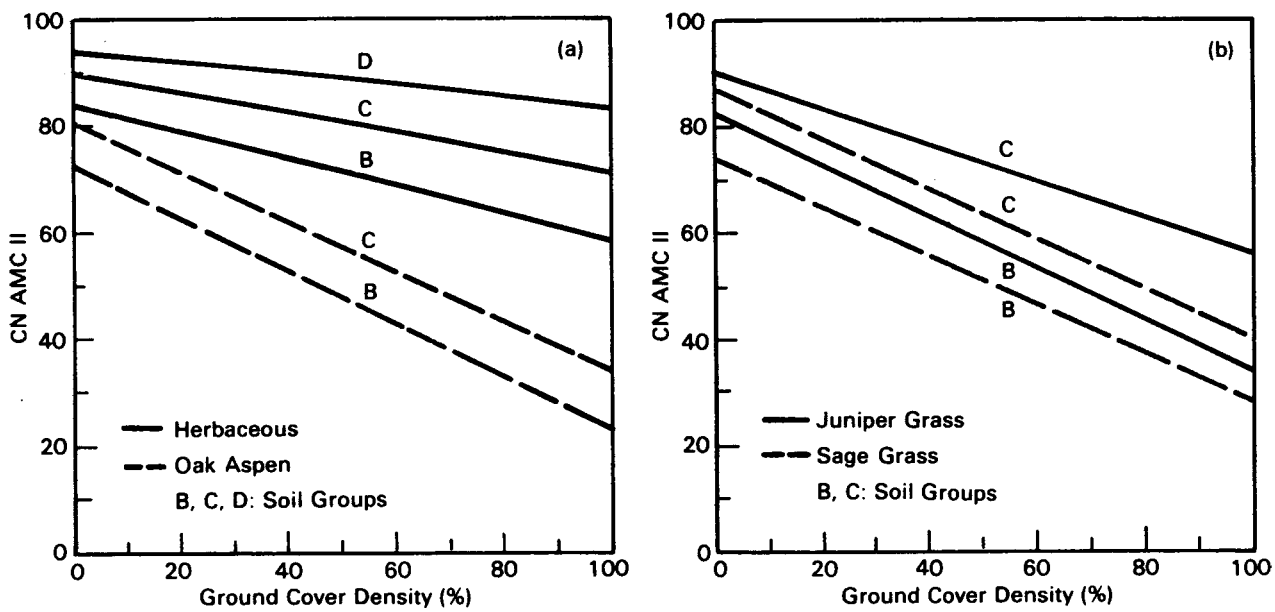

FIGURE 4.7. Chart for Determining Curve Number for Forest Range Areas in the Western United States (After USBR 1977)

matter and mineral soil. Humus depth increases with the age of a forest stand until an equilibrium is reached between the processes that build humus up and those that break it down. A humus depth of 12 to 15 cm (5 to 6 in.) is considered maximum under favorable management conditions (i.e., proper use, protection, and improvement). Humus is porous and has high infiltration and storage capacities. Under poor management conditions (burning, overcutting, or overgrazing), humus can be compacted to impede the absorption of water.

- compactness factor -- Humus is also characterized by its degree of compaction.
  - compact: Mulls are firm; mors are felty (watertight, heavy layers of organic fibers). Frost in compact humus would be considered a compact form.
  - moderately compact: A transition stage exists.
  - loosely compact: Mulls are not firm; mors are not felty.
- hydrologic condition class -- The hydrologic condition represents the runoff-producing potential of a forest area. The condition is indicated by a number ranging from 1 to 6; the lower the number, the higher the runoff-producing potential.

The relationship between the condition class, soil group, and curve number for the AMC-II humus depth and compaction is illustrated in Figure 4.6. The USBR (1977) suggests that if field data on forest watershed conditions are meager, Table 4.4 may be used to estimate the runoff curve number.

Forest in the Western United States

In the forest range regions of the western United States, USBR (1977) indicates that the principal parameters for estimating the curve number are soil group, cover type, and cover density. Figure 4.7 illustrates the relationship between these factors and curve numbers for current soil-cover complexes. The cover types are defined as follows (USBR 1977):

- herbaceous -- grass-weed-brush mixtures, with brush the minor element
- oak-aspen -- mountain brush mixtures of oak, aspen, mountain mahogany, litter brush, maple, and other brush
- juniper grass -- juniper or piñon with an understory of grass
- sage grass -- sage with an understory of grass.

When Figure 4.7 is being used, the amount of litter should be taken into account in estimating the density of cover. If data pertaining to the ground cover density are unavailable, runoff curve numbers may be estimated from Table 4.5.

4.2.4 Monthly Overland Runoff Volume

The SCS CN technique (Kent 1973; SCS 1972, 1982; USBR 1977) is used to compute the overland runoff portion of the monthly water balance at the waste site. Computations for computing landfill infiltration using the CN technique are based on the landfill surface characteristics. The soil cover will represent the soil type, and the vegetation cover will represent the vegetation type. To distribute the monthly volume of precipitation, we assume the following:

1. The monthly volume of precipitation can be equally distributed among the total number of recorded precipitation events with 3.9×10^{-3} cm (0.01 in.) or more of volume.
2. The number of precipitation events can be defined by LCD summaries (see Figure 3.2).
3. Precipitation is stored on the land surface in the form of snow when adjusted average monthly temperatures are equal to or below freezing; precipitation is in the form of rainfall when temperatures are above freezing.

Using the CN technique, the overland flow equation for a single precipitation event is described by

$$V_i = \frac{(P_i - 0.2\ S)^2}{(P_i + 0.8\ S)} \quad \text{for } P_i \geq 0.2\ S \tag{4.7}$$

in which

$$S = \frac{[1000 - 10\ (CN)]\ a}{(CN)} \tag{4.8}$$

where V_i = actual runoff volume for a storm event for the i-th month (cm)

P_i = net daily precipitation for the i-th month (cm)

S = potential maximum retention by any means <u>after</u> runoff begins (cm)

a = conversion parameter between centimeters and inches ($a = 2.54$)

CN = curve number.

The daily or event precipitation can be computed by

$$P_i = \frac{Pm_i}{m_i} \tag{4.9}$$

where m_i = mean number of days during the month i with 3.9×10^{-3} cm (0.01 in.) or more of precipitation.

The m_is are obtained from LCDs, as illustrated in Figure 3.2.

The total monthly runoff from the waste site can be computed by summing the runoff from the individual storm events.

$$Vm_i = \sum_{j=1}^{m_i} V_i = \sum_{j=1}^{m_i} \left[\frac{(Pm_i/m_i - 0.2\ S)^2}{Pm_i/m_i + 0.8\ S}\right] = \left[\frac{(Pm_i - 0.2\ m_i\ S)^2}{(Pm_i + 0.8\ m_i\ S)}\right] \tag{4.10}$$

where Vm_i = monthly runoff volume for the i-th month (cm)

j = index on the mean number of days during the month i with 3.9×10^{-3} cm (0.01 in.) or more precipitation ($1 \leq j \leq m_i$).

Combining Equations (4.8) and (4.10) gives the total monthly runoff as

$$Vm_i = \frac{[Pm_i\ (CN) - 0.2\ a\ m_i\ [1000 - 10\ (CN)]]^2}{(CN)\ [Pm_i\ (CN) + 0.8\ a\ m_i\ [1000 - 10\ (CN)]]} \tag{4.11}$$

It is assumed that the runoff calculations using the CN technique are applicable even though snow may be covering the land. This condition rarely occurs, however, because most snow is usually melted in the first month the average temperature rises above freezing. By substituting the monthly precipitation adjusted for snowmelt [see Equation (3.37)] for the average monthly precipitation volume (i.e., Pm_i), Equation (4.11) becomes

$$Vm_i = \frac{[Pms_i\ (CN) - 0.2\ a\ m_i [1000 - 10\ (CN)]]^2}{(CN)\ [Pms_i\ (CN) + 0.8\ a\ m_i\ [1000 - 10\ (CN)]]} \tag{4.12}$$

$$\text{for} \begin{cases} [Pms_i\ (CN)] \geq [0.2\ a\ m_i\ [1000 - 10\ (CN)]] \\ T_i > 0^0C \end{cases}$$

$$Vm_i = 0 \tag{4.13}$$

$$\text{for} \begin{cases} [Pms_i\ (CN)] < [0.2\ a\ m_i\ [1000 - 10\ (CN)]] \\ T_i \leq 0^0C \end{cases}$$

4.2.5 Summary of Runoff Volume Computations

This subsection presents the algorithms for estimating the volume of precipitation that eventually represents overland flow. The calculations are based on the SCS CN technique. Equation (4.6) can be rearranged to use a CN to estimate the maximum potential retention (S). The actual monthly overland runoff volume (Vm) is then computed by using Equations (4.12) and (4.13).

4.3 SEDIMENT LOSS CALCULATIONS

The most widely used method for predicting soil loss from overland areas is the USLE (Novotny and Chesters 1981; Overcash and Davidson 1980; Mitchell and Bubenzer 1980). Overcash and Davidson (1980) note that the USLE "is and will continue to be for the forseeable future, the best equation for estimating long term, average-annual and monthly soil loss." The USLE was developed to predict average-annual soil loss from sheet, rill, and interrill erosion. Sheet erosion refers to sediment movement from small natural areas having little topographic relief (Eagleson 1970). Rill erosion refers to concentrated soil movement due to channelized flow (Meyer 1974). Interrill erosion refers to uniform soil movement in the remaining areas between rills; interrill erosion results primarily from raindrop impact (Meyer 1974).

Wischmeier (1976) notes that the USLE may be used to predict average-annual soil loss from a field-sized plot with specified land use conditions (Mitchell and Bubenzer 1980). The assumptions associated with the USLE are as follows (Goldman el al. 1986; Novotny and Chesters 1980; Foster 1976; Onstad and Foster 1975):

- The USLE is an empirically derived algorithm and does not mathematically represent the actual erosion process.
- The USLE was developed to estimate long-term, average-annual or seasonal soil loss. Unusual rainfall seasons, especially higher than normal rainfall and atypically heavy storms, may produce more sediment than estimated.
- The USLE estimates soil loss on upland areas only; it does not estimate sediment deposition. Sediment deposition generally occurs at the bottom of a slope (i.e., change in grade) where the slope becomes milder.
- The USLE estimates sheet, rill, and interrill erosion and does not estimate channel or gully erosion. Gully erosion, caused by concentrated flows of water, is not accounted for by the equation and yet can produce large volumes of eroded soil.

- The USLE was developed originally to address soil loss from field-sized plots, although with proper care, watersheds can be addressed.
- Because the USLE only estimates the volume of sediment loss (i.e., the volume of soil detached and transported some distance), it can be used to estimate sediment transport capacity at a site.
- Because the USLE represents an empirically derived expression, consistently accurate estimates of soil loss are fortuitous at best.[a]
- The USLE does not estimate soil loss from single storm events unless a modified form of the original equation is used.

The general form of the USLE, as expressed in metric units, is as follows (Goldman et al. 1986):

$$A = R\ K\ LS\ C\ P \tag{4.14}$$

where A = average-annual soil loss (t/ha)[b]
R = rainfall erosivity factor (J/ha)
K = soil erodibility factor (t/J)[c]
LS = slope length and steepness factor (dimensionless)
C = vegetative cover factor (dimensionless)
P = erosion control practice factor (dimensionless)

To calculate soil loss, each of the factors is assigned a numerical value. The five factors are then multiplied together to produce an estimate of the soil eroded from the site in an average year. Goldman et al. (1986) note that the USLE is most effective when evaluation of site characteristics is done over areas no larger than 40 ha (100 ac). To produce the most representative

(a) Although the USLE is best used to evaluate the relative effectiveness of different land use patterns and practices, this does not diminish its utility for predicting soil loss, especially as it relates to the RAPS methodology.
(b) One hectare (ha) equals 10,000 m^2.
(c) The parameter "t" refers to metric tonnes.

results, the soil loss analysis at the waste site should be conducted over areas that have similar conditions. Generally, the waste sites are small enough such that these criteria are approximately met. At sites where these conditions cannot be approximated, the site can be subdivided into smaller areas. The five factors comprising the USLE are discussed in more detail as follows.

4.3.1 Rainfall Erosivity Factor

The rainfall erosivity factor (R-factor) is based on kinetic energy considerations of falling rain (Whelan 1980) and represents a measure of the erosive force and intensity of rain in a normal year (Goldman et al. 1986). Two components of the factor are the total energy and the maximum 30-min intensity of storms (i.e., EI factor as defined by Wischmeier and Smith 1978, 1958). The R-factor is the sum of the product of these two components for all major storms in the area during an average year. Values for the R-factor have been computed for the United States from rainfall records and probability statistics and are presented in Figure 4.8. The values presented in Figure 4.8 should not be considered a precise factor for any given year or location.

Although R-factors have been estimated for the entire United States and presented in Figure 4.8, they only reflect regional-type conditions; as such, Goldman et al. (1986) note that irregular topography in the western portions of the United States makes use of Figure 4.8 impractical. For the western United States, they suggest basing the R-factor on rainfall data. Wischmeier and Smith (1978) report that results of an investigation at the Runoff and Soil Loss Data Center at Purdue University showed that the R-factor could be approximated with reasonable accuracy by using the 2-year, 6-hr rainfall frequency distribution. Based on this frequency distribution, regression equations were developed to define R-factors for three different storm types (i.e., Type I, Type IA, and Type II).

A Type II storm is characterized by gradually increasing rainfall followed by a strong peak in rainfall intensity that tapers off to low-intensity rain. Type II storms occur in 1) the eastern portions of California (i.e., east of the Sierra Nevada), Washington, and Oregon (Kent 1973; Goldman et al. 1986; Mitchell and Bubenzer 1980); 2) all of Idaho, Montana, Nevada, Utah, Wyoming,

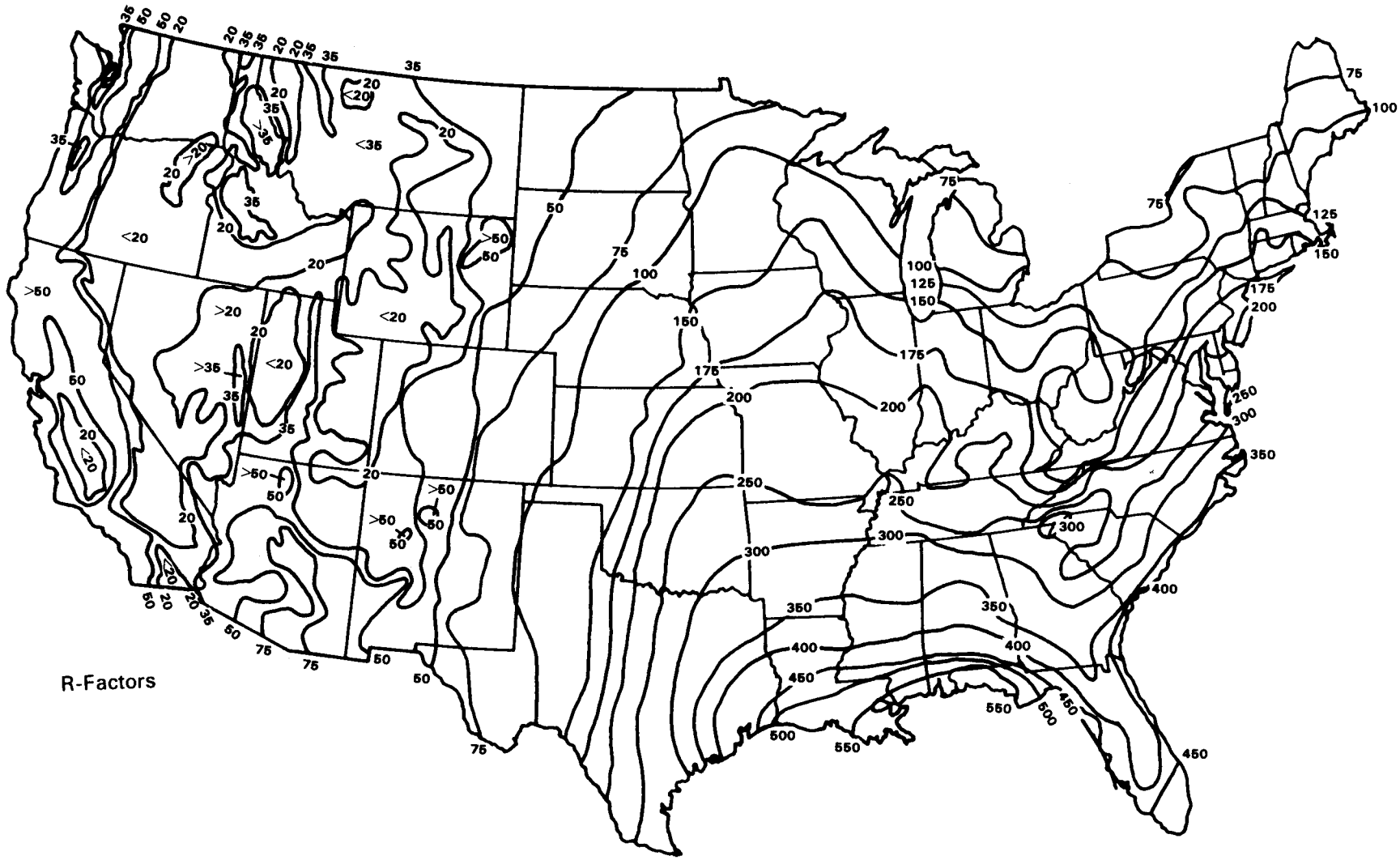

FIGURE 4.8. Average R-Factor Values for the Continental United States (After Wischmeier and Smith 1978)

Arizona, and New Mexico (Kent 1973; Goldman et al. 1986; Mitchell and Bubenzer 1980); and 3) the remaining portions of the United States not covered by Type I and Type IA storms (Kent 1973; Mitchell and Bubenzer 1980).

Type I and IA storms occur in the maritime climate. Type I is typical of storms that occur in southern and central western California; these storms have a milder but definite peak similar to that of Type II storms. Type IA storms, which are characteristic of storms in coastal areas of northern California, Oregon, Washington, and the western slopes of the Sierra Nevada, have a low broad peak in the rainfall distribution (Goldman et al. 1986; Mitchell and Bubenzer 1980). Each storm type is illustrated in Figure 4.9.

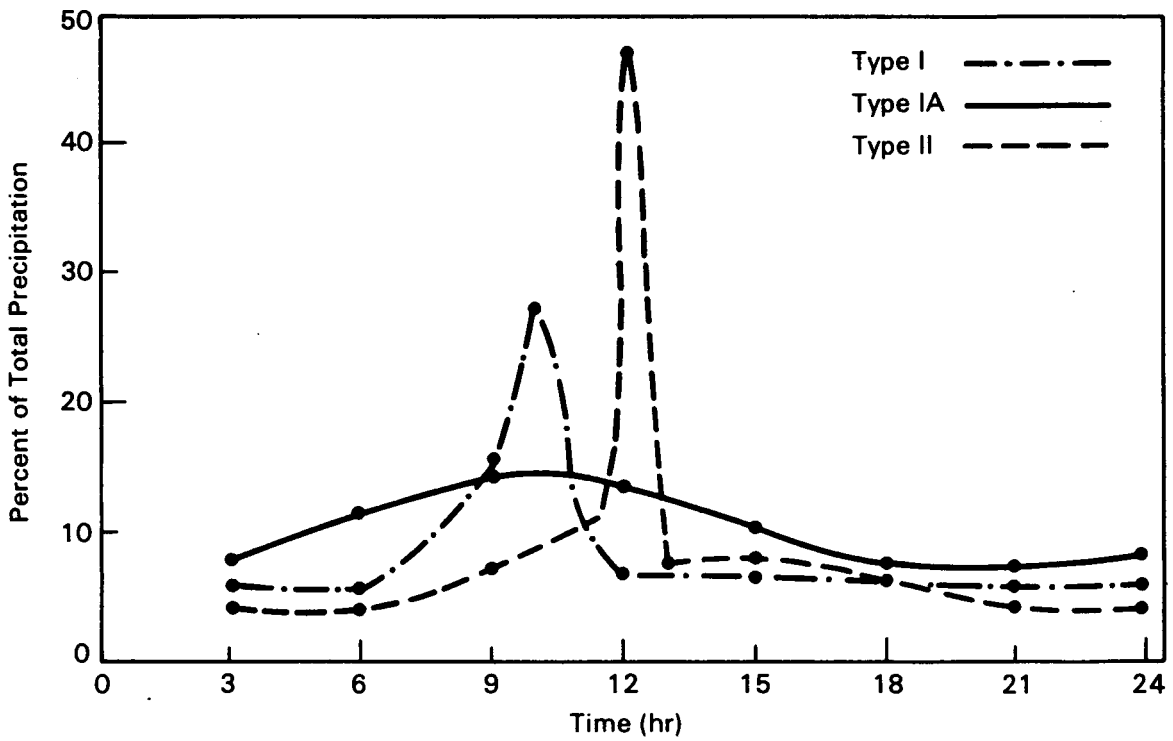

FIGURE 4.9. Time Distribution of Rainfall Within Storm Types (After unpublished data provided by Wendell Styner, U.S. Department of Agriculture, Soil Conservation Service, West Technical Service Center, Portland, Oregon, October 28, 1981; as reported by Goldman et al. 1986)

The equations that have been developed for estimating R-factors, based on storm type and rainfall-frequency distribution, are presented as follows (Mitchell and Bubenzer 1980; Goldman et al. 1986):

$$R = 2.124\ (P_{2,6})^{2.20} \qquad \text{for Type I storm} \qquad (4.15)$$

$$R = 1.312\ (P_{2,6})^{2.20} \qquad \text{for Type IA storm} \qquad (4.16)$$

$$R = 3.239\ (P_{2,6})^{2.17} \qquad \text{for Type II storm} \qquad (4.17)$$

where $P_{2,6}$ = the 2-year recurrence interval, 6-hr duration rainfall (cm).

When the rainfall volume for the 2-year, 6-hr rainfall-frequency distribution and the corresponding R-factors are compared, it is evident that the stronger the peak intensity of the typical storm that is characteristic of a given area, the larger the rainfall erosivity factor.

The R-factors described by Equations (4.15) through (4.17) do not include the erosive forces from thaw or snowmelt. Mitchell and Bubenzer (1980) note that McCool et al. (1974, 1976) show that a major erosion potential occurs in the form of low-intensity rainfall or snow during winter months. Wischmeier and Smith (1978) suggest modifying the R-factor at those sites where snowmelt may be important. To provide more discrimination between those sites that traditionally have snowmelt runoff from those where it occurs occasionally, the average-annual R-factors, as defined by Equations (4.15) through (4.17), are increased by an amount equaling 0.591 times the December through March precipitation (in cm).(a)

(a) This modification is associated with those months having an average monthly temperature below freezing, including the first month following the last freezing month. Note that Wischmeier and Smith (1978) suggest using the precipitation total for the entire period from December through March. Because the runoff volume associated with the RAPS methodology is based on historically averaged monthly precipitation amounts, it is difficult to determine a priori which locations will traditionally have significant snowmelt runoff. To provide some differentiation between sites, the monthly average temperature is used to help determine the effects of snowmelt runoff.

At sites where characteristics associated with major sediment producing individual storm events are known or at those sites where design storm events are to be analyzed, Foster (1976) recommends a modification to the R-factor of the USLE to account for peak runoff rate and runoff volume. The resulting modified USLE (MUSLE) is defined for individual storm events as follows (Onstad and Foster 1975; Onstad et al. 1976; Mitchell and Bubenzer 1980; Novotny and Chesters 1981):

$$A = W\ K\ SL\ C\ P \tag{4.18}$$

in which

$$W = a\ R + 132\ (1 - a)\ V\ (q_{max} / h_{max})^{1/3} \tag{4.19}$$

where W = modified R-factor (J/ha)
a = coefficient that represents the relative importance of rainfall energy compared with runoff energy for detaching soil ($0 < a < 1$)
V = actual runoff volume (cm)
q_{max} = peak runoff discharge per unit width (cm^2/s)
h_{max} = peak flow depth (cm).

Onstad and Foster (1975) and Foster (1976) suggest a value of 0.5 for the coefficient "a."

To use Equations (4.18) and (4.19) in any analysis, q_{max} and h_{max} have to be estimated. Eagleson (1970) uses the method of characteristics with the kinematic wave approximation to temporally and spacially distribute rainfall excess (i.e., actual runoff volume). The method of characteristics defines the path of wave propagation along which partial differential equations become ordinary differential equations with analytical solutions. Using this technique, both q_{max} and h_{max} can be defined. A complete discussion of the method of characteristics is presented in Section 4.4.

4.3.2 Soil Erodibility Factor

The soil erodibility factor, K, is a quantitative description of the inherent erodibility of a particular soil; it is a measure of the

susceptibility of soil particles to detach and transport by rainfall and runoff. For a particular soil, the soil erodibility factor is the rate of erosion per unit erosion index from a standard plot. The factor reflects the fact that different soils erode at different rates when the other factors that affect erosion (e.g., infiltration rate, permeability, total water capacity, dispersion, rain splash, and abrasion) are the same. Texture is the principal factor affecting K, but structure, organic matter, and permeability also contribute. The soil erodibility factor ranges in value from 0.02 to 0.69 (Goldman et al. 1986; Mitchell and Bubenzer 1980).

Goldman et al. (1986) note that several methods can be used to estimate the K-factor. The most frequently used are 1) Soil Conservation Service (SCS) Soil County Survey reports compiled for many counties in the United States and 2) nomographs relating K-factors to topsoil conditions. The SCS county soil surveys contain soil maps superimposed on aerial photographs. The maps permit easy location of sites and tentative determination of soil series. Recent surveys list K-factors for the soil series in the table outlining the soil's physical and chemical properties. Goldman et al. (1986) note that this method of determining K-factors should only be used if minimal soil disturbance at the site is anticipated and a site analysis is unavailable.

The preferred method, according to Goldman et al. (1986), for determining K-factors is the nomograph method. The soil erodibility nomograph is illustrated in Figure 4.10. Figure 4.10 is based on the work by Wischmeier et al. (1971) and is mathematically represented as follows:

$$K = 2.1\ 10^{-6}\ M^{1.14}\ (12 - \%OM) + 0.0325\ (S - 2) + 0.025\ (P - 3) \quad (4.20)$$

in which

$$M = \%Si\ (100 - \%C) \quad (4.21)$$

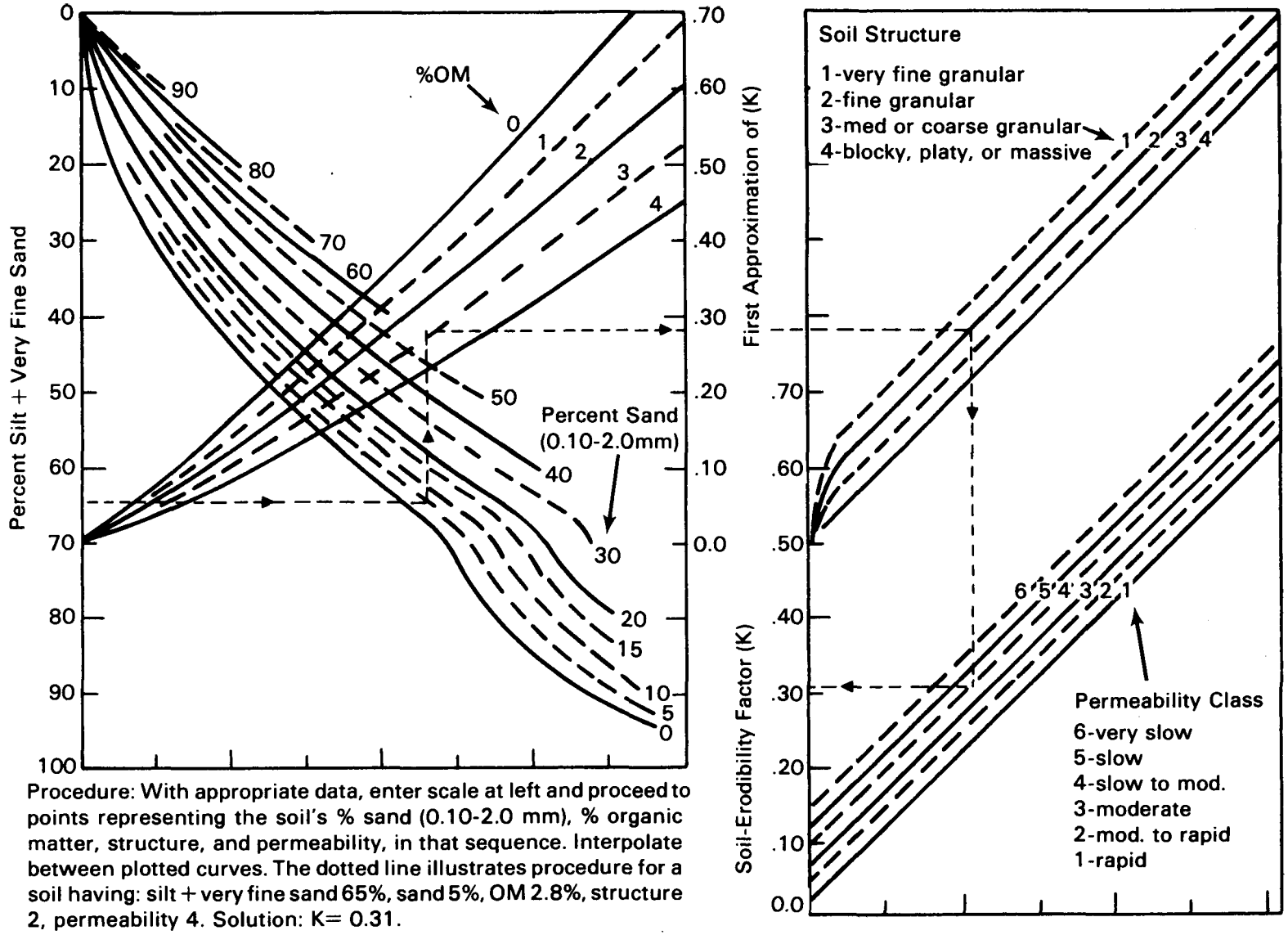

Procedure: With appropriate data, enter scale at left and proceed to points representing the soil's % sand (0.10-2.0 mm), % organic matter, structure, and permeability, in that sequence. Interpolate between plotted curves. The dotted line illustrates procedure for a soil having: silt + very fine sand 65%, sand 5%, OM 2.8%, structure 2, permeability 4. Solution: K= 0.31.

FIGURE 4.10. Soil Erodibility Nomograph (After Novotny and Chesters 1981; Mitchell and Bubenzer 1980; Wischmeier and Smith 1978)

where M = particle size parameter

%OM = percent organic matter

S = soil structure index (= 1 for very fine granular soil; = 2 for fine granular soil; = 3 for medium or coarse granular soil; = 4 for blocky, platy, or massive soil)

P = profile-permeability class (= 1 for very slow infiltration; = 2 for slow infiltration; = 3 for slow to moderate infiltration; = 4 for moderate infiltration; = 5 for moderate to rapid infiltration; = 6 for rapid infiltration)

%Si = percent silt plus very fine sand

%C = percent clay

Erickson (1977), as reported by Goldman et al. (1986), used the information from the nomograph and superimposed K-factors for 2% organic matter on a U.S. Department of Agriculture (USDA) soil textural classification triangle. An example is provided in Figure 4.11. Goldman et al. (1986) also presents tables to modify the results in Figure 4.11 to account

- soils with greater than 15% very fine sand
- soils with organic matter content different from that of 2%
- soils with rock (i.e., soil particle size greater than 2 mm) content greater than 14% by volume
- permeability
- structure.

Stewart et al. (1975) -- as reported by Mills et al. (1985), Mitchell and Bubenzer (1980), and Novotny and Chesters (1981) -- also used the information in Figure 4.11 and developed a table indicating the general magnitude of the K-factor as a function of organic matter content and and soil textural class. Their results are presented in Table 4.6.

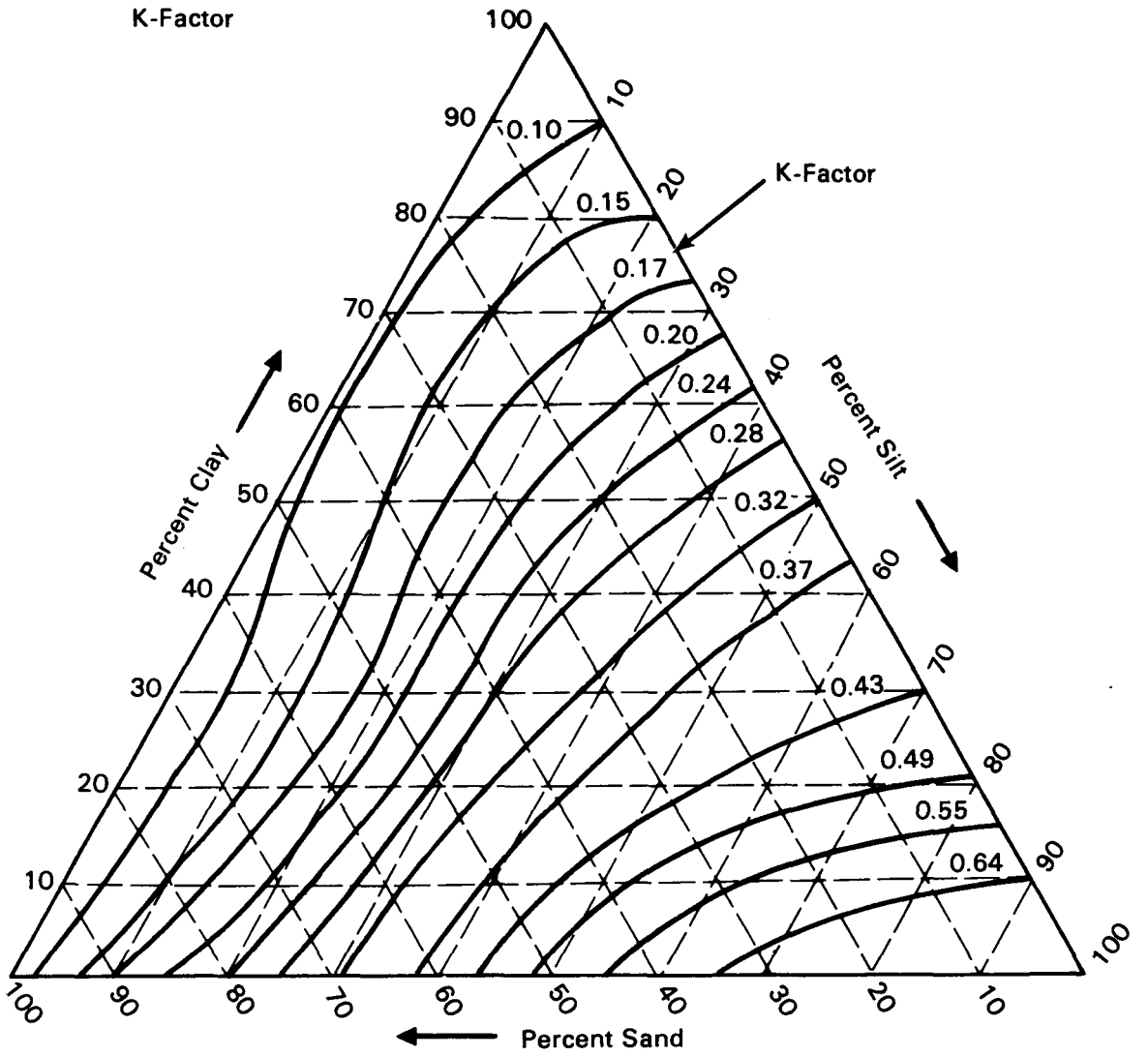

FIGURE 4.11. Triangular Nomograph for Estimating K-Factors, Assuming 2% Organic Matter Content (after Erickson 1977, as reported by Goldman et al. 1986).

Goldman et al. (1986) note that if a site inspection or data analyses indicate significant variations in the soil erodibility, different K-factors can be assigned to different areas of the site. They also note that a simpler and more conservative approach is to use the highest value obtained for all parts of the site, because it may not be possible to know exactly what soils will be exposed or how varied the soils are.

TABLE 4.6. Soil Erodibility Factor K (After Stewart et al. 1975[a])

Textural Class	Organic Matter Content (%) <0.5	2	4
Sand	0.05	0.03	0.02
Fine sand	0.16	0.14	0.10
Very fine sand	0.42	0.36	0.28
Loamy sand	0.12	0.10	0.08
Loamy fine sand	0.24	0.20	0.16
Loamy very fine sand	0.44	0.38	0.30
Sandy loam	0.27	0.24	0.19
Fine sandy loam	0.35	0.30	0.24
Very fine sandy loam	0.47	0.41	0.33
Loam	0.38	0.34	0.29
Silt loam	0.48	0.42	0.33
Silt	0.60	0.52	0.42
Sandy clay loam	0.27	0.25	0.21
Clay loam	0.28	0.25	0.21
Silty clay loam	0.37	0.32	0.26
Sandy clay	0.14	0.13	0.12
Silty clay	0.25	0.23	0.19
Clay		0.13-0.2	

(a) The values shown are estimated averages of broad ranges of specific soil values. When a texture is near the border line of two texture classes, use the average of the two K values.

4.3.3 Slope Length and Steepness Factor

The slope length and steepness factor describes the combined effects of slope length (i.e., flow length) and slope gradient (i.e., grade or relief); it represents the ratio of soil loss per unit area on a site to the corresponding loss from a 22.1-m- (72.6-ft-) long experimental plot with a 9% slope. Slope length is defined as the distance from the point of origin of overland flow to the point where the slope decreases sufficiently for deposition to occur or to the point where runoff enters a defined channel (wet or dry). The slope steepness is the segment or site slope, usually expressed as a percentage.

Although the LS-factor is traditionally expressed as two parameters in the USLE equation, it is universally computed as a combined term (Mitchell and Bubenzer 1980; Goldman et al. 1986).

Slope length and slope steepness strongly influence the transport of soil particles once the soil particles are dislodged by raindrop impact or runoff. Because the LS-factor can be defined to be substantially greater than unity, it can have a considerable effect on the predicted erosion. For this reason, averaging over large areas is not advised. In fact, Foster et al. (1980) suggest not basing the LS-factor solely on USGS topographic maps, as they usually suggest excessively long slope lengths.

Goldman et al. (1986) have mathematically expressed the LS-factor as follows:

$$LS = (65.41\ S^2 / a^2 + 4.56\ S / a + 0.065)\ (4.53\ 10^{-4}\ L)^m \qquad (4.22)$$

in which

$$a = (S^2 + 10{,}000)^{0.5} \qquad (4.23)$$

where S = slope gradient (%)
a = parameter
L = slope length (cm)
m = exponent in the LS-factor equation (0.2 for slopes <1%, 0.3 for slopes 1% to 3%, 0.4 for slopes 3.5% to 4.5%, and 0.5 for slopes >5%).

Equations (4.22) and (4.23) have been expressed as a figure by a number of authors (e.g., Shultz et al. 1986; Novotny and Chesters 1981; Mitchell and Bubenzer 1980; Wischmeier and Smith 1978); one such figure is presented as Figure 4.12.

4.3.4 Vegetative Cover Factor

The vegetative cover factor is defined as the ratio of soil loss from land under specified vegetative or mulch conditions to the corresponding loss from tilled, bare soil (Goldman et al. 1986). Any vegetation or management condition that reduces the amount of soil exposed to raindrop impact will reduce

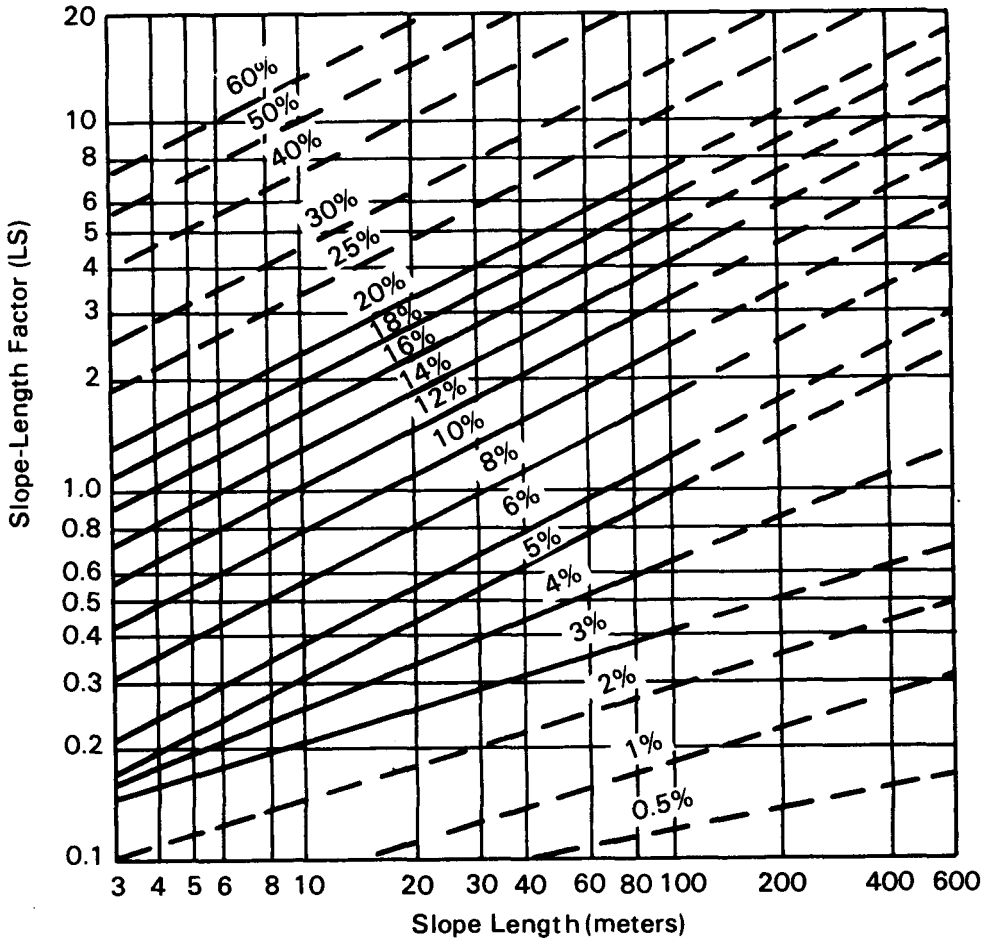

FIGURE 4.12. Slope Length and Gradient Factor (LS) for Use with the Universal Soil Loss Equation (After Mitchell and Bubenzer 1980)

erosion. In the USLE, the C-factor reduces the soil loss estimate according to the effectiveness of vegetation and mulch at preventing detachment and transport of soil particles. The effect of vegetation on erosion rates results from canopy protection, reduction of rainfall energy, and protection of soil by plant residues, roots, and mulches. When the surface is bare, the C-factor is considered to equal unity.

Typical values for C-factors are presented in Table 4.7. Many reports have been published defining the C-factor for numerous vegetative conditions. These documents include Goldman et al. (1986), Shultz et al. (1986); Mills

TABLE 4.7. C-Factor Values for the Universal Soil Loss Equation (After Kay 1983; USDA 1977; Wischmeier and Smith 1978; as reported by Goldman et al. 1986)

Type of Cover	C Factor	Soil Loss Reduction, %
None	1.0	0
Native vegetation (undisturbed)	0.01	99
Temporary seedings:		
90% cover, annual grasses, no mulch	0.1	90
Wood fiber mulch, 3/4 ton/acre (1.7 t/ha), with seed[a]	0.5	50
Excelsior mat, jute[a]	0.3	70
Straw mulch[a]		
1.5 tons/acre (3.4 t/ha), tacked down	0.2	80
4 tons/acre (9.0 t/ha), tacked down	0.05	95

(a) For slopes up to 2:1.

et al. (1985), Kay (1983), Novotny and Chesters (1981), Mitchell and Bubenzer (1980), Wischmeier and Smith (1978, 1965), USDA (1977), Stewart et al. (1975), and Wischmeier (1972).

4.3.5 Erosion Control Practice Factor

The erosion control practice factor (P-factor) is defined as the ratio of soil loss with a given surface condition to soil loss with up-and-down-hill plowing. P-factor values involve treatments that retain liberated particles near the source and prevent further transport.[a] The P-factor accounts for the erosion control effectiveness of such land treatments as contouring, compacting, establishing sediment basins, and other control structures. At sites where there is or has been much human and vehicular traffic, the P-factor reflects the roughening of the soil surface by tractor treads or by rough grading, raking, or disking. Practices that reduce the velocity of runoff and

(a) Note that protection of the soil surface against the impact of rain droplets and subsequent loss of soil particles is reflected in the C-factor (Novotny and Chesters 1981).

the tendency of runoff to flow directly downslope reduce the P-factor (Goldman et al. 1986; Novotny and Chesters 1981).

Table 4.8 presents typical values for sites with varying practice conditions and structures. Note that most of the P-factor values are around unity; changing the surface conditions does not provide much direct reduction in P-factor, although other USLE factors may change and may have a significant effect on the amount of soil loss.

TABLE 4.8. P-Factor Values for Various Practice Conditions (After Ports 1973, as reported by Novotny and Chester 1981)

Erosion Control Practice	P
Surface Condition with No Cover	
Compact, smooth, scraped with bulldozer or scraped up and down hill	1.30
Same as above, except raked with bulldozer and root-raked up and down hill	1.20
Compact, smooth scraped with bulldozer or scraped across the slope	1.20
Same as above, except raked with bulldozer and root-raked across slope	0.90
Loose, as a disked plow layer	1.00
Rough irregular surface, equipment tracks in all directions	0.90
Loose with rough surface >0.3 m depth	0.80
Loose with smooth surface >0.3 m depth	0.90
Structures	
Small sediment basins:	
0.09 basins/ha	0.50
0.13 basins/ha	0.30
Downstream sediment basins:	
With chemical flocculants	0.10
Without chemical flocculants	0.20
Erosion control structures:	
Normal rate usage	0.50
High rate usage	0.40
Strip building	0.75

4.3.6 Summary of Soil Loss Calculations

This subsection presents the algorithms for estimating the soil loss from a waste site with contaminated surface sediments. The calculations are based on the USLE, which provides long-term, average-annual soil loss due to rill, interrill, and sheet erosion.

4.4 SINGLE-EVENT OVERLAND FLOW EQUATIONS

This subsection presents the algorithms for spacially and temporally distributing the overland flow volume for a single precipitation event; these algorithms are not used to estimate long-term, average-annual overland runoff characteristics. This subsection is presented to support the application of the modified USLE [see Equations (4.18) and (4.19)] at a specific site. The calculations are based on the kinematic wave approximation for estimating overland flow using the method of characteristics solution technique.

4.4.1 Basic Equations

The one-dimensional flow equation as described by the equations of motion (continuity and momentum) is expressed as

$$\frac{1}{g}\frac{\partial u}{\partial t} + \frac{u}{g}\frac{\partial u}{\partial x} + \frac{\partial h}{\partial x} = S_o - S_f - \frac{i}{g}\frac{u}{h} \qquad (4.24)$$

where g = gravitational acceleration (cm/s^2)
u = overland flow velocity (cm/s)
t = time (s)
x = distance (cm)
h = overland flow depth (cm)
S_o = overland slope (dimensionless)
S_f = friction slope (dimensionless)
i = rainfall excess rate (cm/s).

Croley (1978) notes that Equation (4.24) can be simplified by omitting terms that are found to be unimportant for overland flow (Lighthill and Whitham 1955; Henderson 1966b; Woolhiser and Liggett 1967; Eagleson 1970). This simplification is known as the kinematic wave approximation for steady, uniform flow (gradually varied flow) in a wide rectangular channel. Under the kinematic wave approximation, inflow, free surface slope, and inertial terms are considered negligible as compared to the overland slope and friction slope. Equation (4.24) can thus be written as

$$S_o = S_f \tag{4.25}$$

Based on the assumptions of Equation (4.25), the continuity and momentum equations are written in their respective forms as

$$\frac{\partial h}{\partial t} + \frac{\partial q}{\partial x} = i \tag{4.26}$$

$$q = \alpha h^m \tag{4.27}$$

where q = discharge per unit width of overland segment (cm^2/s)
α = coefficient that is a function of overland roughness and slope
m = parameter that is determined by the roughness equation employed in the analysis.

Because steady, uniform flow in a wide rectangular channel is assumed, the coefficients α and m can be assumed by using the Darcy-Weisbach, Chezy, or Manning equation (see Henderson 1966b; Chow 1959). These equations and their corresponding values for α and m are as follows (Eagleson 1970):

Darcy-Weisbach Equation

$$S_f = \frac{k \nu q}{8 g h^3} \tag{4.28}$$

or

$$q = \left(\frac{8\ g\ S_f}{k\ \nu}\right) h^3 \tag{4.29}$$

and

$$\alpha = \frac{8\ g\ S_f}{k\ \nu} \tag{4.30}$$

$$m = 3 \tag{4.31}$$

Chezy Equation

$$q = \left(C\ S_f^{1/2}\right) h^{3/2} \tag{4.32}$$

and

$$\alpha = C\ S_f^{1/2} \tag{4.33}$$

$$m = 3/2 \tag{4.34}$$

Manning Equation

$$q = \left(\frac{a}{n}\ S_f^{1/2}\right) h^{5/3} \tag{4.35}$$

and

$$\alpha = \frac{a}{n}\ S_f^{1/2} \tag{4.36}$$

$$m = 5/3 \tag{4.37}$$

where k = roughness parameter [$k = f(Re)$]

f = Darcy-Weisbach friction factor

$f(Re)$ = function of Reynolds number ($u\,D/\nu$)

u = flow velocity (cm/s)

D = characteristic depth parameter (cm)

ν = kinematic viscosity (cm^2/s)

C = Chezy coefficient

a = units conversion factor equaling unity for metric units (when meters and seconds are employed) and 1.49 for English units (when feet and seconds are employed)

n = Manning coefficient.

Using a relationship such as that shown in Equation (4.27), Horton (1938) found that natural surfaces give $m \approx 2$, which is generally supported by the works of other investigators (e.g., Horner and Jens 1942; Hicks 1944; and Jens 1948, as reported by Eagleson 1970). If Horton's definition of m is used in the analysis, the roughness parameters k, C, and n -- as defined in Equations (4.29), (4.32), and (4.35), respectively -- do not retain their original definitions. Note that under the original definitions, empirical values can be assigned to these roughness parameters (i.e., k, C, and n) (see Chow 1959; Henderson 1966b); however, values for these parameters do not exist if Horton's definitions are used. Because modified values for these parameters do not currently exist, the definitions as outlined by Equations (4.31), (4.34), and (4.37) will be assumed.

The method of characteristics -- as outlined by Eagleson (1970), Hjelmfelt (1976), and Croley (1978) and as used by Witinok (1979), Croley (1979),[a] Whelan (1980), Witinok and Whelan (1980), and Knisel (1980) -- forms the basis for temporally distributing the overland runoff volume. Based on

(a) Croley, T. E., II. 1979. Unsteady Overland Sedimentation. Working Paper, Iowa Institute of Hydraulic Research, University of Iowa, Iowa City, Iowa.

Equations (4.26) and (4.27) and using the definition of total differentials, a set of differential equations can be developed for use by the method of characteristics:

$$\frac{\partial h}{\partial t} + \frac{\partial q}{\partial x} = i \tag{4.26}$$

$$\frac{\partial q}{\partial t} = \alpha\, m\, h^{m-1} \frac{\partial h}{\partial t} \tag{4.38}$$

$$dq = \frac{\partial q}{\partial x}\, dx + \frac{\partial q}{\partial t}\, dt \tag{4.39}$$

$$dh = \frac{\partial h}{\partial x}\, dx + \frac{\partial h}{\partial t}\, dt \tag{4.40}$$

When Equations (4.26), (4.38), (4.39), and (4.40) are solved along characteristic x-t curves defined by the wave celerity (wave celerity = $\alpha\, m\, h^{m-1}$), the equations reduce to the following total derivatives:

$$\frac{dq}{dx} = i \tag{4.41}$$

$$\frac{dh}{dt} = i \tag{4.42}$$

$$\frac{dq}{dt} = i\, \alpha\, m\, h^{m-1} \tag{4.43}$$

$$\frac{dh}{dx} = \frac{i}{\alpha\, m\, h^{m-1}} \tag{4.44}$$

For Equations (4.41) through (4.44) to be valid, rainfall excess must be spacially and temporally constant over the overland segment. In addition, the equations are valid only along the given path defined by the wave celerity (c):

$$\frac{dx}{dt} = c = \alpha\, m\, h^{m-1} \tag{4.45}$$

The initial and boundary conditions are imposed as

$$h = 0 \qquad \text{for} \quad 0 \leq x < L\,,\ t = 0 \tag{4.46}$$

$$h = 0 \qquad \text{for} \quad x = 0\,,\ t > 0 \tag{4.47}$$

By assuming that no infiltration occurs after cessation of rainfall, the characteristics are derived by integrating Equations (4.42) and (4.43):

$$x - x_o = \alpha\, i^{m-1}\, (t - t_o)^m \qquad \text{for } t \leq t_r \tag{4.48}$$

where L = overland flow length (cm)
x_o = initial spacial location (cm)
t_o = initial time (s)
t_r = duration of rainfall excess (s).

When t_r goes to infinity (hypothetical case), the time of concentration (i.e., the time for a particle of water to travel the length of the overland segment) can be computed by rearranging Equation (4.48) and by noting that at $x_o = 0$ and $x = L$, $t_o = 0$ and $t = t_c$, respectively:

$$t_c = \left(\frac{L\, i^{1-m}}{\alpha}\right)^{1/m} \tag{4.49}$$

where t_c = time of concentration.

The time of concentration helps identify the point when the rainfall excess equals the outflow rate at the downgradient end of the segment.

When the duration of the rainfall excess is not infinite, two possibilities exist:

1) The duration of rainfall excess is longer than the time of concentration (i.e., $t_r \geq t_c$) or

2) The duration of rainfall excess is shorter than the time of concentration (i.e., $t_r > t_c$).

Each condition is discussed below.

Condition 1: $t_c \leq t_r < \infty$

Where $t < t_c$, Equation (4.42) can be integrated to give

$$h_L = i\ t \qquad \text{for} \quad 0 \leq t \leq t_c \leq t_r \tag{4.50}$$

where h_L = overland flow depth at the downgradient end of the segment (i.e., h at x = L).

Where $t_c \leq t \leq t_r$, Equations (4.49) and (4.50) are combined to give

$$h_L = \left(\frac{L\ i}{\alpha}\right)^{1/m} \qquad \text{for} \quad t_c \leq t \leq t_r \tag{4.51}$$

Note that the depth of flow has stopped increasing with time and that the rainfall excess equals the outflow rate at the downgradient end of the segment. The maximum depth on the overland segment is defined by Equation (4.51).

When t exceeds t_r (i.e., $t_c \leq t_r \leq t$), the depth of flow begins to decrease, as does the outflow discharge. The depth decreases asymptotically with time toward zero. Up to the cessation of rainfall excess, the relationship between distance, time, and flow depth is described by 1) combining and integrating Equations (4.42) and (4.45) to give Equation (4.48), 2) integrating Equation (4.42), and 3) substituting Equation (4.42) into Equation (4.40) for the time, t. This relationship reduces to

$$x = \frac{\alpha\ h^m}{i} \tag{4.52}$$

Note that when x = L, Equation (4.52) reduces to Equation (4.51). As the water flows from the overland segment following the cessation of rainfall excess, a

wave of water moves down the segment; the depth-distance profile at different times (e.g., t_1, t_2, and t_3) is shown in Figure 4.13.

To describe the wave (i.e., constant depth location) as it moves downgradient, as the overland flow subsides, a constant depth moves downgradient with time. After cessation of the rainfall excess (i.e., when $t > t_r$), Equations (4.41) through (4.44) become

$$\frac{dq}{dx} = \frac{dq}{dt} = \frac{dh}{dx} = \frac{dh}{dt} = 0 \qquad (4.53)$$

Equation (4.53) states that the discharge and depth are independent of distance and time along a characteristic curve (i.e., discharge and depth are constant). Because the depth is constant, Equation (4.45) can be integrated for $t > t_r$ to give

$$\Delta x = \alpha\, m\, h^{m-1}\, (t - t_r) \qquad \text{for} \quad t \geq t_r \qquad (4.54)$$

As illustrated by Figure 4.13,

$$x_1 = x + \Delta x \qquad \text{for} \quad t > t_r \qquad (4.55)$$

Combining Equations (4.52), (4.54), and (4.55) and calculating constant depths at the downgradient end of the segment (i.e., when $x_1 = L$) gives

$$L = \frac{\alpha\, h^m}{i} + \alpha\, m\, h^{m-1}\, (t - t_r) \qquad \text{for} \quad t_c \leq t_r \leq t \qquad (4.56)$$

Because Equation (4.56) asymptotically decreases toward zero, a linear approximation is assumed for the outflow discharge recession limb. The time defining the end of overland runoff (t_e) is computed by assuming that the runoff volume (V_r) in cubic centimeters (assumed to be equivalent to the rainfall excess volume) equals the volume of water represented by the area under the

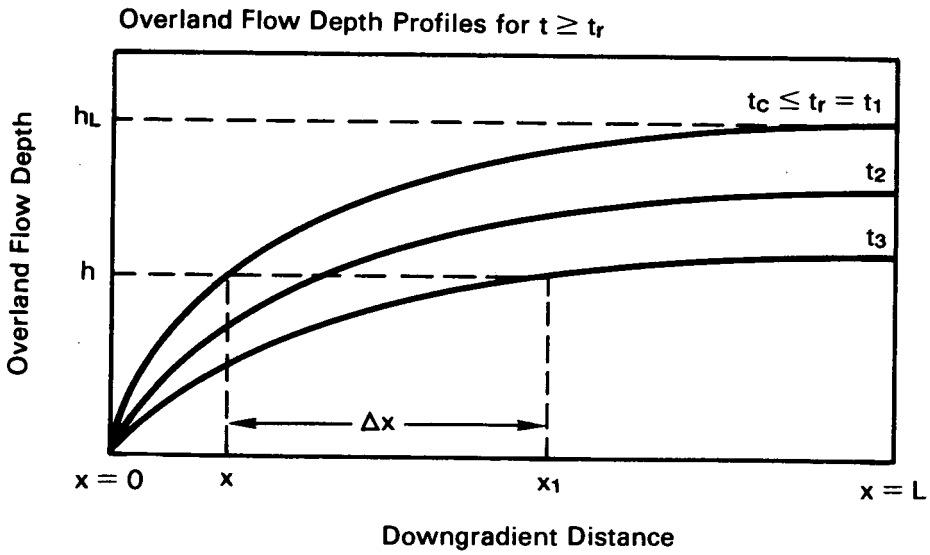

FIGURE 4.13. Water Flow Depth Profile as a Function of Downgradient Distance and Time for $t \leq t_r \leq t_c$ (After Eagleson 1970)

overland hydrograph times the width of the overland segment (W). This computation is schematically illustrated in Figure 4.14a.

By making this assumption, the approximation for the overland flow depth for the recession limb of the overland hydrograph can be computed as follows:

$$V_r = W \left[\frac{\alpha \ i^m \ t_c^{m+1}}{m+1} + i \ L \ (t_r - t_c) + \frac{i \ L \ (t_e - t_r)}{2} \right] \qquad (4.57)$$

$$t_e = \frac{2 \ V_r}{i \ L} + \frac{2 \ \alpha \ i^{m-1} \ t_c^{m+1}}{L \ (m+1)} + 2 \ t_c - t_r \qquad (4.58)$$

$$h_L = i \ t_c \left(\frac{t_e - t}{t_e - t_r} \right)^{1/m} \qquad \text{for} \quad t_c \leq t_r \leq t \leq t_e \qquad (4.59)$$

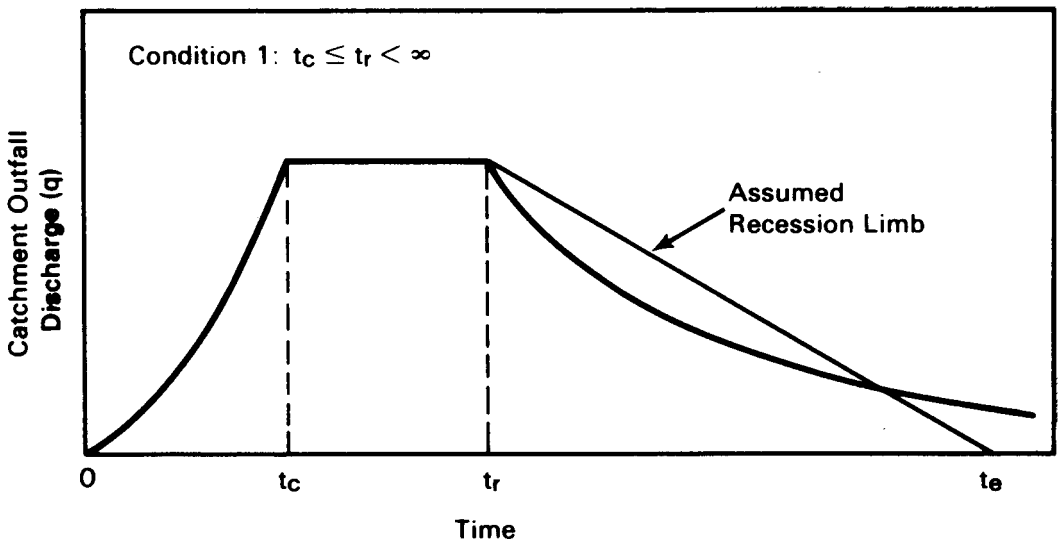

(a)

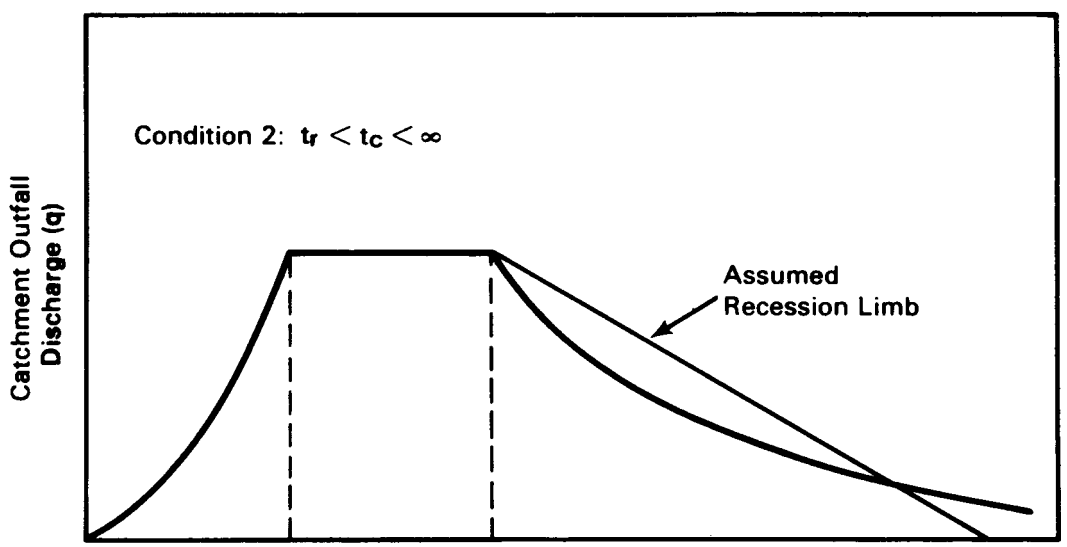

(b)

FIGURE 4.14. Schematic Illustration of the Procedure Used in Computing t_c for the Conditions when a) $t_c \leq t_r < \infty$ and b) $t_r < t_c < \infty$

The equations used for computing the outflow discharge hydrograph from the overland segment for Condition 1 are Equations (4.27), (4.50), (4.51), and (4.59).

Condition 2: $t_r < t_c < \infty$

For the case when $t \leq t_r < t_c$ (see Figure 4.14b), an equation similar to Equation (4.50) is applicable:

$$h_L = i\, t \qquad \text{for} \qquad t \leq t_r < t_c \tag{4.60}$$

For the case when the rainfall excess ceases before the initial disturbance has reached the catchment outfall (i.e., $t_r < t_c$), the depth-distance profile at different times (t_1, t_2, and t_3) on the overland segment is pictorially described by Figure 4.15. At $t = t_r$, the depth has reached a maximum and is located at point B (see Figure 4.15). Point B represents the peak of the rising limb of the hydrograph. Based on earlier arguments, point B will move to point C as the water flows downgradient at a constant depth. The depth at the end of the segment remains constant until point B coincides with point D. This time, t_p (the time to peak flow), can be calculated as follows.

After the cessation of rainfall excess, the flow depth at the end of the segment remains constant from t_r to t_p. During this time, the flood wave moves with a velocity equal to that of Equation (4.45), as h is constant. The time (t*) for the wave to move from point x_1 (at t_r) on Figure 4.15 to point L is equal to the distance divided by the wave celerity:

$$t^* = \frac{L - x_1}{c} = \frac{L - x_1}{\alpha\, m\, h^{m-1}} \tag{4.61}$$

The total time for a particle of water to move the length of the segment is equal to

$$t_p = t_r + \frac{L - x_1}{\alpha\, m\, h^{m-1}} \tag{4.62}$$

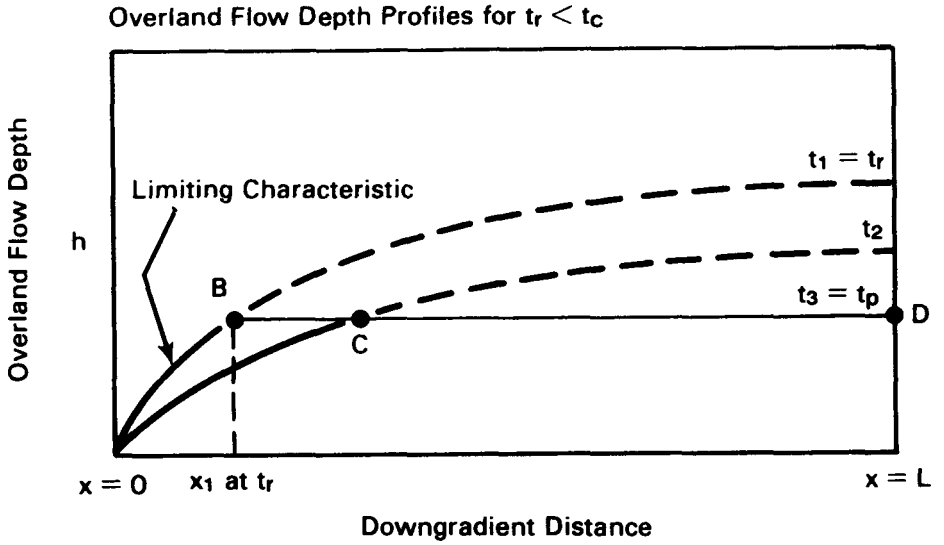

FIGURE 4.15. Water Flow Depth as a Function of Downgradient Distance and Time for $t_r < t_c$ (After Eagleson 1970)

Note however that x_1 can be described by Equation (4.52). Substituting Equation (4.52) into Equation (4.62) gives

$$t_p = t_r + \frac{i\,L - \alpha\,h_L^m}{\alpha\,i\,m\,h^{m-1}} \qquad (4.63)$$

Based on this explanation, the end depth from t_r to t_p is a constant and equal to the depth of flow at t_r, which is described by the integration of Equation (4.40):

$$h_L = i\,t_r \qquad \text{for} \quad t_r < t_c\ ;\ t_r \leq t \leq t_p \qquad (4.64)$$

The recession limb for $t_r < t_c$ can be described in a manner similar to that for $t_c < t_r$. Based on similar reasoning, the flow depth at the end of the segment is implicitly computed as

$$L = \alpha\,h_L^{m-1}\left[\frac{h_L}{i} + m\,(t - t_r)\right] \qquad \text{for} \quad t_p < t \qquad (4.65)$$

Because Equation (4.65) asymptotically decreases toward zero, a linear approximation is assumed for the recession limb. The time defining the end of overland runoff (t_e) is computed by assuming that the runoff volume (V_r) in cm^3 (assumed to be equal to the rainfall excess volume) equals the volume of water represented by the area under the overland hydrograph. This computation is schematically illustrated in Figure 4.14b. By making this assumption, the approximation for the overland flow depth for the recession limb of the overland hydrograph can be computed as follows:

$$V_r = W\left[\frac{\alpha\, i^m\, t_r^{m+1}}{m+1} + \left(\frac{\alpha\,(i\,t_r)^m}{2}\right)(t_p + t_e - 2\,t_r)\right] \tag{4.66}$$

$$t_e = \frac{2\,V_r}{\alpha\,(i\,t_r)^m} + \frac{2\,m\,t_r}{m+1} - t_p \tag{4.67}$$

$$h_L = i\,t_r\left(\frac{t_e - t}{t_e - t_p}\right)^{1/m} \qquad \text{for} \quad t_r < t_c\,;\; t_p \leq t \leq t_e \tag{4.68}$$

The equations used for computing the outflow discharge hydrograph from the overland segment for Condition 2 are Equations (4.27), (4.60), (4.64), and (4.68).

4.4.2 Summary of Overland Flow Equations

This subsection presents the algorithms for spacially and temporally distributing the overland flow volume. The calculations in this section are used to compute the outflow hydrograph from the overland segment and are based on the kinematic wave approximation for estimating overland flow using the method of characteristics technique.

4.5 OVERLAND CONTAMINANT FLUX CALCULATIONS

As initially noted in Section 4.1, once surface soils are contaminated, the constituents can migrate to the subsurface environment by

precipitation-generated leaching and to nearby surface water bodies with contaminated runoff water and contaminated surface soil loss. When a storm event occurs, the contaminants in the soil are partitioned between soil and water (i.e., dissolved-liquid phase and adsorbed-solid phase). Contaminant levels in the dissolved-liquid phase can be used in calculating the contaminant flux leaching into the subsurface environment and migrating with overland runoff. Contaminant levels in the adsorbed-solid phase can be used in calculating the contaminant flux associated with sediment loss at the site.

The degree of soil-water partitioning expected for a given compound can be calculated based on the method used in recording the concentration associated with the sample. Leonard and Wauchope (1980) note that the standard convention for recording concentration units, when a soil sample is removed and analyzed for contaminant content, is to express the concentration in mass of constituent per dry mass of soil. Based on this convention, the dissolved-liquid and adsorbed-solid (or particulate) concentrations can be expressed as follows:

$$D = C_{Tp}\ \beta\ /\ (\theta + \beta\ Kd) \tag{4.69}$$

$$P = C_{Tp}\ \beta\ Kd\ /\ (\theta + \beta\ Kd) \tag{4.70}$$

in which

$$Kd = P\ /\ D \tag{4.71}$$

where D = dissolved-liquid phase concentration, expressed as per volume of liquid (Ci/ml or g/ml)

C_{Tp} = total contaminant concentration, expressed in weight of dry soil (Ci/g or g/g)

β = bulk density of the soil (g/cm^3)

θ = moisture content

Kd = equilibrium (partition or distribution) coefficient (ml/g)

P = particulate concentration, expressed in weight of dry soil (Ci/g or g/g)

Equations (4.69) through (4.71) assume that the contaminant sorption process can be described by a constant (i.e., Kd) representing the ratio between the contaminant adsorbed to the soil particle (i.e., P) and the contaminant dissolved in solution (i.e., D).

If the soil contaminant concentrations are presented on a per unit volume basis (i.e., mass of contaminant per total volume of sample), the dissolved and particulate concentrations can be expressed as follows:

$$D = C_T / (\theta + \beta Kd) \tag{4.72}$$

$$P = C_T Kd / (\theta + \beta Kd) \tag{4.73}$$

where C_T = total contaminant concentration, expressed in total volume (Ci/cm^3 or g/cm^3)

Similar equations have been expressed in the literature by other authors (e.g., Mills et al. 1985; Haith 1980; Shultz et al. 1986; Leonard and Wauchope 1980).

Based on 1) the flow equations presented in Sections 4.2 and 4.4, 2) the soil loss equations in Section 4.3, and 3) the contaminant concentration equations presented in this section [i.e., Equations (4.69) through (4.72)], the contaminant flux leaching into the subsurface environment and migrating with overland runoff can be calculated at the site. In each case, the contaminant flux is equal to the flux of liquid or soil times the appropriate constituent concentration. The contaminant flux in the dissolved-liquid phase is expressed as

$$Qc_d = Q D \tag{4.74}$$

where Qc_d = contaminant flux in the dissolved-liquid phase (Ci/s or g/s)
Q = liquid flux (cm^3/s)

The contaminant flux in the solid phase is expressed as

$$Qc_p = Qs\ P \tag{4.75}$$

where Qc_p = contaminant flux in the solid phase (Ci/s or g/s)
Qs = sediment flux (g/s).

4.6 SUMMARY

Many of the characteristics describing the watershed and hazardous waste site are used in computing overland water movement and subsequent contaminant transport. If an unlimited supply of contamination were available for transport, then the overland flow rate would control the mass flux of contaminant moving downgradient. As the flow rate increases, the potential for increasing the contaminant mass flux would also rise. The algorithms describing the overland pathway are based on data that are easily attainable. Estimation techniques are based on the curve (CN) number technique of the U.S. Department of Agriculture's SCS, the Universal Soil Loss Equation (USLE), and the method of characteristics.

The SCS CN technique incorporates into its computations soil classifications, soil cover, land use treatment or practice, hydrologic condition for infiltration, locale (i.e., location within the United States), initial moisture abstraction, antecedent moisture conditions, and potential maximum moisture retention. The algorithms are empirically based and represent a method of estimating direct runoff volumes from storms.

The USLE (or the modified USLE) estimates the soil loss from a site whose surface soils are contaminated. The USLE considers 1) the erosive force and intensity of precipitation and runoff, 2) the susceptibility of soil particles to detachment and transport by precipitation and runoff, 3) the combined effects of slope length and gradient, and 4) the soil loss from lands under varying vegetative conditions.

The direct runoff inventory of flow and contaminants can be temporally distributed using the method of characteristics with the kinematic wave approximation. The method of characteristics defines the path of wave propagation along which partial differential equations become ordinary differential equations with analytical solutions.

4.7 REFERENCES

Chow, V. T. 1959. Open-Channel Hydraulics. McGraw-Hill, New York.

Crawford, N. H., and R. K. Linsley. 1966. Digital Simulation in Hydrology, Stanford Watershed Model 4. Technical Report 39, Dept. of Civil Engineering, Stanford University, Stanford, California.

Croley, T. E., II. 1978. "Notes on Hydrologic Computations." Iowa Institute of Hydraulic Research, University of Iowa, Iowa City, Iowa.

Eagleson, P. S. 1970. Dynamic Hydrology. McGraw-Hill, New York.

Erickson, A. J. 1977. Aids for Estimating Soil Erodibility -- "K" Value Class and Tolerance. U.S. Department of Agriculture, Soil Conservation Service, Salt Lake City, Utah.

Foster, G. R. 1976. "Sediments, General: Reporter's Comments." In Proceedings of the National Symposium on Urban Hydrology, Hydraulics, and Sediment Control, pp. 129-138. University of Kentucky, Lexington, Kentucky, July 26-29, 1976.

Foster, G. R., and W. H. Wischmeier. 1973. "Evaluating Irregular Slopes for Soil Loss Prediction". Trans. ASAE (Am. Soc. Agric. Eng.) 17.

Foster, G. R., L. D. Meyer and C. A. Onstad. 1977. "An Erosion Equation Derived from Basic Erosion Principles." Trans. ASAE (Am. Soc. Agric. Eng.) 20:678-682.

Foster, G. R., L. J. Lane and J. D. Nowlin. 1980. "Chapter 2. A Model to Estimate Yield from Field-Sized Areas; Selection of Parameter Values." In CREAMS: A Field Scale Model for Chemicals, Runoff, and Erosion from Agricultural Management Systems -- Volume II User Manual. Conservation Report No. 26, U.S. Department of Agriculture, Washington, D.C.

Goldman, S. J., K. Jackson and T. A. Bursztynsky. 1986. Erosion and Sediment Control Handbook. McGraw-Hill, New York.

Haith, D. A. 1980. "A Mathematical Model for Estimating Pesticide Losses in Runoff." J. Environ. Qual. 9(3):428-433.

Haun, C. F., and B. J. Barfield. 1978. Hydrology and Sedimentology of Surface-Mined Lands. University of Kentucky, Lexington, Kentucky.

Henderson, F. M. 1966a. Open Channel Flow. Macmillan, New York.

Henderson, F. M. 1966b. "Flood Waves in Prismatic Channels." Proc. ASCE 89(HY4):39-69.

Hicks, W. I. 1944. "Discussion of Paper 'Preliminary Report on Analysis of Runoff Resulting from Simulated Rainfall on a Paved Plot'." Trans. Am. Geophys. Union 25:1039-1041.

Hjelmfelt, A. T., Jr. 1976. Modeling of Soil Movement Across a Watershed. Completion Report for Project A-076-MO, Missouri Water Resources Center, University of Missouri, Columbia, Missouri.

Horner, W. W., and S. W. Jens. 1942. "Surface Runoff Determination from Rainfall Without Using Coefficients." Trans. ASCE 107:1039-1117.

Horton, R. E. 1938. "The Interpretation and Application of Runoff Plot Experiments with Reference to Soil Erosion Problems." Proc. Soil Sci. Soc. Am. 3:340-349.

Jens, S. W. 1948. "Drainage of Airport Surfaces: Some Basic Design Considerations." Trans. ASCE 113:785-809.

Kay, B. L. 1983. Straw As an Erosion Control Mulch. Agronomy Process Report No. 140. University of California at Davis, Agricultural Experiment Station Cooperative Extension, Davis, California.

Kent, K. M. 1973. A Method for Estimating Volume and Rate of Runoff in Small Watersheds. SCS-TP-149, U.S. Department of Agriculture, Soil Conservation Service, Washington, D.C.

Knisel, W. G., ed. 1980. CREAMS: A Field-Scale Model for Chemical, Runoff, and Erosion from Agricultural Management Systems. Conservation Report No. 26, U.S. Department of Agriculture, Washington, D.C.

Kuh, H., D. L. Raddell and E. A. Hiler. 1976. Two-Dimensional Model of Erosion from a Watershed. Paper 76-2539. American Society of Agricultural Engineers, St. Joseph, Michigan.

Langbein, W. B., and S. A. Schumm. 1958. "Yield of Sediment in Relation to Mean Annual Precipitation." Trans. Am. Geophys. Union 39:1076-84.

Langbein, W. B., et al. 1949. Annual Runoff in the United States. Circular 52, U.S. Geological Survey, Washington, D.C.

Leonard, R. A., and R. D. Wauchope. 1980. "The Pesticide Submodel." In CREAMS: A Field Scale Model for Chemicals, Runoff, and Erosion from Agricultural Management Systems. Conservation Report No. 26, Chapter 5, pp. 88-112. U.S. Department of Agriculture, Washington, D.C.

Lighthill, M. H., and G. B. Whitham. 1955. "On Kinematic Waves, I. Flood Movement in Long Rivers." Proc. R. Soc. Lond. A 229:281-316.

Meyer, L. D. 1974. "Overview of the Urban Erosion and Sedimentation Processes." In Proceedings of the National Symposium on Urban Rainfall and Runoff and Sediment Control, University of Kentucky, Lexington, Kentucky, July 29-31, 1974.

McCool, D. K., W. H. Wischmeier and L. C. Johnson. 1974. Adapting the Universal Soil Loss Equation to the Pacific Northwest. Paper No. 74-2523. American Society of Agricultural Engineers, St. Joseph, Michigan.

McCool, D. K., R. I. Papendick and F. L. Brooks. 1976. "The Universal Soil Loss Equation as Adapted to the Pacific Northwest." In Proceedings of the Third Federal Interagency Sedimentation Conference, PB-245-100, pp. 2.135-2.147. Water Resources Council, Washington, D.C.

Mills, W. B., D. B. Porcella, M. J. Ungs, S. A. Gherini, K. V. Summers, L. Mok, G. L. Rupp and G. L. Bowie. 1985. WATER QUALITY ASSESSMENT: A Screening Procedure for Toxic and Conventional Pollutants in Surface and Groundwater. Vols. I and II. EPA/600/6-85/002. NTIS PB86-12249 6, U.S. Environmental Protection Agency, Athens, Georgia.

Mitchell, J. K., and G. D. Bubenzer. 1980. "Soil Loss Estimation." In Soil Erosion, eds. M. J. Kirby and R. P. C. Morgan. Wiley, New York.

Morgan, R. P. C. 1980. "Implications." In Soil Erosion, eds. M. J. Kirby and R. P. C. Morgan. Wiley, New York.

Novotny, V. 1976. Hydrologic and Hydraulic Conceptual Models Applicable to Overland and River Transport Modeling. Literature Review No. 4, August 1976. Water Resources Center, University of Wisconsin, Madison, Wisconsin.

Novotny, V., and G. Chesters. 1981. Handbook of Nonpoint Pollution. Van Nostrand Reinhold, New York.

Onstad, C. A., and G. R. Foster. 1975. "Erosion Modeling over Watershed." Trans. ASAE (Am. Soc. Agric. Eng.) 18(2):288-292.

Onstad, C. A., R. F. Piest and K. E. Saxton. 1976. "Watershed Erosion Model Validation for Southwest Iowa." In Proceedings of the Third Federal Inter-Agency Sedimentation Conference, PB-245-100, pp. 1.22-1.34. Water Resources Council, Washington, D.C.

Onstad, C. A., C. K. Mutchler and A. J. Bowie. 1977. "Predicting Sediment Yields." In National Symposium on Soil Erosion and Sedimentation by Water. American Society of Agricultural Engineers Proceedings, St. Joseph, Michigan, December 1977.

Overcash, M. R., and J. M. Davidson. 1980. Environmental Impact of Nonpoint Source Pollution. Ann Arbor Science, Ann Arbor, Michigan.

Ports, M. A. 1973. Use of the Universal Loss Equation as a Design Standard. Water Resources Engineering Meeting, American Society of Agricultural Engineers, Washington, D.C.

Rovey, E. W., D. A. Woolhiser and R. E. Smith. 1977. A Distributed Kinematic Model of Upland Watersheds. Hydrology Paper No. 93, Colorado State University, Fort Collins, Colorado, 52 p.

SCS. 1972. "Hydrology Guide for Use in Watershed Planning." SCS National Engineering Handbook, Section 4, Hydrology, Supplement A. U.S. Department of Agriculture, Soil Conservation Service, Washington, D.C.

SCS. 1982. SCS National Engineering Handbook, Section 4, Hydrology. 1982 Update. U.S. Department of Agriculture, Soil Conservation Service, Washington, D.C.

Schroeder, P. R., A. C. Gibson and M. D. Smolen. 1984. The Hydrologic Evaluation of Landfill Performance (HELP) Model. U.S. Environmental Protection Agency, Cincinnati, Ohio.

Schumm, A. A. 1977. The Fluvial System. Wiley, New York.

Shultz, H. L., W. A. Palmer, G. H. Dixon and A. F. Gleit. 1986. Superfund Exposure Assessment Manual. OSWER Directive 9285.5-1. U.S. Environmental Protection Agency, Office of Emergency and Remedial Response, Washington, D.C. (Draft).

Stewart, B. A., D. A. Woolhiser, W. H. Wischmeier, J. H. Caro and M. H. Frere. 1975. Control of Water Pollution from Croplands. Vols. I and II. EPA-600/2-75-026, U.S. Environmental Protection Agency, Washington, D.C.

USBR. 1977. Design of Small Dams. U.S. Department of the Interior, Bureau of Reclamation. U.S. Government Printing Office, Washington, D.C.

USDA. 1975. Guides for Erosion and Sediment Control in California. U.S. Department of Agriculture, Soil Conservation Service, Davis, California.

Whelan, G. 1980. Distributed Model for Sediment Yield. Master's Thesis, Iowa Institute of Hydraulic Research, University of Iowa, Iowa City, Iowa.

Williams, J. R., and H. D. Berndt. 1976. Sediment Yield Prediction Based on Watershed Hydrology. Paper No. 76-2535, American Society of Agricultural Engineers, St. Joseph, Michigan.

Wischmeier, W. H. 1976. "Use and Misuse of the Universal Soil Loss Equation." J. Soil Water Conserv. 31(1): 5-9.

Wischmeier, W. H., and D. D. Smith. 1958. "Rainfall Energy and Its Relationship to Soil Loss." Trans. Am. Geophys. Union 39(2):258-291.

Wischmeier, W. H., and D. D. Smith. 1965. Predicting Rainfall Erosion Losses from Cropland East of the Rocky Mountains. Agricultural Handbook No. 282, U.S. Department of Agriculture, Washington, D.C.

Wischmeier, W. H., and D. D. Smith. 1978. Predicting Rainfall Erosion Losses: A Guide to Conservation Planning. Agricultural Handbook No. 537. U.S. Department of Agriculture, Washington, D.C.

Wischmeier, W. H., C. B. Johnson and B. V. Cross. 1971. "A Soil Erodibility Nomograph for Farmland and Construction Sites." J. Soil Water Conserv. 26:189-193.

Witinok, P. M. 1979. Distributed Watershed and Sedimentation Model. Master's Thesis, University of Iowa, Iowa City, Iowa.

Witinok, P. M., and G. Whelan. 1980. "Distributed Parameter Sedimentation Model." Proc. Iowa Acad. Sci. 87(3)103-111.

Woolhiser, D. A., and J. A. Liggett. 1967. "Unsteady, One-Dimensional Flow Over a Plane: The Rising Hydrograph." Water Resour. Res. 3(3):752-771.

Woolhiser, D. A. 1974. "Simulation of Unsteady Overland Flow," Chapter 12. Institute on Unsteady Flow, Fort Collins, Colorado.

5.0 GROUNDWATER PATHWAY

5.1 INTRODUCTION

The groundwater component of the RAPS methodology provides estimates of groundwater contaminant concentrations and/or fluxes at various transporting medium interfaces (i.e., water table surface and edge of stream) and at withdrawal wells. Contaminant concentrations at transporting medium interfaces and withdrawal wells provide contaminant levels for the exposure assessment component of RAPS. Contaminant fluxes at transporting medium interfaces represent boundary conditions for the next medium that is to simulate contaminant migration and fate (e.g., groundwater contamination entering a surface water environment). A schematic diagram illustrating the groundwater environment is presented in Figure 5.1.

The migration and fate of contaminants through the groundwater (i.e., subsurface) environment are described by the three-dimensional advective-dispersive equation for solute transport. The results are based on semi-analytical solutions (e.g., solutions that require numerical integration) that are well established in the scientific literature. To increase the computational efficiency of the integration, limits of integration are also identified.

The groundwater model accounts for the major mechanisms of constituent mobility (i.e., adsorption/desorption), persistence (i.e., degradation or decay), advection, and hydrodynamic dispersion. Mobility is described by an equilibrium coefficient that assumes instantaneous adsorption/desorption between the soil matrix and the pore water. Persistence is described by a first-order degradation/decay coefficient; for radionuclides, the groundwater component of RAPS also accounts for decay products. Advection is described by constant, unidirectional flow in the vertical direction in the partially saturated zone and in the longitudinal direction in the saturated zone. Hydrodynamic dispersion is described in three dimensions.

Other assumptions associated with the groundwater component of RAPS include the following:

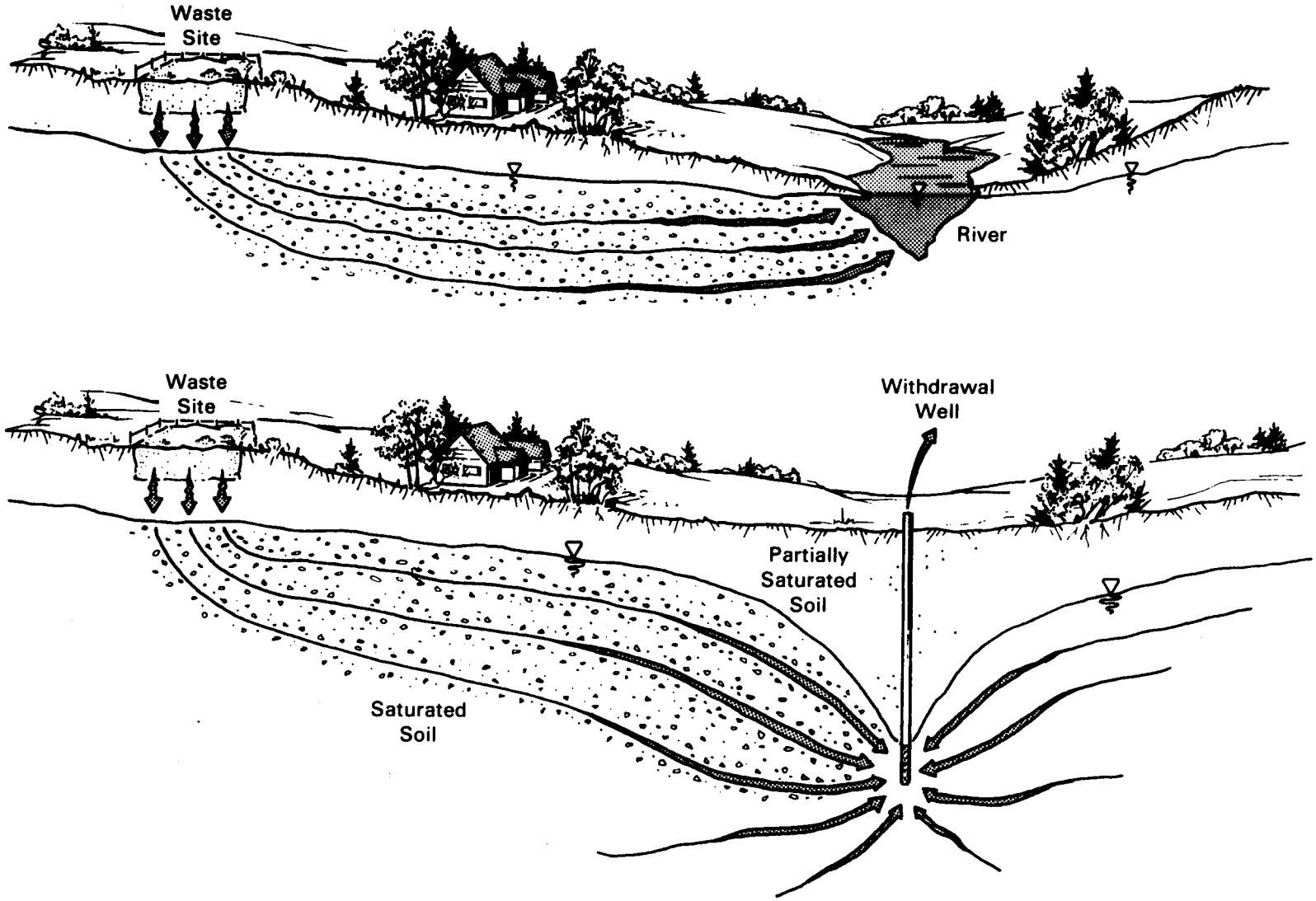

FIGURE 5.1. Schematic Diagram Illustrating the Groundwater Environment: a) Contaminant Levels or Fluxes at a Surface Water Boundary and b) Contaminant Levels at a Withdrawal Well

- All aquifer properties are homogeneous and isotropic.
- Flow in both the partially saturated and saturated zones is uniform.
- The groundwater environment is initially free of contamination.
- The effects of withdrawal well drawdown and other transient stresses on the saturated aquifer are not considered in the semianalytical solutions. Hydraulic gradients and flow velocities are assumed to be provided by the user.

The groundwater pathway of the RAPS methodology models solute transport through the partially saturated and saturated zones of the groundwater (i.e., subsurface) environment. The numerical algorithms describing the mathematical formulations of each groundwater component are presented in this chapter. The topics addressed in this chapter are as follows:

- advective-dispersive equation -- The advective-dispersive equation describes solute migration in the groundwater environment (both partially saturated and saturated zones). The form of the equation used by the groundwater component is briefly discussed.
- contaminant concentration equations -- The various semianalytical (i.e., combined analytical and numerical algorithms) solutions to the advective-dispersive equation are presented. The solutions describe solute concentrations.
- contaminant flux equations -- The various equations describing contaminant fluxes from one medium to another are presented. The equations describe solute movement between a series of partially saturated zones, partially saturated and saturated zones, and/or a saturated zone and a surface water body.
- integration limits -- Because the solutions to the advective-dispersive equation are semianalytical and must be integrated over time, integration limits that increase the computational efficiency are described.
- mixing length -- Lateral and vertical mixing lengths are defined; these describe the respective distances in which the migrating solute

plume is fully mixed. The time for the contaminant to travel from the waste site through groundwater porous media to a receptor of concern is described. The travel time is used in determining mixing lengths.

- contaminant degradation/decay -- The technique for computing the degradation of chemicals and/or the decay of radionuclides is described.

5.2 ADVECTIVE-DISPERSIVE EQUATION

The advective-dispersive equation for solute movement through a porous medium with a constant, steady-state flow velocity forms the basis of all groundwater solution algorithms. As noted by Codell et al. (1982), the algorithms are developed for the limiting case of unidirectional advective transport with three-dimensional dispersion in a homogeneous, saturated aquifer. Let n and n_e represent total and effective porosities, respectively; then $n - n_e$ is the remaining void fraction devoted to nonflowing waters. A mass balance on the differential volume $dV = dx\ dy\ dz$ gives the expression:

$$\underset{(a)}{n_e \frac{\partial C}{\partial t}} + \underset{(b)}{(n - n_e) \frac{\partial G}{\partial t}} + \underset{(c)}{(1 - n) \frac{\partial P}{\partial t}} + \underset{(d)}{n_e u \frac{\partial C}{\partial x}} =$$

$$n_e \left[E_x \frac{\partial^2 C}{\partial x^2} + \underset{(e)}{E_y \frac{\partial^2 C}{\partial y^2}} + E_z \frac{\partial^2 C}{\partial z^2}\right] +$$

$$(n - n_e) \left[E'_x \frac{\partial^2 G}{\partial x^2} + \underset{(f)}{E'_y \frac{\partial^2 G}{\partial y^2}} + E'_z \frac{\partial^2 G}{\partial z^2}\right] - \qquad (5.1)$$

$$\underset{(g)}{n_e \lambda C} - \underset{(h)}{(1 - n) \lambda P} - \underset{(i)}{(n - n_e) \lambda G}$$

where n = total porosity (dimensionless)

n_e = effective porosity (dimensionless)

C = dissolved concentration in the liquid phase in the flowing voids (g/ml or Ci/ml)[a]

t = time (s)

G = dissolved concentration in the liquid phase in the nonflowing voids (g/ml or Ci/ml)

P = particulate concentration on the solid phase (g/g or Ci/g)

u = the x-component groundwater (pore water) velocity (cm/s)

E_x, E_y, E_z = the dispersion coefficients in the flowing voids in the x-, y-, and z-directions, respectively (cm^2/s)

E'_x, E'_y, E'_z = the diffusion coefficients in the nonflowing voids in the x-, y-, and z-directions, respectively (cm^2/s)

λ = the decay constant [= (ℓn 2)/(half-life)] (s^{-1}).

In Equation (5.1), term (a) is the accumulation (storage) in the liquid phase in the flowing void; (b) is the accumulation in the liquid phase in the nonflowing void; (c) is the accumulation in the solid phase; (d) is the x-direction advective transport in the flowing voids in the liquid phase; (e) is the dispersive transport in the flowing voids in the liquid phase in the x-, y-, and z-directions; (f) is the diffusive transport in the nonflowing voids in the liquid phase in the x-, y-, and z-directions, respectively; and (g), (h), and (i) are, respectively, the chemical degradation or radioactive decay in the liquid phase in the flowing void, in the solid phase, and in the liquid phase in the nonflowing void.

Equation (5.1) can be streamlined with some simplifying assumptions. One assumption is that the dissolved concentration in the nonflowing voids (G) equals the dissolved concentration in the flowing voids (C). A second assumption is that the contaminant sorption process can be described by a constant (i.e., Kd) representing the ratio between the contaminant adsorbed to the soil matrix (i.e., P) and the contaminant dissolved in solution (C). A final

---

(a) When two sets of units are provided, the first refers to chemicals, and the second refers to radionuclides.

assumption is that the diffusion in the nonflowing void is comparable with the dispersion in the flowing void. Using these assumptions, Equation (5.1) can be rewritten as

$$\frac{\partial C}{\partial t} + \frac{u}{R_{f_1}} \frac{\partial C}{\partial x} = \frac{D_x}{R_{f_1}} \frac{\partial^2 C}{\partial x^2} + \frac{D_y}{R_{f_1}} \frac{\partial^2 C}{\partial y^2} + \frac{D_z}{R_{f_1}} \frac{\partial^2 C}{\partial z^2} - \lambda C \tag{5.2}$$

in which

$$D = \frac{n\ E}{n_e} \tag{5.3}$$

$$R_{f_1} = \frac{n}{n_e} + \frac{\beta}{n_e} Kd \tag{5.4}$$

where D = pseudodispersion coefficient (cm^2/s)
R_f = retardation factor (dimensionless)
β = bulk density (g/ml)
Kd = equilibrium (partition or distribution) coefficient (ml/g).

The retardation factor (i.e., coefficient) is used as a measure of the mobility of constituents in a porous medium. It represents the ratio of the mean pore water velocity to the mean contaminant migration velocity and can be expressed in a number of ways. Other forms describing the retardation factor have also appeared in the literature (e.g., any groundwater textbook) and have been expressed by

$$R_{f_2} = 1 + \frac{\beta}{n_e} Kd \tag{5.5}$$

$$R_{f_3} = 1 + \frac{\beta}{n} Kd \tag{5.6}$$

$$R_{f_4} = 1 + \frac{\beta}{\theta} Kd \tag{5.7}$$

where θ is the moisture content of partially saturated zone.

Equation (5.4) assumes that the porous medium is composed of interconnected pore spaces through which flow occurs (i.e., n_e) and dead-end pore spaces through which no flow occurs (i.e., $n - n_e$). The contaminant in Equation (5.4) is assumed to migrate through the interconnected pore spaces, diffuse into dead-end pore spaces, and instantaneously adsorb to or desorb from the soil matrix where fluid is and is not flowing. Equation (5.4) also assumes that the solute concentration in the dead-end pore spaces is equivalent to the solute concentration in the free-flowing spaces and that the dispersion coefficients in both locations are equivalent. Equation (5.5) includes the same processes as Equation (5.4) except that the contaminant does not diffuse into dead-end pore spaces. For this second case, the pseudodispersion coefficients (D_x, D_y, and D_z) equal the dispersion coefficients (E_x, E_y, and E_z, respectively). Equation (5.6) includes the same phenomena as Equation (5.4) except that the porous medium contains no dead-end pore spaces. Again, the pseudodispersion coefficients equal the dispersion coefficients because effective porosity equals the porosity. Equations (5.6) and (5.7) describe the retardation of the contaminant in a similar manner; the major difference between them is that the porosity in Equation (5.6) is replaced by the moisture content to give Equation (5.7). Equations (5.4) through (5.6) are used in the saturated zone, while Equation (5.7) is used in the partially saturated zone. By making the following substitutions

$$u^* = u/R_f \tag{5.8}$$

and

$$D^* = D/R_f \tag{5.9}$$

Equation (5.2) can be rewritten as

$$\frac{\partial C}{\partial t} + u^* \frac{\partial C}{\partial x} = D_x^* \frac{\partial^2 C}{\partial x^2} + D_y^* \frac{\partial^2 C}{\partial y^2} + D_z^* \frac{\partial^2 C}{\partial z^2} - \lambda C \tag{5.10}$$

As written, Equation (5.1) specifically addresses the general conditions for saturated flow and solute movement. However, Equation (5.1) can also be applied to the partially saturated zone if minor modifications are made. To apply the equation to the partially saturated zone, the porosities (n and n_e) are assumed to be equal to the soil matrix moisture content. In addition, one-dimensional, unidirectional flow and dispersion are assumed only in the vertical (z) direction. Note that with these assumptions 1) Equation (5.7) defines the retardation factor, 2) Equation (5.10) is applicable if the coordinate system is rotated such that the x-axis corresponds to the z-direction, and 3) dispersion is only considered in the flow direction. The solution algorithm to the advective-dispersive equation is based on homogeneous and isotropic soil parameters (Van Genuchten and Alves 1982; Donigian et al. 1983). The partially saturated soil beneath the waste site is assumed at a unit potential hydraulic gradient. The moisture content is assumed to fluctuate between field capacity and saturation. The hydraulic conductivity is based on an empirical equation proposed by Gardner (1960), Gardner et al. (1970), Campbell (1974), and Clapp and Hornberger (1978) and is expressed as (Hillel 1980)

$$K(\theta) = K_s \, (\theta/n)^{1/m} \qquad (5.11)$$

where $K(\theta)$ = hydraulic conductivity (cm/s)
θ = moisture content (dimensionless)
K_s = saturated hydraulic conductivity (i.e., permeability) (cm/s)
n = total porosity (dimensionless)
m = empirically based parameter that is a function of soil properties.

Hillel (1980) notes that although attempts have been made to develop theoretically based equations relating hydraulic conductivity to moisture content, the state of the art is such that consistently accurate a priori predictions of $K(\theta)$ from basic soil properties are difficult.

Whelan et al. (1986) note that if the infiltration rate (leach rate) of water from the waste site is less than the soil transmission rate, as described by the general equation for liquid flow in the partially saturated zone (Hanks

and Ashcroft 1980; Hillel 1980), the water moves through the soil at the infiltration rate, accounting for adjustments in the soil moisture content. For an infiltration rate equal to or greater than the transmission rate, the leachate is assumed to move at the transmission rate.

For ponded waters, Hillel (1971) notes that the downward infiltration into an initially partially saturated soil generally occurs under the combined influence of suction and gravity gradients. As the water penetrates deeper and the wetted part of the profile lengthens, the average suction gradient decreases, because the overall difference in pressure head (between the saturated soil surface and the unwetted soil inside the profile) divides itself along an ever-increasing distance. This trend will continue until eventually the suction gradient in the upper part of the profile becomes negligible, leaving the constant gravitational gradient as the only remaining force moving water downward in this upper or transmission zone. Because the gravitational head gradient has the value of unity, it follows that the flux tends to approach the hydraulic conductivity as the limiting value. Therefore, in a uniform soil without crust under prolonged ponding, the water content of the wetted zone approaches the saturated hydraulic conductivity. Based on this reasoning, a unit hydraulic gradient and saturated conditions, as described by a saturated hydraulic conductivity, are assumed for the subsurface region below ponded sites.

5.3 CONTAMINANT CONCENTRATION EQUATIONS

By solving Equation (5.10) with the appropriate boundary and initial conditions, a set of semianalytical expressions is obtained that characterize the transport of contaminants through the partially saturated and saturated groundwater zones. These expressions are based on Green's functions and have been reported by several researchers (e.g., Selim and Mansell 1976; Yeh and Tsai 1976; Yeh 1981; Codell et al. 1982). Various analytical expressions describing solute concentrations at selected locations and times can be described by one basic equation:

$$Ci_{\ell} = \alpha_m X_i Y_j Z_k \qquad (5.12)$$

where Ci_{ℓ} = instantaneous solute concentration at location x, y, z and time t for an instantaneous source release for the ℓ-th solution $(cm^{-3})^{(a,b)}$

α_m = parameter that ensures mass balance and that is based on initial and boundary conditions for the m-th assumption

X_i = Green's function in the x-direction for the i-th solution (cm^{-1})

Y_j = Green's function in the y-direction for the j-th solution (cm^{-1})

Z_k = Green's function in the z-direction for the k-th solution (cm^{-1})

in which

$$\alpha_1 = \frac{1}{R_{f_1} n_e} \tag{5.13}$$

$$\alpha_2 = \frac{1}{R_{f_2} n_e} \tag{5.14}$$

$$\alpha_3 = \frac{1}{R_{f_3} n} \tag{5.15}$$

$$\alpha_4 = \frac{1}{R_{f_4} \theta} \tag{5.16}$$

(a) Based on unit mass in grams.
(b) When included in an equation, "Ci" refers to instantaneous solute concentration; otherwise, it refers to the unit "curies."

5.3.1 Green's Functions

The various solutions associated with X_i, Y_j, and Z_k can be derived using Green's relationships (Carslaw and Jaeger 1959; Yeh and Tsai 1976; Yeh 1981) or by the method of separation of variables (Ritger and Rose 1968; Codell et al. 1982). X_i, Y_j, and Z_k reflect the geometry associated with the source (i.e., boundary conditions) releasing the contaminants; for example, a point source and a line source will each have a different solution. The expressions describing X_i, Y_j, and Z_k by source-term type that are incorporated into the RAPS methodology are as follows:

$$X_1 = \left(\frac{1}{4 \pi D_x^* t}\right)^{1/2} \exp(-\lambda t) \exp\left[-\frac{(x - u^* t)^2}{4 D_x^* t}\right] \qquad (5.17)$$

with C = 0 at t = 0 and x = ± ∞

where X_1 = the point-source solution in the x-direction with flow in the x-direction only (cm^{-1}).

$$X_2 = \frac{1}{2 \ell} \exp(-\lambda t)\left\{\operatorname{erf}\left[\frac{x + \frac{\ell}{2} - u^* t}{(4 D_x^* t)^{1/2}}\right] - \operatorname{erf}\left[\frac{x - \frac{\ell}{2} - u^* t}{(4 D_x^* t)^{1/2}}\right]\right\} \qquad (5.18)$$

with C = 0 at t = 0 and x = ± ∞

where X_2 = line-source solution in the x-direction with flow in the x-direction only (cm^{-1})

ℓ = length of contaminated line source in the x-direction (cm).

$$Y_1 = \left(\frac{1}{4 \pi D_y^* t}\right)^{1/2} \exp\left(-\frac{y^2}{4 D_y^* t}\right) \qquad (5.19)$$

with C = 0 at t = 0 and y = ± ∞

where Y_1 = point-source solution in the y-direction for an aquifer of infinite width (cm^{-1}).

$$Y_2 = \left(\frac{1}{2\,b}\right)\left\{\text{erf}\left[\frac{y + \frac{b}{2}}{(4\,D_y^*\,t)^{1/2}}\right] - \text{erf}\left[\frac{y - \frac{b}{2}}{(4\,D_y^*\,t)^{1/2}}\right]\right\} \qquad (5.20)$$

with $C = 0$ at $t = 0$ and $y = \pm \infty$

where Y_2 = line-source solution in the y-direction for an aquifer of infinite width (cm^{-1})

b = length of contaminated line or area source in the y-direction (cm).

$$Z_1 = \left(\frac{1}{4\,\pi\,D_z^*\,t}\right)^{1/2} \exp\,(-\lambda\,t)\ \exp\left[-\frac{(z - w^*\,t)^2}{4\,D_z^*\,t}\right] \qquad (5.21)$$

with $C = 0$ at $t = 0$ and $z = \pm \infty$

where Z_1 = point-source solution in the z-direction with flow in the z-direction (cm^{-1}). (Note: This expression represents the one-dimensional solution of the advective-dispersive transport equation [i.e., Equation (5.1)] in the z-direction.)

w^* = flow velocity in the z-direction, adjusted for retardation (i.e., ratio of the seepage rate and retardation factor) (cm/s);

$$Z_2 = \frac{1}{h_m} \qquad (5.22)$$

with $C = 0$ at $t = 0$; $\partial C/\partial z = 0$ at $z = 0$ and $z = h_m$

where Z_2 = vertically averaged solution over the aquifer depth h_m (cm^{-1})

h_m = vertical distance over which contaminant is assumed to be uniformly distributed ($0 < h_m \leq h$; see Section 5.6.1) (cm)

h = depth of saturated aquifer (cm).

$$Z_3 = \frac{1}{h} \tag{5.23}$$

with $C = 0$ at $t = 0$; $\partial C/\partial z = 0$ at $z = 0$ and $z = h$ (cm^{-1})
where Z_3 = vertically averaged solution over the aquifer depth h (cm^{-1}).

5.3.2 Solute Concentrations

Solute concentrations are computed by combining Green's functions (i.e., X_i, Y_j, and Z_k) in a multiplicative manner. The types of configurations at the source considered in the RAPS methodology are point source, line source (in x- and y-direction), and area source (in x-y plane).[a] The various instantaneous solute concentration options addressed by the RAPS methodology are as follows. Each is presented in a form similar to that expressed by Equation (5.12).

Partially Saturated Zone:

$$Ci_1 = \frac{\alpha_1 \, Z_1}{b \, \ell} \tag{5.24}$$

where Ci_1 = solute concentration with flow only in the z-direction for an instantaneous release (cm^{-3}).

Saturated Zone:

Point Source:

$$Ci_2 = \alpha_1 \, X_1 \, Y_1 \, Z_2 \quad \text{when } h_m < h \tag{5.25}$$

$$Ci_3 = \alpha_1 \, X_1 \, Y_1 \, Z_3 \quad \text{when } h_m \geq h^{(b)} \tag{5.26}$$

(a) The terms "point source," "line source," and "area source" refer to the source-term configuration, which reflects simplifying assumptions, and do not refer to the exact technical definition associated with the instantaneous concentration equation. Note, for example, that a vertically averaged point source represents a line source in the z-direction.

(b) When h_m is greater than h, h_m is set equal to h. See Section 5.6.1 for more information.

where Ci_2 = vertically integrated solute concentration over the aquifer depth h_m at a well for a point source (cm^{-3})

Ci_3 = vertically integrated solute concentration over the aquifer depth h at a well for a point source (cm^{-3}).

Line Source:

$$Ci_4 = \alpha_1 X_1 Y_2 Z_2 \quad \text{when } h_m < h \tag{5.27}$$

$$Ci_5 = \alpha_1 X_1 Y_2 Z_3 \quad \text{when } h_m \geq h \tag{5.28}$$

$$Ci_6 = \alpha_1 X_2 Y_1 Z_2 \quad \text{when } h_m < h \tag{5.29}$$

$$Ci_7 = \alpha_1 X_2 Y_1 Z_3 \quad \text{when } h_m \geq h \tag{5.30}$$

where Ci_4 = vertically integrated solute concentration over the aquifer depth h_m at a well for a line source in the y-direction (cm^{-3})

Ci_5 = vertically integrated solute concentration over the aquifer depth h at a well for a line source in the y-direction (cm^{-3})

Ci_6 = vertically integrated solute concentration over the aquifer depth h_m at a well for a line source in the x-direction (cm^{-3})

Ci_7 = vertically integrated solute concentration over the aquifer depth h at a well for a line source in the x-direction (cm^{-3})

Area Source:

$$Ci_8 = \alpha_1 X_2 Y_2 Z_2 \quad \text{when } h_m < h \tag{5.31}$$

$$Ci_9 = \alpha_1 X_2 Y_2 Z_3 \quad \text{when } h_m \geq h \tag{5.32}$$

where Ci_8 = vertically integrated solute concentration over the aquifer depth h_m at a well for line sources in the x- and y-directions (i.e., horizontal area source) (cm^{-3})

Ci_9 = vertically integrated solute concentration over the aquifer depth h at a well for line sources in the x- and y-directions (cm^{-3})

Note that when two line-source solutions corresponding to orthogonal directions [e.g., X_2 and Y_2 in Equations (5.31) and (5.32)] are combined, a solution results for an area source. Also note that Equations (5.12) through (5.32) have been formulated in terms of an instantaneous contaminant release (i.e., a pulse release over zero time). Codell et al. (1982) note that these equations can be generalized for arbitrary time-varying releases by using the convolution integral

$$C(\tau) = \int_0^{\tau} f(t)\ Ci_{\ell}(\tau - t)\ dt \qquad (5.33)$$

where τ = the time over which contaminant concentration is computed (s)

$f(t)$ = source term expressed as a temporally varying contaminant flux (g/s or Ci/s).

5.4 CONTAMINANT FLUX EQUATIONS

Contaminant fluxes are computed to indicate the transfer of contaminants between successive media (between partially saturated layers, partially saturated and saturated zones, etc.). The fluxes are computed when they leave one medium (e.g., the groundwater environment) and act as boundary conditions to the next medium to be modeled (e.g., the surface water environment). The RAPS methodology can calculate the discharge rate of a contaminant entering a partially saturated layer, the saturated zone, and a surface water body that has intercepted the aquifer containing the transported material. It is assumed that if the surface water body is the final transporting medium, then all

contaminants entering the subsurface environment will eventually enter the water body, except for the portion of the contaminants that has been lost through degradation/decay.

The RAPS methodology assumes a unidirectional flow field and bases its flux computations on contaminated material crossing an area perpendicular to the flow axis. Using the flow (i.e., x) direction in the saturated zone as an example, the instantaneous flux perpendicular to the x-direction can be described by the following equation:

$$\frac{dFi_{\ell}}{dA} = n_e \left(u\ Ci_{\ell} - D_x \frac{\partial Ci_{\ell}}{\partial x} \right) \tag{5.34}$$

where Fi_{ℓ} = instantaneous contaminant flux resulting from an instantaneous release (g/s or Ci/s)

A = cross-sectional area perpendicular to the flow direction ($dA = dy\ dz$) (cm^2).

The total flux across the plane is, therefore, described by laterally and vertically integrating Equation (5.43):

$$Fi_{\ell} = n_e \int_0^{h_m} \int_{-\infty}^{+\infty} \left(u\ Ci_{\ell} - D_x \frac{\partial Ci_{\ell}}{\partial x} \right) dy\ dz \tag{5.35}$$

The temporally distributed contaminant flux (Fi_1) in the longitudinal direction resulting from an instantaneous release of a point source at $x = 0$ and $t = 0$, as described by Equation (5.25) or (5.26), is given by

$$Fi_1 = \left[\frac{x + u^* t}{16\ \pi\ D_x^*\ t^3}^{1/2} \right] \exp - \left[\left(\frac{(x - u^* t)^2}{4\ D_x^* t} + \lambda t \right) \right] \tag{5.36}$$

The temporally distributed contaminant flux (Fi_2) in the longitudinal direction resulting from an instantaneous release of an area source at x = 0 and t = 0, as described by Equation (5.31) or (5.32), is given by

$$Fi_2 = \left[\frac{\exp(-\lambda t)}{\ell}\right]\left(\frac{1}{4\pi D_x^* t}\right)^{1/2}\left\{u^*(\pi D_x^* t)^{1/2}\left[\text{erf}(A_1) - \text{erf}(A_2)\right] - D_x^*\left[\exp\left(-A_1^2\right) - \exp\left(-A_2^2\right)\right]\right\} \quad (5.37)$$

in which

$$A_1 = \frac{x + \ell/2 - u^* t}{(4 D_x^* t)^{1/2}} \quad (5.38)$$

$$A_2 = \frac{x - \ell/2 - u^* t}{(4 D_x^* t)^{1/2}} \quad (5.39)$$

The contaminant flux in the vertical direction (Fi_3) resulting from an instantaneous release of a point source at z = 0 and t = 0, as described by Equation (5.25), is given by

$$Fi_3 = \frac{z + w^* t}{\left(16\pi D_z^* t^3\right)^{1/2}} \exp\left[-\left(\frac{(z - w^* t)^2}{4 D_z^* t} + \lambda t\right)\right] \quad (5.40)$$

Equations (5.36), (5.37), and (5.40) have been formulated in terms of an instantaneous contaminant release. These equations can be generalized for arbitrary time-varying releases by the use of the convolution integral

$$F(\tau) = \int_0^\tau f(t)\, Fi_\ell(\tau - t)\, dt \quad (5.41)$$

Note that when Equations (5.36), (5.37), and (5.40) were simplified, the α_m terms factored out of the solutions.

5.5 INTEGRATION LIMITS

Equations (5.33) and (5.41) are evaluated in RAPS by a standard Simpson's rule for numerical integration (Carnahan et al. 1969). As noted by Codell et al. (1982), several special precautions are taken, however, to preserve computational accuracy and efficiency. The terms within the integral sign of the equations can be very nearly equal to zero over part of the computational range, if $f(t)$ is equal to zero or if $Ci_\ell(\tau - t)$ or $Fi_\ell(\tau - t)$ is very nearly zero or equal to zero. If we ensure that $Ci_\ell(\tau - t)$ or $Fi_\ell(\tau - t)$ is small enough to provide little to the integration, integration limits can be developed. Because an area source represents the most general description, it is used in developing integration limits.

By inspection, the argument of the error function in Equation (5.18) provides the best opportunity for developing integration limits. So that all of the terms in the argument of the error function do not have to be continually rewritten, let

$$W = \frac{x \pm \ell/2 - u^* t}{(4 D_x^* t)^{1/2}} \tag{5.42}$$

For an area source, the solution for X_2 involves an error function. As the argument of the error function becomes larger and larger, the error function moves closer to unity, and the difference between the error functions in Equation (5.18) approaches zero, thereby providing little to the integration. By supplying an upper and lower bound to the integral, a reasonable and efficient time frame can be developed for defining the source term for routing contaminants through successive media.

Upper and lower cutoff times can be defined by approximating the error function with a series expansion. Approximating the error function with the rational approximation series (Abramowitz and Stegun 1964) gives

$$\text{erf}\,(W) \simeq 1 - \left[\frac{\exp(-W^2)}{W\sqrt{\pi}}\right]\left[1 - \frac{2!}{1!\,(2W)^2} + \frac{4!}{2!\,(2W)^4} \cdots \frac{(2n)!}{n!\,(2W)^{2n}}\right] \tag{5.43}$$

By neglecting terms other than unity in the series expansion, the error function can be approximated as

$$\text{erf}\ (W) \simeq 1 - \frac{\exp\ (-\ W^2)}{W\ \sqrt{\pi}} \tag{5.44}$$

By setting the argument of the exponential equal to the negative of a parameter γ such that γ reduces the exponential to approximately zero, the integrand will contribute nothing to the integration. By adjusting the argument of the exponential for degradation/decay, the parameter γ can be defined as

$$\gamma = W^2 + \lambda\ t \tag{5.45}$$

and solving for t in Equation (5.45), upper and lower temporal limits can be defined. The lower temporal limit (t_1) is then

$$t_1 = \frac{1}{2}\left\{\left[\frac{2\ u^*\ (x - \ell/2) + 4\ D_x^*\ \gamma}{(u^*)^2 + 4\ D_x^*\ \lambda}\right] - \left[\left(\frac{2\ u^*\ (x + \ell/2) + 4\ D_x^*\ \gamma}{(u^*)^2 + 4\ D_x^*\ \lambda}\right)^2 - \left(\frac{4\ (x - \ell/2)^2}{(u^*)^2 + 4\ D_x^*\ \lambda}\right)\right]^{1/2}\right\} \tag{5.46}$$

The upper temporal limit (t_2) becomes

$$t_2 = \frac{1}{2}\left\{\left[\frac{2\ u^*\ (x + \ell/2) + 4\ D_x^*\ \gamma}{(u^*)^2 + 4\ D_x^*\ \lambda}\right] + \left[\left(\frac{2\ u^*\ (x + \ell/2) + 4\ D_x^*\ \gamma}{(u^*)^2 + 4\ D_x^*\ \lambda}\right)^2 - \left(\frac{4\ (x - \ell/2)^2}{(u^*)^2 + 4\ D_x^*\ \lambda}\right)\right]^{1/2}\right\} \tag{5.47}$$

If γ is chosen such that it is fairly large (e.g., 50), the limits of the integration ensure that only that portion of the integrand significantly contributing to the integral is considered in the computation. When successive media are modeled, γ should be defined such that only the important portion of the temporally varying concentrations is retained for successive computations. The value for γ was determined by a set of example runs and has been experimentally set equal to 50.

Equations (5.46) and (5.47) can be used to compute integration limits associated with the convolution integrals of Equations (5.33) and (5.41). The lower integration limit (t_ℓ) is defined as

$$t_\ell = 0 \qquad \text{for } t_2 \geq \tau \tag{5.48}$$

$$t_\ell = \tau - t_2 \qquad \text{for } t_2 < \tau \tag{5.49}$$

The upper integration limit (t_u) becomes

$$t_u = \tau - t_1 \tag{5.50}$$

5.6 MIXING LENGTH

When a contaminant travels from a waste site to a receptor of concern (e.g., well or river), the contaminant is temporally and spacially redistributed -- longitudinally, vertically, and laterally -- by the transporting medium. Because contaminant levels are spacially distributed at any designated receptor (e.g., well), one contaminant concentration does not describe the spacial distribution unless the fully mixed condition exists. Because the exposure component of the RAPS methodology requires only one temporally distributed contaminant concentration per receptor location, the contaminant concentration of the fully mixed region is used.

At some distance downgradient from a waste site releasing contaminants to an aquifer of constant depth, the concentration near the surface of the water table can be considered to be fully mixed over some distance in the vertical direction. As Codell et al. (1982) note, the vertical dispersion is not influenced by the vertical dimensions of the aquifer close to the point of release; the mixed region is considered to be very small. As the vertical dimension of the aquifer becomes more of an influence in the spacial distribution of the contaminants, the mixed region increases in vertical extent until a fully mixed condition exists over the depth of the aquifer.

This section briefly identifies the basis for defining the spacial extent of the mixing regions used in the saturated zone component of the RAPS methodology. A vertical mixing length is defined and is used when computing the contaminant levels at a well. A lateral mixing length is defined and is used when computing the spacial extent of groundwater contamination at the edge of a surface water body.

5.6.1 Vertical Mixing Length

The vertical mixing length is the vertical distance over which contamination at a well is considered fully mixed. Over this vertical region, the contaminant concentration is assumed to be uniformly mixed in the vertical direction and is used in computing the potential risk to populations surrounding the well.

The vertical mixing length is estimated by employing the advective-dispersive equation and its associated Gaussian distribution solution. The one-dimensional advective-dispersive equation in the vertical direction is written as

$$\frac{\partial C}{\partial t} = D_z^* \frac{\partial^2 C}{\partial z^2} \tag{5.51}$$

The unit area solution to Equation (5.51) in an aquifer of infinite vertical extent is described by

$$C = \frac{M}{\sigma_v (2\pi)^{1/2}} \exp\left(-\frac{z^2}{2\sigma_v^2}\right) \quad (5.52)$$

in which

$$\sigma_v = \left(2 D_z^* t\right)^{1/2} \quad (5.53)$$

where M = contaminant mass per unit area (g/cm^2 or Ci/cm^2)
σ_v = standard deviation in the vertical direction (cm)
t = representative contaminant travel time (s).

With the assumption that no contaminant diffusion occurs through the water table surface once the contaminant has entered the saturated aquifer, contaminant spreading (excluding lateral and longitudinal directions) is only downward in the vertical direction. Because no contaminant flux crosses the water table surface because of dispersion, the vertical mixing depth for the fully mixed condition is assumed as the dispersive distance associated with one-half the standard deviation:

$$h_m = \frac{1}{2}\sigma_v = \left(\frac{D_z^* t}{2}\right)^{1/2} \quad (5.54)$$

where h_m = vertical distance over which the contaminant is assumed to be uniformly distributed (equivalent to one-half the standard deviation) (cm).

To illustrate that Equation (5.54) has a physical basis, a mixing depth similar to that identified by Equation (5.54) can be developed by defining a time scale associated with complete vertical mixing as similar to the one found in Codell et al. (1982):

$$t_m = \xi \frac{(h'_m)^2}{D^*_z} \tag{5.55}$$

where t_m = time to achieve the fully mixed condition (i.e., representative contaminant travel time) (s)

ξ = proportionality coefficient (dimensionless)

h'_m = alternative vertical distance over which the contaminant is assumed to be uniformly distributed (cm).

By rearranging Equation (5.55), the effective depth, which represents the fully mixed condition, can be solved for

$$h'_m = \left(\phi\, t_m\, D^*_z\right)^{1/2} \tag{5.56}$$

in which

$$\phi = \frac{1}{\xi} \tag{5.57}$$

where ϕ = proportionality constant (dimensionless).

Codell et al. (1982) note that when $\phi \leq 3.3$, the fully mixed condition can be assumed, because the release may be considered, for the most part, to be unaffected by the confining layer beneath the plume. When ϕ is between 3.3 and 12, the release is considered to be neither fully mixed over the depth of the aquifer nor unaffected by the aquifer boundary. Because Equation (5.54) represents a more conservative expression than Equation (5.56) when ϕ equals 3.3 and because its derivation is consistent with other mixing-length estimations used in the RAPS methodology, Equation (5.54) is used to describe the vertical mixing length in the groundwater environment.

The groundwater contaminant levels at a well or at the boundary of a surface water body that represents the receptor of concern are computed based on the vertical mixing depth h_m and the thickness of the saturated aquifer. The

RAPS methodology computes h_m to identify the mixing depth. If h_m is larger than the aquifer depth, the aquifer depth is used in the calculations [i.e., Equations (5.26), (5.28), (5.30), and (5.32)]. When the opposite is true, the mixing depth is used in the calculations. This procedure ensures a continuous transition between the fully mixed condition and non-fully mixed condition.

Equation (5.54) is valid as long as the waste site remains above the water table surface. When the waste site penetrates the saturated aquifer (i.e., a portion of the waste site is situated below the water table surface in the saturated zone of the groundwater environment), the vertical mixing zone, with respect to the depth of the saturated aquifer, is increased by that portion of the waste site below the water table surface. For a partially penetrating waste site, the mixing depth can be expressed as

$$h_m = \left(\frac{D_z^* t}{2}\right)^{1/2} + h_w \qquad (5.58)$$

where h_w = depth of the waste site below the water table surface (cm).

5.6.2 Lateral Mixing Length

The groundwater pathway interacts with the surface water pathway by supplying the necessary boundary conditions (i.e., temporally varying contaminant fluxes). Unfortunately, the lateral distance over which the groundwater pathway supplies contaminated water may be considered infinite. To alleviate this problem, the RAPS methodology computes an effective length for the line source used as the source term for the surface water transport computations. The lateral mixing length (i.e., effective length of line source) for a conservative substance at the edge of a surface water body identifies the extent over which contamination in the groundwater at the interface (i.e., a surface water body boundary) is considered fully mixed in the lateral direction. The contaminant level is assumed to be uniformly distributed over this lateral region and is used in computing the boundary conditions for modeling the surface water environment.

As in the case of the vertical mixing length, the lateral mixing length is estimated by employing the advective-dispersive equation and its associated Gaussian distribution solution. The one-dimensional advective-dispersive equation in the lateral direction is written as

$$\frac{\partial C}{\partial t} = D_y^* \frac{\partial^2 C}{\partial y^2} \tag{5.59}$$

The unit area solution to Equation (5.59) in an aquifer of infinite lateral extent is described by

$$C = \left(\frac{M}{\sigma_\ell \ (2 \ \pi)^{1/2}} \right) \exp \left(- \frac{y^2}{2 \ \sigma_\ell^2} \right) \tag{5.60}$$

in which

$$\sigma_\ell = \left(2 \ D_y^* \ t \right)^{1/2} \tag{5.61}$$

where σ_ℓ = standard deviation in the lateral direction (cm).

The lateral mixing distance for the fully mixed condition, approximately adjusted for a source term of width b, is assumed equal to the dispersion distance associated with one standard deviation:

$$\ell_m = \sigma_\ell + b \tag{5.62}$$

where ℓ_m = lateral distance over which the contaminant is assumed to be uniformly mixed (cm).

To illustrate that Equation (5.62), in conjunction with Equation (5.61), has a physical basis, a mixing width similar to that identified by Equation (5.62) can be developed by equating the longitudinal travel time to the

receptor of concern with the time for complete lateral mixing. An estimate of the time scale associated with complete lateral mixing is given by

$$t_m = \xi \frac{(\ell'_m)^2}{D^*_y} \tag{5.63}$$

where ℓ'_m = alternative lateral distance over which the contaminant is assumed to be uniformly distributed (cm).

By rearranging Equation (5.63), an effective width that represents the fully mixed condition can be calculated:

$$\ell'_m = \left(\phi\ t_m\ D^*_y\right)^{1/2} \tag{5.64}$$

The mixing length, when approximately adjusted for a source term of width b, can be estimated as

$$\ell'_m = \left(\phi\ t_m\ D^*_y\right)^{1/2} + b \tag{5.65}$$

As noted in the previous section, when $\phi \leq 3.3$ in a flow field with a fixed width, the fully mixed condition can be assumed. Because Equation (5.62) represents a more conservative expression than Equation (5.65) when ϕ equals 3.3 and because its derivation is consistent with the other mixing-length estimations used in the RAPS methodology, Equation (5.62) is used to describe the lateral mixing length in the groundwater environment.

5.6.3 Representative Travel Time

To define a vertical or lateral mixing length [see Equations (5.54) and (5.62), respectively], a representative travel time has to be identified. As the plume migrates downgradient from the source, some contaminant particles migrate faster than others (i.e., attenuation effect); therefore, a representative travel time must be determined. One technique of estimating the travel

time of a contaminant in a groundwater system is to divide the distance the contaminant travels by the flow velocity, adjusted for retardation:

$$t_t = \frac{x}{u^*} \tag{5.66}$$

where t_t = estimated travel time (s)
x = longitudinal distance traveled (cm).

Equation (5.75) usually provides a good estimate of the travel time of a contaminant; it assumes, however, that dispersion in the flow direction and degradation/decay are negligible.

A more precise estimate of the travel time of a contaminant that does account for dispersion and degradation/decay can be developed; this estimate computes the travel time of the peak contaminant concentration. By doing so, the highest concentration is known. The time to the peak concentration (i.e., travel time) can be estimated by 1) assuming a point source and its accompanying analytical Green's function solution in the direction of flow [e.g., Equation (5.17) or (5.21)], 2) taking its derivative with respect to time, 3) setting the derivative to zero, and 4) solving for the travel time. The point-source solution is used, as opposed to the line-source solution, because tests indicate that it provides an accurate estimation of the travel time and because its formulation is less complicated than that of a line source. Using Equation (5.17) as an example, we have

$$X_1 = \left(\frac{1}{4 \pi D_x^* t_p}\right)^{1/2} \exp(-\lambda t_p) \exp\left[-\frac{(x - u^* t_p)^2}{(4 D_x^* t_p)}\right] \tag{5.67}$$

where t_p = time to the peak contaminant concentration (i.e., representative travel time) (s^{-1}).

Solving for the time to maximum concentration gives

$$t_p = \frac{\left[(u^* x)^2 + 4 \lambda D_x^* x^2 + (D_x^*)^2\right]^{1/2} - D_x^*}{4 \lambda D_x^* + (u^*)^2} \qquad (5.68)$$

If dispersion and degradation/decay are negligible, Equation (5.68) reduces to Equation (5.66), as expected.

5.7 CONTAMINANT DEGRADATION/DECAY

Although many chemicals have degradation rates that are different for dissolved and adsorbed phases, known degradation rates in many cases are lacking for each. At this time, first-order degradation/decay is assumed for all contaminants that do not result in decay products. For contaminants that do produce decay products, the groundwater model treats the transport of the decay products like a conservative substance (i.e., the parent contaminant). Once the contaminant reaches the receptor of concern, the model corrects for radiological decay in a separate calculation and subsequently computes the temporal distribution of each daughter product at the receptor. Performing the decay computation after calculating the conservative-substance concentration allows for manageable computations in the case of long decay chains.

The transport model calculates the quantities of the parent (first) member of the decay chain as if it were a conservative substance. The Bateman equation (Bateman 1910) is then used to calculate the concentrations of all important decay products in the chain. This calculation is complicated because the decay products have chemical properties different from the parent and, in all probability, are absorbed on the soil medium to a greater or lesser extent than the parent. This difference has two implications (Codell et al. 1982):

- The decay product travels in the ground faster or slower than the parent.
- The decay product is partitioned between the soil and interstitial water differently from the parent. The concentration of the decay radionuclide in the groundwater must, therefore, be corrected for its equilibrium coefficient.

The first implication above is violated because RAPS assumes that decay products travel at the same speed as the parent. An analytical solution that accounts for these implications has been expressed by Lester et al. (1974) for the one-dimensional transport equation for radioactive chains with up to three components. The three-member chain model is useful for establishing the important conclusion that highest concentrations result where all members travel at the same speed as the parent. This fact is well illustrated by Codell et al. (1982). Because of the relatively poor state of knowledge about distribution coefficients and other transport parameters and the inherent conservatism this assumption ensures, the assumption that the parent and decay products travel at the same speed is tacitly made. The assumption of equal transport speeds makes a relatively small difference to the calculated concentrations of the most important components; the radioactive elements at the upper end of the periodic table have long decay chains, terminating with stable elements. Codell et al. (1982) again illustrate these conclusions. The concentration of the i-th decay product in terms of the parent concentration is given as

$$C_i = \left(\frac{\lambda_i\, C_1}{\lambda_1}\right)\left(\prod_{j=1}^{i-1} \lambda_j\right)\left[\sum_{j=1}^{i}\left(\frac{e^{-\lambda_j t}}{\prod_{\substack{r=1 \\ r\neq j}}^{i} (\lambda_r - \lambda_j)}\right)\right] \qquad (5.69)$$

where C_1 = parent concentration (Ci/ml)

λ_i = radiological decay coefficient of the i-th decay product (s^{-1}).

5.8 SUMMARY

In the subsurface environment, contaminants migrate through a partially saturated or saturated groundwater zone. In the partially saturated zone, flow is usually assumed to be in a vertical direction. Because this flow is generally unidirectional, one-dimensional modeling is performed. The RAPS methodology uses a one-dimensional, unsteady, semianalytical code to simulate contaminant leaching and movement through the partially saturated zone. The solution algorithm to the advective-dispersive equation is based on homogeneous and isotropic soils parameters. The partially saturated soil beneath the waste

site is assumed at a unit potential hydraulic gradient. The moisture content is assumed to fluctuate between field capacity and saturation with the hydraulic conductivity based on an empirical equation.

The predominant movement of the leachate in the saturated zone is assumed to be in the direction of the groundwater flow. A three-dimensional advective-dispersive equation describes the migrating plume as it disperses and attenuates through the saturated aquifer. Advection represents the transport of solute caused by the mass motion of water, while dispersion represents solute transport by unaccounted variations in the fluid velocity and molecular motion. Dispersion is considered in the longitudinal, lateral, and vertical directions. Soil properties are assumed homogeneous, and the flow is assumed steady and only in the longitudinal direction.

The advective-dispersive equation describing solute transport in the saturated zone can also be applied to the partially saturated zone if minor modifications are made. To apply the equation to the partially saturated zone, the total and effective porosities are assumed to be equal to the soil matrix moisture content. In addition, one-dimensional, unidirectional flow and dispersion are assumed only in the vertical (z) direction.

Solutions for the advective-dispersive equations for the partially saturated and saturated zones have been formulated in terms of an instantaneous contaminant release (i.e., a pulse release over zero time). The RAPS methodology generalizes these solutions for arbitrary time-varying releases by convoluting response functions (i.e., temporally varying contaminant leach or flow rates) with instantaneous contaminant release solutions. The RAPS groundwater component computes contaminant levels at wells and at the edge of streams and calculates solute fluxes from the groundwater environment to the surface water environment.

5.9 REFERENCES

Abramowitz, M. A., and I. A. Stegun. 1964. Handbook of Mathematical Functions. AMS 55, U.S. Department of Commerce, National Bureau of Standards, Washington, D.C.

Bateman, H. 1910. "The Solution of a System of Differential Equations Occurring in the Theory of Radioactive Transformations." Proc. Cambridge Philos. Soc. 16:423-427.

Campbell, G. S. 1974. "A Simple Method for Determining Unsaturated Conductivity from Moisture Retention Data." Soil Sci. 117:311-314.

Carnahan, B., H. A. Luther and J. O. Wilkes. 1969. Applied Numerical Methods. Wiley, New York.

Carslaw, H. S., and J. C. Jaeger. 1959. Conduction of Heat in Solids. Oxford University Press, London.

Clapp, R. B., and G. M. Hornberger. 1978. "Empirical Equations for Some Soil Hydraulic Properties." Water Resour. Res. 14(4):601-604.

Codell, R. B., K. T. Key and G. Whelan. 1982. A Collection of Mathematical Models for Dispersion in Surface Water and Groundwater. NUREG-0868, U.S. Nuclear Regulatory Commission, Washington, D.C.

Donigian, A. S. Jr., T. Y. R. Lo and E. W. Shanahan. 1983. Rapid Assessment of Potential Groundwater Contamination under Emergency Response Conditions. Anderson-Nichols and Co., Athens, Georgia.

Gardner, W. R. 1960. "Soil Water Relations in Arid and Semi-Arid Conditions." UNESCO 15:37-61.

Gardner, W. R., D. Hillel and Y. Benyamini. 1970. "Postirrigation Movement of Soil Water, 1. Redistribution." Water Resour. Res. 6:851-861.

Hanks, R. J., and G. L. Ashcroft. 1980. Applied Soil Physics. Springer-Verlag, New York.

Hillel, D. 1971. Soil and Water: Physical Principles and Processes. Academic Press, New York.

Hillel, D. 1980. Fundamentals of Soil Physics. Academic Press, New York.

Lester, D. H., G. Jansen and H. C. Burkholder. 1974. Migration of Radionuclide Chains Through an Adsorbing Medium. BNWL-SA-5079, Pacific Northwest Laboratory, Richland, Washington.

Ritger, P. D., and N. J. Rose. 1968. Differential Equations with Applications. McGraw-Hill, New York.

Selim, H. M., and R. S. Mansell. 1976. "Analytical Solution of the Equation for Transport of Reactive Solutes Through Soils." Water Resour. Res. 12(3):528-532.

Van Genuchten, M. Th., and W. J. Alves. 1982. Analytical Solutions of the One-Dimensional Convective-Dispersive Solute Transport Equation. Tech. Bull. No. 1661. U.S. Department of Agriculture, Washington, D.C.

Whelan, G., B. L. Steelman, D. L. Strenge and J. G. Droppo. 1986. "Overview of the Remedial Action Priority System (RAPS)." In Pollutants in a Multimedia Environment, ed. Y. Cohen, pp. 191-227. Plenum Press, New York.

Yeh, G. T. 1981. AT123D: Analytical Transient One-, Two-, and Three-Dimensional Simulation of Waste Transport in the Aquifer System. ORNL-5602, Oak Ridge National Laboratory, Oak Ridge, Tennessee.

Yeh, G. T., and Y. Tsai. 1976. "Analytical Three-Dimensional Transient Modeling of Effluent Discharges." Water Resour. Res. 12(3):533-540.

6.0 SURFACE WATER PATHWAY

6.1 INTRODUCTION

The surface water component of the RAPS methodology provides estimates of surface water contaminant concentrations at downstream locations from the release point. The computed contaminant concentrations are used by the exposure assessment component of RAPS to calculate dose to the surrounding population and subsequent health effects associated with that dose. Potential exposure of humans to contaminants via the surface water pathway can be associated with ingestion (e.g., drinking contaminated water), dermal contact (e.g., swimming), or external dose (e.g., swimming). A schematic diagram illustrating the surface water environment is presented in Figure 6.1.

Because contaminant releases to a surface water body in the RAPS methodology are relatively long term, the migration and fate of contaminants through the surface water environment are described by the steady-state, two-dimensional advective-dispersive equation for solute transport. The results are based on analytical solutions that are well established in the literature. The surface water solutions account for the major mechanisms of constituent persistence (i.e., degradation/decay), advection, and hydrodynamic dispersion. Persistence is described by a first-order degradation/decay coefficient; for radionuclides, the surface water component also accounts for decay products. Advection is described by constant unidirectional flow in the longitudinal direction. Hydrodynamic dispersion is accounted for in the longitudinal (for travel time estimations) and lateral (for contaminant concentration calculations) directions. The processes associated with adsorption/desorption between the water column and suspended and bed sediments are not addressed. The complexities and subsequent data requirements associated with instream sediment transport and sedimentation processes preclude their use in this simplified assessment methodology. Neglecting these processes should, in most cases, represent a conservative assumption with regard to water column contaminant concentrations.

Contamination can enter the surface water environment in one of three ways. The groundwater environment can supply transient contaminant fluxes

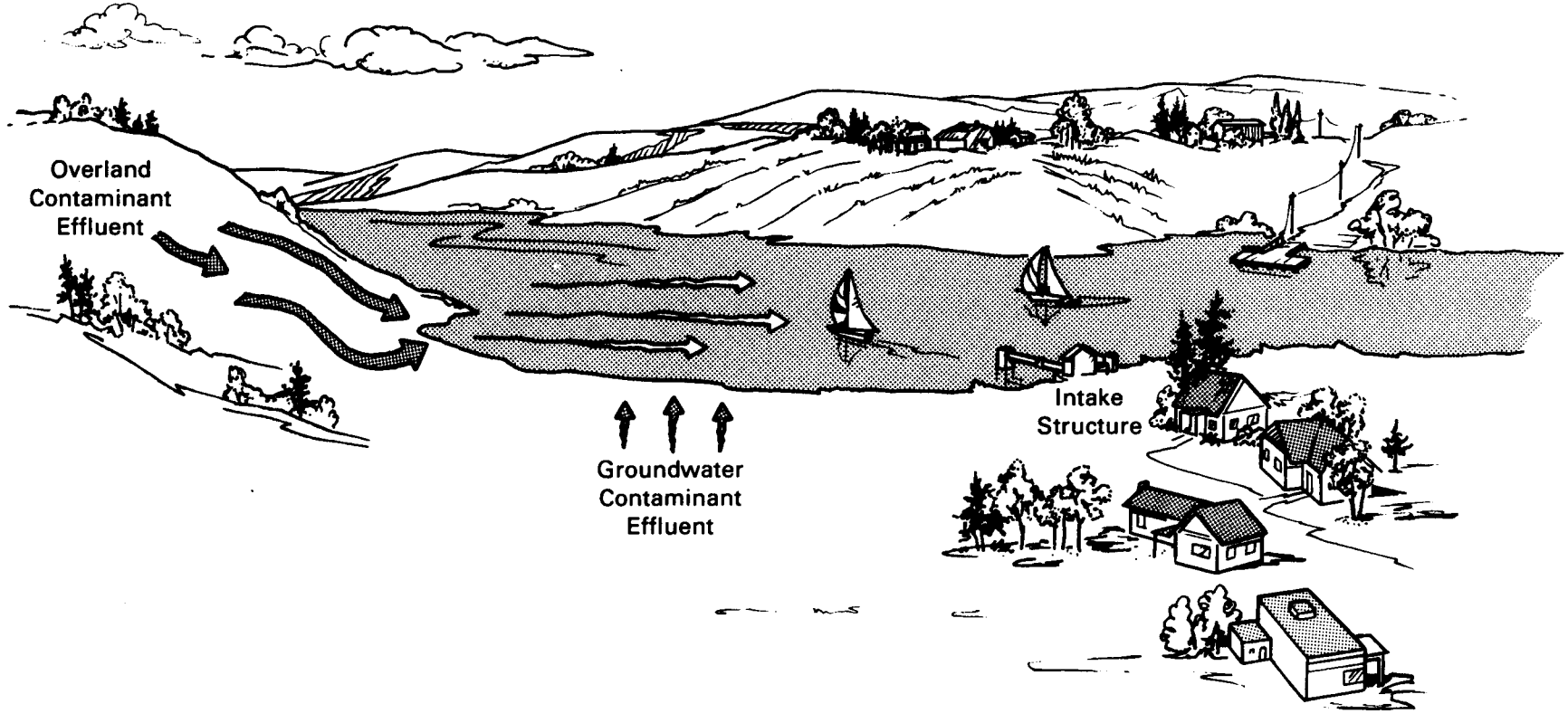

FIGURE 6.1. Schematic Diagram Illustrating the Surface Water Environment

along the stream bank adjacent to the subsurface aquifer. The overland runoff can supply nonpoint-source steady-state contaminant fluxes from the land adjacent to the stream. Finally, the surface water component of RAPS can address direct discharge to the stream.

The numerical algorithms describing the mathematical formulations of the surface water component are presented in this section. The following topics are addressed:

- advective-dispersive equation -- The advective-dispersive equation describes solute migration in the surface water environment. The form of the equation used in the surface water component is briefly discussed.
- contaminant concentration equations -- The various solutions to the advective-dispersive equation are presented. The solutions describe contaminant concentrations.
- mixing length -- A lateral mixing length is defined; this describes the distance in which the migrating solute plume is fully mixed. The time for the contaminant to travel from the waste site through the surface water medium to a receptor of concern is also described. The travel time is used in determining mixing lengths.
- dispersion coefficients -- Longitudinal and lateral dispersion coefficients that are used in determining mixing lengths are described in this section.
- contaminant degradation/decay -- The technique for computing the degradation of chemicals and/or the decay of radionuclides is described in this section.

6.2 ADVECTIVE-DISPERSIVE EQUATION

The advective-dispersive equation for solute movement through a riverine surface water body forms the basis of all surface water algorithms. The surface water flow is assumed to be steady and uniform; the algorithms are developed for the limiting case of unidirectional advective transport with

three-dimensional (longitudinal, lateral, and vertical) dispersion. The advective-dispersive equation for surface waters can be described by the following expression:

$$\frac{\partial C}{\partial t} + u \frac{\partial C}{\partial x} = E_x \frac{\partial^2 C}{\partial x^2} + E_y \frac{\partial^2 C}{\partial y^2} + E_z \frac{\partial^2 C}{\partial z^2} - \lambda C \qquad (6.1)$$

where C = dissolved instream contaminant concentration (g/ml or Ci/ml)[a]

u = average instream flow velocity (cm/s)

E_x, E_y, E_z = dispersion coefficients in the x-, y-, and z-directions, respectively (cm^2/s)

λ = degradation/decay constant [= (ℓn 2) / (half-life)] (s^{-1}).

Equation (6.1) does not take into account the effects of contaminant adsorption to or desorption from sediment particles suspended in the water column or in the river bed. This assumption is conservative in most cases.

Contaminant releases to the surface water environment in the RAPS methodology are relatively long term. Because transient solutions for contaminant migration and fate calculations are most applicable for batch and infrequent releases over relatively short periods of time (Codell et al. 1982), steady-state solutions to the advective-dispersive equation are most applicable. The steady-state, vertically integrated mass balance equation for contaminant transport in a riverine environment (where longitudinal advection dominates longitudinal dispersion) can be written as follows:

$$u \frac{\partial C}{\partial x} = E_y \frac{\partial^2 C}{\partial y^2} - \lambda C \qquad (6.2)$$

in which

(a) When two sets of units are provided, the first refers to chemicals, and the second refers to radionuclides.

$$\frac{\partial C}{\partial y} = 0 \text{ at } y = 0 \text{ and } y = B \qquad (6.3)$$

where B = width of stream channel (cm).

6.3 CONTAMINANT CONCENTRATION EQUATIONS

When Equation (6.2) is solved with the appropriate boundary conditions [i.e., Equation (6.3)], the surface water pathway is described by an analytical expression that characterizes the transport of contaminants through a river environment. For a point-source[a] contaminant release from the bank of a stream, the solution to Equation (6.2) employing the boundary conditions defined by Equation (6.3) is very similar to those outlined by Codell et al. (1982), Strenge et al. (1986), and Whelan et al. (1986):

$$C = \left(\frac{Qc}{u\ B\ h}\right) \exp\left(-\frac{\lambda\ x}{u}\right) \left\{1 + 2 \sum_{n=1}^{\infty} \left[\exp\left(-\frac{n^2\ \pi^2\ E_y\ x}{u\ B^2}\right) \left(\cos\frac{n\ \pi\ y}{B}\right)\right]\right\} \qquad (6.4)$$

where Qc = contaminant flux at the source
h = depth of stream (cm)
x = distance downstream (cm)
n = index on series expansion
y = lateral distance from bank where source release is located (cm) (where y is equivalent to B) (cm).

All other terms retain their previous definitions.

When a contaminant is released from a source along the stream bank, it is spacially redistributed -- longitudinally, vertically, and laterally -- by the transporting medium. Because contaminant levels are spacially distributed at any designated receptor (e.g., intake structure), one contaminant concentration

(a) The term "point source" refers to the source-term configuration, which reflects simplifying assumptions, and does not refer to the exact technical definition associated with the concentration equation. Note, for example, that a vertically averaged point source represents a line source in the z-direction.

does not describe the spacial distribution unless the contaminant is uniformly mixed in the stream. Because the exposure component of the RAPS methodology requires only one temporally distributed contaminant concentration per receptor location per time interval, the contaminant concentration of the fully mixed region is used.

Under a fully mixed condition in the river, the concentration is assumed to be vertically integrated. Lateral contaminant migration is bounded by the banks of the water body, and complete lateral mixing occurs at some distance downstream from the contaminant source. However, if the fully mixed condition across the entire width of the stream is not reached, an effective concentration must be developed for use by the exposure pathway model. The RAPS methodology computes an effective concentration, based on the fully mixed condition and the longitudinal distance the contaminant has migrated. The lateral distance in the surface water body over which contamination is considered to be fully mixed begins on the side of the river where the contaminant was released and extends some distance (ℓ_m) across the river. Within this region (i.e., $0 \leq y \leq \ell_m$), the contaminant level is assumed to be spacially constant; therefore, the concentration at $y = 0$ is used in computing the exposure levels for the exposure component of the RAPS methodology. By assuming that y equals 0, Equation (6.4) reduces to

$$C = \left(\frac{Qc}{u\,\ell_m\,h}\right) \exp\left(-\frac{\lambda x}{u}\right) \left[1 + 2\sum_{n=1}^{\infty} \exp\left(-\frac{n^2 \pi^2 E_y x}{u B^2}\right)\right] \qquad (6.5)$$

A line source along the edge of the stream can be represented by distributing a series of point sources equivalent in length to the line source. As the downstream receptor location is moved farther away, the line source resembles a point source located at the center of the line source. As the receptor location is moved closer to the center of the line source, only that portion of the source term upstream of the receptor has an opportunity to influence contaminant levels at the receptor; in effect, the strength of the source term is

reduced. Under these circumstances, the line source can be approximated as a point source that is located at one-half the distance between the receptor location and the upstream end of the line source.

6.4 TRANSVERSE DISPERSION COEFFICIENTS

To estimate the instream concentration, the transverse dispersion coefficient is required. Accurately defining this parameter for all riverine systems under all conditions is difficult. The coefficient is, therefore, defined such that representative properties of the water body are considered in the estimation.

Fisher et al. (1979) note that dispersion in rivers is generally related to the characteristics of the river using the following relationship:

$$E_y = \phi\ d\ u^* \tag{6.6}$$

where ϕ = proportionality constant (dimensionless)
d = average depth of flow (cm)
u^* = shear velocity (cm/s).

To analyze Equation (6.6), it is necessary to define ϕ and the shear velocity. Fischer[a] and Fischer et al. (1979) note that researchers (e.g., Orlob 1959; Sayre and Chamberlain 1964; Sayre and Chang 1968; Engelund 1969; Prych 1970; Elder 1959; Okoye 1970; Glover 1964; Fischer 1967; Yotsukura et al. 1970) have defined a range of values for ϕ. In laboratory flumes, ϕ ranges from 0.5 to 2.4. For practical purposes, Fischer (1967) suggests that $\phi = 0.6$.

The shear velocity is estimated by Fischer (1974) by assuming that it was directly proportional to the average flow velocity of the stream:

$$u^* = 0.10\ u \tag{6.7}$$

(a) Fischer, H. B. Date Unknown. "Longitudinal Dispersion and Turbulent Mixing in Open Channel Flow." Working Paper. University of California at Berkeley, California.

Equation (6.16) was suggested for streams with Manning's roughness coefficients on the order of 0.04. By combining Equations (6.6) and (6.7) with $\phi = 0.6$, the dispersion coefficient in the lateral direction can be roughly estimated as

$$E_y = 0.06\ d\ u \tag{6.8}$$

6.5 CONTAMINANT DEGRADATION/DECAY

First-order degradation and decay is assumed for all contaminants that do not result in decay products. For contaminants that do result in decay products, the surface water model treats the transport of the decay products like a conservative substance (i.e., the parent contaminant). Once the contaminant reaches the location of concern, the model corrects for radiological decay in a separate calculation using the Bateman equation (Bateman 1910; Codell et al. 1982) and then computes the temporal distribution of each decay product. The concentration of the i-th decay product in terms of the parent concentration is given by Equation (5.69). For more information, refer to the discussion of contaminant degradation/decay in Section 5.7.

6.6 SUMMARY

Of the many surface water components (e.g., nontidal rivers, estuaries, lakes, open coasts, reservoirs, impoundments, etc.), RAPS is currently capable of addressing nontidal rivers. Nontidal rivers refer to freshwater bodies with unidirectional flow in definable channels. Because the RAPS methodology is compositely coupled, other surface water pathways can be added when deemed necessary.

Contaminant releases to the surface water environment in the RAPS methodology are relatively long term. Because transient solutions for contaminant migration and fate calculations are most applicable for batch and infrequent releases over relatively short periods of time (Codell et al. 1982), steady-state solutions to the advective-dispersive equation are most applicable. The steady-state, vertically integrated mass balance equation for contaminant transport in a riverine environment forms the basis of the surface water pathway. Advection is assumed to be only in the longitudinal direction, and it

is assumed to dominate longitudinal dispersion. Dispersion is considered in the lateral direction with degradation/decay being defined by a first-order degradation/decay rate. The surface water pathway supplies contaminant levels to the exposure assessment component of RAPS.

6.7 REFERENCES

Bateman, H. 1910. "The Solution of a System of Differential Equations Occurring in the Theory of Radioactive Transformations." Proc. Cambridge Philos. Soc. 16:423-427.

Codell, R. B., K. T. Key and G. Whelan. 1982. A Collection of Mathematical Models for Dispersion in Surface Water and Groundwater. NUREG-0868, U.S. Nuclear Regulatory Commission, Washington, D.C.

Elder, J. W. 1959. "The Dispersion of Marked Fluid in Turbulent Shear Flow." J. Fluid Mech. 5:544-560.

Engelund, F. 1969. J. Hydraul. Div. 95(HY4,ASCE):1149-1162.

Fischer, H. B. 1967. "The Mechanics of Dispersion in Natural Streams." J. Hydraul. Div. 93(HY6,ASCE):187-216.

Fischer, H. B. 1974. "Turbulent Mixing and Dispersion in Waterways." Presented at the Dispersion and Transport of Pollutants in Waterways Workshop at California State University, Riverside, California, September 24-26, 1974.

Fischer, H. B., E. J. List, R. C. Y. Koh, J. Imberger and N. H. Brooks. 1979. Mixing in Inland and Coastal Waters. Academic Press, New York.

Glover, R. E. 1964. Dispersion of Dissolved or Suspended Materials in Flowing Streams. Prof. Paper 433-B, U.S. Geological Survey.

Okoye, J. K. 1970. Characteristics of Transverse Mixing in Open Channel Flows. Report KH-R-23, Keck Laboratory, California Institute of Technology, Pasadena, California.

Orlob, G. T. 1959. J. Hydraul. Div. 85(HY9,ASCE):75-101.

Prych, E. A. 1970. Effects of Density Differences on Lateral Mixing in Open Channel Flows. Report KH-R-21, Keck Laboratory, California Institute of Technology, Pasadena, California.

Sayre, W. W., and A. R. Chamberlain. 1964. Circular 4840, U.S. Geological Survey.

Sayre, W. W., and F. M. Chang. 1968. A Laboratory Investigation of the Open Channel Dispersion Process for Dissolved, Suspended, and Floating Dispersants. Prof. Paper 433-E, U.S. Geological Survey.

Strenge, D. L., R. A. Peloquin and G. Whelan. 1986. LADTAP II -- Technical Reference and User Guide. NUREG/CR-4013, U.S. Nuclear Regulatory Commission, Office of Nuclear Reactor Regulation, Washington, D.C.

Whelan, G., B. L. Steelman, D. L. Strenge and J. G. Droppo. 1986. "Overview of the Remedial Action Priority System (RAPS)." In Pollutants in a Multimedia Environment, ed. Y. Cohen, pp. 191-227. Plenum Press, New York.

Yotsukura, N., H. B. Fischer and W. W. Sayre. 1970. Measurement of Mixing Characteristics of the Missouri River Between Sioux City, Iowa and Plattsmouth, Nebraska. Water Supply Paper 1899-G, U.S. Geological Survey.

7.0 ATMOSPHERIC PATHWAY

7.1 INTRODUCTION

The atmospheric pathway component of RAPS provides estimates of the long-term average exposures from atmospheric emissions to the regional human population. This component also provides input to the overland transport pathway and the ingestion route of exposure. Contaminant levels are computed for locations defined in terms of a direction and distance from the site. The estimates of contaminant levels for exposure assessment can thus be made for both population centers and less populated rural areas.

The long-term average exposure in the atmospheric pathway based on a 70-year increment (i.e., approximately one human life span) represents the sum of exposures from individual atmospheric plumes. The travel time between release and exposure for these individual plumes is typically expressed in hours and minutes. Therefore, relatively short-term processes need to be incorporated into the computation of long-term, average concentrations.

The approach taken for modeling the long-term, average exposures in the atmospheric pathway involves a weighted summation of exposures from individual hourly average plumes. Exposures are computed for a matrix of cases spanning ranges of ambient atmospheric conditions. Climatological data are used to represent the average conditions over the 70-year exposure period. These climatological summaries are in terms of the average frequency of occurrence of the various combinations of ambient atmospheric conditions. These climatological frequencies allow the computation of a long-term, average exposure by a weighted summation of the matrix of exposures.

The fate of a contaminant released to the atmosphere depends on a number of complex processes including release mechanisms and characteristics, dilution and transport, chemical reactions, washout by cloud droplets and precipitation, and deposition onto the underlying surface cover (Cupitt 1980). The RAPS atmospheric pathway model accounts for each of these processes in computing long-term exposures. A schematic diagram illustrating the atmospheric pathway is presented in Figure 7.1.

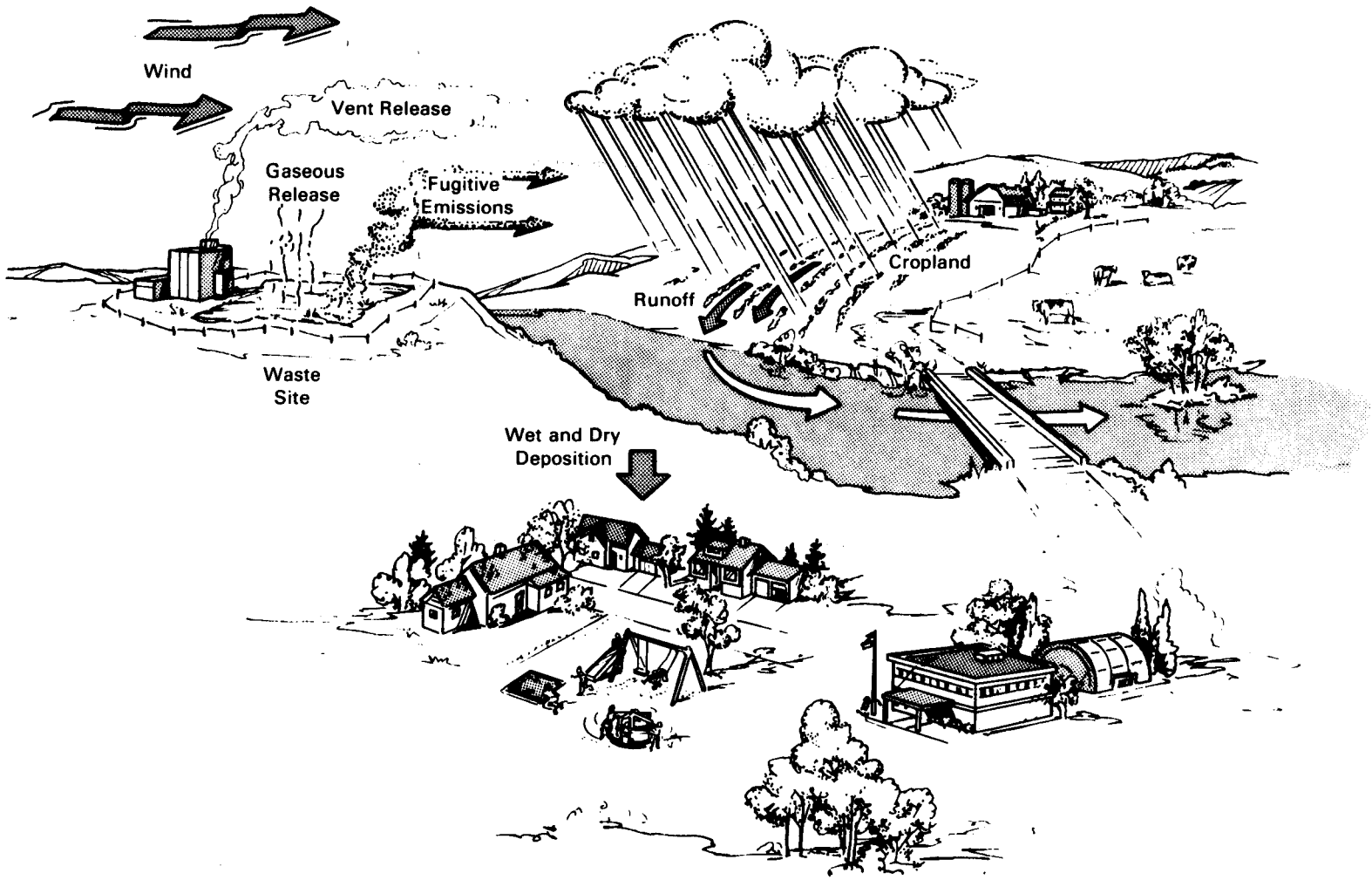

FIGURE 7.1. Schematic Diagram Illustrating the Atmospheric Environment

The atmospheric pathway considers contaminant air concentrations and deposited surface concentrations. Air concentrations are needed for inhalation pathways. Surface concentrations resulting from dry and wet removal processes are needed for overland transport and for ingestion pathways.

The atmospheric pathway has several sequential components: suspension/emission, atmospheric transport and dispersion, and wet and dry deposition (Figure 7.2). The relationship of these atmospheric components in the RAPS model is shown in Figure 7.1. Input of site-specific data is required. From these data, the gaseous and particulate release rates are estimated. An atmospheric transport and dispersion model is used to compute downwind air concentrations. As the plume travels away from the site, these airborne concentrations are reduced both by dispersion and deposition processes. Wet and dry deposition models are used to compute the total deposition to the surface.

The atmospheric pathway model components are modeled to maximize the validity of comparisons of environmental trends between sites. The suspension/emission rates, atmospheric transport and dispersion, and the deposition rates are based on empirical relationships that incorporate site characteristics (i.e., location, surface cover, climatology). The output concentrations represent a reasonable estimate of an order-of-magnitude analysis for impacts associated with the risk assessment component of RAPS. Contaminant transport is assumed to occur on a short time scale so that chemical transformations can normally be neglected. The validity of this assumption needs to be checked on a case-by-case basis for various contaminants.

In summary, the prediction of contaminant movement through the atmospheric pathway uses algorithms that address atmospheric suspension/emission of contaminants at a site and the subsequent transport, diffusion, and deposition of these airborne contaminants. Input to the model includes site-specific climatological information such as wind speed and direction, stability, and precipitation. Output from the model consists of average air and surface contaminant levels that are then used in the inhalation and ingestion components, respectively, of the exposure assessment analysis. The surface contaminant levels also represent input to the overland transport components of RAPS.

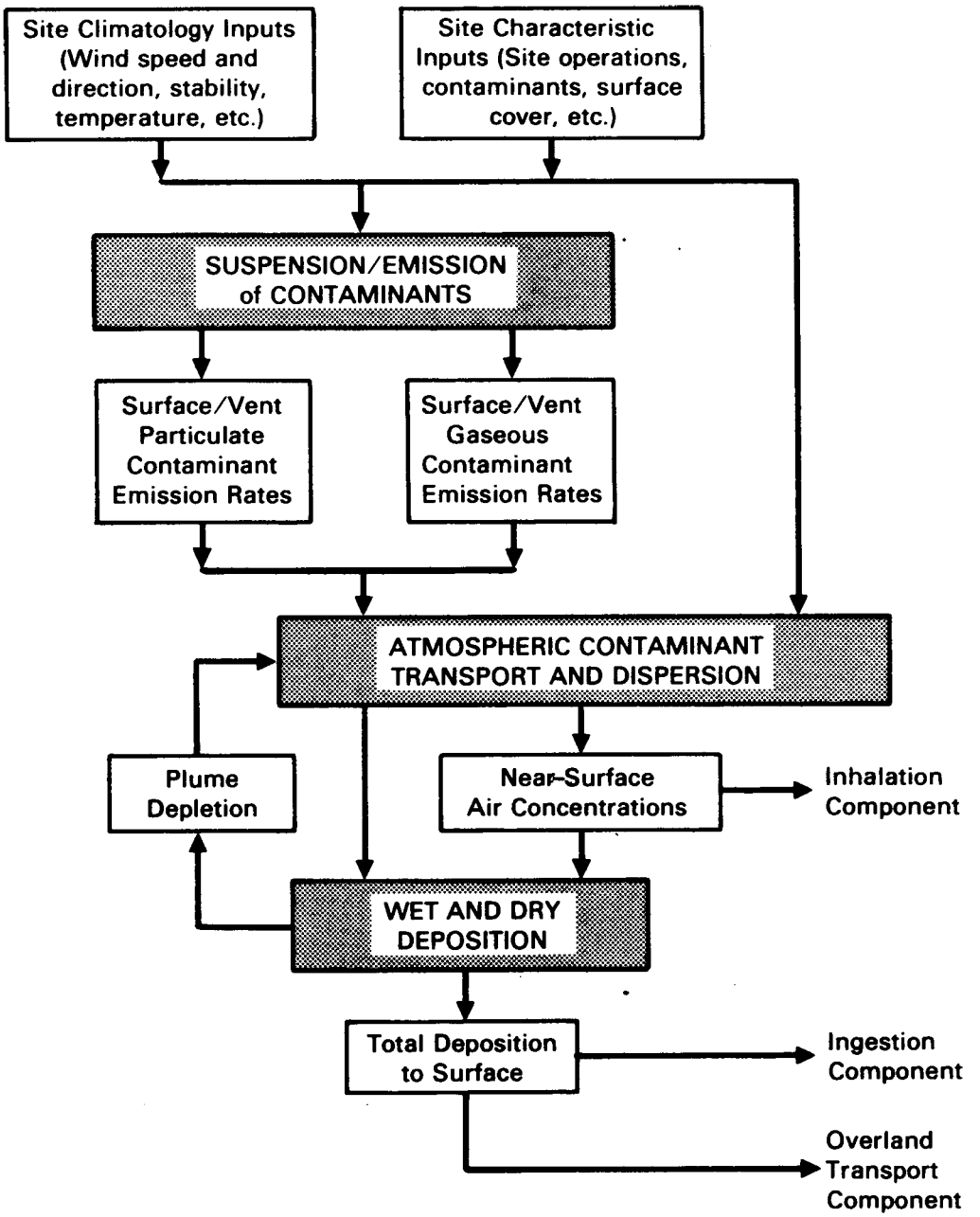

FIGURE 7.2. Atmospheric Pathway Computation Diagram

7.2 EMISSION CHARACTERIZATION

The release of contaminants into the atmosphere involves processes such as volatilization, suspension, leakage, etc. These processes vary with factors such as temperature; moisture; wind speed; surface characteristics (i.e., crust

formation, roughness, vegetation cover); the physical state and chemical form of the contaminant (i.e., gas or particulate, reactive or nonreactive); and location of the contaminant (i.e., on the surface, buried under a soil layer, in a tank).

The emission characterization was not in the original scope of the atmospheric pathway component. However, as the framework for the RAPS model was developed, the emission modeling appeared to fit best in the atmospheric component; the emissions feed directly into the atmospheric pathway computation, and the emission rates depend on many of the same variables as needed in the atmospheric pathway computation. The formulations for emission rates are still under development. The following subsections describe the approaches that are being taken in that effort.

7.2.1 Suspension of Surface Particles

Particulate fugitive releases of contaminants are defined as emissions resulting from the suspension of exposed surface contamination. If a site has exposed surfaces with contamination, the potential suspension of the contaminants depends on factors such as the physical and chemical surface characteristics, surface contamination, ambient wind speed, turbulence, and local mechanical activity on the surface.

A surface cover with contaminants may be the result of either waste storage (i.e., mill tailings) or contamination by the operation of a facility. The latter contamination may occur on natural surfaces (i.e., soil) or manmade surfaces (i.e., concrete pads, roadways). The potential for suspension of contaminants varies greatly because of the wide variety of surface types and activities expected on the surfaces.

The suspension of particles from the surface may occur as the result of wind action (Bagnold 1941; Sehmel and Lloyd 1976) or other physical action on the surface (Sehmel 1976). Atmospheric turbulence plays a role in determining the extent to which the air movement over the surface can suspend surface particles. Local mechanical activity on the surface such as animal grazing, vehicular traffic, walking, and earth moving can greatly increase the fugitive particulate release rates compared to an undisturbed surface.

The suspension of respirable particles (those with diameters less than 10 μm) from contaminated areas at DOE sites is calculated using empirical relationships based on studies of wind erosion and surface disruption. The RAPS outputs for suspension from contaminated surface areas are expressed in terms of an airborne soil concentration normalized to a unit surface contamination. These soil concentration arrays are converted to arrays of contaminant concentrations using the fraction of surface contamination in the suspended soil.

The computation of the suspension of contaminants from a surface into the atmosphere requires both contaminant and site data. These data are used to define which formulations, if any, apply to the site. Then, if a computation is appropriate, these data are used to compute the suspension rates.

The RAPS methodology for computing suspension rates is an adaptation of the methodology proposed by Cowherd et al. (1984) for rapid computation of potential long-term impacts from spills of hazardous materials. This methodology includes formulations for suspension by winds, vehicular traffic, and other physical disturbances of the surface.

7.2.2 Wind Erosion

Cowherd et al. (1984) define the steps for determining potential respirable particulate emission from wind erosion. The soil particle size distribution, apparent roughness of the site, vegetation cover, presence of a crust on the soil, and presence of nonerodible elements (e.g., large stones) are used to define the potential for suspension. Depending on the results of this procedure, the site is characterized having 1) unlimited erosion potential, 2) limited erosion potential, or 3) no erosion potential.

The methodology uses different formulations for the two cases with wind erosion potential. Cowherd et al. (1984) suggest that if the site is completely covered with vegetation or if there is a thick crust (or a wet, saturated soil) and if no mechanical disturbances occur at the site, it can be assumed that no contaminants are suspended. However, for certain contaminants, even very small suspension rates from well-stabilized surfaces may be

significant. Testing was needed to determine if the erosion formulations give reasonable results over the range from bare, unstabilized surfaces to well-stabilized surfaces.

The potential for wind erosion is quantified in terms of a threshold friction velocity. The greater the value of the threshold friction velocity for a site, the lower the potential for particle suspension. The threshold friction velocity for the contaminated area is determined by knowing the mode of the aggregate size distribution (which is derived from the soil composition) and using a formula derived from the graphical relationship given by Gillette et al. (1980):

$$u_c^* = N \exp [0.004118428 \log (X) + 0.04167173] \quad (7.1)$$

where u_c^* = threshold friction velocity (m/s)
X = aggregate size distribution (mm)
N = nonerodible elements correction factor (dimensionless).

The correction factor in Equation (7.1) allows for the effects of any nonerodible elements in the contaminated area. This correction factor is based on the fraction of surface coverage. This factor is based on graphical results given by Cowherd et al. (1984) derived from wind tunnel studies by Marshall (1971). As the silhouette area of nonerodible elements increases, so does the threshold friction velocity.

Once the threshold friction velocity has been determined, the erosion potential of the contaminated area can be classified by calculating the equivalent wind speed at a given height above the surface using the equation

$$u' = r\, u_c^* \log (z/z_0) \quad (7.2)$$

where u' = wind speed at 7-m height (m/s)
r = von Karman constant (0.4; dimensionless)
z = reference height above the surface (7.0 m)
z_0 = surface roughness length (m).

The value of z is usually 7 m; the surface roughness length of the site, z_0, is related to the size and spacing of the roughness elements in the area. Figure 7.3 illustrates z_0 for various surfaces (Cowherd and Guenther 1976).

Once the threshold friction velocity has been calculated, the erosion potential of the area can be determined. If the threshold friction velocity is less than 0.75 m/s, the area has unlimited erosion potential; otherwise, the area has limited erosion potential.

For estimating particulate emissions from a contaminated area having limited wind-erosion potential, the following equation is used to predict potential emissions:

$$E10 = 0.83 \left[f \, p(u) \, (1 - v) \, / \, (PE \, / \, 50)^2 \right] \qquad (7.3)$$

where E10 = annual-average emission rate per unit surface area ($mg/m^2/hr$)
f = frequency of mechanical disturbances (number/mo)
u = observed maximum wind speed for periods between disturbances (m/s)
p(u) = erosion potential (g/m^2)
v = vegetation coverage on surface (fraction)
PE = Thornthwaite's Precipitation-Evaporation (PE) Index (dimensionless).

The frequency of disturbances per month, f, is defined as the number of actions that could expose fresh surface material. A disturbance could be vehicular traffic, plowing or turning of the soil, or mining or construction. The erosion potential, p(u), depends on the maximum wind speed, u, so that

$$\begin{aligned} p(u) &= 6.7 \, (u - u') \quad \text{if } u \geq u' \\ p(u) &= 0.0 \quad \text{if } u < u' \end{aligned} \qquad (7.4)$$

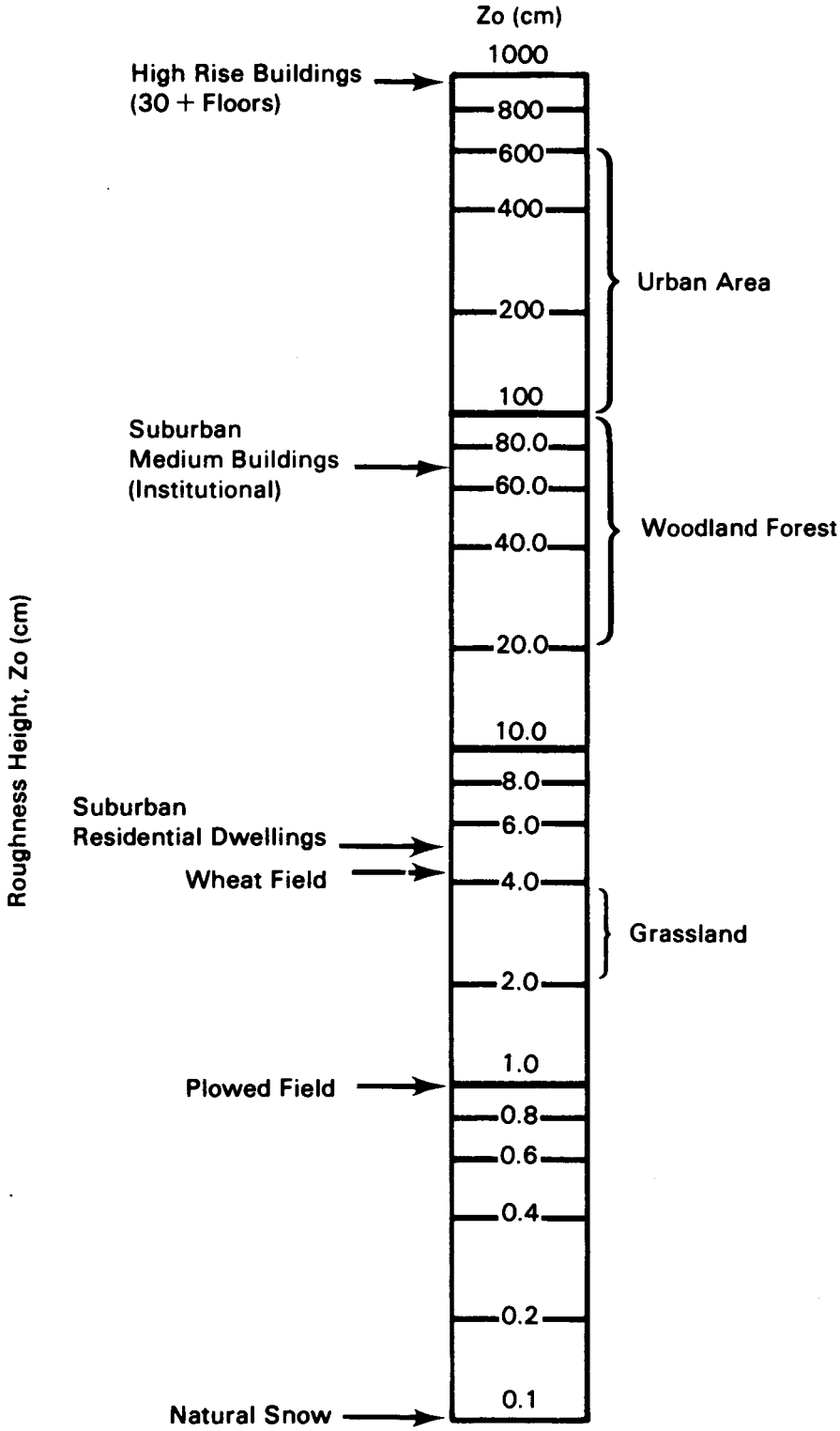

FIGURE 7.3. Roughness Lengths for Various Surfaces

The vegetation fraction varies from 0 for bare ground to 1 for total coverage. The Thornthwaite's Precipitation-Evaporation (PE) Index is used as a moisture-correction parameter for wind-generated emissions. Cowherd et al. (1984) provide a map with values of PE for all regions in the contiguous United States (Figure 7.4).

For an area with unlimited erosion potential, the relationship for the surface emission rate is

$$E10 = 0.036\ (1 - v)\ (\bar{u} / u')^3\ F(x) \qquad (7.5)$$

where $\bar{u}$ = mean annual wind speed (m/s)
$F(x)$ = integration function.

The vertical flux of particles smaller than 10 μm in diameter is assumed to be proportional to the cube of the horizontal wind speed. This relationship was originally developed from measurements made by O'Brien and Rindlaub (1936) in studies at the mouth of the Columbia River and later measurements made by Bagnold (1941) in the Egyptian desert. Chepil (1951) found this same relationship using results from wind-tunnel experiments.

The integration function F(x) comes from the cubic relationship of the vertical transport of particles and the wind speed. It is defined in graphical format by Cowherd et al. (1984). This relationship can be broken into the following four discrete parts:

$$\begin{aligned} F(x) &= 0.0 && \text{if } x < 0.0 \\ F(x) &= 1.91 && \text{if } 0.0 \leq x < 0.5 \\ F(x) &= 1.9 - (x - 0.5)\ 0.6 && \text{if } 0.5 \leq x < 1.0 \\ F(x) &= 1.6 - (x - 1.0)\ 1.3 && \text{if } 1.0 \leq x \end{aligned} \qquad (7.6)$$

where $x = 0.886\ u' / \bar{u}$.

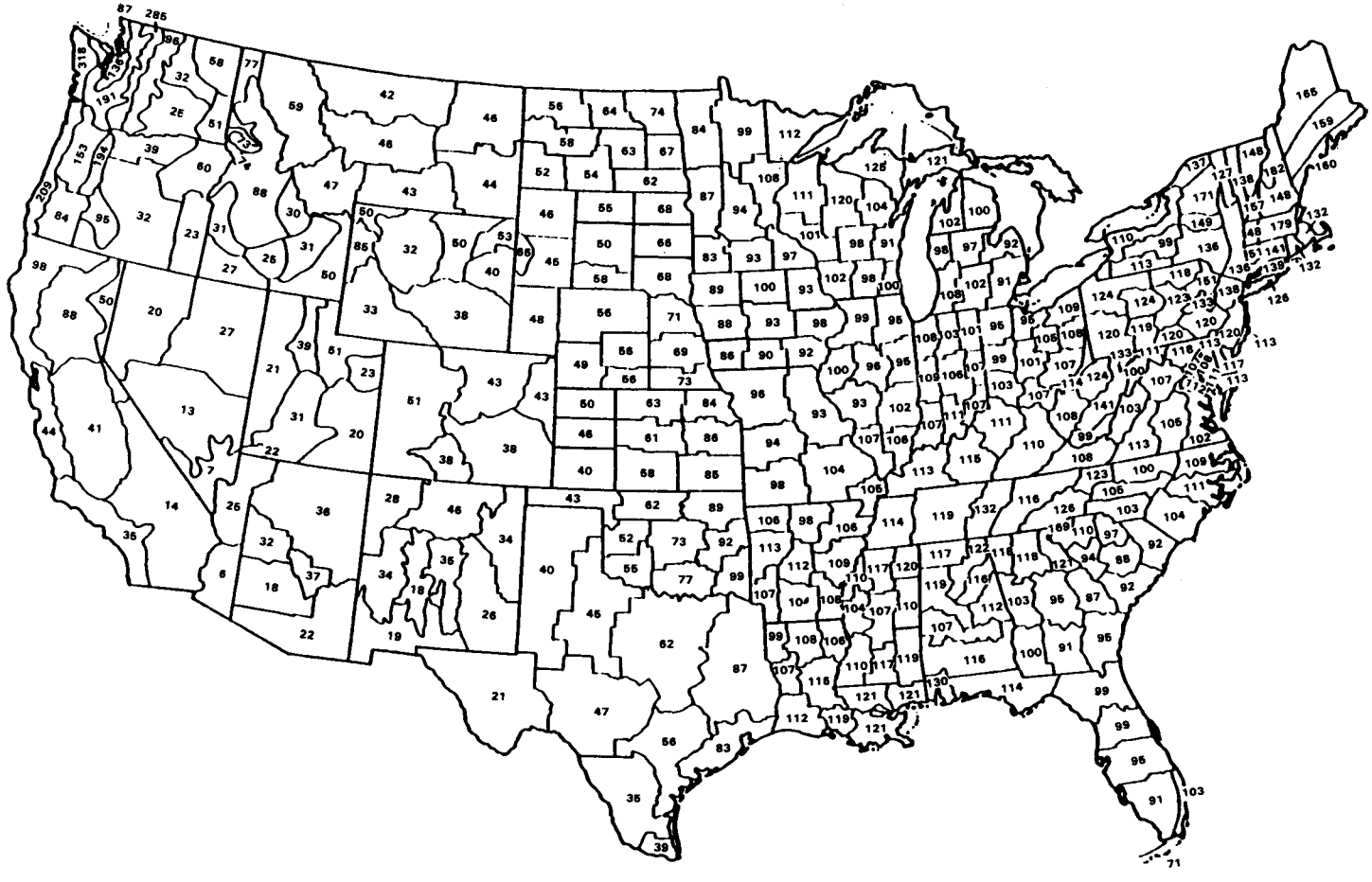

FIGURE 7.4. Map of Precipitation-Evaporation Index for State Climatic Divisions (Cowherd et al. 1984)

7.2.3 Vehicular Suspension of Particles

Formulations used to compute emissions per unit area resulting from the mechanical disturbances by vehicle traffic are also based on Cowherd et al. (1984). The emission from traffic over unpaved surfaces is computed using

$$E10 = \left(0.85\right)^3 \left(\frac{s}{10}\right) \left(\frac{S}{24}\right)^{0.8} \left(\frac{W}{7}\right)^{0.3} \left(\frac{w}{6}\right)^{1.2} \left(\frac{365 - p}{365}\right) \qquad (7.7)$$

where E10 = emission factor for an unpaved expressed as mass suspended per vehicle-kilometer of travel [g/(vehicle-km)]

s = silt content of road surface material (%)

S = mean vehicle speed (km/hr)

W = mean vehicle weight (Mg)

w = mean number of wheels

p = number of days with at least 0.254 mm (0.01 in.) of precipitation per year.

Site-specific information from local sources is normally to be obtained for each of the parameters. In cases in which site-specific data are not available, the default values given by Cowherd et al. (1984), which are listed in Table 7.1, may be used.

Values for p are obtained from a local source of meteorological data.

TABLE 7.1. Default Values for Independent Variables of Equation (7.7)[a,b]

Site	s(%)	S(km/hr)	W(Mg)	w
Rural/Residential	15 (5-68)	48 (40-64)	2	4
Industrial	8 (2-29)	24 (8-32)	3	4
			15	6
			26	10

(a) Based on Cowherd et al. (1984).
(b) Numbers in parentheses are ranges of measured values.

7.2.4 Emission Rate Computation

Once the various emission factors have been determined, the emission rates for respirable particles can be calculated. For wind erosion, the emission rate is calculated from the relationship

$$R10 = E10 \text{ area } / \text{ cpr} \tag{7.8}$$

where R10 = emission rate for wind erosion (g/s)
area = area of source contamination (m^2)
cpr = climatological suspension factor (dimensionless).

The climatological suspension factor allows for the frequency of suspension conditions to be included. This factor is based on original factors tabulated by Cowherd et al. (1984), based on output from a series of runs of the Industrial Source Complex-Long Term (ISCLT) model (Bowers et al. 1979).

For mechanical suspension of particles from vehicle traffic on an unpaved contaminated surfaces, the emission rate is computed from

$$R10 = 1.157\ 10^{-5}\ E10\ L\ T\ /\ cpr \tag{7.9}$$

where R10 = emission rate for traffic (g/s)
L = distance of travel over contaminated surface (km)
T = average number of vehicles traveling over the contaminated surface per day (number/day).

The total emission rate is the sum of the wind-erosion and mechanical-disturbance emission rates. The total emission rate is used as input to the atmospheric dispersion, transport, and deposition model described in Section 7.3.1.

This atmospheric model determines air and surface concentrations of the suspended soil materials. The concentrations resulting from the suspension of a specific surface contaminant, e, are computed using the following equations:

$$C_\theta = \alpha C_s \tag{7.10}$$

and

$$\dot{S}_\theta = \alpha S_s \tag{7.11}$$

where C_θ = airborne contaminant concentration (g/m^3)

C_s = airborne soil concentration (g/m^3)

α = mass fraction of contaminant in the suspended surface soil (g/g)

S_θ = surface concentration of deposited contaminant (g/m^2)

S_s = surface concentration of deposited soil material (g/m^2).

7.2.5 Gaseous Fugitive Releases

Contaminant release in a gaseous form may result from leakage of a stored gaseous material or from the emission of the gaseous product of chemical reaction, biodegradation, or radioactive decay. The rate of release of such gases from the soil is a function of both surface and contaminant properties.

Radon is one of the best known natural gaseous emissions from soil. Most soil- and/or rock-derived materials (i.e., concrete, wood, soil) contain minute amounts of uranium that steadily decay, producing radon gas. Therefore, all natural surface covers have some natural emission of radon. If elevated uranium concentrations occur in the surface cover, then increased radon emission from the cover can be expected.

Detailed models have been developed for computing emissions from uranium-enhanced materials (Momeni 1979; Strenge and Bander 1981). Although these models are not directly included in the RAPS framework, they were used for guidance in developing the model used in the atmospheric transport component of RAPS.

Landfills, such as those containing solvent hazardous chemicals, can potentially release a variety of chemicals to the atmosphere (Bennett 1985). Landfill sites with decaying organic matter have measurable emissions of

methane and other compounds. The potential for methane or other gaseous releases depends on the nature of the materials that have been buried and their production/release rates.

Caravanos et al. (1985) evaluated the validity of two existing theoretical models [by Thibodeaux (1979) and Shen (1980, 1981)] for predicting chemical emission rates from saturated soils in a landfill. Actual/predicted emission ratios of benzene, carbon tetrachloride, and trichlorethylene were computed for three types of soil. Both models provided reasonable order-of-magnitude estimates of emission rates. The equations of Thibodeaux (1979) give results that are in better agreement with the observed emissions than the equations of Shen (1980, 1981). Caravanos et al. (1985) attribute the better agreement to the inclusion of soil quality parameters by Thibodeaux (1979).

The RAPS atmospheric component requires input of gas emission rates. The rates must be obtained either from site emission measurements or from computations based on site characteristics. The objective of RAPS, to provide comparisons between sites, will be best met if a consistent approach is used in an application of RAPS. The following paragraphs briefly outline the basis of one computational methodology for computing organic gas emission rates that can be adopted for an application of RAPS; this methodology is based on OSWFR Directive 9285.5-1.[(a)]

Simplified methods are provided in the OSWFR document for computing the volatilization of organic contaminants at uncontrolled hazardous wastes sites under the following source configurations:

1. Covered landfills - without internal gas generation
2. Covered landfills - with internal gas generation
3. Spills, leaks, land farms - sites having concentrated wastes on the surface or adhered to soil particles below the surface
4. Lagoons - wastes dissolved in or mixed with water.

(a) EPA (1986). Superfund Exposure Assessment Manual (Draft). U.S. Environmental Protection Agency, Washington, D.C., January 14, 1986, pp. 3-19 to 3-33.

Formulations are given for computing emission rates of volatile contaminants from each of these situations. For spills and leaks, formulations are given both for fresh spills and leaks and for old spills and leaks. These computational methods are provided only as a guide, and may need to be changed to apply to a particular series of sites. Also, newer improved approaches may be available for computing gas emission rates.

7.2.6 Vented Emissions

The storage practices for certain contaminants can involve vented emissions. To allow for changes in atmospheric pressure, some tanks have atmospheric vents. Typically, these venting systems include precautions to control the release of large amounts of contaminants to the atmosphere. However, small amounts of particulate and gaseous contaminants can be expected to be routinely released from these vents.

7.2.7 Summary

The characterization of contaminant atmospheric releases is based on the nature and location of the contaminants at the site, the local climatology of conditions favoring suspension, and the extent of physical activities on exposed, contaminated surfaces.

7.3 TRANSPORT, DISPERSION, AND DEPOSITION

Once the contaminant material is airborne, the material is transported and dispersed by air movement. The contaminant will be carried by the winds, and the atmospheric contaminant concentration will be reduced by dispersion and deposition processes. The near-surface atmospheric concentrations computed in this component of the model provide the basis for evaluating inhalation exposures.

The relative importance of the atmospheric pathway at various sites is controlled by a combination of topographic and climatological influences. Controlling parameters include the distance and direction from the inactive waste site and local wind conditions and stability. Because dispersion is a strong function of the downwind distance, the physical distances between the contaminant site and population centers are of prime importance. The local

frequencies of wind directions, particularly in areas with topographic channeling of winds, are important in calculating exposure and risk associated with the atmospheric pathway. The relative rates of atmospheric dilution between the sites are mainly a function of local wind speeds and dilution (stability) parameters.

As a result of surface-induced mechanical mixing, the local surface roughness influences local dispersion rates. The RAPS formulation for local dispersion rates includes the effect of local surface roughness. All other factors being equal, a site with a smoother surface will have slower dilution rates than a site with a rougher surface.

7.3.1 Atmospheric Pathway Model

A standard straight-line, sector-averaged Gaussian model was selected as the basis of the atmospheric pathway model. Such a model meets the RAPS objective of assessing long-term, average risk from the various inactive waste sites. This model provides a consistent framework for computing average exposures, and incorporates the major factors that control the emission, transport and dispersion, and deposition of various contaminants.

The sector-averaged, atmospheric model is particularly applicable in RAPS because it allows direct incorporation of long-term site data. The sector-averaged model computes long-term, average exposures by a weighted summation of exposures. These exposures are for a matrix of cases covering the range of combinations of atmospheric stability, wind speed, and wind direction. Climatological data representing average long-term conditions are used to define the frequency of occurrence of each case in the computation of an average long-term exposure.

The atmospheric model is not expected to be applicable to all sites. The sector-averaged Gaussian model applies best to a site located on a uniform flat plane, and is used only as an approximation for sites located on other types of terrain.

Although sites in complex terrain or on a coastline have atmospheric influences that are quite different than sites located on a flat uniform plane, the use of a straight-line Gaussian model will generally provide reasonable

exposure estimates to the first major terrain feature. As the regional influences become more important at greater distances, the straight-line Gaussian model becomes less accurate.

Complex-terrain models for plumes, such as those proposed by EPA, may be appropriate for use in RAPS at sites with complex terrain. The RAPS atmospheric model is used in such a way that alternative concentration computation codes, such as the EPA atmospheric codes, may be used if they are found to be essential for a specific site.

Applying the sector-averaged model to sites in complex terrain needs careful attention to ensure that the estimate of risk is reasonable. For example, some adjustment of the inputs may be appropriate for sites in complex terrain to reflect local wind fields, such as adjusting the wind frequency as a functional direction to reflect local terrain.

The Gaussian diffusion equation for the concentrations of a contaminant in a plume downwind of a continuous point-source release is given by Slade (1968) as

$$C_k = \frac{Q_k}{2 \pi \sigma_y \sigma_z \bar{u}} \exp\left[- y^2 / (2 \sigma_z^2)\right] f(z,H,\sigma_z) \qquad (7.12)$$

where C_k = time-averaged value of concentration for contaminant form k (g/m^3)

Q_k = amount of material released from a point source of a contaminant form k (g/s)

k = index on elemental contaminant form [k=1, . . . p; p = number of forms representing (p-1) ranges of particle sizes, and a gaseous state]

x,y,z = positions in a Cartesian coordinate system that are oriented such that the x-axis is in the direction of the mean horizontal wind vector, the y-axis is cross-wind, and z-axis is vertical height above local ground level (m)

σ_y = standard deviation of the distribution of material in a plume in the y-direction (m)

σ_z = standard deviation of the distribution of material in a plume in the z-direction (m)

$\bar{u}$ = average value wind speed in the x-direction at the height of the plume centerline (m/s)

H = effective height of release over local ground level (m)

$f(z,H,\sigma_z)$ = functional relationship for the vertical variation of plume concentrations (dimensionless).

The function f in Equation (7.12) has the form of a sum of exponential terms representing the Gaussian dispersion from the actual plume as well from virtual plumes. The use of virtual plumes is a means of accounting for the physical limit on Gaussian vertical dispersion encountered at the ground and at the mixing-height inversion layer. The material mathematically "lost" by dispersion of the actual plume through these layers is "recovered" by adding the contributions of virtual plumes. The virtual plumes are thus a means of accounting for plume reflections and multiple reflections at the ground surface and at the mixing height. The form of the function f is based on a discussion by Ramsdell et al. (1983). The vertical exponential term is approximated with a sum of exponentials

$$f(z,H,\sigma_z) \approx \sum_{n=-\infty}^{\infty} \left\{ \exp\left[-\frac{1}{2}\left(\frac{2\,n\,h - H - z}{\sigma_z}\right)^2 \right] + \exp\left[-\frac{1}{2}\left(\frac{2\,n\,h + H - z}{\sigma_z}\right)^2 \right] \right\} \quad (7.13)$$

As a practical matter, the summation can be truncated after a few terms centered on zero. In RAPS, a range of -4 to +4 is used.

The crosswind-integrated concentration from a continuous source is obtained by integrating Equation (7.12) with respect to the crosswind distance (y) from $-\infty$ to $+\infty$

$$CWI = \frac{Q_k}{\sqrt{2\pi}\ \sigma_z\ \bar{u}}\ f(z,H,\sigma_z) \qquad (7.14)$$

where CWI = crosswind-integrated concentration (i.e., perpendicular to wind direction) (g/m^2).

The frequency of combinations of wind speeds, wind directions, and diffusion rates can be summarized in terms of a speed, direction, and stability joint frequency table. The average concentration is computed by multiplying the integrated concentration formula (Equation 7.12) by the frequency of a given set of conditions divided by the width of the sector at the distance of interest. The sector average concentration for one set of wind speed, direction, and stability conditions is given by

$$C_{ijk}(x,z) = Q_k\ R_k(x)\ \left(\frac{1}{2\pi}\right)^{1/2}\ \frac{1}{u_i\ \sigma_{z_j}\ 2\pi x / n}\ f(z,H,\sigma_{z_i}) \qquad (7.15)$$

where $C_{ijk}(x,z)$ = sector-averaged atmospheric concentrations for wind speed, i, stability condition, j, and contaminant form, k (g/m^3), for the downwind distance x and height z above local ground level

i = index on wind speed (i=1, . . . m; m = number of wind speed classes)

j = index on stability conditions (j=1, . . . n; n = number of stability conditions)

$R_k(x)$ = deposition and/or decay plume source depletion fraction, which varies as a function of the position x of the plume for contaminant form k (dimensionless)

u_i = wind speed central value for wind speed interval class i (m/s)

σ_{z_j} = standard deviation of concentration in vertical for stability class j (m)

n = number of wind direction sectors (n = 16) (dimensionless)

$(2\pi x / n)$ = sector width.

The indexed variables are defined in terms of central values for each atmospheric frequency class (i.e., a set of wind speed, wind direction, and stabilities conditions). The removal of the contaminant from the atmospheric plume, by various depletion processes, is computed using

$$R_k(x) = r\ c\ d\ w \tag{7.16}$$

where fractional losses are defined as

r = radioactive decay term, defined in Section 7.3.3 (dimensionless)

c = chemical decay term, defined in Section 7.3.4 (dimensionless)

d = dry deposition term, defined in Section 7.3.5 (dimensionless)

w = wet deposition term, defined in Section 7.3.6 (dimensionless).

The average air concentration near the earth's surface is input to the inhalation component of the health assessment. The average air concentration, $C(x,z)$ (g/m^3), at ground level ($z = 0$) for a population located at a distance and direction from the waste site is computed as the sum of the concentrations over the i, j, and k indices, given by

$$C(x,z) = \sum_{i=1}^{n} \sum_{j=1}^{m} \sum_{k=1}^{p} [f_{ij}\ C_{ijk}(x,z)] \tag{7.17}$$

where f_{ij} = climatological fractional frequency of occurrence of the wind speed (i) and stability class (j) conditions within the specified direction (dimensionless).

The table of frequencies of occurrence of the f_{ij} values is referred to as a joint frequency summary. These data are available as STAR summaries from the National Climatic Data Center, NOAA, Asheville, North Carolina.

The local surface roughness is characterized by a surface roughness length. Table 7.2 (and Figure 7.3) show examples of the magnitude of this parameter for various surface covers. The surface roughness lengths in the

TABLE 7.2. Typical Surface Roughness Lengths

Surfaces	Roughness Length (cm)
Snow, sea, desert	0.005 - 0.03
Lawn	0.1
Grass (5 cm)	1 - 2
Grass (tall)	4 - 9
Mature root crops	14
Low forest	50
High forest	100
Urban area	>100

region surrounding the release are used to account directly for local influences in both dispersion and dry deposition computations.

The central wind speed, u_i, in a wind speed category is not necessarily applicable to the movement of an atmospheric plume in the region of interest. The wind speed needs to be adjusted for differences in height and local surface roughness. The atmospheric component of RAPS uses relationships from atmospheric surface layer similarity theory given by Paulson (1970), Businger et al. (1971), and Hanna et al. (1982) to compute an equivalent central wind speed at plume height for each wind speed category. To provide a height adjustment of the wind speed as a continuous function of the local surface roughness, these relationships are used in preference to less general power-law approximations (Irwin et al. 1985).(a)

(a) Irwin, J. S., S. E. Gryning, A. A. M. Holtslay and B. Siversten. 1985. Atmospheric Modeling Based on Boundary Layer Parameterization. Draft Report. U.S. Environmental Protection Agency, Washington, D.C.

For unstable atmospheric conditions, the following expression is used to calculate the wind variation with height (Paulson 1970):

$$\bar{u} = \frac{u_*}{4} \ln\left(\frac{z}{z_o}\right) - 2 \ln\left[\frac{1}{2}\left(1 + \frac{1}{\phi_m}\right)\right] - \ln\left[\frac{1}{2}\left(1 + \frac{1}{\phi_m^2}\right)\right] + 2 \tan\left(\frac{1}{\phi_m}\right) - \frac{\pi}{2} \tag{7.18}$$

where $\bar{u}$ = average wind speed (m/s)

u_* = friction velocity (m/s)

z = height over land/water surface (m)

z_o = roughness length of surface (m)

ϕ_m = dimensionless wind gradient parameter.

For stable conditions the following expression is used to calculate the wind variation with height (Hanna et al. 1982):

$$\bar{u} = \frac{u_*}{0.4}\left[\ln\left(\frac{z}{z_o}\right) + 5\frac{z}{L}\right] \tag{7.19}$$

where L is the Monin-Obukhov length (m), a scaling length of atmospheric turbulence. Equations (7.18) and (7.19) are integrated forms of relationships derived from field studies by Businger et al. (1971).

To use Equations (7.18) and (7.19) for determining the wind variation with height, the roughness length, friction velocity, and Monin-Obukhov length must be known or calculated.

The roughness length is an input parameter for over land surfaces. Charnock's relationship for the roughness length (z_o), as described by Joffre (1985), is used for over water surfaces.

$$z_o = m\, u_*^2 / g \tag{7.20}$$

where g = acceleration of gravity (m/s^2)

m = coefficient [= 0.0144; recommended by Garratt (1977)].

Equation (7.21) is used in the RAPS atmospheric model to estimate the friction velocity (u_*) over water surfaces. These friction velocity relationships were taken from drag coefficient relationships reported in Large and Pond (1981) by substituting for the friction velocity using $C_D = u_*^2/u_s$.

$$\begin{aligned} u_* &= 0.0346\ u_x && \text{for } 4 \leq u_x < 11 \text{ m/s} \\ u_* &= 0.0316\ u_x\ (0.49 + 0.065\ u_x)^{1/2} && \text{for } 11 < u_x \leq 25 \text{ m/s} \end{aligned} \qquad (7.21)$$

where u_x = wind speed at the 10-m height.

The Monin-Obukhov length is a function of atmospheric stability and is related to the Pasquill stability class and roughness length using the relationship of Golder (1972).

Using the approach of computing appropriate wind speeds for the underlying surface allows the wind speeds to vary as function of distance downwind of the release. The plume speed is computed at a height of the approximate vertical center of mass of the plume at each downwind distance. This speed is used to compute a travel time for each computation interval. The total travel time divided by the distance traveled defines an average plume speed for use in Equation (7.15).

The deposition to surfaces can occur as the result of both wet or dry removal processes. Wet removal is caused by the scavenging and deposition of the contaminant by precipitation or cloud droplets. Dry deposition is the direct deposition of the airborne contaminant onto a surface by processes such as impaction, sorption, gravitational settling, etc. The total deposition for wet and dry processes provides surface contaminant levels for the overland transport pathway and also provides the basis for evaluating ingestion exposures from the atmospheric pathway.

The total deposition to the surface is input to the exposure component of the RAPS model. The total deposition at a specified location is computed as the sum of the wet and dry deposition fluxes to the surface:

$$T(x,z) = \sum_{i=1}^{n} \sum_{j=1}^{m} \sum_{k=1}^{p} [f_{ij} D_{ijk}(x,z) + g W_{ijk}(x,z)] \quad (7.22)$$

where $T(x,z)$ = total surface concentration (g/m^2)

$D_{ijk}(x,z)$ = dry deposition flux (g/m^2)

$W_{ijk}(x,z)$ = wet deposition flux (g/m^2) for wind speed (i), stability class (j), and contaminant form (k)

g = climatologic fractional frequency of occurrence of the indexed precipitation conditions within the specific direction (dimensionless).

Dry deposition is based on the computed near-surface air concentrations given in Equation (7.15) using

$$D_{ijk}(x,z) = \frac{C_{ijk}(x,z)\, t}{R_{ijk}} \quad (7.23)$$

where R_{ijk} = dry deposition resistance (s/m) for wind speed (i), stability class (j), and contaminant (k)

t = time period for deposition (s).

Wet deposition is given by

$$W_{ijk}(x,z) = g\, t \int_0^Z \Lambda\, C_{ijk}(x,z)\, dz \quad (7.24)$$

where Λ = scavenging coefficient (s^{-1})

Z = depth of the wetted plume layer (m).

7.3.2 Dispersion Coefficients

The RAPS atmospheric component uses six classes of atmospheric stability to characterize the dispersion rates. The atmospheric stability classes are designated by the letters A to F (Slade 1968) and are commonly referred to as the Pasquill Stability Categories (Pasquill and Smith 1983). The classes A, B, and C stand for very unstable, unstable, and slightly unstable conditions, respectively; D stands for a neutral condition; and E and F stand for stable and very stable conditions, respectively. Dispersion varies from being fastest for very unstable conditions to being slowest for very stable conditions.

The Pasquill dispersion curves used in the atmospheric component of RAPS are computed as a function of elapsed plume travel time. The conversion from the distance dependence (as originally published) to the time dependence is based on equivalent wind speeds. The Pasquill curves are applied as a function of time for the conditions for which the curves were originally developed. Following Hasse and Weber (1985), the Pasquill dispersion curves are assumed to apply over rural English countryside (Z_0 = 10 cm). Equations (7.18) and (7.19) are used to compute wind speeds. The plume travel time is computed as the sum of travel times over various surfaces, thus allowing for local wind shear effects in the dispersion computation.

7.3.3 Radioactive Decay

Radioactive materials with short half-lives may undergo significant radioactive decay while still airborne. The radioactive decay plume depletion term (r) [see Equation (7.16)] is computed using an exponential decay based on the following expression:

$$r = \exp\left(-\frac{\lambda x}{u_i}\right) \tag{7.25}$$

where λ = first-order decay coefficient (s^{-1})

x = downwind distance (m).

EPA (1979) relates the decay coefficient to the contaminant half-life $Tp_{1/2}$ (s) using

$$\lambda = \frac{0.693}{Tp_{1/2}} \tag{7.26}$$

7.3.4 Chemical Reactions

Chemical reactions that are fast enough to significantly change the airborne concentrations within the plume may be accounted for using a first-order degradation coefficient (λ). The fraction of the contaminant lost to degradation can be expressed as follows (EPA 1979):

$$c = \exp\left(-\lambda \frac{x}{u_i}\right) \tag{7.27}$$

where c = chemical degradation term in Equation (7.16).

7.3.5 Dry Deposition

The dry deposition rate is computed using a total resistance (R_{ijk}) as shown in Equation (7.23). The total resistance, the inverse of the deposition velocity, is computed at each point as the sum of atmospheric and surface resistances (see Droppo et al. 1987)(a):

$$R_{ijk} = R_{a_{ijk}} + R_{s_{ijk}} \tag{7.28}$$

where $R_{a_{ijk}}$ = atmospheric resistance (s/m)

$R_{s_{ijk}}$ = surface resistance (s/m) for wind speed (i), stability class (j), and contaminant (k).

The atmospheric resistance represents the resistance for the transfer of a contaminant in the atmospheric layer to the ground surface. The atmospheric

(a) Droppo, J. G., L. W. Vail and R. M. Ecker. INSEA's Users' Manual. U.S. Environmental Protection Agency, Washington, D.C. Draft report.

resistance varies with the wind speed, stability, and upwind surface roughness using micrometeorological relationships (Paulson 1970; Businger et al. 1971; Golder 1972). The surface resistance is a function of the surface roughness and the properties of the materials. For particulate matter, the gravitational term is included in the empirical curves used to define the resistances (Sehmel and Hodgson 1978).

A mass budget approach is used to compute the net Gaussian plume source depletion fractions [i.e., parameter d in Equation (7.16)] for dry deposition. Although these removal rates are applied as a source depletion model [see Equation (7.15)] such as the one given in Slade (1968), the surface depletion effects documented by Horst (1984) are accounted for in the RAPS dry deposition model by the atmospheric resistances. The approach computes deposition resistances for each wind speed/stability class over a layer that is deep enough so that corrections for near-surface concentration depletion are unnecessary. The thickness of this layer is assumed to be 10 m. The computation of the atmospheric resistance term is based on assuming empirical shapes of micrometeorological profiles (Van Voris et al. 1984). The atmospheric resistance varies with stability, wind speed, and local surface roughness.

7.3.6 Wet Deposition

The detailed calculation of the scavenging of contaminants from individual plumes requires a complex model with a number of inputs that are difficult to define. The RAPS calculation of climatological scavenging of contaminants is accomplished using a simpler approach (Slinn 1976). The climatological calculation used in RAPS provides estimates of wet deposition rates. This computation accounts for the major factors changing the wet deposition for the various combinations of releases and receptors between sites.

The wet deposition is computed as the integral of the concentration over height in Equation (7.24) using Equation (7.15). The result as given by Hanna et al. (1982) for the wet flux (F_{wet}) is

$$F_{wet} = \frac{\Lambda\, Q_k}{\sqrt{2\,\pi}\,\sigma_{y_j}\,u_i} \tag{7.29}$$

Equation (7.29), converted to a sector-averaged form for the total deposition, is expressed by Van Voris et al. (1984) as

$$W_{ijk} = \frac{\Lambda\, Q_o\, R_k\, 8\, g\, t}{u_i\, \pi\, x} \tag{7.30}$$

The scavenging coefficient for a specified volume of a plume is defined as the ratio of airborne contaminant removal from the volume by precipitation scavenging of the airborne contaminant within the volume. Hanna et al. (1982) point out that the scavenging coefficient varies with the rainfall type and rate, saturation conditions, and contaminant characteristics. The model assumes a neutral stability for all precipitation conditions. The wet deposition plume depletion term [w in Equation (7.16)] is obtained using

$$w = \exp\,(-\,\Lambda\, x\, /\, u_i) \tag{7.31}$$

7.3.7 Plume Rise

Plume rise formulations given by Briggs (1969, 1971, 1972, 1975) and reported in Petersen et al. (1984) are used in the RAPS atmospheric model. The plume rise equations are based on the assumption that plume rise depends on the inverse of the mean wind speed and is directly proportional to the two-thirds power of the downwind distance from the source. Different equations are used for different atmospheric stabilities.

The plume rise equations used for unstable and stable atmospheric conditions are summarized below. For additional details of the plume rise formulation, the reader is referred to the detailed description of the plume rise formulations by Petersen et al. (1984).

7.3.7.1 Unstable and Neutral Atmospheric Conditions

The plume rise relationships are as follows:

$$x_f = 3.5\, x^* \tag{7.32}$$

where x_f = downwind distance of final plume rise (m)

x^* = distance at which atmospheric turbulence begins to dominate entrainment.

The value of x^* is computed from

$$x^* = 14\ F^{5/8} \qquad \text{for } F < 55\ m^4/s^3 \tag{7.33}$$

or

$$x^* = 34\ F^{2/5} \qquad \text{for } F \geq 55\ m^4/s^3 \tag{7.34}$$

where F is the buoyancy flux parameter (m^4/s^3). The final plume rise is given by

$$H = h' + 1.6\ F^{1/3}\ (3.5\ x^*)^{2/3}\ /\ u_h \tag{7.35}$$

where H = effective height of plume (m)

h' = stack height above sea level adjusted for stack downwash (m)

u_h = wind speed at top of stack (m/s).

7.3.7.2 Stable Atmospheric Conditions

The relationships for distance expressed as a function of stability parameter are

$$x_f = 0.0020715\ u_h\ s^{-1/2} \tag{7.36}$$

where s = stability parameter (1/s).

The plume rise height for windy conditions is given by

$$H = h' + 2.6\ [F\ /\ (u_h\ s)]^{1/3} \tag{7.37}$$

or for near-calm conditions

$$H = h' + 4\,F^{1/4}\,s^{-3/8} \qquad (7.38)$$

The lower value of H computed from these two equations is used as the final plume rise.

7.4 SUMMARY

The atmospheric pathway component of the RAPS model takes into account the local site influences. The region around the site is to be assigned one of four roughness classes to define local dispersion rates. The atmospheric and surface deposition concentrations are computed using these dispersion coefficients plus climatologic site data. Major removal and decay mechanisms are incorporated in the atmospheric component of RAPS. These computations are formulated to provide reasonable estimates of contaminant deposition rates as input to the overland transport and exposure assessment components of RAPS.

7.5 REFERENCES

Bagnold, F. A. 1941. The Physics of Blown Sand and Desert Dunes. Matheson, London.

Bennett, G. F. 1985. "Fate of Solvents in a Landfill." In Proceedings of the National Conference on Hazardous Wastes and Environmental Emergencies, May 14-16, 1985, Cincinnati, Ohio.

Bowers, J. F., J. R. Bjorklund and C. S. Cheney. 1979. Industrial Source Complex (ISC) Dispersion Model User's Guide. EPA-450/2-77-018. U.S. Environmental Protection Agency, Research Triangle Park, North Carolina.

Briggs, G. A. 1969. Plume Rise. USAEC Critical Review Series. TID-25075, National Technical Information Service, Oak Ridge, Tennessee. 81 pp.

Briggs, G. A. 1971. "Some Recent Analyses of Plume Rise Observation." In Proceedings of the Second International Clean Air Congress, eds. H. M. Englund and W. T. Berry, pp. 1029-1032. Academic Press, New York.

Briggs, G. A. 1973. Diffusion Estimation for Small Emissions. NOAA Atmospheric Turbulence and Diffusion Laboratory, Contribution File No. 79. Oak Ridge, Tennessee. 59 pp.

Briggs, G. A. 1975. "Plume Rise Predictions." In Lectures on Air Pollution and Environmental Impact Analyses. American Meteorological Society, Boston, Massachusetts.

Businger, J. A., J. C. Wyngaard, Y. Izumi and E. F. Bradley. 1971. "Flux Profile Relationships in the Atmospheric Surface Layer." J. Atmos. Sci. 28:181-189.

Caravanos, J., G. H. Sewell and T. T. Shen. 1985. "Validation of Mathematical Models Predicting Chemical Emission Rates from Saturated Soils." In Proceedings of the 78th Annual Meeting of the Air Pollution Control Association, June 16-21, Detroit, Michigan.

Chepil, W. S. 1951. "Properties of Soil Which Influence Wind Erosion: I. The Governing Principle of Surface Roughness." Soil Sci. 69:142-162.

Cowherd, C., and C. Guenther. 1976. Development of a Methodology and Emission Inventory for Fugitive Dust for the Regional Air Pollution Study. Prepared for U.S. Environmental Protection Agency, Office of Air and Waste Management, Office of Air Quality Planning and Standards, Research Triangle Park, North Carolina.

Cowherd, C., G. E. Muleski, P. J. Englehart and D. A. Gillette. 1984. Rapid Assessment of Exposure to Particulate Emissions from Surface Contamination Sites. Final Report EPA Contract 68-03-3116, Project 7972-L, Midwest Research Institute, Kansas City, Missouri.

Cupitt, L. T. 1980. Fate of Toxic and Hazardous Materials in the Air Environment. EPA-600/3-80-084, U.S. Environmental Protection Agency, Research Triangle Park, North Carolina.

EPA. 1979. Industrial Source Complex Dispersion Model User's Guide. Vols. I and II. EPA-450/4-79-030 and EPA-450/4-79-031. U.S. Environmental Protection Agency, Washington, D.C.

Garratt, J. R. 1977. "Review of Drag Coefficients Over Oceans and Continents." Mon. Weather Rev. 105:915-929.

Gillette, D. A., et al. 1980. "Threshold Velocities for Input of Soil Particles into the Air by Desert Soils." J. Geophys. Res. 85(c10):5621-5630.

Golder, D. 1972. "Relationships Among Stability Parameters in the Surface Layer." Boundary-Layer Meteor. 3:47-58.

Hanna, S. R., G. A. Briggs and R. P. Hosker, Jr. 1982. Handbook on Atmospheric Diffusion. DOE/TIC-11223, U. S. Department of Energy, Washington, D.C.

Hasse, L., and H. Weber. 1985. "On the Conversion of Pasquill Categories for Use Over Sea." Boundary-Layer Meteor. 31:177-185.

Horst, T. W. 1984. "The Modification of Plume Models to Account for Dry Deposition." Boundary-Layer Meteor. 30:413-430.

Joffre, S. M. 1985. The Structure of the Marine Atmospheric Boundary Layer: A Review from the Point of View of Diffusivity, Transport and Deposition Processes. Technical Report No. 29. Finnish Meteorological Institute, Helsinki, Finland.

Large, W. G., and S. Pond. 1981. "Open Ocean Momentum Flux Measurements in Moderate to Strong Winds." J. Phys. Oceanogr. 11(3):324-336.

Marshall, J. 1971. "Drag Measurements in Roughness Arrays of Varying Density and Distribution." Agric. Meteorol. 8:269-292.

Momeni, M. H. 1979. The Uranium Dispersion and Dosimetry (UDAD) Code. NUREG/CR-0553, U.S. Nuclear Regulatory Commission, Washington, D.C.

O'Brien, M. P., and B. D. Rindlaub. 1936. "The Transportation of Sand by Wind." Civil Eng. 6(5):325.

Pasquill, F., and F. B. Smith. 1983. Atmospheric Diffusion. 3rd ed. Wiley, New York.

Paulson, C. A. 1970. "The Mathematical Representation of Wind Speed and Temperature Profiles in the Unstable Atmospheric Surface Layer." J. Appl. Meteorol. 9:857.

Petersen, W. B., J. A. Latalano, T. Chico and T. S. Yuen. 1984. INPUFF - A Single Source Gaussian Puff Dispersion Algorithm User's Guide. EPA-600/8-84-027, U.S. Environmental Protection Agency, Washington, D.C.

Ramsdell, J. V., G. F. Athey and C. S. Glantz. 1983. MESOI Version 2-0. An Interactive Mesoscale Lagrangian Puff Dispersion Model with Deposition and Decay. NUREG/CR-3344 (PNL-4753). U.S. Nuclear Regulatory Commission, Washington, D.C.

Sehmel, G. A. 1976. "Particulate Resuspension from an Asphalt Road." In Atmosphere-Surface Exchange of Particulate and Gaseous Pollutants. Energy Research and Development Administration, ERDA Symposium Series 38, pp. 846-858.

Sehmel, G. A., and W. J. Hodgson. 1978. A Model for Predicting Dry Deposition of Particles and Gases to Environmental Surfaces. PNL-SA-6721, Pacific Northwest Laboratory, Richland, Washington.

Sehmel, G. A., and F. D. Lloyd. 1976. "Resuspension of Plutonium at Rocky Flats." In Atmosphere-Surface Exchange of Particulate and Gaseous Pollutants. Energy Research and Development Administration, ERDA Symposium Series 38, pp. 575-780.

Shen, T. T. 1980. "Emission Estimation of Hazardous Organic Compounds for Waste Disposal Sites." In Proceedings of the 73rd Annual Meeting of the Air Pollution Control Association, Pittsburgh, Pennsylvania.

Shen, T. T. 1981. "Control Techniques for Gas Emissions from Hazardous Waste Landfills." J. Air Pollut. Control Assoc. 31(2):321.

Slade, D. H. 1968. Meteorology and Atomic Energy. U. S. Atomic Energy Commission, TID-24190, National Technical Information Service, Oak Ridge, Tennessee.

Slinn, W. G. N. 1976. "Dry Deposition and Resuspension of Aerosol Particles - A New Look at Some Old Problems." In Atmosphere-Surface Exchange of Particulate and Gaseous Pollutants, ERDA Symposium Series 38, Energy Research and Development Administration, pp. 1-40.

Strenge, D. L., and T. J. Bander. 1981. MILDOS - A Computer Program for Calculating Environmental Radiation Doses for Uranium Recovery Operations. NUREG/CR-0553, U.S. Nuclear Regulatory Commission, Washington, D.C.

Thibodeaux, L. J. 1979. Chemodynamics: Environmental Movement of Chemicals in Air, Water and Soil. Wiley, New York.

Van Voris, P., T. L. Page, W. H. Rickard, J. G. Droppo and B. E. Vaugahan. 1984. Environmental Implications of Trace Element Releases from Canadian Coal-Fired Generating Stations. Phase II, Final report. Volume II, Appendix B. Contract No. 001G194, Canadian Electric Association, Montreal, Quebec.

8.0 EXPOSURE PATHWAYS

8.1 INTRODUCTION

This section presents the exposure pathway components selected for RAPS to estimate exposure of individuals in a defined population group who are exposed to chemical and radioactive contaminants. The primary exposure modes considered are inhalation, external exposure (including dermal contact), and ingestion. The exposure analysis begins with environmental concentrations predicted by the four environmental pathways analyses. Output from the exposure analysis is an estimate of the uptake by individuals in the exposed population group. Use of the uptake to estimate the hazard potential index is discussed in Chapter 9.0.

The mathematical formulations for the exposure pathway analysis were selected for easy application to a variety of sites. The analysis is designed to represent the important site parameters affecting exposure without requiring onerous input data or complex analyses. As such, the analysis is much more simplified than a detailed environmental assessment that may be performed in conjunction with a detailed site analysis.

The exposure pathways by which contaminants may reach the individual and cause human exposures are illustrated by a schematic diagram and flow diagram in Figures 8.1 and 8.2, respectively. In Figure 8.2, rectangles indicate processes and hexagons indicate contaminant concentrations, either in environmental media or in parts of the exposure network. The exposure pathways represented in this figure include the following:

- inhalation -- primary mode of exposure for the atmospheric transport pathway plus inhalation of volatile organics from groundwater while showering
- drinking-water ingestion -- from groundwater, surface water, and overland transport pathways
- aquatic food ingestion -- from fish and shellfish produced in contaminated waters (surface water or overland transport pathways)

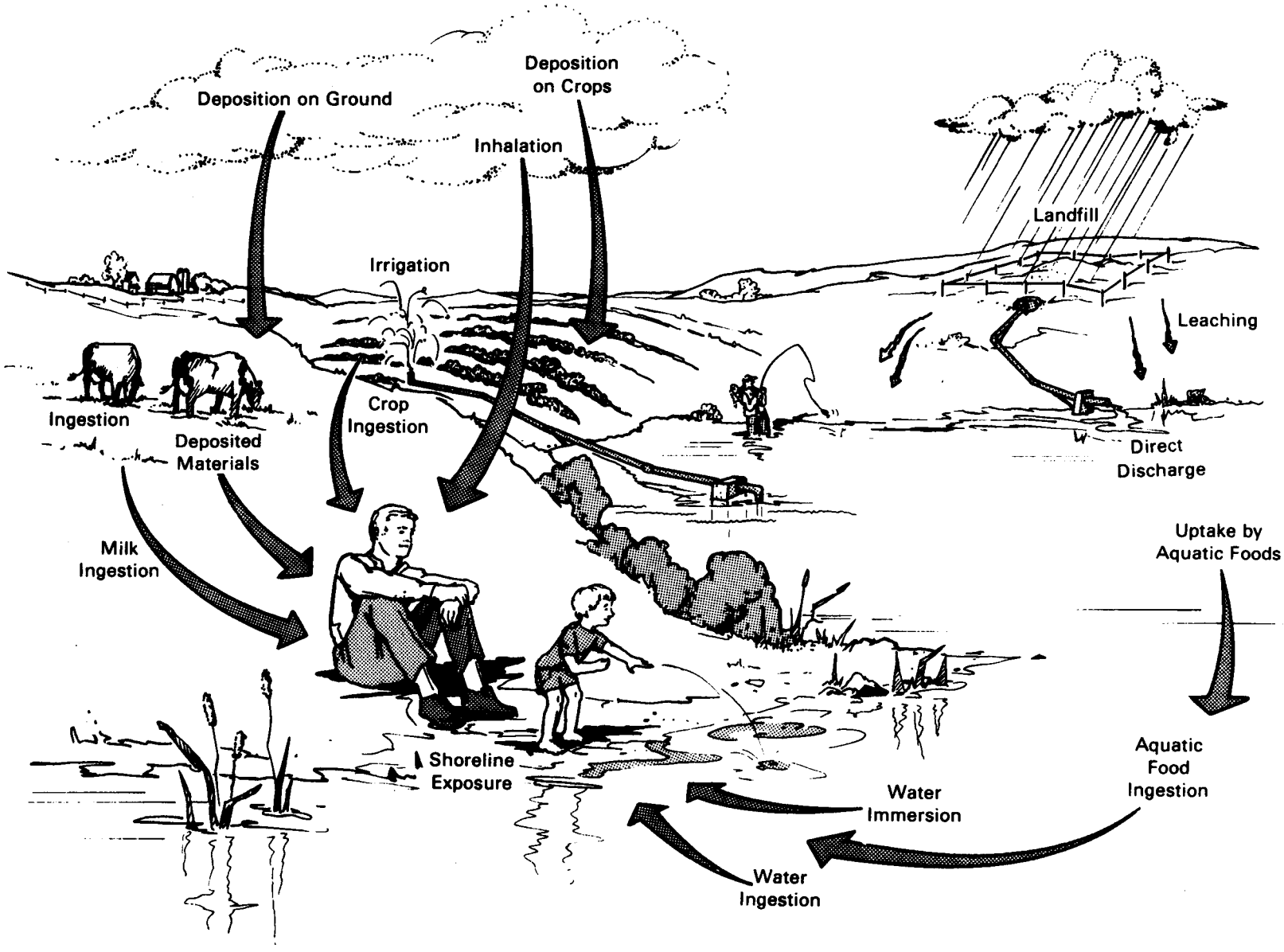

FIGURE 8.1. Exposure Pathways to Humans

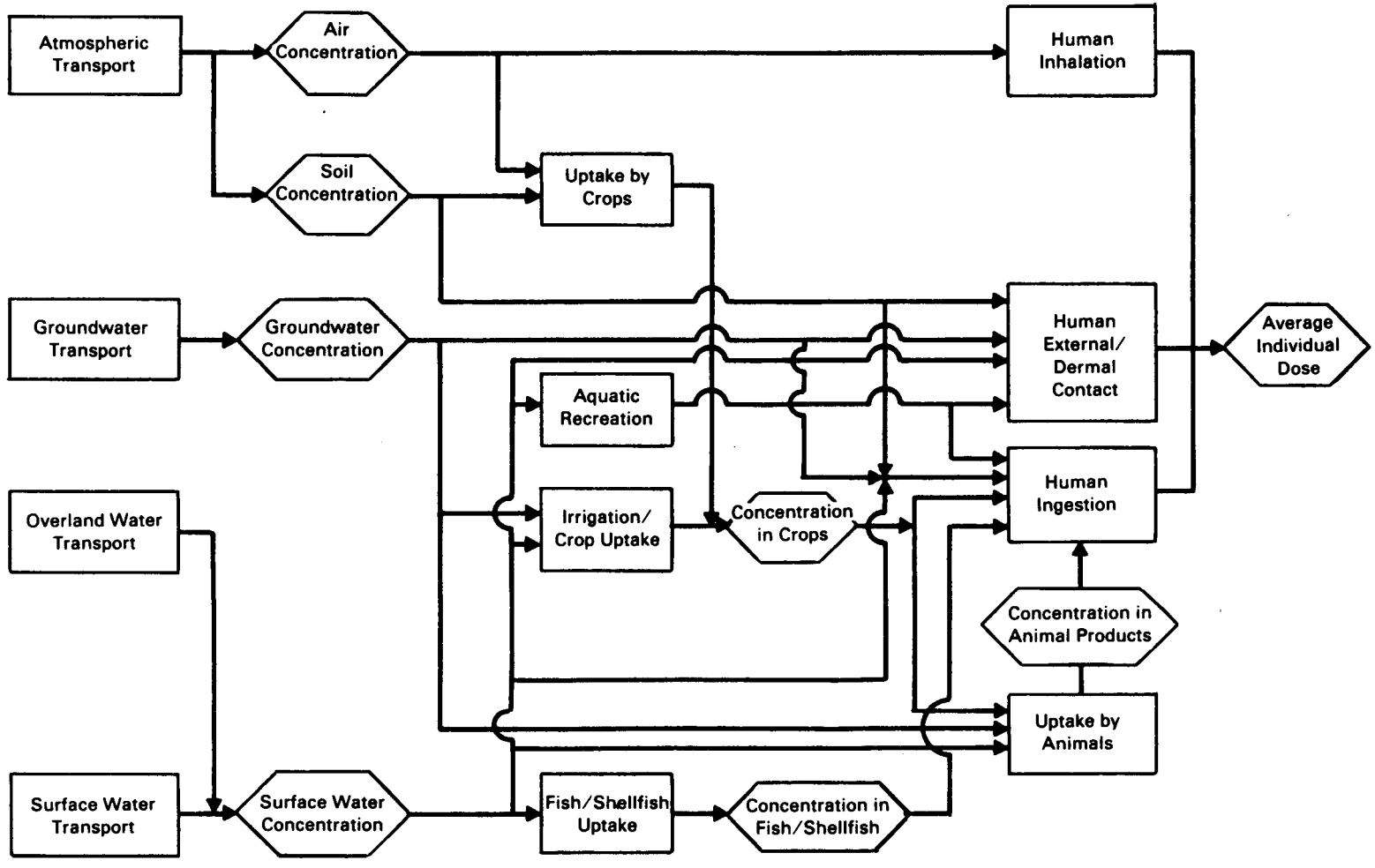

FIGURE 8.2. Exposure Pathways Considered by RAPS (after Bolten et al. 1983; Whelan et al. 1987)

- crop ingestion -- from farmlands contaminated by atmospheric transport and deposition or from irrigation using contaminated water (water transport pathways)
- animal product ingestion -- from animals fed contaminated crops (all transport pathways) or contaminated water (water transport pathways)
- external exposure to radionuclides -- from contaminated soil (air transport pathway) and from aquatic recreational activities (swimming, boating, and shoreline activities for overland and surface water transport pathways)
- dermal contact with chemicals -- from contact and ingestion of contaminated soil (atmospheric transport pathway), from swimming in contaminated water (overland and surface water transport pathways), and from bathing in domestic water (all water transport pathways).

The exposure pathway components discussed here use the long-term average environmental concentrations of each contaminant provided by the transport analyses. Because the analyses are performed assuming no changes to current land use, groundwater, or surface water practices (such as remedial actions to the waste or population changes), the potential exposures may continue for hundreds to thousands of years, particularly for the groundwater transport pathway. The exposure analysis is, therefore, based on 70-year increments (i.e., approximately one human life span), with average concentrations defined for each increment. These average concentrations are defined for media contaminated by the transport pathway being evaluated. The atmospheric transport pathway can potentially contaminate soil and air, while the water transport pathways are only considered to contaminate water (and farm soil through irrigation).

The exposure analysis provides the average individual dose for each contaminant. Two types of doses are calculated: for radioactive contaminants, the dose is expressed as the effective whole-body dose equivalent received from each contaminant over the lifetime of an average member of the population; and for chemical contaminants, dose is expressed as average daily intake (per unit body weight) of each contaminant by an average member of the population. The

basic equations for the two types of contaminants are identical; the differences in dose types are handled through definition of dose conversion factors, as explained in Section 8.9.

The exposure analysis is performed for one transport pathway, one usage location, and one 70-year period at a time. The term "usage location" represents a point in the environment where air, soil, or water may become contaminated and result in the exposure of a local population group. The doses from each calculation are evaluated for each contaminant. The doses are used in the health risk evaluation where a composite hazard potential index is determined for each contaminant. The hazard potential index includes contributions from all transport pathways, usage locations, and time periods.

Environmental degradation and decay are considered for all contaminants relative to three media: air, water, and soil. Radioactive contaminants are assumed at this time to decay at the same rate in all three media, although chemical contaminants may have different decay rates in the three media. In the following sections, the decay rate constants for a given contaminant (i) are represented as λa_i, λw_i, and λs_i for air, water, and soil, respectively.

Details of the mathematical expressions for each exposure pathway are given in the following discussions.

8.2 INHALATION

Two inhalation exposure pathways are included in RAPS. The primary pathway is inhalation of airborne contaminants from the atmospheric transport pathway. All individuals within 80 km (50 miles) of the site are potentially exposed by this route. A secondary exposure pathway is inhalation of volatile organic contaminants while showering. This pathway is only considered for the groundwater pathway because volatile compounds are not expected to remain in surface or overland water for times required to reach usage locations.

The average dose from inhaling contaminated air is calculated from the average individual ventilation rate (inhalation volume rate) and the average air concentration:

$$Db_i = B\ Ca_i\ Dh_i \qquad (8.1)$$

where Db_i = average individual dose from breathing contaminated air for contaminant i (mg/kg/d or rem/70 yr)[a]

i = index on contaminant

B = average ventilation rate for individuals (m^3/d)

Ca_i = average air concentration of contaminant i (mg/m^3 or pCi/m^3)

Dh_i = inhalation dose conversion factor for contaminant i (kg^{-1} or rem/70 yr per pCi inhaled).

The inhalation intake while showering requires an estimate of the amount of volatile contaminant released to the shower air. Because showering represents a system that promotes release of volatiles from the water (i.e., high turbulence, high surface area, and small droplets), the concentration of the contaminant in the shower air is assumed to be in equilibrium with the concentration in the water. The air concentration can be estimated using the Henry's law constant (Lyman et al. 1982) as follows:

$$Cv_i = 10^3\ Cw_i\ H_i\ /\ (R\ T) \qquad (8.2)$$

where Cv_i = concentration of volatile contaminant i in shower air (mg/m^3)

10^3 = units conversion factor (l/m^3)

Cw_i = concentration of contaminant i in shower water (mg/l)

H_i = Henry's law constant for contaminant i (atm-m^3/mol)

R = gas constant, 8.2×10^{-5} [atm-m^3/(mol-°K)]

T = average temperature of the air-shower atmosphere (°K)

A nominal temperature of 311°K (100°F) is assumed for the shower atmosphere in application of Equation (8.2).

Equation (8.2) will predict relatively high air concentrations for highly volatile contaminants; therefore, a mass balance must be performed to ensure

(a) For parameters with two sets of units, the first set refers to chemical contaminants, and the second set refers to radioactive contaminants.

that the amount of contaminant predicted to be in the shower air is not greater than the total amount in the shower water. The mass balance can be represented as

$$Cv_i \; Va \leq Cw_i \; Vw \tag{8.3}$$

where Va = volume of air in the shower stall (m^3)
Vw = volume of water used during a shower (l)

Nominal volumes of 2 m^3 and 190 l (~50 gal) are assumed for the air and water volumes, respectively. By using these values in Equation (8.3), combining the resulting expression with Equation (8.2), and solving for the Henry's law constant, the following expression is obtained:

$$H_i \leq 2.4 \times 10^{-3} \text{ atm-m}^3\text{/mol} \tag{8.4}$$

The value of the Henry's law constant is therefore limited to a maximum value of 2.4×10^{-3} in application of Equation (8.2) to evaluate the shower air concentration. The total amount of pollutant inhaled during a shower is then estimated as follows:

$$Df_i = B \; tv \; Cv_i \; Tf \; Dh_i \; \exp(- \lambda w_i \; tp) \tag{8.5}$$

where Df_i = inhalation intake of contaminant i while showering (mg/kg/d)
tv = average time spent showering per day (d/d)
λw_i = environmental degradation constant for contaminant i in water (d^{-1})
tp = average time of transit through the water distribution system (d)
Tf = water treatment purification factor, fraction of contaminant remaining after treatment (dimensionless)

The shower time is set to an average value of 0.0069 (10 min/d).

The inhalation dose conversion factor for chemical contaminants is equal to the inverse of the average adult body mass, assumed to be 70 kg (ICRP

1975). This representation is used to convert the daily intake (mg/d) to average individual dose (mg/kg/d). The average daily intake for chemical contaminants is assumed to be received by each member of the population over the entire 70-year period. Note that for chemical contaminants, intake by inhalation and ingestion are assumed to give equivalent risk. Alternatively, to consider blood level uptake as the basis for risk equivalence, the dose conversion factors could be modified to include inhalation-to-blood transfer and ingestion-to-blood transfer.

8.3 DRINKING-WATER INGESTION

Exposure to contaminants via the drinking-water ingestion pathway may result from the groundwater, surface water, or overland transport pathway. (The overland transport pathway may contribute to contamination in surface water systems and thus indirectly contribute to drinking-water ingestion.) The dose from ingesting water is calculated from the water concentration, water ingestion rate, a water treatment factor, and a decay correction (for radioactive or unstable contaminants). The average dose to an individual using a contaminated domestic water supply is calculated as follows:

$$Dw_i = Uw\ Cw_i\ Tf\ Dg_i \exp(-\lambda w_i\ tp) \qquad (8.6)$$

where Dw_i = average individual dose from ingesting drinking water for contaminant i (mg/kg/d or rem/70 yr)

Uw = average daily water intake rate for an individual (l/d)

Cw_i = average water concentration of contaminant i (mg/l or pCi/l)

Tf = water treatment purification factor, fraction of contaminant remaining after treatment (dimensionless)

λw_i = environmental degradation or radiological decay constant for contaminant i in water (d^{-1})

tp = average time of transit through the water distribution system (d)

Dg_i = ingestion dose conversion factor for contaminant i (kg^{-1} or rem/70 yr per pCi ingested).

The water treatment purification factor accounts for removal of contaminants during water treatment at municipal water supply facilities. If no water treatment is performed, then the purification factor is unity. The average daily water intake rate is assumed to be 2 l/d. Inadvertent ingestion of water during bathing is represented by an increment to the daily intake rate. This amount is considered to be small compared to the average daily water intake rate and is included to represent uptake from dermal contact during bathing as discussed in Section 8.8.

8.4 AQUATIC FOOD INGESTION

Ingestion of contaminated aquatic foods is an exposure pathway considered for the surface water and overland transport pathways. For the RAPS analysis, two types of aquatic foods are considered: fish and shellfish. Fish represent organisms living in free-flowing waters; shellfish represent organisms living in or feeding on sediments. The contaminant concentration in these organisms is related to the contaminant water concentration by use of bioaccumulation factors. The average individual dose from ingestion of aquatic foods is calculated using the water concentration and uptake rates as follows:

$$Da_i = \sum_{f=1}^{n} [U_f \, Cw_i \, B_{if} \exp(-\lambda w_i \, t_f)] \qquad (8.7)$$

where Da_i = average individual dose from ingestion of aquatic foods for contaminant i (mg/kg/d or rem/70 yr)

n = number of aquatic foods considered (n = 2)

f = index on aquatic food types

U_f = average consumption rate of aquatic food f for individuals in the population (kg/d)

B_{if} = bioaccumulation factor for contaminant i and aquatic food f (l/kg)

t_f = average time for decay from food harvest to consumption for aquatic food type f (d).

The ingestion dose factor is the inverse of the average adult body weight (70 kg). This representation converts daily intake (mg/d) to average individual dose (mg/kg/d). The default value for finfish consumption is 0.0065 kg/d (EPA 1980). The shellfish default consumption rate is 0.0027 kg/d (NRC 1977).

Bioaccumulation factors are available from NRC (1977) for all elemental chemicals from models derived for use in radiological analysis. For chemical contaminants that behave differently from the elemental form, additional data must be obtained. Default correlations for estimating bioaccumulations are available in the RAPS computer program based on octanol-water partition coefficients. These correlations are taken from Chapter 5.0 of Lyman et al. (1982) as prepared by S. E. Bysshe. The correlation equation for fish is based on Veith et al. (1980) as follows:

$$\log (B_{if}) = 0.76 \log (Kow_i) - 0.23 \qquad (8.8)$$

where Kow_i = the octanol-water partition coefficient for contaminant i. An expression similar to Equation (8.8) used for invertebrates (shellfish) is based on Southworth et al. (1978) as follows:

$$\log (B_{if}) = 0.819 \log (Kow_i) - 1.146 \qquad (8.9)$$

Equations (8.8) and (8.9) are to be used only when data for the specific contaminant are not available. These two correlations represent only an order-of-magnitude estimate.

8.5 CROP INGESTION

Irrigation using contaminated water or direct deposition of airborne contaminants onto plants and soil can result in contamination of agricultural crops. Two food products associated with contaminated crop production are considered: leafy vegetables and other vegetables (and fruit). The leafy vegetable category represents plants such as lettuce for which the edible portions of the plant are above ground, exposed, and are eaten directly with little processing. The other vegetable category represents all other crops for which

directly deposited contamination has a much smaller chance of being incorporated directly into the edible portion of the plant. The method that is used to estimate contaminant concentrations in the edible portions of the plant considers uptake from two pathways: direct deposition and absorption through roots from soil. The contribution to plant concentration from direct deposition onto leaves at the time of harvest is calculated as follows:

$$Cl_{ip} = Du_i \; Tv_p \; r \; [1 - \exp(-\lambda e_i \; te_p)] \; / \; (\lambda e_i \; Y_p) \qquad (8.10)$$

where Cl_{ip} = concentration of contaminant i in the vegetable for vegetable type p (leafy or root) from deposition onto leaves (pCi/kg or mg/kg)

p = index on plant or vegetable type (1 = leafy vegetable and 2 = root or other vegetable)

Du_i = deposition rate of contaminant i from air or water onto farmlands ($mg/m^2/d$ or $pCi/m^2/d$)

Tv_p = translocation factor from plant surfaces to edible parts of the plant for plant type p (dimensionless)

r = fraction of deposition, retained on edible parts of the plant (dimensionless)

λe_i = effective weathering and decay constant for contaminant i (d^{-1})

$\lambda e_i = \lambda a_i + 0.04951$

λa_i = environmental degradation and decay constant for contaminant i in air (d^{-1})

0.04951 = weathering decay constant corresponding to a half-time of 14 days (d^{-1})

te_p = duration of the growing period for crop type p (d)

Y_p = yield of crop type p (kg/m^2).

A default growing period of 60 days is assumed for both vegetable crops (NRC 1977).

For the air deposition pathway, the contaminant deposition rate (Du_i) is calculated from the air concentration and an average deposition velocity as follows:

$$Du_i = 86400\ Ca_i\ Vd_i \tag{8.11}$$

where Vd_i = the deposition velocity for contaminant i (m/s)
86,400 = the unit conversion factor (s/d).

For the water pathways, the contaminant deposition rate is calculated from the irrigation rate and water concentration as follows:

$$Du_i = Cw_i\ I\ /\ 30 \tag{8.12}$$

where I = the irrigation water application rate ($l/m^2/mo$)
30 = the units conversion factor (d/mo).

The contribution to contaminant concentration in plants from the root uptake pathway is calculated as follows for air deposition pathways:

$$Cr_{ip} = Cs_i\ Bv_i\ /\ P \tag{8.13}$$

where Cr_{ip} = plant concentration from uptake through roots for contaminant i and plant uptake pathway p (pCi/kg or mg/kg)
Cs_i = soil concentration of contaminant i (mg/m^2 or pCi/m^2)
P = area soil density (kg/m^2)
Bv_i = soil-to-plant transfer factor for contaminant i (dimensionless).

The calculation of contaminant concentration in plants from contaminated water involves estimating the average soil concentration over the irrigation period (usually defined as the growing period for the site). The plant concentration at the time of harvest is estimated as follows:

$$Cr_{ip} = Bv_i \frac{Du_i}{P\ \lambda_i} [1 - \exp(-\lambda_i\ te_p)] \tag{8.14}$$

The soil-to-plant transfer factor (Bv_i) is available for all elements from NRC (1977). For chemical contaminants that are not well described by elemental

parameters, an estimate for the transfer factor can be made using the correlation of Baes (1982) based on octanol-water partition coefficients:

$$\log (Bv_i) = 2.71 - 0.62 \log (Kow_i) \qquad (8.15)$$

Equation (8.15) is an order-of-magnitude estimate and should only be used when contaminant-specific data are unavailable. This equation is included in RAPS and is used whenever a value for the transfer factor is not supplied.

Equations (8.10) through (8.15) are used to estimate the concentration of contaminants in plants based on a farming cycle of 1 year. The concentration of contaminants in plants from irrigation and from atmospheric contaminant deposition onto plant leaves is estimated as 70 times the 1-year value. This estimate is appropriate because the plants are harvested annually and no contaminant accumulation occurs. However, for contributions to contaminant concentration in plants via root uptake from soil, a correction must be made to account for contaminant accumulation in soil from repeated atmospheric deposition of contaminants or contaminated irrigation water applications each year. This correction is made by applying a factor to the root uptake plant concentration. The factor includes contribution in soil from previous years of atmospheric deposition or irrigation as follows:

$$Sf_i = \frac{1}{25600\ \lambda s_i} \sum_{n=1}^{70} [1 - \exp (-\lambda s_i\ n\ 365)] \qquad (8.16)$$

where Sf_i = soil retention factor for 70 years of atmospheric deposition or irrigation for contaminant i (dimensionless)

λs_i = environmental degradation and decay constant for contaminant i in soil (d^{-1})

n = index on year within the 70-year period

365 = days per year

25,600 = days per 70 years.

The average total plant concentration at the time of consumption is then calculated as the sum of the contributions from direct deposition and soil uptake (including a term from background soil concentration levels) as follows:

$$C_{ip} = (Cl_{ip} + Sf_i \, Cr_{ip} + Cb_i \, Bv_i) \, [\exp (- \lambda w_i \, th_p)] \qquad (8.17)$$

where C_{ip} = average concentration of contaminant i in the vegetable for vegetable type p (leafy vegetables or other vegetables) at time of consumption (mg/kg or pCi/kg).

Cb_i = background soil concentration of contaminant i (mg/kg or pCi/kg)

th_p = time between harvest and consumption for the vegetable type p (d).

Equation (8.17) is used for computing the average concentration of most contaminants in plants. However, a more realistic model is required for the contaminant tritium because it is associated more closely with water. The concentration of tritium in plants is assumed to have the same specific activity as the contaminating medium (air or water). The fractional content of hydrogen in the plant is then used to estimate the tritium content in the food product. The concentration of tritium in vegetables from atmospheric deposition is calculated for air pathways as follows:

$$C_{ip} = 9 \, Ca_i \, Fh_p \, / \, Ha \qquad (8.18)$$

where 9 = inverse of hydrogen mass fraction in water (kg H_2O/kg H)

Fh_p = total fraction of hydrogen in plants of plant uptake pathway p (kg H/kg plant)

Ha = absolute humidity (kg H_2O/m^3).

A default absolute humidity of 0.008 (kg/m^3) is assumed.

A similar expression is used to estimate plant uptake of tritium from the water pathways:

$$C_{ip} = 9\ Cw_i\ Fh_p \qquad (8.19)$$

A default value for the plant hydrogen fraction for leafy vegetables and vegetables is assumed as 0.10 (Napier et al. 1980).

The average individual dose from ingestion of agricultural crops is estimated from the plant concentration, as determined by Equation (8.17), (8.18), or (8.19), and the average consumption rate of vegetables is computed as follows:

$$Dv_i = \sum_{p=1}^{2} U_p\ C_{ip}\ Dg_i \qquad (8.20)$$

where Dv_i = average dose from consumption of contaminated crops for contaminant i (mg/kg/d or rem/70 yr)

U_p = average daily consumption rate of vegetable product p (leafy vegetable or other vegetable) (kg/d).

The summation is over the two vegetable types. Default values for vegetable consumption rates are taken from NRC (1977) as follows: 0.082 kg/d for leafy vegetables and 0.52 kg/d for other vegetables.

8.6 ANIMAL PRODUCTS

Atmospheric deposition of contaminants onto feed crops and use of contaminated water to irrigate feed crops can result in the ingestion of contaminated crops by animals. In addition, contaminated water can be used as part of the animals' drinking-water supply. Human exposure to contaminants can then result from subsequent ingestion of contaminated animal products. The two animal products considered in the RAPS program are cow's milk and beef. In evaluating the contaminant concentration in the milk and meat, the animals are assumed to be fed crops containing contaminant levels defined by Equation (8.17), without considering the decay correction between harvest and consumption [the exponential term with th_p in Equation (8.17)]. The animal product concentration resulting from animal ingestion of contaminated feed is calculated as follows:

$$Cf_{im} = C_{ip} F_{mi} f Qf \exp(-\lambda w_i th_m) \quad (8.21)$$

where Cf_{im} = concentration of contaminant i in animal product m (milk or meat) from animal ingestion of contaminated feed (pCi/l or mg/l for milk and pCi/kg or mg/kg for meat)

m = index on animal product

C_{ip} = concentration of contaminant i in feed crop p used by the animal (pCi/kg or mg/kg)

F_{mi} = transfer coefficient for contaminant i that relates daily intake rate by an animal to the concentration in an edible animal product m (pCi/l milk per pCi/d or mg/l milk per mg/d for milk and pCi/kg meat per pCi/d or mg/kg meat per mg/d for meat)

f = fraction of animal feed that is contaminated (dimensionless)

Qf = consumption rate of feed by the animal (kg/d)

th_m = holdup time between harvest or slaughter and consumption for the animal product m (d).

In evaluating the feed concentration (C_{ip}) from Equation (8.17), parameter values representative of animal feed production are used, which differ from vegetable production parameters for human consumption. For example, the growing period is set to 30 days to represent animal grazing habits. Also, the crop yield is less (0.7 kg/m^2) for animal feed production. The animal consumption rate of feed is set to 55 kg/d for milk production and 68 kg/d for meat production.

The contribution to animal product concentration from animal ingestion of contaminated water is calculated as follows:

$$Cw_{im} = Cw_i F_{mi} fw Qw \exp(-\lambda w_i th_m) \quad (8.22)$$

where Cw_{im} = concentration of contaminant i in an animal product m from animal ingestion of water (pCi/l or mg/l for milk and pCi/kg or mg/kg for meat)

fw = fraction of animal water that is contaminated (dimensionless)

Qw = consumption rate of water by the animal (l/d).

Milk cows are assumed to consume 60 l/d of water, and beef animals are assumed to consume 50 l/d. As a conservative default, both types of animals are assumed to derive all of their drinking water from the contaminated source. The time between harvest and consumption by individuals is assumed to be 4 days for milk production and 20 days for meat production.

The transfer coefficients for milk and meat production have been defined for each element of the periodic table by NRC (1977). Default values for chemical contaminants can be estimated from the octanol-water partition coefficients using expressions presented by Kenega and Goring (1980). For milk the expression is

$$\log (F_{mi}) = -6.13 + 0.50 \log (Kow_i) \tag{8.23}$$

and for meat, the expression is

$$\log (F_{mi}) = -5.15 + 0.50 \log (Kow_i) \tag{8.24}$$

The total contaminant concentration in the animal product is the sum of the contributions from feed and water intake.

$$C_{im} = Cw_{im} + Cf_{im} \tag{8.25}$$

where C_{im} = concentration of contaminant i in animal product m (mg/l or pCi/l for milk and mg/kg or pCi/kg for meat.

A special model is used to estimate tritium concentration in animal products. The concentration of tritium is assumed to have the same specific

activity as the total animal intake of feed and water. For air and water pathways, the animal product tritium concentration is estimated as follows:

$$C_{im} = \frac{C_{ip}\ Qf + Cw_i\ Qw}{Fh_p\ Qf + Qw\ /\ 9}\ Fh_m \qquad (8.26)$$

where C_{ip} = tritium concentration in plant type p used for animal feed (pCi/kg)

Cw_i = tritium concentration in water used for animal drinking water (pCi/l)

Fh_m = the fraction of hydrogen in animal product m (kg H/kg animal product)

Fh_p = the fraction of hydrogen in animal feed plant type p (kg H/kg plant)

For air pathways, the concentration in animal drinking water (Cw_i) is set to zero.

Beef cattle are assumed to be fed primarily on grain and milk cows on grass. Hydrogen fraction values used by RAPS for feed plants and animal products are given in Table 8.1, as suggested by Napier et al. (1980).

The average individual dose is calculated from the animal product concentration and the average consumption rate of the products as follows:

$$D_{mi} = \sum_{m=1}^{n} U_m\ C_{im}\ Dg_i \qquad (8.27)$$

where D_{mi} = average individual dose for contaminant i from ingestion of contaminated animal product m (mg/kg/d or rem/70 yr)

U_m = average daily consumption rate of animal product m (milk or meat) (l/d for milk and kg/d for meat).

The summation is over both animal product types, milk and meat. Default values for the average daily intake of milk and meat are 0.30 l/d and 0.26 kg/d, respectively (NRC 1977).

TABLE 8.1. Fractions of Hydrogen Used in Animal Product Analysis

Animal Product	Animal Feed Plant Fraction, Fh_p (kg H/kg Plant)	Animal Product Fraction, Fh_m (kg H/kg Animal Product)
Meat	0.068	0.10
Milk	0.10	0.11

8.7 EXTERNAL EXPOSURE TO RADIONUCLIDES

External radiation exposure is considered for individuals exposed to land surfaces contaminated by atmospheric deposition and for individuals involved in aquatic recreational activities associated with contaminated overland and surface waters. Aquatic recreational activities include boating, swimming, and shoreline fishing or hiking. The radiation dose is calculated from the water concentration or soil concentration (depending on which transport pathway is being studied) as described below. For water pathways, the recreational dose is

$$De_i = 70\ (0.5\ tb + ts)\ Cw_i\ Db_i + 70\ tf\ Cd_i\ W\ Ds_i \qquad (8.28)$$

where De_i = radiation dose to an individual from external exposure for contaminant i (rem/70 yr)

tb = average time spent by an individual in boating (hr/yr)

ts = average time spent by an individual swimming (hr/yr)

Db_i = external dose conversion factor for radionuclide i for immersion in water (rem/hr per pCi/l)

tf = average time spent by an individual in shoreline activities (e.g., hiking, fishing, etc.) (hr/yr)

Cd_i = average sediment concentration of contaminant i deposited on shoreline from contaminated water (mg/m^2 or pCi/m^2)

W = shore-width factor to correct for finite size of shoreline (dimensionless)

Ds_i = external dose conversion factor for exposure to a contaminated plane of radionuclide i (rem/hr per pCi/m^2).

Default values for exposure times associated with boating, swimming, and shoreline fishing are 12 hr/yr, 12 hr/yr, and 12 hr/yr, respectively (NRC 1977). The water immersion dose factors are for total immersion; therefore, the boating dose is reduced by a factor of 0.5 to account for approximately half immersion while in a boat (i.e., exposure from one side instead of both sides).

The average contaminant concentration in shoreline sediment is estimated from a code developed by Soldat et al. (1974) relating water concentration to sediment concentration following a long period of deposition. The contaminant concentration in sediment is given by the expression below. The equation estimates an effective surface contamination for use in calculating gamma exposure rates to persons standing on sediment:

$$Cd_i = 100\ t_i\ Cw_i\ [1 - \exp\ (-\lambda s_i\ \ tw)] \qquad (8.29)$$

where 100 = transfer constant from water to sediment ($1/m^2/d$)

t_i = physical half-life of radionuclide i (d)

tw = length of time the shoreline sediment is exposed to the contaminated water, set to 35 years to represent the midpoint of the 70-yr evaluation period (12,780 d).

The value of the transfer constant was derived for several radionuclides by using data obtained from an analysis of water and sediment samples taken from the Columbia River at Richland, Washington, and at Tillamook Bay, Oregon, 75 km south of the river mouth (Nelson 1965; Toombs and Cutler 1968).

The shore-width factor (W) represents the fraction of dose from an infinite horizontal plane source that would be received from a given shoreline situation that may not be well represented as an infinite plane (for which the dose factors are defined). The shore-width factor is essentially a geometric correction to account for the finite size of shorelines. Suggested values for W are derived from experimental data (Dunster 1971) and are presented in Table 8.2.

TABLE 8.2. Suggested Values for Shore-Width Factor

Shoreline Type	Shore-Width Factor
River shoreline	0.2
Lake shore[a]	0.3
Nominal ocean site[a]	0.5
Tidal basin[a]	1.0

(a) Currently not addressed by the RAPS methodology.

Exposure to contaminated ground is considered only for atmospheric deposition because the water transport pathways will not result in widespread contamination exposing large population groups. Large areas of farmlands may become contaminated from irrigation with contaminated water; however, relatively few people will be subject to exposure (e.g., farm workers). Airborne deposition is assumed to cover the entire region of the defined population group, and all individuals are potentially exposed. The radiation dose received in one time period (i.e., 70 years) is calculated from the average soil concentration from air deposition as follows:

$$Dx_i = 70\ tg\ \ Cs_i\ Ds_i \qquad (8.30)$$

where Dx_i = radiation dose to an individual from exposure to contaminated ground for contaminant i (rem/70 yr)

70 = units conversion factor (yr/70 yr)

tg = average time of exposure per year to contaminated ground (hr/yr).

A default value of 8760 hr is used for tg, representing continuous exposure.

8.8 DERMAL CONTACT/INADVERTENT INGESTION

Uptake of contaminants may result from dermal contact with soil contaminated from atmospheric deposition or water contaminated from groundwater, surface water, or overland transport pathways. Soil contact represents either

ingestion from hand-to-mouth contact or absorption through the skin. Water contact may result in uptake during recreational swimming or domestic bathing. The effective uptake of contaminants from dermal contact with soil is estimated based on inadvertent ingestion of soil. The actual intake through the skin is assumed to be small compared to the intake through the ingestion route. To ensure that intake through the skin is small (relative to ingestion), the ingestion rate is estimated conservatively. Kimbrough et al. (1983) presented conservative estimates of soil ingestion as a function of age (Table 8.3). Using the values from this table, an estimate of average soil ingestion over the lifetime of an individual can be obtained (e.g., 410 mg/d). However, McKone (1985) suggested using a value of 40 mg/d equivalent uptake through dermal contact with skin. The average individual dose from dermal contact with soil is then estimated as follows:

$$Dd_i = 410\ Cs_i\ Dg_i\ /\ (1.5 \times 10^7) \qquad (8.31)$$

where Dd_i = average dose to an individual from soil ingestion for contaminant i (mg/kg/d or rem/70 yr)

410 = daily average soil ingestion rate (mg soil/d)

1.5×10^7 = areal soil density (mg soil/m^2).

TABLE 8.3. Soil Ingestion by Age

Age Group	Soil Ingested (mg/d)
0 - 9 mo	0
9 - 18 mo	1,000
1.5 - 3.5 yr	10,000
3.5 - 5 yr	1,000
>5 yr	100

The areal soil density is based on an average soil density of 1.5 g/cm^3 and a mixing depth of 1 cm for the contamination deposited from the air.

The dermal uptake during domestic bathing is assumed to be a minor dose contribution relative to inadvertent ingestion of water; this may be more true for shower bathing than for tub bathing. For the present analysis, each person is assumed to bathe once per day and ingest an average of 10 ml of contaminated water per day. The dose from this exposure pathway is estimated as follows:

$$Dc_i = 0.010\ Cw_i\ Tf\ Dg_i\ \exp\ (-\lambda w_i\ tp) \qquad (8.32)$$

where Dc_i = average daily dose to an individual from dermal contact with water during domestic bathing for contaminant i (mg/kg/d or rem/70 yr)

0.010 = ingestion rate from domestic bathing (l/d).

The ingestion of water during bathing is normally insignificant compared to the ingestion of drinking water (0.01 l/d as compared to 2 l/d); however, for locations where water is used for bathing but not for drinking, the bathing dose may be significant. Inadvertent ingestion of water may also occur during recreational swimming. The amount ingested is assumed to be 100 ml for every hour of swimming. The average time spent swimming per year [ts as defined for Equation (8.28)] is used to estimate the average exposure as follows:

$$Dr_i = 0.10\ Cw_i\ ts\ Dg_i\ /\ 365 \qquad (8.33)$$

where Dr_i = average dose to an individual from inadvertent ingestion of water during swimming for contaminant i (mg/kg/d or rem/70 yr)

0.10 = inadvertent water ingestion rate during recreational swimming (l/hr)

365 = days per year.

Exposure from inadvertent ingestion of water and soil is considered for both chemical and radioactive contaminants.

8.9 DOSE CONVERSION FACTORS

Factors must be defined for each contaminant to relate the rate of exposure to dose. For radiological contaminants, dose is measured as effective dose equivalent for the lifetime of an individual (i.e., 70 years). Inhalation and ingestion dose conversion factors are available from ICRP (1977, 1979-1982). The dose factors from this ICRP publication give the 50-year dose commitment from 1 year of intake. Multiplying these values by 70 (as is done in the RAPS methodology) results in a conservative estimate of lifetime dose; an individual would have to live 120 years (as opposed to 70 years) to receive the full dose implied in the calculations. This estimate is conservative to within a factor of two and is approximately correct for many radionuclides. External dose factors for human exposure to soil, sediments, and water contaminated with radioactive material are available from several sources. The values presented by Napier et al. (1980) are employed in the RAPS methodology.

Dose factors for chemical contaminants essentially represent unit conversion factors because the exposure and dose are the same. For inhalation, the dose factor relates the average amount of contaminant inhaled per day to the daily dose per unit body weight. The dose factor is the same for all chemical contaminants:

$$Dh_i = 1 \; / \; 70 \text{ kg} \tag{8.34}$$

For ingestion, the dose factor similarly relates daily intake to daily dose per unit body weight:

$$Dg_i = 1 \; / \; 70 \text{ kg} \tag{8.35}$$

8.10 SUMMARY

Results from each of the four transport pathways are used in the exposure assessment component to help calculate the HPI for each important waste site contaminant. The exposure assessment component considers potential exposure of

the surrounding population through the following exposure routes: 1) inhalation of airborne contaminants; 2) ingestion of contaminated drinking water, aquatic foods, soil crops, and animal products; 3) external dose from radiation; and 4) external dermal contact to chemicals. First, the important exposure routes and populations are defined. On the basis of the air, water, and soil contaminant levels provided by the transport pathway analyses, an estimate is then made of the average daily exposure to each contaminant. Estimation of the daily exposure is based on simple multiplicative models describing the transfer of contaminants from air, water, or soil to humans.

8.11 REFERENCES

Baes, C. F., III. 1982. "Prediction of Radionuclide Kd Values from Soil-Plant Concentration Ratios." Trans. Am. Nucl. Soc. 41:53-54.

Bolten, J. G., P. F. Morrison and K. A. Soloman. 1983. Risk-Cost Assessment Methodology for Toxic Pollutants from Coal-Fired Power Plants. WD-1589 EPRI RP1826-5, Electric Power Research Institute, Palo Alto, California.

Dunster, H. J. (chairman). 1971. Handbook of Radiological Protection Part 1: Data. SNB 11=360079-8. Radioactivity Advisory Committee, Department of Employment, Department of Health and Social Security, Ministry of Health and Social Services, Northern Ireland. Her Majesty's Stationery Office, London.

EPA (U.S. Environmental Protection Agency). 1980. "Water Quality Criteria Documents: Availability." 45 Fed. Reg. 79318-79379.

ICRP. 1975. Report of The Task Group on Reference Man. ICRP Publication 23, International Commission on Radiological Protection. Pergamon Press, New York.

ICRP. 1977. Recommendations of the International Commission on Radiological Protection. ICRP Publication 26, International Commission on Radiological Protection. Pergamon Press, New York.

ICRP. 1979-1982. Limits for Intakes of Radionuclides by Workers. ICRP Publication 30, Part 1 (and subsequent parts and supplements), Vol. 2, No. 3/4 through Vol. 8, No. 4. International Commission on Radiological Protection. Pergamon Press, New York.

Kenega, E. E., and C. A. I. Goring. 1980. "Relationship Between Water Solubility, Soil Sorption, Octanol-Water Partitioning and Concentration of Chemicals in Biota." In Aquatic Toxicology Proceedings, ASTM STP, 707:78-115.

Kimbrough, R. D., H. Falk, P. Stehr and G. Fries. 1983. "Health Implications of 2,3,7,8,-Tetrachlorodibenzodioxin (TDCC) Contamination of Residential Soil." In Proceedings of Public Health Risks of the Dioxins. William Kaufmann, Los Angeles, California.

Lyman, W. J., W. F. Reehl and D. H. Rosenblatt. 1982. Handbook of Chemical Property Estimation Methods. McGraw-Hill, New York.

McKone, T. E. 1985. The Use of Environmental Health-Risk Analysis for Managing Toxic Substances. UCRL-92329. Lawrence Livermore National Laboratory, Livermore, California.

Napier, B. A., W. E. Kennedy, Jr. and J. K. Soldat. 1980. PABLM - A Computer Program to Calculate Accumulated Radiation Doses from Radionuclides in the Environment. PNL-3209, Pacific Northwest Laboratory, Richland, Washington.

Nelson, J. L. 1965. "Distribution of Sediments and Associated Radionuclides in the Columbia River Below Hanford." In Hanford Radiological Sciences Research and Development Report for 1965, eds. D. W. Reece and J. K. Green. USAEC Report BNWL-36, Pacific Northwest Laboratory, Richland, Washington.

NRC. 1977. Calculation of Annual Doses to Man from Routine Releases of Reactor Effluents for the Purpose of Evaluating Compliance with 10 CFR Part 50, Appendix I. Regulatory Guide 1.109, U.S. Nuclear Regulatory Commission, Washington, D.C.

Soldat, J. K., N. M. Robinson and D. A. Baker. 1974. Models and Computer Codes for Evaluating Environmental Radiation Doses. BNWL-1754, Pacific Northwest Laboratory, Richland, Washington.

Southworth, G. R., J. J. Beauchamp and P. K. Schmeider. 1978. "Bioaccumulation Potential and Acute Toxicity of Synthetic Fuels Effluents in Fresh Water Biota: Azaarenes." Environ. Sci. Technol. 12:1062-1066.

Toombs, G. L., and P. B. Cutler (compilers). 1968. Comprehensive Final Report for the Lower Columbia River Environmental Survey in Oregon June 5, 1961 - July 31, 1967. Oregon State Board of Health, Division of Sanitation and Engineering, Salem, Oregon.

Veith, G. D., K. J. Macek, S. R. Petrocelli and J. Carroll. 1980. "An Evaluation of Using Partition Coefficients and Water Solubility to Estimate Bioconcentration Factors for Organic Chemicals in Fish." J. Fish. Res. Board Can. (prepublication copy).

Whelan, G., S. M. Brown, D. L. Strenge, A. P. Schwab and P. J. Mitchell. 1987. Contaminant Assessment Modeling Under the Resource Conservation and Recovery Act. EA-5342. Electric Power Research Institute, Palo Alto, California.

9.0 HEALTH RISK EVALUATION

9.1 INTRODUCTION

Evaluating the Hazard Potential Index (HPI) for a site requires that a measure of health risk be determined for the doses estimated by the exposure pathway analysis. The steps in determining the HPI from the average individual dose are illustrated in Figure 9.1. The first step is to determine a risk factor based on one of three contaminant types under consideration: 1) radioactive, 2) carcinogenic, and 3) noncarcinogenic. Risk factors are evaluated for each exposure resulting from each 1) transport pathway, 2) population group exposed, and 3) time period (i.e., each 70-year period during which contaminants are in the environment causing human exposures). The risk factors calculated for each contaminant type must be comparable. The RAPS analysis is based on a risk level of 10^{-6} as the point of comparability. For carcinogens and radioactive contaminants, risk functions are available from which the dose at a risk level of 10^{-6} can be evaluated. For noncarcinogenic contaminants, the reference dose, RFD, is assumed to correspond to a risk level of 10^{-6}, which is in agreement with current EPA philosophy.

EPA (1986) noted that guidance on response actions under CERCLA "requires that the analysis of cleanup alternatives include options in the 10^{-4} to 10^{-7} risk range with at least one alternative utilizing a 10^{-6} risk level . . . (EPA 1985a). Options are often chosen corresponding to a 10^{-6} risk level. Within the RCRA program the draft guidance manual for Alternate Concentration Limits (ACL), under the groundwater protection program (40 CFR 264.94) identifies 10^{-6} as the point of departure within a risk range of 10^{-4} to 10^{-8} . . . (EPA 1985b)[a]." The State of New York Bureau of Environmental Protection has also suggested (Johnson and Newell 1986) that a risk level of 10^{-6} be applied to exposures at reference dose levels.

The RAPS analysis evaluates the risk factor as the calculated dose to an individual divided by the dose corresponding to a risk level of 10^{-6}. The risk

(a) EPA. 1985b. Alternate Concentration Limit Guidance Based on Section 264.94b Criteria. Part I. Information Required in ACL Demonstrations. U.S. Environmental Protection Agency, Washington, D.C. (Draft).

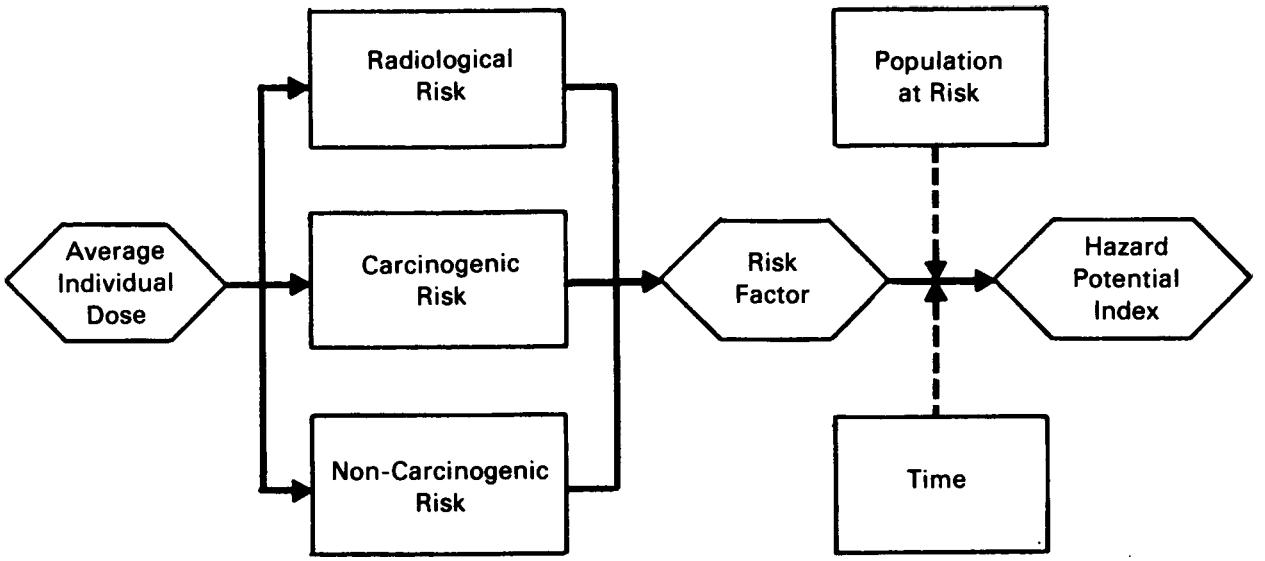

FIGURE 9.1. Health Risk Pathway Analysis Considered by RAPS [after Bolten et al. 1983; Whelan et al. (1987)]

factors for these evaluations are then combined mathematically with the population exposed and a time-of-exposure function to arrive at the HPI for the site. Details of these evaluations are provided in the following sections.

9.2 RADIOACTIVE CONTAMINANTS

Radiation exposure can cause health effects ranging in severity from minor genetic abnormalities to death. The magnitude and duration of the exposure are important parameters in determining the effects that are likely to occur. For the present analysis, long-term exposure over the lifetime of an individual is of interest. The primary health effect for such long-term exposures is cancer. Considerable research has been done on dose-response relationships for radiation exposure, particularly as related to the incidence of cancer. The National Research Council subcommittee on the Biological Effects of Ionizing Radiations has performed a detailed review of available data (NAS 1980).[a]

(a) Known as the BEIR III Report.

Based on this report and additional calculations, Buhl and Hansen (1984) have recommended methods for estimating health effects related to low levels of radiation exposure. Based on their analysis, the following expression has been selected for estimating a radiation health risk for RAPS:

$$R_{ij} = 2.7 \times 10^{-4} D_{ij} \qquad (9.1)$$

where R_{ij} = health risk for exposure to radiation for radionuclide i and exposure pathway j (dimensionless)

2.7×10^{-4} = health effect risk factor (per rem lifetime dose)

D_{ij} = average individual lifetime dose summed over all exposure pathways using the expressions described in Chapter 8.0 for radionuclide i (rem/70 yr).

The average dose to an individual for radioactive contaminants is evaluated as described in Section 8 for each exposure pathway. A summary of exposure pathways for radionuclides is as follows:

Db_i = inhalation
Df_i = inhalation while showering
Dw_i = drinking water ingestion
Da_i = aquatic food ingestion
Dv_i = vegetable crop ingestion
Dm_i = animal product ingestion
De_i = external exposure during aquatic recreation
Dx_i = external exposure from contaminated land
Dd_i = ingestion of soil
Dc_i = ingestion of water while bathing
Dr_i = ingestion of water while swimming.

The risk factor for radiation exposure is evaluated as the ratio of the individual dose, D_{ij}, to the dose corresponding to a health risk of 10^{-6} [i.e., 0.0037 rem, from Equation (9.1)]. The risk factor is given by the following:

$$RF_{ij} = 270 D_{ij} \qquad (9.2)$$

where RF_{ij} = risk factor for exposure to radiation for radionuclide i from pathway j (dimensionless)

270 = inverse of 10^{-6} risk level dose of 0.0037 rem (rem^{-1}).

9.3 CHEMICAL CARCINOGENS

The risk associated with exposure to chemical carcinogens is estimated using cancer potency factors developed by the EPA's Cancer Assessment Group (EPA 1982). These factors relate the average daily intake per unit body mass to the risk of developing cancer. The risk model is as follows:

$$R_{ij} = 1.0 - \exp\ (-\ D_{ij}\ q_i) \tag{9.3}$$

where R_{ij} = health risk for exposure to chemical carcinogen i for exposure pathway j (dimensionless)

D_{ij} = average daily intake rate of chemical carcinogen i (mg/kg/d)

q_i = cancer potency factor for chemical carcinogen i [$(mg/kg/d)^{-1}$].

When the exponent of Equation (9.3) is small (i.e., <0.01), the risk is approximated as equal to the exponent ($D_{ij}\ q_i$). This approximation is used in the RAPS program.

Cancer potency factors are defined for the inhalation and ingestion intake routes. The total risk factor for exposure to carcinogens is the sum of contributions from inhalation and ingestion.

$$RF_{ij} = 10^6\ qh_i\ Dh_{ij} \tag{9.4}$$

or

$$RF_{ij} = 10^6\ qg_i\ Dg_{ij} \tag{9.5}$$

where RF_{ij} = risk factor for exposure to chemical carcinogen i for exposure pathway j (dimensionless)

qh_i = inhalation cancer potency factor for chemical i [$(mg/kg/d)^{-1}$]

Dh_{ij} = average daily intake rate via inhalation of chemical carcinogen i for exposure pathway j (mg/kg/d)

qg_i = ingestion cancer potency factor for chemical i $[(mg/kg/d)^{-1}]$

Dg_{ij} = average daily intake rate via ingestion of chemical carcinogen i for exposure pathway j (mg/kg/d).

Inhalation pathways include air inhalation (Db_i) and inhalation while showering (Df_i). Other pathways are ingestion pathways (external exposure pathways are not considered for chemicals).

9.4 NONCARCINOGENIC CONTAMINANTS

Noncarcinogenic contaminants are those that exhibit a threshold dose below which no observable adverse health effects have been noted. This category generally includes all chemicals not considered to be carcinogenic, although carcinogenic chemicals may also exhibit threshold properties for effects other than cancer.

The noncarcinogenic analysis is based on reference dose levels as established by EPA for intake via ingestion and inhalation. These reference dose values are available for many chemicals on EPA's Integrated Risk Information System (IRIS). Exposure at the reference dose level is assumed to correspond to a health risk of 10^{-6}, as discussed in the introduction to this section. The risk factor is then given by

$$RF_{ij} = Dth_i \; / \; RfDh_i \qquad (9.6)$$

or

$$RF_{ij} = Dg_{ij} \; / \; RfDg_i \qquad (9.7)$$

where RF_{ij} = risk factor for exposure to noncarcinogenic chemical i for exposure pathway j (dimensionless)

Dh_{ij} = average daily inhalation intake rate of chemical i for exposure pathway j (mg/kg/d)

$RfDh_i$ = reference dose for inhalation of chemical i (mg/kg/d)

Dg_{ij} = average daily ingestion intake rate of chemical i for exposure pathway j (mg/kg/d)

$RfDg_i$ = reference dose for ingestion of chemical i (mg/kg/d).

The risk factors are used in evaluation of the hazard potential index for the site, as described in the following section.

9.5 HAZARD POTENTIAL INDEX EVALUATION

The risk factors (RF_{ij}) are combined with the population exposed and a time factor to determine the HPI for a site. A risk factor is defined for each contaminant (i), for each transport pathway considered for a site (groundwater, surface water, overland, or atmospheric), for each population group (one or more per site), and for each 70-year time period (as required for each transport pathway). The time factor is included to discount the importance of exposures that occur in the distant future, thus giving importance to the sites imposing an immediate hazard. The time factor is given an exponential representation with an assumed degradation half-life of 70 years (one human lifetime) and no minimum value. With these considerations, a preliminary hazard index is evaluated as follows:

$$PI_i = \sum_{n=1}^{N} \sum_{k=1}^{K_n} \left[\exp(-L\, t_k) \sum_{m=1}^{M_n} \sum_{j=1}^{J_n} RF_{ijkmn}\, P_{jmn} \right] \qquad (9.8)$$

where PI_i = preliminary hazard potential index for contaminant i for the site (persons)

n = index on transport pathway

m = index on usage location

j = index on exposure pathway

k = index on time period

L = time constant for the time weighting function based on a half-time of 70 years (0.01/yr) (yr^{-1})

N = number of transport pathways considered for the current site

M_n = number of usage locations considered for the current site and transport pathway

J_n = number of exposure pathways considered for the current site and transport pathway

K_n = number of 70-year time periods considered for the transport pathway n

t_k = time between the beginning of the calculation and the beginning of the current time period k (years)

P_{jmn} = number of people in population group m exposed by pathway j for transport pathway n (persons)

RF_{ijkmn} = risk factor for contaminant i, the current exposure pathway j, usage location m, transport pathway n, and time period k per person (dimensionless).

The preliminary hazard potential index (PI_i) is converted to the final hazard potential index for each contaminant (HPI_i) using the following numerical algorithm, which puts the HPI on a scale approximately from 0 to 100.

$$HPI_i = H_1 (H_2 + \log_{10} PI_i) \tag{9.9}$$

where H_1, H_2, = coefficients of the HPI function (dimensionless). Current values of H_1 and H_2 are 10.0 and 0.0, respectively.

These values result in an HPI value of zero for a PI_i of unity and a value of 100 for a PI_i of 10^{10}. Most sites are expected to have HPIs in the range of 0 to 100. Sites that score below zero are considered to be relatively innocuous to the surrounding human population although environmental damage may have occurred. Sites that score near 100 are considered to be a potential health hazard to the surrounding population. Adjustments may be made to the coefficient values after experience is gained in application of RAPS to specific sites.

Note that the parameter RF_{ijkm} in Equation (9.8) is the same as parameter RF_{ij} in Equations (9.2), (9.4), (9.5), (9.6), and (9.7). For simplicity, the dependence on transport pathway, population group, and time period were not shown in the earlier equations.

9.6 SUMMARY

The exposure assessment analysis supplies average contaminant dose to individuals for use in determining subsequent health effects (i.e., risk). The average exposure is then converted to an average individual risk factor using mathematical models for radionuclides, carcinogenic chemicals, and noncarcinogenic chemicals. The risk factor is intended to indicate the relative level of potential exposure to an average member of the exposed population.

For radionuclides, the risk factor is based on cancer risk estimates of the National Academy of Sciences Committee on the Biological Effects of Ionizing Radiation. The risks from chemical carcinogens are currently based on cancer potency factors defined by EPA. The cancer potency factors relate the average daily intake per unit body mass to the risk of developing cancer. Risk estimates for noncarcinogenic chemicals are based on reference doses, RfD, as estimated by the EPA. Risk factors are evaluated as the average daily intake (or dose) divided by the intake corresponding to a lifetime risk of 10^{-6}. The risk factors for radioactive, chemical carcinogenic, and chemical noncarcinogenic constituents are then combined with the population exposed and a time factor to determine the HPI for the site. The HPI is the parameter that is used for comparing waste sites according to their relative risks.

9.7 REFERENCES

Bolten, J. G., P. F. Morrison and K. A. Soloman. 1983. Risk-Cost Assessment Methodology for Toxic Pollutants from Coal-Fired Power Plants. WD-1589 EPRI RP1826-5. Prepared for the Electric Power Research Institute by Rand Corporation, Santa Monica, California.

Buhl, T. E., and W. R. Hansen. 1984. Estimating the Risks of Cancer Mortality and Genetic Defects Resulting from Exposures to Low Levels of Ionizing Radiation. LA-9893-MS, Los Alamos National Laboratory, Los Alamos, New Mexico.

EPA. 1982. Health Effects Assessment Summary for 300 Hazardous Organic Constituents. Environmental Criteria and Assessment Office, U.S. Environmental Protection Agency, Cincinnati, Ohio.

EPA. 1985a. Guidance on Feasibility Studies Under CERCLA. EPA-540/G-E5-003. U.S. Environmental Protection Agency, Office of Emergency and Remedial Response, Washington, D.C.

EPA. 1986. "Hazardous Waste Management System Land Disposal Restrictions; Proposed Rule." Part III. U.S. Environmental Protection Agency. 40(260) Fed. Reg. 1601-1766 (January 14, 1986).

Johnson, D. W., and A. J. Newell. 1986. Risk to Wildlife from Eating Contaminated Fish. Paper presented at the Annual Meeting of the Society of Environmental Toxicology and Chemistry, 2-5 Nov. 1986, Alexandria, Virginia.

Lewis, R. J. Sr., and R. L. Tatken. 1982. Registry of Toxic Effects of Chemical Substances. DHHS(NIOSH) Publication No. 81-116, two volumes. U.S. Department of Health and Human Services, Washington, D.C.

NAS. 1980. The Effects on Populations of Exposure to Low Levels of Ionizing Radiation. National Academy of Sciences Committee on the Biological Effects of Ionizing Radiations, National Research Council, Washington, D.C.

Whelan, G., S. M. Brown, D. L. Strenge, A. P. Schwab and P. J. Mitchell. 1987. Contaminant Assessment Modeling Under the Resource Conservation and Recovery Act. EA-5342. Electric Power Research Institute, Palo Alto, California.

10.0 EXAMPLE TEST APPLICATIONS OF THE RAPS METHODOLOGY[a]

10.1 INTRODUCTION

The results of applying the RAPS methodology to four hypothetical case studies are presented in this chapter. These simplified case studies are presented to demonstrate the utility of RAPS in simulating the migration and fate of hazardous and radioactive mixed wastes through and between various environmental media and their interaction with the media. The case studies are simplified for illustrative and comparative purposes. The subsurface information is partially based on data presented by Perlmutter and Lieber (1970) and Anderson (1979), as given in Codell et al. (1982). Data pertaining to the transport pathways and constituent characteristics can also be found in Whelan et al. (1987), Mills et al. (1985), EPA (1980), ICRP (1977, 1979-1982), Napier et al. (1980), NRC (1977), Mualem (1976), and Israelsen and Hansen (1962). (Data were also received from EPA on cancer potency factors.)

The first two example case studies (i.e., Cases 1 and 2) are presented to illustrate the applications and differences of the HRS, mHRS, and RAPS methodologies to a hazardous and radioactive mixed-waste disposal site. These simplified case studies are presented to demonstrate typical limitations associated with HRS and mHRS methodologies and how these limitations are addressed by RAPS. The final two example case studies (i.e., Cases 3 and 4) use only the RAPS methodology at sites where contaminant migration and fate are through multiple media and routes of human exposure. Example Cases 3 and 4 illustrate the application of RAPS at more complex sites than those considered in Cases 1 and 2.

10.2 GENERAL ASSUMPTIONS ASSOCIATED WITH EACH EXAMPLE CASE STUDY

Each of the four example case studies assumes that identical hazardous and radioactive mixed-waste sites are located above an unconfined, unconsolidated aquifer. The transporting pathway of importance to Cases 1 and 2 is the

(a) This chapter is based on Whelan et al. (1985, 1986).

saturated zone of the groundwater environment; the important transport pathways for Cases 3 and 4 are the partially saturated and saturated zones of the groundwater environment and a river, which represents the surface water environment.

Arsenic and strontium-90 represent the important respective chemical and radioactive contaminants leaching from the waste site. In these examples, arsenic represents a persistent and relatively immobile substance; strontium-90 represents a mobile and decaying substance. The waste is represented by a mixture of chemical and radioactive sludge wastes and soil aggregate. For each case study, first-order degradation/decay is assumed for each potentially important contaminant, with constituent-soil matrix interaction described by an equilibrium coefficient. Climatic and meteorologic conditions for each case study are assumed to be equivalent. Although RAPS is capable of computing a leach rate from the waste site, it is assumed for simplification that the leach rate is equal to 20% of the average-annual precipitation.

Under the RAPS analysis, contaminant levels of arsenic and strontium-90 contained in the waste site were chosen so that if an individual ingested the leachate leaving the site, the resulting risk to the individual from arsenic and strontium-90 would be equal. By setting the waste concentrations so that they initially pose equivalent risk, the effects of persistence, mobility, and dilution on the relative risks to important receptors are more clearly discerned. For computing the relative risk for Cases 1 through 4, arsenic is assumed to be a carcinogen with a cancer potency factor of 14 $(mg/kg/d)^{-1}$,(a) and the radiological dose for strontium-90 is based on an ingestion dose factor of 1.2×10^{-8} rem per pCi ingested and a risk factor of 2.4×10^{-4} per person-rem (ICRP 1977, 1979-1982; Buhl and Hansen 1984).

Site, constituent, and exposure assessment characteristics for Cases 1 through 4 are presented in Tables 10.1 through 10.6. Table 10.1 presents general information pertaining to each of the example cases. Table 10.2 presents data associated with the saturated zone of the groundwater pathway for

---

(a) The cancer potency factor for arsenic was obtained from a soon-to-be-published EPA draft document. At the time of this writing, the document was unavailable for citation.

TABLE 10.1. Information Pertaining to Cases 1 Through 4 (After Whelan et al. 1985, 1986)

Parameter	Value
Precipitation infiltration rate[a,b]	8.0×10^{-7} cm/s (2.3×10^{-3} ft/d)
Area of square disposal site (Codell et al. 1982)	2,916 m^2 (31,390 ft^2)
Life of disposal site	No remediation
Human life span (NRC 1977)	70 yr
Half-life of arsenic[c]	∞ yr
Half-life of strontium-90 (Codell et al. 1982)	28.5 yr
Population of Town W[b]	500 people
Population of Town X[b]	500 people
Population of Town Y[b]	500 people
Population of Town Z[b]	500 people

(a) Assumed equal to 20% of the average-annual rainfall.
(b) Assumed for descriptive purposes.
(c) Whelan, G., S. M. Brown, D. L. Strenge, A. P. Schwab and P. J. Mitchell (1987). Containment Assessment Modeling Under the Resource Conservation and Recovery Act. EPRI Project EA-5342. Electric Power Research Institute, Palo Alto, California.

Cases 1 through 4. Tables 10.3 and 10.4 list data associated with the partially saturated zone for Case 4, while Table 10.5 presents the Case 4 hydraulic information assumed for River Z. Finally, Table 10.6 lists the data related to the exposure assessment component of the RAPS methodology for Cases 1 through 4. Much of this information is based on standard parameter values provided by NRC (1977).

TABLE 10.2. Information Pertaining to the Saturated Zone for Cases 1 Through 4 (After Whelan et al. 1985, 1986)

Parameter	Value
Depth (Codell et al. 1982)	43 m (140 ft)
Soil porosity (Codell et al. 1982)	35.0%
Bulk density (Codell et al. 1982)	1.92 g/cm^3 (120 lb/ft^3)
Distance between waste site and Well W for Cases 1 and 2[a]	1.0 km (0.6 mi)
Distance between waste site and Well X for Cases 1 and 2	6.0 km (3.7 mi)
Distance between waste site and Well Y for Case 3	1.0 km (0.6 mi)
Distance between waste site and River Z for Case 4[a]	0.5 km (0.3 mi)
Groundwater pore water velocity (Codell et al. 1982)	43.2 cm/d (1.42 ft/d)
x-direction dispersivity (Codell et al. 1982)	2130 cm (69.9 ft)
y-direction dispersivity (Codell et al. 1982)	427 cm (14.0 ft)
z-direction dispersivity (Mills et al. 1985)	2.47 cm (0.08 ft)
Equilibrium coefficient for arsenic[a]	15 ml/g
Equilibrium coefficient for strontium-90 (Codell et al. 1982)	3.4 ml/g

(a) Assumed for descriptive purposes.

10.3 APPLICATION OF HRS, mHRS, AND RAPS METHODOLOGIES TO EXAMPLE CASE STUDIES 1 AND 2

Example Case Studies 1 and 2 assume that a hazardous and radioactive mixed-waste site is located above a saturated, alluvial aquifer. This aquifer supplies municipal drinking water to the surrounding populations and represents the only unthreatened municipal drinking-water supply. The waste is stored in an unlined landfill. The bottom of the landfill coincides with the water table surface.

TABLE 10.3. Information Pertaining to the Top Layer (Clay) of the Partially Saturated Zone for Case 4 (After Whelan et al. 1986)

Parameter	Value
Depth[a]	0.5 m (1.6 ft)
Soil porosity (Mualem 1976)	49.5%
Bulk density (Mualem 1976)	1.32 g/cm^3 (82.5 lb/ft^3)
Field capacity (Israelsen and Hansen 1962)	28.0%
Hydraulic conductivity at field capacity (Mualem 1976; Israelsen and Hansen 1962)	6.9 x 10^{-8}cm/s (2.0 x 10^{-4} ft/d)
Hydraulic conductivity at saturation (Mualem 1976)	1.2 x 10^{-5}cm/s (3.4 x 10^{-2} ft/d)
z-direction dispersivity (Mills et al. 1985)	1 cm (0.4 in.)
Equilibrium coefficient for arsenic[b]	150 ml/g
Equilibrium coefficient for strontium-90[b]	34 ml/g

(a) Assumed for descriptive purposes.
(b) For descriptive purposes, the equilibrium coefficients for the clay layer were assumed to be one order of magnitude higher than that for the alluvial layer.

The waste site is located 1 km (0.6 mi) from the drinking-water well (Well W) for Town W and 6 km (3.7 mi) from the drinking-water well (Well X) for Town X (Figures 10.1 and 10.2). Each town is assumed to have a constant population of 500 people. Each population center is assumed to obtain its drinking-water supplies only from its respective well, with ingestion of drinking water representing the only route of exposure to contaminants.

For illustration, this example is evaluated under two separate scenarios. Case 1 (Figure 10.1) illustrates contaminant movement from the waste site toward Well X and away from Well W. Case 2 (Figure 10.2) assumes the same hydrologic and geologic conditions as Case 1, except the groundwater

TABLE 10.4. Information Pertaining to the Bottom Layer (Sand) of the Partially Saturated Zone for Case 4 (After Whelan et al. 1986)

Parameter	Value
Depth[a]	1.0 m (3.3 ft)
Soil porosity (Codell et al. 1982)	35%
Bulk density (Codell et al. 1982)	1.92 g/cm^3 (120 lb/ft^3)
Field capacity (Israelsen and Hansen 1962)	8.5%
Hydraulic conductivity at field capacity (Mualem 1976; Israelsen and Hansen 1962)	4.9 x 10^{-4} cm/s (1.4 ft/d)
Hydraulic conductivity at saturation (Mualem 1976)	1.5 x 10^{-2} cm/s (42.5 ft/d)
z-direction dispersivity (Mills et al. 1985)	1 cm (0.4 in.)
Equilibrium coefficient for arsenic[a]	15 ml/g
Equilibrium coefficient for strontium-90 (Codell et al. 1982)	3.4 ml/g

(a) Assumed for descriptive purposes.

TABLE 10.5. Information Pertaining to River Z for Case 4 (After Whelan et al. 1986)

Parameter[a]	Value
Flow velocity	0.30 m/s (1.0 ft/s)
Flow depth	1.5 m (5.0 ft)
Width	91.4 m (300 ft)
Distance downstream to usage location	1000 m (3281 ft)

(a) Assumed for descriptive purposes.

TABLE 10.6. Exposure Assessment Data for Cases 1 Through 4 (After Whelan et al. 1986)

Parameter	Value	
	Cases 1, 2, and 3	Case 4
Drinking water?[a]	Yes	Yes
Water purification?[a]	No	Yes
Purification factor for arsenic (Napier et al. 1980)	---	0.7
Purification factor for strontium-90 (Napier et al. 1980)	---	0.2
Water consumption rate (EPA 1980)	2.0 l/d (0.53 gal/d)	2.0 l/d (0.53 gal/d)
Crop ingestion[a]	No	Yes
Animal product ingestion[a]	No	Yes
Consumption rate of vegetables (NRC 1977)	---	0.52 kg/d (1.15 lb/d)
Consumption rate of leafy vegetables (NRC 1977)	---	0.08 kg/d (0.18 lb/d)
Consumption rate of meat (NRC 1977)	---	0.26 kg/d (0.57 lb/d)
Consumption rate of milk (NRC 1977)	---	0.30 l/d (0.08 gal/d)
Crop growing period[a]	---	120 d
Irrigation rate[a]	---	100 (3.8×10^{-7} l/s/m^2)

Transfer Factor	Arsenic	Strontium-90
Soil-to-Plant (NRC 1977)	0.01	0.20
Water/Feed-to-Meat (NRC 1977)	1.5×10^{-3} d/kg (6.8×10^{-4} d/lb)	3.0×10^{-4} d/kg (1.4×10^{-4} d/lb)
Water/Feed-to-Milk (NRC 1977)	3.0×10^{-3} d/l (1.1×10^{-2} d/gal)	1.5×10^{-4} d/l (5.7×10^{-4} d/gal)

(a) Assumed for descriptive purposes.

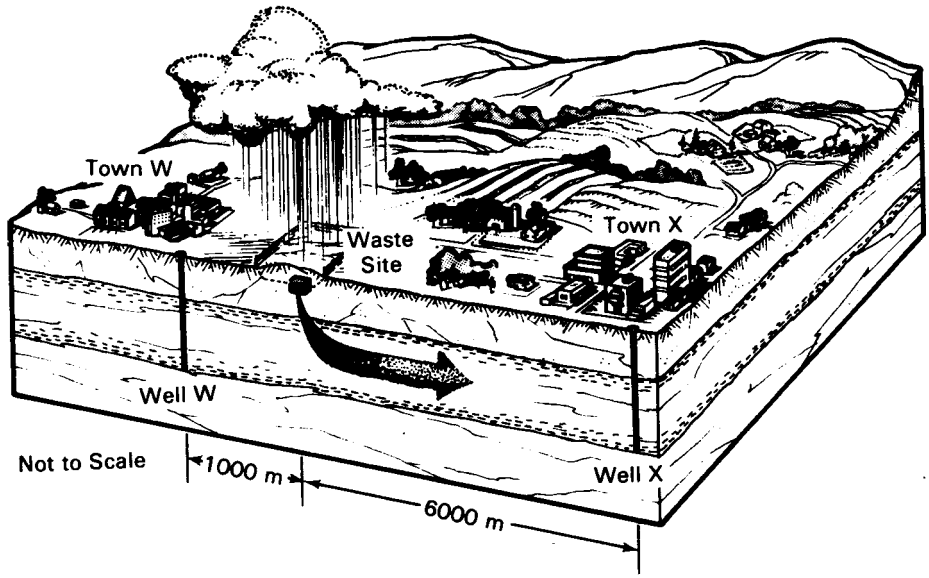

FIGURE 10.1. Case 1 Scenario: Contaminated Wastes Leaching from the Disposal Site and Migrating Toward Well X and Town X (After Whelan et al. 1985)

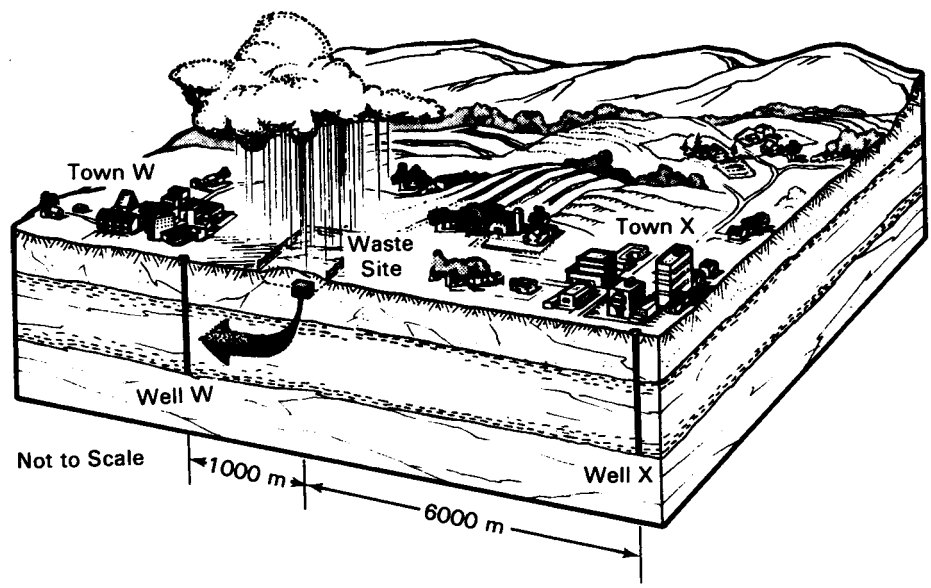

FIGURE 10.2. Case 2 Scenario: Contaminated Wastes Leaching from the Disposal Site and Migrating Toward Well W and Town W (After Whelan et al. 1985)

flow is in the opposite direction, away from Well X and toward Well W. Only population X is potentially affected by exposure to contaminated groundwaters in Case 1; Town W represents the only potentially exposed population in Case 2.

10.3.1 Application of the HRS and mHRS Methodologies to Cases 1 and 2

Case Studies 1 and 2 have been structured such that only the groundwater route of exposure is of any importance when the HRS and mHRS methodologies are applied. Figures 2.2 and 2.3 illustrate the manner in which the groundwater routes of HRS and mHRS, respectively, are applied to the case studies. Results of each case study are presented in Table 10.7. Because HRS has been described and applied many times, only those aspects pertaining to the HRS/mHRS results from analyzing these case studies are discussed here. For more information on

TABLE 10.7. HRS and mHRS Site Rankings for Cases 1 and 2 (After Whelan et al. 1985)

Route Component	HRS		mHRS	
	Case 1	Case 2	Case 1	Case 2
Release characteristics	45/45[a]	45/45	45/45	45/45
Route characteristics	NS[b]	NS	NS	NS
Arsenic waste characteristics	26/26	26/26	26/26	26/26
Strontium-90 waste characteristics	26/26	26/26	11/26	11/26
Target characteristics	25/49	25/49	25/49	25/49
Normalized route score for arsenic	51.02	51.02	51.02	51.02
Normalized route score for strontium-90	51.02	51.02	21.59	21.59
Normalized total migration score for arsenic	29.49	29.49	29.49	29.49
Normalized total migration score for strontium-90	29.49	29.49	12.47	12.47
Site assessment score	29.49	29.49	29.49	29.49

(a) 45 of a possible 45 points assigned.
(b) Not scored according to the provisions of the HRS or mHRS methodologies.

the HRS and mHRS methodologies, refer to EPA (1982) for the HRS methodology and Stenner et al. (1986), Hawley et al. (1986), and Hawley and Napier (1984) for the mHRS methodology.

As Figures 2.2 and 2.3 and Table 10.7 illustrate, both methodologies evaluate the chemical waste characteristics component in an identical way. Each methodology evaluates the type of chemical with regard to toxicity/persistence and the total quantity of material, not contaminant, disposed of at the waste site.

HRS and mHRS differ in their assessment approach when evaluating the waste characteristics component. The HRS evaluates all radionuclides as strong carcinogens (i.e., the most toxic rating possible). When using HRS, both arsenic (toxic metal) and strontium-90 (carcinogenic radionuclide) are assigned maximum toxicity/persistence scores. The hazardous waste quantity, on the other hand, is scored by including all waste (innocuous waste included) present at the facility. The problem with this assumption is that if a small quantity of hazardous material is distributed throughout a large volume of innocuous material (e.g., a large quantity of soil contaminated with a relatively small quantity of hazardous waste), the total volume of disposed material determines the quantity score. According to this approach, the same amount of hazardous waste, if disposed undiluted, would receive a much lower score than if it were blended with an innocuous material, such as soil. Because of the large volume of contaminated soil considered in both Cases 1 and 2, the quantity score would receive a maximum value -- regardless of the concentration of contaminants.

The radioactive wastes characteristics component for the mHRS, however, would be based on the maximum observed concentration of radionuclides in the groundwater and the estimated maximum potential concentration. The estimated concentration is a function of the quantity of the waste disposed of at the site and a transport coefficient that is based on a substantial amount of field/laboratory data. The resulting mHRS analysis more accurately reflects the relative hazards between radionuclides. Both the observed (if available) and estimated concentrations are factored into a concentration/dose matrix table to derive a waste characteristics score. Using the mHRS approach,

strontium-90 is assigned a score 58% lower than that assigned by HRS (see Table 10.7); however, arsenic is still assigned the maximum waste characteristics score, so the mHRS site assessment score is the same as the HRS score.

The HRS/mHRS method does not consider the direction of groundwater flow in evaluating the population at risk. Well W may be in close proximity to the site, but if it is up gradient from the contamination, as in Case 1, Well W is unlikely to be impacted by releases from the facility. The structure of the HRS/mHRS is such that it cannot distinguish between the two case studies. According to its scoring method, only Population W and Well W for both Cases 1 and 2 would be evaluated and scored. Because the HRS/mHRS is insensitive to the groundwater gradient, the final normalized total migration score of 29.49 applies to both Cases 1 and 2.

The chemical waste score dominates the total score assigned for both Cases 1 and 2 (see Table 10.7). The mHRS assigns a lower score, 12.47, to the strontium-90 waste; however, according to EPA protocol, the chemical's score would dominate the ranking. Using current EPA guidance, this score is sufficient to place this waste site, under either scenario, on EPA's National Priority List (NPL).

10.3.2 Application of the RAPS Methodology to Cases 1 and 2

The various pathways and interactions comprising the RAPS methodology are illustrated in Figure 2.5. The sequential procedure for implementing the methodology from the contaminant source through the computation of the HPI for this case study is illustrated in this figure. Contaminants leaching from the waste site are assumed to directly enter the saturated groundwater zone because the bottom of the waste site coincides with the surface of the water table. The migration and fate of the contaminants are modeled using semianalytical solute transport algorithms similar to those expressed by Codell et al. (1982) and Yeh (1981). The surrounding population inhabiting Town X (Case 1) or Town W (Case 2) are assumed exposed via the drinking water pathway only. An analysis of the source term is not presented because the levels of arsenic and strontium-90 in the waste site were chosen so that their leachate concentrations would result in equal risk if the leachate itself was ingested.

The risk to a population surrounding a waste site depends on each contaminant's mobility, persistence (degradation/decay), transport direction, temporal and spacial distribution, time of population exposure, and duration of exposure. A contaminant that is more mobile represents a greater threat to a surrounding population than an equally hazardous contaminant that is immobile. Likewise, a contaminant that degrades/decays generally presents less of a risk than one that does not (assuming equal environmental conditions). The numerical algorithms forming the basis of the RAPS methodology consider each of these conditions with regard to site and constituent characteristics.

For example, Case 1 results (see Table 10.8) indicate that, although strontium-90 (HPI = -32) decays (i.e., a half-life of 28.5 years), it is significantly more mobile than arsenic (HPI = -52) and therefore poses a greater potential hazard to Town X (i.e., -32 is greater than -52).[a] Case 2

TABLE 10.8. RAPS Site Rankings for Cases 1 and 2

Case	Town and Well Designation	Contaminant	Contaminant HPI[a]
1	X	Arsenic	-52
1	X	Strontium-90	-32
2	W	Arsenic	60
2	W	Strontium-90	42

(a) The scoring system associated with the RAPS methodology is not related in any way to the scoring system of the HRS/mHRS methodology. Also, the scoring system presented in Whelan et al. (1986) is different from the one outlined in this report. (Note: HPI = Hazard Potential Index.)

(a) It should be noted that sites that score below zero are considered to be relatively innocuous to the surrounding human population although environmental damage may have occurred. Most sites, however, will score between 0 and 100.

results indicate that the potential hazards to Town W associated with arsenic (HPI = 60) are higher than the relative risk posed by the significantly more mobile, nonpersistent contaminant strontium-90 (HPI = 42).[a]

The RAPS methodology also assessed the population size and exposure for Cases 1 and 2. The HPIs computed for each case were directly proportional to the size of the population exposed. The HPIs also considered the time at which exposure of the population to the contaminants occurred, duration of exposure, and relative level of exposure. RAPS gives preference to sites where 1) contaminant levels are high, 2) the travel time of the contaminant from the waste site to a receptor of concern is short, and 3) exposure durations occur over long periods of time. The contaminant levels are higher for Case 2 than for Case 1; the contaminant travel times are also shorter. On the other hand, the surrounding population for Case 1 is exposed to contaminants over longer periods of time, although the concentrations are less than those of Case 2. The lower concentrations result from contaminant retention and degradation/decay.

The overall risk at the hazardous waste site, however, represents the potential risk posed by the contaminant with the highest HPI. The risks to the respective populations for Cases 1 and 2 are presented in Table 10.8. As indicated in Table 10.8, Town W (Case 2) would be potentially more heavily impacted by contaminant releases from the waste site (as one would expect because of its proximity) than Town X (Case 1).

10.3.3 Summary of the HRS, mHRS, and RAPS Applications to Cases 1 and 2

Two simplified case studies are presented illustrating the use of the HRS, mHRS, and RAPS methodologies in assessing the potential migration, fate, exposure, and effects of a chemical (arsenic) and radionuclide (strontium-90) released to a groundwater system supplying the only source of drinking water to two identical towns: a town 1 km (0.6 mi) north of the waste site (Town W for Case 2) and a town 6 km (3.7 mi) south (Town X for Case 1). Case 1 assumes

(a) It should be noted that sites that score near 100 are considered to be a potential health hazard to the surrounding population. Most sites, however, will score between 0 and 100.

solute transport toward Town X, while Case 2 assumes solute transport toward Town W. All other geologic and hydrologic conditions are assumed equal between the cases.

When the HRS and mHRS methodologies are employed in analyzing Cases 1 and 2, the results indicate that no differences exist between the cases. These methodologies are insensitive to the direction of solute transport, population size and location, time until exposure occurs, duration of exposure, or the relative level of contamination. The mHRS results do indicate a lower score for strontium-90 than that calculated by the HRS methodology; however, the cases are equivalently ranked because arsenic levels control each analysis.

In its analysis of Cases 1 and 2, the RAPS methodology indicates that the waste site as described by Case 2 is potentially more dangerous to the surrounding population than that of Case 1. These results are expected because Town W, under Case 2, is one-sixth the distance from the waste site that Town X is under Case 1. Even though strontium-90 is more mobile than arsenic, the persistence of arsenic (i.e., no degradation) causes it to be a long-term potential hazard in Case 2. Strontium-90, on the other hand, is also important in Case 2 because the transport time to the exposure location (i.e., Well W) is relatively short such that strontium-90 does not decay to very low levels.

These simplified case studies illustrate that the RAPS methodology is more sensitive than HRS/mHRS to site and constituent characteristics; it is also more discriminating in its analysis by directly considering the location and size of the exposed population; duration of exposure; time until exposure occurs; each contaminant's mobility, persistence, and transport direction; and the relative level of contamination.

10.4 APPLICATION OF THE RAPS METHODOLOGY TO EXAMPLE CASE STUDIES 3 AND 4

Application of the RAPS methodology to Cases 3 and 4 illustrates its use at two sites with different contaminant transport pathways and exposure routes to surrounding populations. Descriptions highlighting the characteristics associated with Cases 3 and 4 are presented below.

10.4.1 Application of the RAPS Methodology to Case 3

Under Case 3, the contaminated waste is stored in an unlined landfill with a bottom that coincides with the water table surface. The waste is assumed to leach at a constant average-annual rate from the site and enter an alluvial saturated aquifer. The leachate then travels 1.0 km (0.6 mi) through the saturated aquifer to the nearby municipal drinking-water well, Well Y. Well Y supplies drinking water to the surrounding population of Town Y and represents the only municipal drinking-water supply. For simplicity, ingesting drinking water is assumed to represent the only route of exposure to these contaminants. Dermal contact during bathing is not considered a significant pathway for the contaminants, as compared to direct ingestion of water. The well water is assumed to be used directly, without purification. It is also assumed that no other populations are exposed to these contaminated waters. Under Case 3, only one transport pathway, the saturated zone of the groundwater environment, is considered. The Case 3 scenario is illustrated in Figure 10.3.

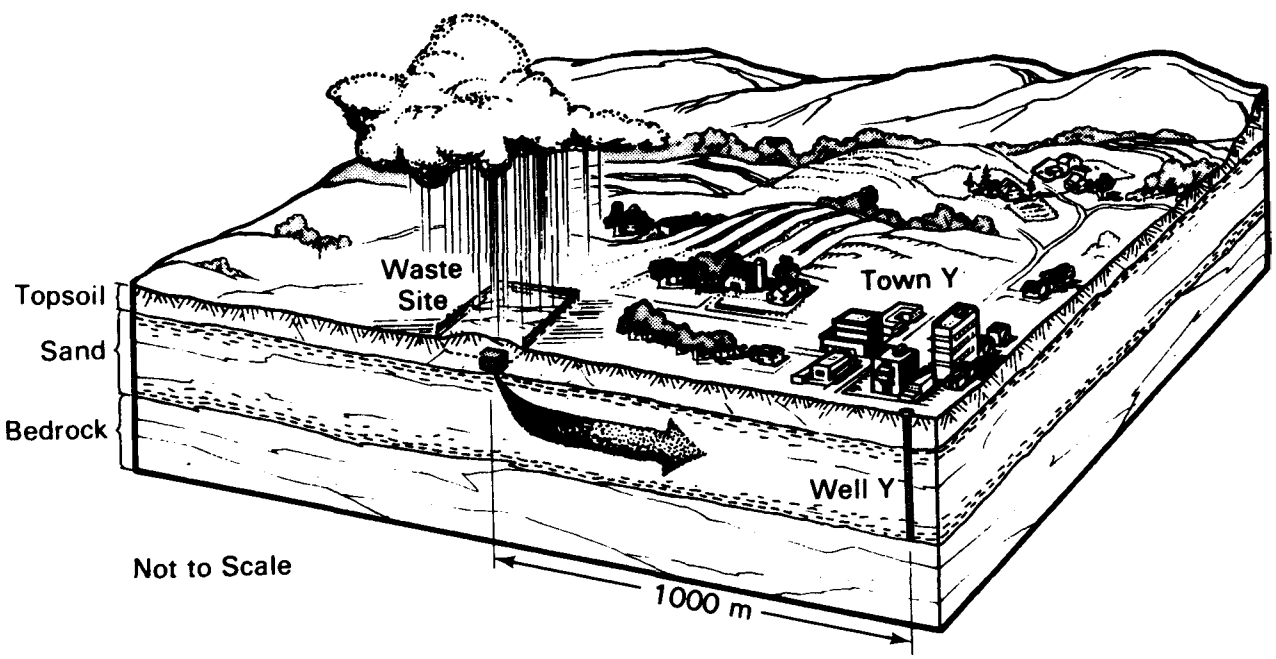

FIGURE 10.3. Case 3 Scenario: Contaminated Wastes Leaching from the Disposal Site and Migrating Toward Well Y and Town Y (After Whelan et al. 1986)

10.4.2 Application of the RAPS Methodology to Case 4

Under Case 4, contaminated water is stored in a landfill that is situated on 6 m (20 ft) of partially saturated soil. This partially saturated zone is composed of two distinct layers. The topmost layer (i.e., the one touching the bottom of the landfill) is 1 m (3 ft) thick and is composed of claylike material. The soil layer beneath the clay layer consists of alluvial material and is 5 m (17 ft) thick. The bottom of this layer coincides with the water table surface of a saturated aquifer composed of the same alluvial material. The saturated aquifer supplies groundwater to a nearby river (River Z), 500 m (1640 ft) from the waste site. The waste is assumed to leach from the site and migrate through four consecutive transport pathways: two partially saturated zones, one saturated zone, and one river. The RAPS methodology computes contaminant fluxes between transport pathways and contaminant levels in the final transporting medium (i.e., River Z) for use by the exposure assessment component.

The migration and fate of the contaminants leaching from the waste site under Case 4 are explained as follows. The leachate percolates into and through the clay layer, then into and through the alluvial layer of the partially saturated zone. Because the percolation rate (i.e., leach rate) is less than the maximum transmission rate of either soil layer, the flux of water through each layer is equivalent to the percolation rate. Although the fluid movement through the clay and sand layers is not hindered by the respective characteristics of each soil layer, the characteristics of each soil layer affect the adsorption-desorption process and affect the rates of contaminant transport through each layer. Because of its higher affinity for adsorbing contaminants (assuming an infinite supply of adsorption sites), the clay layer has a greater impact on impeding solute movement than does the alluvial layer. On leaving the partially saturated zone, the waste enters the saturated alluvium below and travels, adsorbing to the surrounding soil matrix and dispersing as it migrates, toward River Z.

The contaminants eventually enter the river and are transported to a surface water intake structure where drinking-water supplies for Town Z, irrigation water for locally grown crops, and stock water for locally grown animals

are collected. River Z supplies drinking water to Town Z and represents the only municipal drinking-water supply. The drinking water, though, is assumed to pass through a treatment plant that removes different fractions of each contaminant. In addition, the water from River Z is assumed to irrigate nearby agricultural lands that supply food crops to milk- and meat-producing animals; these food crops and animal products are assumed to be harvested for human consumption. It is further assumed that no populations other than Town Z are exposed to these contaminated waters. For simplicity, this scenario limits the routes of exposure to the surrounding population to ingestion of crops irrigated with contaminated water, livestock that have ingested contaminated water, and contaminated drinking water. The Case 4 scenario is illustrated in Figure 10.4.

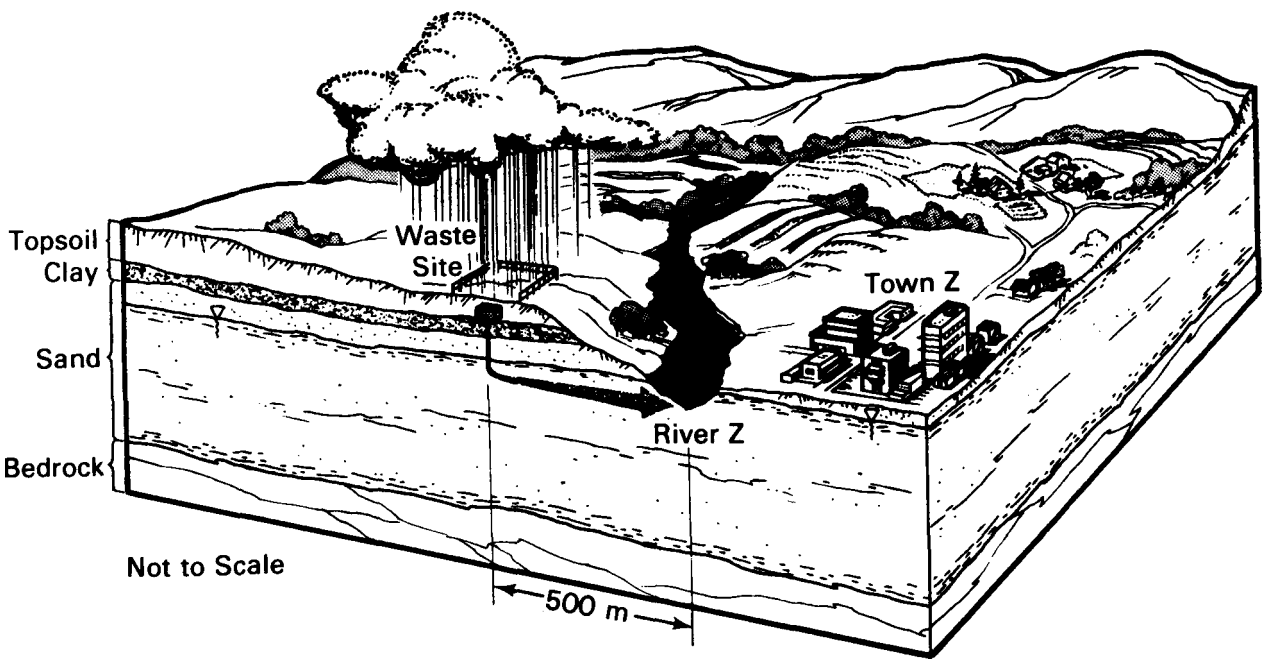

FIGURE 10.4. Case 4 Scenario: Contaminated Wastes Leaching from the Disposal Site and Migrating Toward River Z and Town Z (After Whelan et al. 1986)

10.4.3 RAPS Application Results for Cases 3 and 4

Two simplified examples (i.e., Cases 3 and 4) demonstrate the application of the RAPS methodology. These examples have been constructed to illustrate the effects of certain constituent characteristics and various environmental media on contaminant transport and eventual exposure of a surrounding population. For the examples presented, five factors help determine the relative importance of arsenic and strontium-90: mobility (adsorption-desorption effects), persistence (degradation/decay), duration of exposure of a population to a contaminant, arrival time of the contaminant, and dilution effects. The example case studies are structured to minimize the effects of other important characteristics such as climate, site geometry, etc. The results of each example application are briefly described as follows.

Case 3. Because strontium-90 is more mobile in the environment than arsenic, it arrives at Well Y first. However, it undergoes decay (half-life of 28.5 years) before reaching Well Y [1.0 km (0.6 mi) from the waste site] and, subsequently, the population of Town Y; in contrast, arsenic does not degrade. Because arsenic is more persistent in the environment and because of its lower mobility (i.e., attenuation characteristics), the population of Town Y is exposed to arsenic significantly longer than it is to strontium-90. Arsenic potentially poses a greater hazard to Town Y (HPI = 99) than the hazard presented by strontium-90 (HPI = 96). The results of the HPI evaluation for Case 3 are presented in Table 10.9.

TABLE 10.9. Hazard Potential Index (HPI) Values for Cases 3 and 4

Case	Town and Well/ River Designation	Contaminant	Contaminant HPI
3	Y	Arsenic	60
3	Y	Strontium-90	42
4	Z	Arsenic	-13
4	Z	Strontium-90	-63

Case 4. Although the clay layer in the partially saturated zone does not affect the transmission rate of fluid through the layer, it does effectively attenuate the movement of arsenic and strontium-90. Although strontium-90 decays, it is more mobile (as in Case 3) than arsenic. Because of arsenic's persistence, though, Town Z is exposed significantly longer to arsenic than strontium-90. In this case, the relative risk posed by the less mobile, persistent contaminant arsenic, which is exposed to the surrounding population for a longer duration of time, is significantly higher than the relative risk posed by the more mobile, nonpersistent contaminant strontium-90.

Comparison Between Cases 3 and 4. The results of applying the RAPS methodology to Cases 3 and 4 indicate that Case 3, with a maximum HPI based on arsenic of 9, poses a greater potential hazard to the surrounding population than that of Case 4, which has a maximum HPI for arsenic of 19. The attenuation and retardation characteristics inherent to the clay layer and the dilution effects of contaminant mixing in River Z in Case 4 significantly reduce the adverse effects associated with the proximity of River Z to the waste site. Based on these results alone, a further detailed site characterization of Site Y would be recommended before site characterization of Site Z.

10.4.4 Summary of the RAPS Application to Cases 3 and 4

Two simplified case studies (i.e., Cases 3 and 4) illustrate the use of the RAPS methodology in assessing the migration, fate, exposure, and relative risks associated with the release of a chemical (arsenic) and radionuclide (strontium-90) to a multimedia environment. Arsenic is an immobile, persistent, suspected carcinogen, and strontium-90 is a relatively mobile, nonpersistent, known carcinogen. Case 3 illustrates the transport of arsenic and strontium-90 from a waste site through one environmental medium (i.e., a saturated alluvial aquifer of a groundwater system) to a well (Well Y) that supplies drinking water to a nearby town (Town Y). Case 4 illustrates arsenic and strontium-90 movement through four environmental media [i.e., two partially saturated soil layers (one composed of clay and one composed of sand) beneath the waste site, one saturated alluvial aquifer, and one river] to a water intake structure in a river (River Z) that supplies the only drinking, irrigation, and stock water to a nearby town (Town Z).

Under the Case 3 analysis, arsenic represents the dominant constituent of concern to the surrounding population. Even though strontium-90 is more mobile than arsenic, the transport time to the exposure location (i.e., Well Y) is long enough that strontium-90 can sufficiently decay to relative risk levels that are below that of arsenic. On the other hand, the persistence of arsenic (i.e., no degradation) causes it to be a long-term potential hazard. Case 3 illustrates the tradeoff between strontium-90's mobility and arsenic's persistence.

For the Case 4 analysis, the results also indicate that arsenic is more dominant than strontium-90. Analysis using the RAPS methodology indicates that the waste site as described by Case 3 is potentially more dangerous to the surrounding population than that of Case 4. With Case 4, the clay layer beneath the site significantly reduces the contaminant transport rate to other environmental media; in addition, dilution from mixing in the river also reduces contaminant levels.

10.5 SUMMARY

The RAPS methodology is being developed to provide DOE with a better management tool for prioritizing inactive hazardous and radioactive mixed-waste sites according to their relative risks to surrounding populations and for funding allocations for further site investigations and possible remediation. The RAPS methodology addresses many of the typical limitations associated with other simplified ranking systems: 1) more site information and constituent characteristics associated with potential contaminant transport pathways; 2) chemical and radioactive wastes; 3) the potential direction of contaminant movement; 4) contaminant mobility, persistence, and toxicity; 5) time until a population is exposed (i.e., contaminant arrival time); and 6) duration of exposure.

The risk to a population surrounding a hazardous waste site depends on each contaminant's mobility, persistence (degradation/decay), transport direction, time of population exposure, and duration of exposure. A contaminant that is more mobile represents a greater threat to a surrounding population than an equally hazardous contaminant that is immobile. Likewise, a

contaminant that degrades/decays is less risk than one that does not degrade/decay, assuming equal environmental conditions. The numerical algorithms forming the basis of the RAPS methodology consider each of these conditions when assessing a hazardous waste site.

Four simplified case studies are presented illustrating the use of the RAPS methodology in assessing the migration, fate, exposure, and relative risks associated with the release of a chemical (arsenic) and radionuclide (strontium-90) to a multimedia environment. Arsenic is an immobile, persistent, suspected carcinogen, and strontium-90 is a relatively mobile, nonpersistent, known carcinogen. The first two case studies employ the HRS, mHRS, and RAPS methodologies; these case studies illustrate the differences that exist between HRS/mHRS and RAPS. The latter two case studies illustrate the application of RAPS to significantly more complex situations than those presented in the first two case studies.

The first two simplified case studies illustrate that the RAPS methodology is more sensitive than HRS/mHRS to site and constituent characteristics. RAPS is also more discriminating in its analysis by directly considering the location and size of the exposed population; duration of exposure; time until exposure occurs; each contaminant's mobility, persistence, and transport direction; and the relative levels of risk associated with the contamination.

The final two case studies illustrate the applicability of RAPS to a diverse and complex environment. Although these case studies are relatively simple, they addressed four transporting media (i.e., two partially saturated zones in the groundwater environment, a saturated zone, and a surface water environment); various routes of exposure (i.e., ingestion of contaminated crops, animal products, and drinking-water supplies); different contaminant types (i.e., carcinogenic chemical and radioactive constituents); and the relative risk associated with each contaminant.

These simplified examples illustrate the application of the RAPS methodology to a multimedia environment. The RAPS methodology is structured such that it requires minimum user knowledge of contaminant transfer between various environmental media and risk assessment.

10.6 REFERENCES

Anderson, M. P. 1979. "Using Models to Simulate the Movement of Contaminants through Groundwater Flow System." CRC Crit. Rev. Environ. Control 2:97-156.

Codell, R. B., K. T. Key and G. Whelan. 1982. A Collection of Mathematical Models for Dispersion in Surface Water and Groundwater. NUREG-0868. Nuclear Reactor Regulation, U.S. Nuclear Regulatory Commission, Washington, D.C.

EPA. 1980. "Appendix C - Guidelines and Methodology in the Preparation of Health Effect Assessment Chapters of the Consent Decree Water Criteria Documents." U.S. Environmental Protection Agency, 47 Fed. Reg. 79347-79357.

EPA. 1982. "Appendix A - Uncontrolled Hazardous Waste Site Ranking System: A User's Manual." U.S. Environmental Protection Agency, 37 CFR(137) Fed. Reg. 31219-31243.

Hawley, K. A., and B. A. Napier. 1984. "A Ranking System for Mixed Radioactive and Hazardous Waste Sites." In Proceedings of the Fifth DOE Environmental Protection Information Meeting, CONF-841187, U.S. Department of Energy, Washington, D.C.

Hawley, K. A., R. A. Peloquin and R. D. Stenner. 1986. Modified Hazard Ranking System for Sites with Mixed Radioactive and Hazardous Wastes -- User Manual. PNL-5841, Pacific Northwest Laboratory, Richland, Washington.

ICRP. 1977. Recommendations of the International Commission on Radiological Protection. International Commission on Radiological Protection, ICRP Publication 26, Pergamon Press, New York.

ICRP. 1979-1982. Limits for Intakes of Radionuclides by Workers. International Commission on Radiological Protection, ICRP Publication 30, Part 1 (and subsequent parts and supplements), Vol. 2, No. 3/4 through Vol. 8, No. 4. Pergamon Press, New York.

Israelsen, O. W., and V. E. Hansen. 1962. Irrigation Principles and Practices. Wiley, New York.

Mills, W. B., D. B. Porcella, M. J. Ungs, S. H. Gherini, K. V. Summers, L. Mok, G. L. Rupp and G. L. Bowie. 1985. Water Quality Assessment: A Screening Procedure for Toxic and Conventional Pollutants. EPA/600/-6-85/0026, U.S. Environmental Protection Agency, Environmental Research Laboratory, Athens, Georgia.

Mualem, Y. 1976. A Catalogue of the Hydraulic Properties of Unsaturated Soils," Research Project 442. Technion Israel Institute of Technology, Haifa, Israel.

Napier, B. A., W. E. Kennedy, Jr. and J. K. Soldat. 1980. PABLM - A Computer Program to Calculate Accumulated Radiation Doses from Radionuclides in the Environment. PNL-3209. Pacific Northwest Laboratory, Richland, Washington.

NRC. 1977. Calculation of Annual Doses to Man from Routine Releases of Reactor Effluents for the Purpose of Evaluating Compliance with 10 CFR Part 50, Appendix I. Regulatory Guide 1.109, U.S. Nuclear Regulatory Commission, Washington, D.C.

Perlmutter, N. M., and M. Lieber. 1970. Disposal of Plating Waste and Sewer Contaminants in Ground Water Surface Water, South Farmingdale-Massapequa Area, Nassau County, New York. U.S. Geological Survey Water-Supply Paper 1979-G.

Stenner, R. D., R. A. Peloquin and K. A. Hawley. 1986. Modified Hazard Ranking System/Hazard Ranking System for Sites with Mixed Radioactive and Hazardous Wastes -- Software Documentation. PNL-6066. Prepared for the U.S. Department of Energy, Office of Environment, Safety, and Health, Washington, D.C.

Whelan, G., B. L. Steelman, D. L. Strenge and J. G. Droppo. 1986. "Overview of the Remedial Action Priority System (RAPS)." In Pollutants in a Multimedia Environment, ed. Y. Cohen, pp. 191-227. Plenum Press, New York.

Whelan, G., B. L. Steelman, D. L. Strenge and K. A. Hawley. 1985. "Development of the Remedial Action Priority System: An Improved Risk Assessment Tool for Prioritizing Hazardous and Radioactive Mixed-Waste Disposal Sites." In Proceedings of Management of Uncontrolled Hazardous Waste Sites, Hazardous Materials Control Research Institute, Silver Spring, Maryland.

Whelan, G., S. M. Brown, D. L. Strenge, A. P. Schwab and P. J. Mitchell. 1987. Contaminant Assessment Modeling Under the Resource Conservation and Recovery Act. EA-5342. Electric Power Research Institute, Palo Alto, California.

Yeh, G. T. 1981. AT123D: Analytical Transient One-, Two-, and Three-Dimensional Simulation of Waste Transport in the Aquifer System. Publication No. 1439, ORNL-5602, Oak Ridge National Laboratory, Oak Ridge, Tennessee.

DISTRIBUTION

No. of Copies

OFFSITE

153 DOE Technical Information Center

Administrator, Economic Regulatory Administration, RG-1
U.S. Department of Energy
1000 Independence Ave., S.W.
Washington, DC 20585

Administrator, Energy Information Administration, EI-1
U.S. Department of Energy
1000 Independence Ave., S.W.
Washington, DC 20585

Assistant Secretary for Congressional Intergovernmental and Public Affairs, CP-1
U.S. Department of Energy
1000 Independence Ave., S.W.
Washington, DC 20585

Assistant Secretary for Conservation and Renewable Energy, CE-1
U.S. Department of Energy
1000 Independence Ave., S.W.
Washington, DC 20585

Assistant Secretary for Defense Programs, DP-1
U.S. Department of Energy
1000 Independence Ave., S.W.
Washington, DC 20585

Assistant Secretary for Fossil Energy, FE-1
U.S. Department of Energy
1000 Independence Ave., S.W.
Washington, DC 20585

No. of Copies

Assistant Secretary for International Affairs and Energy Emergencies, IE-1
U.S. Department of Energy
1000 Independence Ave., S.W.
Washington, DC 20585

Assistant Secretary for Management and Administration, MA-1
U.S. Department of Energy
1000 Independence Ave., S.W.
Washington, DC 20555

Assistant Secretary for Nuclear Energy, NE-1
U.S. Department of Energy
1000 Independence Ave., S.W.
Washington, DC 20585

Director, Office of Civilian Radioactive Waste Management, RW-1
U.S. Department of Energy
1000 Independence Ave., S.W.
Washington, DC 20585

Director, Office of Energy Research, ER-1
U.S. Department of Energy
1000 Independence Ave., S.W.
Washington, DC 20585

Director, Office of General Counsel, GC-1
U.S. Department of Energy
1000 Independence Ave., S.W.
Washington, DC 20585

Director, Office of Inspector General, IG-1
U.S. Department of Energy
1000 Independence Ave., S.W.
Washington, DC 20585

No. of Copies

Director, Office of Minority Economic Impact, MI-1
U.S. Department of Energy
1000 Independence Ave., S.W.
Washington, DC 20585

Director of Office of Policy, Planning, and Analysis, PE-1
U.S. Department of Energy
1000 Independence Ave., S.W.
Washington, DC 20585

20 R. J. Aiken
Office of Environmental Audit
EH-24
U.S. Department of Energy
1000 Independence Ave., S.W.
Washington, DC 20585

M. Arehart
Alaska Power Administration
U.S. Department of Energy
P.O. Box 50
Juneau, AK 99802

J. Barker
U.S. Department of Energy, EH-24
1000 Independence Ave., S.W.
Washington, DC 25585

J. Barry
Assistant Manager
Environmental, Safety & Health Programs
Idaho Operations Office
U.S. Department of Energy
785 Doe Place
Idaho Falls, ID 83402

R. Berube, Acting Director
Office of Environmental Guidance and Compliance
U.S. Department of Energy
1000 Independence Ave., S.W.
Washington, DC 20585

No. of Copies

J. H. Capps
Environment, Safety & Health Manager
Office of Resource Management
Morgantown Energy Technology Center
U.S. Department of Energy
P.O. Box 880
3610 Collins Ferry Rd.
Morgantown, WV 26505

B. W. Church
Director, Health Physics Division
Nevada Operations Office
U.S. Department of Energy
P.O. Box 14100
Las Vegas, NV 89114-4100

T. Clark
Nevada Operations Office
U.S. Department of Energy
P.O. Box 14100
Las Vegas, NV 89114

J. A. Coleman
U.S. Department of Energy, NE-24
1000 Independence Ave., S.W.
Washington, DC 25585

J. Davis
Director, Environment, Safety & Quality Assurance Division
San Francisco Operations Office
U.S. Department of Energy
1333 Broadway
Oakland, CA 94612

Joseph C. Dobes
U.S. Department of Energy, DP-226
1000 Independence Ave., S.W.
Washington, DC 25585

No. of
Copies

R. DuVal
San Francisco Operations Office
U.S. Department of Energy
1333 Broadway
Oakland, CA 94612

R. Egli
Assistant Manager for Safety & Environment
Oak Ridge Operations Office
U.S. Department of Energy
P.O. Box E
Oak Ridge, TN 37831

J. Farley
U.S. Department of Energy, ER-65
19901 Germantown Road
Germantown, MD 20874

R. Folstein, Director
Bartlesville Project Office
U.S. Department of Energy
P.O. Box 1398
Virginia and Cudahy Sts.
Bartlesville, OK 74005

R. Gale
Office Of Civilian Radioactive Waste Management, RW-40
U.S. Department of Energy
1000 Independence Ave., S.W.
Washington, DC 25585

C. George
U.S. Department of Energy, DP-12
1000 Independence Ave., S.W.
Washington, DC 25585

W. Griffing
Assistant Director for Environmental Protection
Chicago Operations Office
U.S. Department of Energy
9800 South Cass Ave.
Argonne, IL 60439

No. of
Copies

R. Guida
Naval Reactors Office, NE-60
U.S. Department of Energy
Crystal City
Arlington, VA 22202

D. J. Hamilla
Director, Radiological/Environmental Control & Safety Division
Schenectady Naval Reactors Office
Thru: Deputy Assistant Secretary for Naval Reactors, NE-60, HQ
U.S. Department of Energy
P.O. Box 1069
Schenectady, NY 12301

W. Hibbitts
Director, Environmental Protection Division
Oak Ridge Operations Office
U.S. Department of Energy
P.O. Box E
Oak Ridge, TN 37831

W. Holman
San Francisco Operations Office
U.S. Department of Energy
1333 Broadway
Oakland, CA 94612

W. Jamison
Assistant to the Administrator for Conservation & Environment
Western Area Power Administration
U.S. Department of Energy
P.O. Box 3402
Goldon, CO 80401

W. D. Jensen
Director, Operational Safety Division
Idaho Operations Office
U.S. Department of Energy
785 Doe Place
Idaho Falls, ID 83402

No. of
Copies

J. G. Johnson
U.S. Department of Energy, FE-13
1000 Independence Ave., S.W.
Washington, DC 25585

R. Jump
U.S. Department of Energy
at Oak Ridge
Waste Programs Branch
P.O. Box E
Oak Ridge, TN 37831

S. L. Katz, Director
Environmental Guidance Division
U.S. Department of Energy
1000 Independence Ave., S.W.
Washington, DC 20585

M. C. Keller
Associate Director for
Administration
Pittsburgh Energy Technology
Center
U.S. Department of Energy
P.O. Box 10940
Pittsburgh, PA 15236

D. Krenz
Assistant Manager for Safeguards
and Safety
Albuquerque Operations Office
U.S. Department of Energy
P.O. Box 5400
Albuquerque, NM 87115

J. LaGrone
Oak Ridge Operations Office
U.S. Department of Energy
P.O. Box E
Oak Ridge, TN 37831

J. Lehr
U.S. Department of Energy, DP-124
1000 Independence Ave., S.W.
Washington, DC 25585

No. of
Copies

J. E. Lytle
U.S. Department of Energy, DP-12
1000 Independence Ave., S.W.
Washington, DC 25585

R. Mayes
Director, Operational &
Environmental Safety Division
Chicago Operations Office
U.S. Department of Energy
9800 S. Cass Ave.
Argonne, IL 60439

J. McKnight
Safety & Occupational Health
Manager
Office of Human Resources
Southwestern Power Administration
U.S. Department of Energy
P.O. Box 1619
Tulsa OK 74101

A. Morell
Environmental Manager
Bonneville Power Administration
U.S. Department of Energy
P.O. Box 3621
Portland, OR 97208

R. Morgan
Savannah River Operations Office
U.S. Department of Energy
P.O. Box A
Aiken, SC 29801

K. Morris
U.S. Department of Energy, DP-3
1000 Independence Ave., S.W.
Washington, DC 25585

H. Myers
U.S. Department of Energy, CE-43
1000 Independence Ave., S.W.
Washington, DC 25585

No. of Copies

D. Newquist
Office of Safety, Health and Environment
Naval Petroleum and Oil Shale Reserves in Wyoming, Utah & Colorado
U.S. Department of Energy
800 Werner Court, Suite 342
Casper, WY 82601

H. Rauch
Chicago Operations Office
U.S. Department of Energy
9800 South Cass Ave.
Argonne, IL 60439

R. Romatowski
Albuquerque Operations Office
U.S. Department of Energy
P.O. Box 5400
Albuquerque, NM 87115

D. Rushworth
U.S. Department of Energy, NE-60
1000 Independence Ave., S.W.
Washington, DC 25585

20 K. Samec
Office of Environmental Guidance and Compliance
EH-23
U.S. Department of Energy
1000 Independence Ave., S.W.
Washington, DC 20585

G. Sherwood
U.S. Department of Energy, NE-43
19901 Germantown Road
Germantown, MD 20874

E. D. Shollenberger
Technical Support Project Officer
Pittsburgh Naval Reactors Office
Thru: Deputy Assistant Secretary for Naval Reactors, NE-60, HQ
U.S. Department of Energy
P.O. Box 109
West Mifflin, PA 15122-0109

No. of Copies

M. Smith
Environmental Safety & Health Division
Strategic Petroleum Reserve Project Management Office
U.S. Department of Energy
900 Commerce Rd. E.
New Orleans, LA 70123

G. A. Smithwick
Environment, Safety and Health
U.S. Department of Energy
1000 Independence Ave., S.W.
Washington, DC 20585

R. W. Taft
Assistant Manager for Engineering & Safety
Nevada Operations Office
U.S. Department of Energy
P.O. Box 14100
Las Vegas, NV 89114

K. Taimi
U.S. Department of Energy, EH-232
1000 Independence Ave., S.W.
Washington, DC 25585

J. G. Themelis
Environment and Health Division
Albuquerque Operations Office
U.S. Department of Energy
P.O. Box 5400
Albuquerque, NM 87115

V. Trebules
U.S. Department of Energy, RW-42
1000 Independence Ave., S.W.
Washington, DC 25585

J. Tseng
U.S. Department of Energy, DP-3
1000 Independence Ave., S.W.
Washington, DC 25585

No. of
Copies

K. E. Tucker
Director, Division of
Administrative Management
Southeastern Power Administration
U.S. Department of Energy
P.O. Box 1619
Tulsa, OK 74101

G. Turi
U.S. Department of Energy, NE-23
1000 Independence Ave., S.W.
Washington, DC 25585

T. Wade
Idaho Operations Office
U.S. Department of Energy
550-2nd St.
Idaho Falls, ID 83401

H. Walter
U.S. Department of Energy, NE-24
1000 Independence Ave., S.W.
Washington, DC 25585

R. P. Whitfield
Assistant Manager for Health
Safety & Environment
Savannah River Operations Office
U.S. Department of Energy
P.O. Box A
Aiken, SC 29802

E. Williams
U.S. Department of Energy, EH-22
1000 Independence Ave., S.W.
Washington, DC 25585

F. Wobber
ER-75 GTN
Ecological Research
Division
U.S. Department of Energy
Washington, DC 20545

No. of
Copies

S. R. Wright
Director, Environmental Division
Savannah River Operations Office
U.S. Department of Energy
P.O. Box A
Aiken, SC 29802

G. S. Sherrod
A & B Industrial Services, Inc.
5100 W. Michigan Ave.
Kalamazoo, MI 49007

S. S. Prasad
AEPCO, Inc.
5272 River Road, Suite 600
Bethesda, MD 20816

W. Cibulas
Agency for Toxic Substances and
Disease Registry
Chamblee 28 S.
1600 Clifton Rd.
Atlanta, GA 30333

B. L. Johnson
Director
Agency for Toxic Substances and
Disease Registry
Chamblee 28 S.
1600 Clifton Rd.
Atlanta, GA 30333

D. Jones
Agency for Toxic Substances and
Disease Registry
Chamblee 28 S.
1600 Clifton Rd.
Atlanta, GA 30333

J. Reyes
Office of Health Assessments
Agency for Toxic Substances and
Disease Registry
Chamblee 28 S.
1600 Clifton Rd.
Atlanta, GA, 30333

No. of
Copies

J. Goldman
The Aluminum Association
900 19th St. N.W.
Washington, DC 20006

D. Garin
Amoco Oil Company
5001 W. 80th St. Suite 890
Minneapolis, MN 55437

M. M. Accardo
Anheuser-Busch Company, Inc.
One Busch Place 202-4
St. Louis, MO 63118

A. S. Donigian, Jr., President
Aqua Terra Consultants
2666 East Bayshore Road
Palo Alto, CA 94303

G. D. Keil
Barr Engineering, Company
7803 Glenroy Rd.
Minneapolis, MN 55435

J. Conner
Battelle Memorial Institute
Battelle Project Management
Division
Battelle, Columbus Laboratories
505 King Avenue
Columbus, OH 43201

P. Hofmann
Battelle Memorial Institute
Battelle Project Management
Division
Battelle, Columbus Laboratories
505 King Avenue
Columbus, OH 43201

J. M. Doesburg
Office of Waste Technology
Development
Battelle
7000 S. Adams St.
Willowbrook, IL 60521

No. of
Copies

S. Sneider
Office of Waste Technology
Development
Battelle
7000 S. Adams St.
Willowbrook, IL 60521

A. Bakeberg
Bay West, Inc.
5 Empire Dr.
St. Paul, MN 55103

J. Berg
Bay West, Inc.
5 Empire Dr.
St. Paul, MN 55103

M. Wangensteen
Bay West, Inc.
5 Empire Dr.
St. Paul, Mn 55103

T. Gass
Blasland and Bouck Engineers
5793 Widewaters Pkwy
Syracuse, NY 13214

C. W. Wilson
Bureau of Land Management, D-155
Denver Federal Center
Building 50
Denver, CO 80225

R. Dorrler
Bymamac Corporation
Fort Lee Executive Park
2 Executive Drive
Ft. Lee, NJ 07024

N. Ball
Hazardous Materials Laboratory
California Department of
Health Services
2151 Berkeley Way
Berkeley, CA 94704

No. of
Copies

N. Ostiguy
Hazardous Materials Laboratory
California Department of
Health Services
2151 Berkeley Way
Berkeley, CA 94704

R. Stephens
Hazardous Materials Laboratory
California Department of
Health Services
2151 Berkeley Way, Room 234
Berkeley, CA 94704

R. B. Howell
California Department of
Transportation
P.O. Box 19128
Sacramento, CA 95819

R. Woodard
California Department of Water
Resources
P.O. Box 942836
Sacramento, CA 94236-0001

M. Cohen
California Institute of
Technology
Mail Code 206-41
Pasadena, CA 91125

M. Gildart
California Waste Management Board
1020 9th St., Suite 300
Sacramento, CA 95814

J. Rowden
California Waste Management Board
1020 9th St., Suite 300
Sacramento, CA 95814

M. Small
Department of Civil Engineering
Carnegie-Mellon University
Schenley Park
Pittsburgh, PA 15213

No. of
Copies

D. C. Lager
Case International Company
P.O. Box 40
Roselle, IL 60172

R. T. Zagraniski
Division of Birth Defects and
Developmental Disabilities
Center for Environmental Health
Center for Disease Control
Koger Center Room 2008
1600 Clifton Road, N.E.
Atlanta, GA 30333

M. Lev-On
CE-Environmental Monitoring and
Services, Inc.
2421 W. Hillcrest Dr.
Newbury Park, CA 91320

S. M. Brown
CH2M-Hill
P. O. Box 91500
Bellevue, Washington 98009

W. G. Goold
CH2M Hill
P.O. Box 4400
Reston, VA 22090

T. D. Van Epp
CH2M Hill
P.O. Box 4400
Reston, VA 22090

J. C. Davies
The Conservation Foundation
1255 23rd St., N.W.
Washington, DC 20037

A. Jankousky
Cotter Corporation
12596 West Bayaud, Suite 350
Lakewood, CO 80201

T. E. Croley, II
1808 Linwood
Ann Arbor, MI 48103

No. of
Copies

P. Deisler
11215 Wilding Lane
Houston, TX 77025

K. Sullivan
Detox, Inc.
P.O. Box 4735
Ithaca, NY 14852

B. Fischback
Dow Chemical U.S.A.
P.O. Box 1398
Pittsburg, CA 94595

B. Neeley
Dow Chemical Company
P.O. Box 1706
Midland, MI 48640

E. D. Grossmann
Department of Chemical
Engineering
Drexel University
Philadelphia, PA 19104

M. D. Olson
E. A. Hickok & Associates
545 Indian Mound
Wayzata, MN 55391

J. D. Skalbeck
Earth Technology Corporation
3777 Long Beach Blvd.
Long Beach, CA 90807

R. Thomasser
Earth Technology Corporation
3777 Long Beach Blvd.
Long Beach, CA 90807

M. Amdurer
EBASCO Services, Inc.
2000 15th St. N.
Arlington, VA 22201

No. of
Copies

G. B. Wiersma, Manager
Earth and Life Sciences
EG&G Idaho, Inc.
P.O. Box 1625
Idaho Falls, ID 83415

I. P. Muraka
Energy Analysis and Environmental
Division
Electric Power Research Institute
3412 Hillview Avenue
Palo Alto, CA 94303

R. E. Wyzga
Environmental and Conservation
Division
Electric Power Research Institute
P.O. Box 10412
Palo Alto, CA 94303

S. L. Brown
Project Manager
Environ Corporation
1000 Potomac St., N.W.
Washington, DC 20007

J. V. Rodricks
Environ Corporation
1000 Potomac St., N.W.
Washington, DC 20007

C. Morton
Environ Corporation
1000 Potomac St., N.W.
Washington, DC 20007

J. Rodricks
Environ Corporation
1000 Potomac St., N.W.
Washington, DC 20007

E. Silbergeld
Chief Toxics Scientist
Toxic Chemicals Program
Environmental Defense Fund
1616 P St., N.W., Room 150
Washington, DC 20036

No. of
Copies

G. Colovos
Environmental Monitoring and
Services, Inc.
2421 W. Hillcrest Dr.
Newbury Park, CA 91320

M. Rambelle
Environmental R & T
696 Virginia Rd.
Concord, MN 01742

M. J. Hewitt
EPA Monitoring Systems
Laboratory
P.O. Box 15027
Las Vegas, NV 89114-5027

A. Huggins
E.R.M., Inc.
999 West Chester Pike
West Chester, PA 19382

N. Drobny
ERM Midwest
2000 West Henderson Road
Columbus, OH 43220

A. Nugent
Fred C. Hart, Associates, Inc.
1110 Vermont Ave., N.W.
Washington, DC 20005

D. Buss
GeoTrans, Inc.
250 Exchange Place, Suite A
Herndon, VA 22070

P. S. Huyakorn
GeoTrans, Inc.
250 Exchange Place, Suite A
Herndon, VA 22070

S. Chatman
Geraghty and Miller, Inc.
1026 Westdale Road
Lawrence, KS 66044

No. of
Copies

M. Olson
Gradient Corporation
44 Brattle St.
Cambridge, MA 02138

S. Wilson
Groundwater Technology
4080 Pike Lane, Suite B
Concord, CA 94520

P. Yaniga
Groundwater Technology, Inc.
P.O. Box 309
Chadds Ford, PA 19317

M. Grube
Geologist
878 Maple Lane
Waterville, OH 43566

L. P. Smith
H & A of New York
50 Chestnut Plaza
Rochester, NY 14604

M. G. Turner
Halliburton Services
1311 Cornwall
Casper, WY 82609

L. Wallace
Harvard School of Public Health
665 Huntington Ave.
Boston, MA 02115

N. Currier
Hill Air Force Base, EMO
2329 E. 3025 N.
Layton, UT 84041

B. Owens
Hill Air Force Base, Base
Contracting Division
Ogden ALC PMKS, Bldg. 1299
Hill Air Force Base,
UT 84056-5320

No. of
Copies

B. Huggins
1103 Hickory Club Road
Antioch, TN 37013

P. S. Huyakorn
HydroGeologic, Inc.
503 Carlisle Drive
Suite 250
Herdon, VA 22070

J. B. Robertson
HydroGeologic, Inc.
503 Carlisle Drive
Suite 250
Herndon, VA 22070

T. W. Gallagher
Hydroqual, Inc.
1 Lethbridge Plaza
Mahwah, NJ 07430

L. A. Smith
ICAIR, Life Systems, Inc.
24755 Highpoint Road
Cleveland, OH 44122

G. Dawson
ICF Northwest
HAPO Bldg., 4th Floor
601 Williams Blvd.
Richland, WA 99352

T. J. McTaggart
Illinois Power Company
500 S. 27th St.
Decatur, IL 62525

B. Morrison
Industrial Economics, Inc.
2067 Massachusetts Ave.
Cambridge, MA 02140

T. Walker
Industrial Economics, Inc.
2067 Massachusetts Ave.
Cambridge, MA 02140

No. of
Copies

L. B. Gratt
I.W.G. Corporation
975 Hornblend St. #C
San Diego, CA 92109

M. McDermott
Keck Consulting Services
1099 W. Grand River Ave.
Williamson, MI 48895

M. Serafini
Keck Consulting Services
1099 W. Grand River Ave.
Williamson, MI 48895

W. L. Lappenbusch
Lappenbusch Environmental Health, Inc.
6480 Overlook Dr.
Alexandria, VA 22312

T. E. McKone
Lawrence Livermore National Laboratory
P.O. Box L-196
Livermore, CA 94550

T. Johnson
Levine-Fricke, Inc.
629 Oakland Ave.
Oakland, CA 94611

M. J. Kangas
Life Systems, Inc.
24755 Highpoint Road
Cleveland, OH 44122

P. A. Lang
L. Lehman & Associates
1103 W. Burnsville Pkwy.
Burnsville, MN 55337

A. K. Stoker
Environmental Surveillance
Los Alamos National Laboratory
P.O. Box 1663, MSK 490
Los Alamos, NM 87545

No. of
Copies

R. Vocke
University of California
Los Alamos National Laboratory
Mail Stop K-490
P.O. Box 990
Los Alamos, NM 87545

W. North
Decision Focus, Inc.
Los Altos Office Center
Suite 200
4984 El Camino Real
Los Altos, CA 94022

L. J. Thibodeaux
Hazardous Waste Research Center
3418 CEBA Bldg.
Louisiana State University
Baton Rouge, LA 70803

D. K. Cohen
Malcolm Pirnie, Inc.
100 Eisenhower Dr.
Paramus, NJ 07653

P. Jagucki
Malcolm-Pirine, Inc.
6161 Busch Blvd.
Columbus, OH 43229

B. P. Keenan
The Mennen Company
Hanover Ave.
Morristown, NJ 07960

G. F. Carpenter
Michigan Department of Natural
Resources
Environmental Response Division
P.O. Box 30028
Lansing, MI 48909

B. L. White
Michigan Department of Natural
Resources
350 Ohawa N.W.
Grand Rapids, MI 49503

No. of
Copies

E. Porcher
Minnesota Pollution Control
Agency
520 Lafayette Rd. N.
St. Paul, MN 55155

S. Saari
Energy, Resource & Environmental
Systems Division
The MITRE Corporation
1820 Dolley Madison Blvd.
McLean, VA 22102

M. P. Wang
Energy, Resource & Environmental
Systems Division
The MITRE Corporation
1820 Dolley Madison Blvd.
McLean, VA 22102

D. Sayala
Energy Resource and Environmental
Systems Division
The MITRE Corporation
1820 Dolley Madison Blvd.
McLean, VA 22102

R. Vargo
Field Research and Development
Agricultural Chemicals Division
Mobay Chemical Corporation
1317 Tulip Lane
Davis, CA 95616

R. Freeman
Monsanto Corporation
800 N. Lindbergh
St. Louis, MO 63167

D. Carfagno
Monsanto Research Corporation
MOUND
Miamisburg, OH 45342

R. Neff
Monsanto Research Corporation
MOUND
Miamisburg, OH 45342

No. of
Copies

W. Stigliani
National Academy of Science
JH804
2101 Constitution Ave., N.W.
Washington, DC 20418

R. A. Chemerys
Oceanic and Atmospheric Research
National Oceanic and Atmospheric
Administration
6010 Exec. Blvd., Room 927
Rockville, MD 20852

R. Pavia
National Oceanic and Atmospheric
Administration, OMA34
7600 Sandpoint Way NE
Seattle, WA 98115

R. Petty
National Water Well Association
6375 Riverside Dr.
Dublin, OH 43017

Major J. Klube
Director, Planning Analysis &
Program Support Division
Naval Petroleum Reserves in
California
P.O. Box 11
Tupman, CA 93276

P. Brookner
Nebraska Department of
Environmental Cont.
P.O. 94877 State House Station
Lincoln, NE 68509-4877

R. Ehrman
Nebraska Department of
Environmental Cont.
P.O. 94877 State House Station
Lincoln, NE 68509-4877

No. of
Copies

T. Burke
Deputy Commissioner
New Jersey Department of Health
Room 805, State Health, CN360
Trenton, NJ 08625

M. Sosnow
New York DEC
50 Wolf Rd.
Albany, NY 12233-3011

K. Clayman
Bureau of Hazardous Materials
Program
New York City Department of
Environmental Protection
1 Center St., Room 2444
New York, NY 10007

J. L. Arndt
North Dakota State University
Box 5575
Fargo, ND 58102

J. L. Richardson
North Dakota State University
Box 5575
Fargo, ND 58102

P. Alexandro
NUS Corporation
910 Clopper Road
Gaithersburg, MD 20879

J. Skridules
NUS Corporation
1300 N. 17th St., Suite 1320
Arlington, VA 22209

R. Talbert
NUS Corporation
Park West Two
Cliff Mine Road
Pittsburgh, PA 15275

No. of
Copies

A. Toblin
NUS Corporation
910 Clopper Road
Gaithersburg, MD 20879

L. Barnthouse
Martin-Marietta Energy Systems
Oak Ridge National Laboratory
Oak Ridge, TN 37831

L. D. Eyman
Martin-Marietta Energy Systems
Oak Ridge National Laboratory
Oak Ridge, TN 37831

D. Kocher
Martin-Marietta Energy Systems
Oak Ridge National Laboratory
Oak Ridge, TN 37831

M. R. Patterson
Martin-Marietta Energy Systems
Oak Ridge National Laboratory
Oak Ridge, TN 37831

G. Suter
Martin-Marietta Energy Systems
Oak Ridge National Laboratory
Oak Ridge, TN 37831

C. Travis
Martin-Marietta Energy Systems
Oak Ridge National Laboratory
Oak Ridge, TN 37831

P. vanHaagen
Office of Management and Budget
Rm. 8222
726 Jackson Pl. N.W.
Washington, DC 20503

C. D. Palmer
Department of Environmental
Science and Engineering
Oregon Graduate Center
19600 N. W. Van Neumann Dr.
Beaverton, OR 97006

No. of
Copies

J. E. Ort
Pennsylvania Department of
Environmental Res.
P.O. Box 2063
Harrisburg, PA 17120

G. Aron
Department of Civil Engineering
Pennsylvania State University
University Park, PA 16801

D. F. Kibler
Department of Civil Engineering
Pennsylvania State University
University Park, PA 16801

A. Miller
Department of Civil Engineering
Pennsylvania State University
University Park, PA 16801

S. G. Termaath
SAF/MIQ
The Pentagon, Room 4C916
Washington, DC 20330-1000

M. Sands
Pope-Reid and Associates
245 E. 6th St., #813
St. Paul, MN 55101

K. P. Vidmar
Pratt & Whitney
400 Main St.
E. Hartford, CT 06108

G. Pinder, Chairman
Department of Civil Engineering
Princeton University
Princeton, NJ 08544

K. J. Yost
Division of Sponsored Programs
Purdue Research Foundation
303 Hovde Hall
West Lafayette, IN 47907

No. of
Copies

T. W. Tesche
Radian Corporation
10395 Old Placerville Road
Sacramento, CA 95827

N. Duan
Rand Corporation
1700 Main St.
Santa Monica, CA 90406

J. A. Detamore
Rockwell International
P.O. Box 3150
Albuquerque, NM 87190-3150

B. L. Anderson
Prog. Mgr. Staff Office
AMXRM-PM-R
Rocky Mountain Arsenal, Bldg. 111
Commerce City, CO 80022-2180

W. C. Mason
Project Manager
Roy F. Weston, Inc.
5301 Central Avenue, N.E.
Suite 1000
Albuquerque, NM 87108

J. Mauro
Roy F. Weston, Inc.
1 Weston Way
West Chester, PA 19380

P. Germann
Department of Soils and Crops
Rutgers, The State University of
New Jersey
P. O. Box 231
New Brunswick, New Jersey 08903

R. Rechard
Division 6431
Sandia National Laboratory
Albuquerque, NM 87185

No. of
Copies

C. Comiskey
Science Applications,
International
800 Oak Ridge Turnpike
Oak Ridge, Tennessee 37830

G. S. Monson
Shell Western E & P, Inc.
Grandview Plaza
Traverse City, MI 49684

S. Hanna
Sigma Research Corporation
394 Lowell St., Suite 11
Lexington, MA 02173

S. Dickey
Southern California Edison
P.O. Box 800
Rosemead, CA 91770

C. Doyle
Southern California Edison
P.O. Box 800
Rosemead, CA 91770

E. C. Ellis
Research and Development
Southern California Edison
P.O. Box 800
Rosemead, CA 91770

A. A. Elseewi
Research and Development, G01
Southern California Edison
P.O. Box 800
Rosemead, CA 91770

J. J. Ospital
Southern California Edison
P.O. Box 800
Rosemead, CA 91770

J. B. Palmer
Southern California Edison
P.O. Box 800
Rosemead, CA 91770

No. of
Copies

R. Sholes
Southern California Edison
P.O. Box 800
Rosemead, CA 91770

D. C. Bomberger
S.R.I. International
333 Ravenswood Ave.
Menlo Park, CA 94025

J. O. Leckie
Department of Civil Engineering
Stanford University
Stanford, CA 94305-4020

S. Burton
Systems Applications
101 Lucas Valley Road
San Rafael, CA 94903

G. E. Moore
Systems Applications, Inc.
101 Lucas Valley Road
San Rafael, CA 94903

C. Seigneur
Systems Applications, Inc.
101 Lucas Valley Road
San Rafael, CA 94903

K. M. Johnson
Environmental Systems Engineering
Tetra Tech, Inc.
3746 Mt. Diablo Boulevard
Lafayette, CA 94549

R. Conway
Corporate Development Fellow
Union Carbide Corporation
P.O. Box 8361
770/342
South Charleston, WV 25303

A. Hirata
Union Oil of California
P.O. Box 7600
Los Angeles, CA 90051

No. of
Copies

D. Allen
Department of Chemical
Engineering
5531 Boelter Hall
University of California,
Los Angeles
Los Angeles, CA 90024

Y. Cohen
Department of Chemical
Engineering
5531 Boelter Hall
University of California,
Los Angeles
Los Angeles, CA 90024

C. Dragoescu
Department of Chemical
Engineering
5531 Boelter Hall
University of California,
Los Angeles
Los Angeles, CA 90024

T. Estes
Department of Chemical
Engineering
5531 Boelter Hall
University of California,
Los Angeles
Los Angeles, CA 90024

S. K. Friedlander
Department of Chemical
Engineering
5531 Boelter Hall
University of California,
Los Angeles
Los Angeles, CA 90024

D. Goldsmith
Toxic Substances Research and
Teaching Program
University of California, Davis
Davis, CA 95616

No. of
Copies

C. Kakalak
Department of Chemical
Engineering
5531 Boelter Hall
University of California,
Los Angeles
Los Angeles, CA 90024

W. E. Kastenberg
Mechanical, Aerospace and Nuclear
Engineering
5730 Boelter Hall
University of California,
Los Angeles
Los Angeles, CA 90024

W. W. L. Lee
Department of Nuclear Engineering
University of California at
Berkeley
Berkeley, CA 94720

C. Mackiewicz
Department of Chemical
Engineering
5531 Boelter Hall
University of California,
Los Angeles
Los Angeles, CA 90024

T. Matonak
Department of Chemical
Engineering
5531 Boelter Hall
University of California,
Los Angeles
Los Angeles, CA 90024

G. Mayer
Department of Chemical
Engineering
5531 Boelter Hall
University of California,
Los Angeles
Los Angeles, CA 90024

No. of
Copies

P. Ryan
Department of Chemical
Engineering
5531 Boelter Hall
University of California,
Los Angeles
Los Angeles, CA 90024

R. Shah
Department of Chemical
Engineering
5531 Boelter Hall
University of California,
Los Angeles
Los Angeles, CA 90024

J. Svihra, Librarian
Earthquake Engineering Research
Center Library 04TT16
RFS Building 453
University of California
1301 S. 46th St.
Richmond, CA 94804

H. Tagahavi
Department of Chemical
Engineering
5531 Boelter Hall
University of California,
Los Angeles
Los Angeles, CA 90024

V. Vilker
Department of Chemical
Engineering
5531 Boelter Hall
University of California,
Los Angeles
Los Angeles, CA 90024

A. Akanbi
Department of Civil and
Environmental Engineering
ML 71
University of Cincinnati
Cincinnati, OH 45221

No. of
Copies

F. M. Holly
Iowa Institute of Hydraulic
Research
University of Iowa
Iowa City, IA 52240

S. Jain
Iowa Institute of Hydraulic
Research
University of Iowa
Iowa City, IA 52240

J. F. Kennedy, Director
Iowa Institute of Hydraulic
Research
University of Iowa
Iowa City, IA 52240

J. Schnoor
Civil and Environmental
Engineering Department
Iowa Institute of Hydraulic
Research
University of Iowa
Iowa City, IA 52240

J. Doull
Professor of Pharmacology and
Toxicology
University of Kansas
Medical Center
Kansas City, KS 66103

H. T. Spencer
Department of Chemical
Engineering
University of Louisville
Louisville, KY 40292

R. H. Kadlec
Department of Chemical
Engineering
3094 Dow Building
University of Michigan
Ann Arbor, MI 48109-2136

No. of
Copies

D. J. Kirkner
Department of Civil Engineering
University of Notre Dame
Notre Dame, Indiana 46556

R. C. Loehr
Civil Engineering Department
8.614 ECJ Hall
University of Texas
Austin, TX 78712

E. A. Cassell
School of Natural Resources
George D. Aiken Center
University of Vermont
Burlington, VT 05405

Wu-Seng Lung
Department of Civil Engineering
Thornton Hall
University of Virginia
Charlottesville, VA 22901

J. A. Cherry
Department of Earth Sciences
University of Waterloo
Waterloo, Ontario N2L 3G1

L. Barry
U.S. Air Force
Ogden Air Logistics Center
Hill Air Force Base,
UT 84056-5990

D. M. Parks
U.S. Army, APG Support Act
Attn: STEAP-FE-M
Aberdeen Proving Ground,
MD 21005

P. Reibel
U.S. Army/HQ ARDEC
Attn: SMCAR-ISE-M, Bldg. 3124
Picatinny Arsenal, NJ 07806-5000

No. of
Copies

W. Dorough, Chief
Water and Sediment Section
U.S. Army Corps of Engineers
Omaha District
U.S. Post Office Building
North 17th and Capitol Sts.
Omaha, NB 67192

C. D. Kealy
U.S. Bureau of Mines Spokane
Research Center
East 315 Montgomery Avenue
Spokane WA 99207

D. Rosenberger
CERCLA Program -- 301 Project
U.S. Department of the Interior
Washington, DC 20545

J. J. Barich, III
U.S. Environmental Protection
Agency, Region 10
1200 Sixth St.
Seattle, WA 98101

J. V. Behar
U.S. Environmental Protection
Agency, EMSL-LV
P.O. Box 15027
Las Vegas, NV 89114

M. Burns
Office of Solid Waste (WH5628)
U.S. Environmental Protection
Agency
Washington, DC 20460

K. W. Conway
Deputy Director
Science Advisory Board
U.S. Environmental Protection
Agency
401 M St., S.W.
A101-F, Washington, DC 20460

No. of
Copies

C. DeRosa
Environmental Criteria and
Assessment Office
U.S. Environmental Protection
Agency
26 W. St. Clair
Cincinnati, OH 45268

J. Falco, Director
Office of Environmental Processes
and Effects Research
U.S. Environmental Protection
Agency
401 M St., S.W.
Washington, DC 20460

L. Fernandez
Office of Science and
Research
New Jersey Office of U.S.
Environmental Protection Agency
401 East State St., CN-40
Trenton, NJ 08625

F. Fong
Environmental Research Laboratory
U.S. Environmental Protection
Agency
College Station Road
Athens, GA 30613

K. Garrahan
Exposure Assessment Group
Office of Research and
Development
U.S. Environmental Protection
Agency (RD-689)
401 M St., S.W.
Washington, DC 20460

J. A. Goodrich
U.S. Environmental Protection
Agency
26 W. St. Clair
Cincinnati, OH 45268

No. of
Copies

M. J. Hewitt
GIS Coordinator
Office of Research and
Development
Remote Air Monitoring Branch
Advanced Monitoring Systems
Division
Environmental Monitoring
Systems Laboratory
U.S. Environmental Protection
Agency
P.O. Box 15027
Las Vegas, NV 89114-5027

S. T. Hwang
Exposure Assessment Group
Office of Research and
Development
U.S. Environmental Protection
Agency (RD-689)
401 M St., S.W.
Washington, DC 20460

R. Madison, PM-220
Office of Policy Analysis
U.S. Environmental Protection
Agency
401 M St., S.W.
Washington, DC 20460

J. Metcalf, WH-548E
U.S. Environmental Protection
Agency
401 M St., S.W.
Washington, DC 20460

L. A. Mulkey
Environmental Research Laboratory
U.S. Environmental Protection
Agency
College Station Road
Athens, GA 30613

No. of
Copies

A. Ortiz
Office of Solid Waste
U.S. Environmental Protection
Agency
WH-562B
401 M St., S.W.
Washington, DC 20460

C. Wolff
Office of Policy Analysis, PM-220
U.S. Environmental Protection
Agency
401 M St., S.W.
Washington, DC 20460

M. Rosen
Office of Science and Research
New Jersey Office of U.S.
Environmental Protection Agency
401 East State St.
Trenton, NJ 08625

M. Shirazi
Corvallis Environmental Research
Laboratory
U.S. Environmental Protection
Agency
Corvallis, OR 97333

S. Williamson
Environmental Monitoring Systems
Laboratory
U.S. Environmental Protection
Agency
P.O. Box 15027
Las Vegas, NV 89114

J. R. Yearsley
U.S. Environmental Protection
Agency, Region 10
1200 Sixth Ave. (M/S 329)
Seattle, WA 98110

No. of
Copies

T. F. Yosie
U.S. Environmental Protection
Agency, Sci. Adv. Brd.
A-101/Room 1145 West Tower
401 M St., S.W.
Washington, DC 20460

L. R. Larson
U.S. Geological Survey
P.O. Box 1125
Cheyenne, WY 82003

R. P. Michel
U.S. Geological Survey
P.O. Box 1125
Cheyenne, WY 82003

D. Pollock
Office of Groundwater
U.S. Geological Survey
411 National Center
Reston, VA 22092

D. F. Wickenberg
U.S. Geological Survey
P.O. Box 1125
Cheyenne, WY 82003

R. B. Codell
Mail Stop 623-SS
U.S. Nuclear Regulatory
Commission
Washington, DC 20555

L. D. James
Utah Water Research Laboratory
Utah State University
Logan, Utah 84332-8200

J. L. Sims
Research Scientist
Utah Water Research Laboratory
UMC 82
Utah State University
Logan, UT 84332

No. of
Copies

J. C. Parker
334 Smyth Hall
Virginia Polytechnic Institute
Blackburgs, Virginia 24061

M. L. Blough
Virginia Power
5000 Dominion Blvd.
Glen Allen, VA 23060

K. E. Hartz
Environmental Engineering
Department
Washington State University
141 Sloan
Pullman, WA 99164

W. Stone
New York State Department of
Environmental Conservation
Wildlife Resources Center
Delmar, New York 12054

P. D. DuBois
Wisconsin Geological Survey
3817 Mineral Point Rd.
Madison, WI 53705

J. D. Dean
Woodward-Clyde Consultants
100 Pringle Ave.
Walnut Creek, CA 94596

D. R. Gaboury
Woodward-Clyde Consultants
100 Pringle Ave.
Walnut Creek, CA 94596

P. Mangarella
Woodward-Clyde Consultants
100 Pringle Ave.
Walnut Creek, CA 94596

A. Salhotra
Woodward-Clyde Consultants
100 Pringle Ave.
Walnut Creek, CA 94596

No. of Copies

FOREIGN

T. G. Chapman
School of Civil Engineering
The University of New South Wales
P.O. Box 1
Kensington, New South Wales
AUSTRALIA 2033

D. Mackay
Department of Chemical Engineering and Applied Chemistry and Institute for Environmental Studies
University of Toronto
Toronto, Ontario
CANADA M5S 1A4

H. E. Turner
Air Quality Research Branch
Atmospheric Environment Service
4905 Dufferin St.
Downsview, Ontario
CANADA

V. Hanusik
Institute of Radioecology and Applied Nuclear Techniques
Garbiarska 2
P.O. Box A-41
040 61 Kosice
CZECHOSLOVAKIA

A. Kerekes
Orszagos "Frederic Joliot-Curie"
Sugarbiologiai Es Sugaregeszsegugyi
Kutato Intezet
Budapest, XXII. Pentz Karoly u. 5.
1775. Budafok 1. Postafiok 101
HUNGARY

K. C. Pillai, Head
Environmental Studies Section
Bhabha Atomic Research Center
Health Physics Division
Bombay-400 085
INDIA

No. of Copies

M. Sadiq
KFUPM 417
Dhaharan 31261
SAUDIA ARABIA

G. Rippen
Battelle
Battelle-Institut e. V.
Postfach 900160
Am Romerhof 35
D-6000 Frankfurt am Main 90
WEST GERMANY

J. Foric
Ruder Boskovic Institute
POB 1016
41001 Zagreb
Croatia
YUGOSLAVIA

ONSITE

6 DOE Richland Operations Office

P. K. Clark
R. Gerton
P. Krupin
M. J. Lawrence
A. J. Rizzo
J. J. Sutey

UNC United Nuclear Industries

G. Tarcza

94 Pacific Northwest Laboratory

J. L. Baer
R. D. Brockhaus
J. W. Buck (2)
D. B. Cearlock
C. R. Cole
K. H. Cramer
J. L. Downs
D. W. Dragnich
J. G. Droppo (2)
P. A. Eddy

No. of
Copies

M. J. Fayer
M. D. Freshley
J. S. Fruchter
G. W. Gee
M. J. Graham
L. K. Grove
J. M. Hales
K. R. Hanson
J. N. Hartley
K. A. Hawley
P. C. Hays
E. A. Jacobson
C. T. Kincaid
S. A. Kreml
T. J. McLaughlin
P. J. Mellinger
B. A. Napier
R. W. Nelson
P. L. Oberlander

No. of
Copies

Y. Onishi
L. S. Prater
D. S. Renne
R. G. Schreckhise
D. R. Sherwood
C. S. Simmons
D. R. Simpson
R. L. Skaggs
J. K. Soldat
B. L. Steelman (10)
T. L. Stewart
J. A. Stottlemyre
D. L. Strenge (2)
R. W. Wallace
M. B. Walter
G. Whelan (30)
R. E. Wildung
Publishing Coordination (2)
Technical Report Files (5)